Faculdade de Ciências e Tecnologia
da Universidade de Coimbra

Mitochondria and Cancer: Opening Pandora's Box

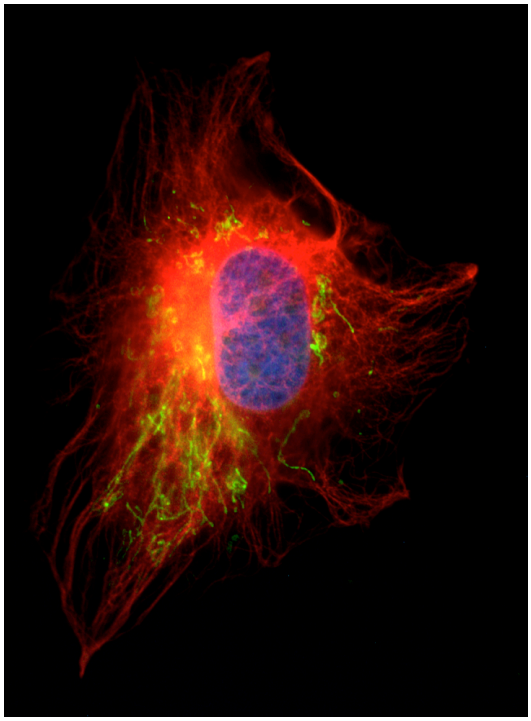

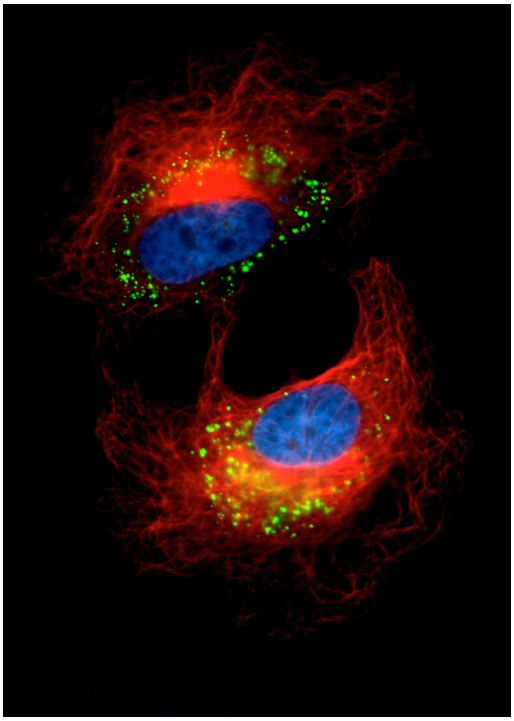

Teresa Laura Mendes Serafim
2011

Dissertação apresentada à Faculdade de Ciências e Tecnologia da Universidade de Coimbra para cumprimento dos requisitos necessários à obtenção de grau de Doutor em Biociências, Especialidade em Toxicologia.

Dissertation presented to the Faculty of Sciences and Technology of the University of Coimbra as requirement for Ph.D. graduation in Biosciences, Toxicology branch.

Supervisors: Paulo Jorge Oliveira, Ph.D
Maria Paula Marques, Ph.D

This work was conducted at the Center for Neuroscience and Cell Biology, Department of Life Sciences, University of Coimbra, Coimbra, Portugal, at the School of Medicine, Department of Anatomy, Microbiology & Pathology, University of Minnesota, Duluth (USA) and at the Department of Biomedical Sciences, Mercer University School of Medicine, Savannah Campus, Georgia (USA). This thesis was supported by a Ph.D. fellowship from the Portuguese FCT to T.L.S. (SFRH/BD/38067/2007).

À minha família

ACKNOWLEDGEMENTS

To *Fundação para a Ciência e Tecnologia*, for the Ph.D. Fellowship that supported my work (SFRH / BD /38067/2007) and for the research grant PTDC/QUI-QUI/101409/2008 (PI: Paulo J. Oliveira).

To Doctor Paulo Oliveira, for inviting me to join your group, for all your support, dedication, friendship but especially for being always there for me, trusting me and making this project possible;

To Doctor Maria Paula Marques, for your supervision, friendship and support during my PhD work;

To Doctor Jon Holy, for receiving me at University of Minnesota-Duluth (USA), for being supervisor, a teacher and a friend, for listening to me;

To Doctor Edward Perkins, for sharing your lab at Mercer University School – Savannah (USA) and guiding me in the genetics field, and for receiving and sharing with me your home together with Doctor Amy Greene;

To Doctor António Moreno and Doctor Maria Sancha Santos, for being always there, for being the pillars of my work but most fundamentaly for being such warm people;

To Doctor Fernanda Borges and Doctor Fernanda Roleira, for your support and friendship and for allowing me to test your phenolic compounds;

To Doctor Pavel Krasutsky, for allowing me to use your triterpenoids compounds and for being such a great person, a great scientist;

To all my collegues of the Mitochondrial Toxicology and Disease group for the team work and the good moments we spent with laughs and parties, but also for the bad ones, fo being there with your friendship. A very special thank you to Filipa Carvalho, for being such friend and my "right harm";

To Paula, Júlia and Clara for making the lab work much easier, with your backstage work, but essentially with your daily good humor;

To all the friends that I made during my PhD, that were fundamental for my growth as a scientist as well as a person;

To Sónia Fiuza, for being you, my syncronized friend;

To Filipe Ceia, for being so patient, supportive and goofy, showing that life can be simple;

To my mom and sister, for being my pillars, giving me such strength;

To Laura Ceia, "my life", for showing me that anything is possible with courage, strength and love.

SCIENTIFIC PAPERS

2011 – T. L. Serafim, Vilma A. Sardão, Amy Greene, Edward Perkins and Paulo J. Oliveira. Characterization of mitochondria physiology in breast cancer (*in preparation*);

2011 – T. L. Serafim, Filipa S. Carvalho, Gonçalo Pereira, Telma Bernardo, Edward Perkins, Jon Holy, Dmytro A. Krasutsky, Oksana N. Kolomitsyna, Pavel A. Krasutsky and Paulo J. Oliveira. New derivatives of lupane triterpenoids as promising mitochondria disturbers in breast cancer (*in preparation*);

2011 – Teresa L. Serafim, Filipa S. Carvalho, Maria P.M. Marques, Rita Calheiros, Tiago Silva, Jorge Garrido, Nuno Milhazes, Fernanda Borges, Fernanda Roleira, Elisiário T. Silva, Jon Holy and Paulo J. Oliveira. Lipophilic Caffeic and Ferulic Acid Derivatives Presenting Cytotoxicity against Human Breast Cancer Cells. Chem Res Toxicol. 16;24(5):763-774;

2011 – Cátia Diogo, Nuno Machado, Inês Barbosa, Teresa L. Serafim, Ana Burgeiro, Paulo J. Oliveira. Berberine as a Promising Safe Anti-Cancer Agent - Is there a Role for Mitochondria? Curr Drug Targets. 12(6):850-9;

2008 – Teresa L. Serafim, Maria P. Marques, Fernanda M. Borges and Paulo J. Oliveira. Mitochondria as a target for novel chemotherapeutic agents based on phenolic acids. Journal Theoretical & Experimental Pharmacology. 1 (1): 3-13;

2008 – Teresa L. Serafim, Júlio A. Matos, Vilma A. Sardão, Gonçalo C. Pereira, Ana F. Branco, Sandro L. Pereira, Donna Parke, Edward L. Perkins, António J.M. Moreno, Jon Holy, Paulo J. Oliveira. Mechanisms of Sanguinarine Cytotoxicity on Mouse Melanoma K1735-M2 Cells – Nuclear versus Mitochondrial Effects. Biochemical Pharmacology. 76 (11): 1459-1475;

2008 - Teresa L. Serafim, Paulo J. Oliveira, Vilma A. Sardão, Ed Perkins, Donna Parke,

Jon Holy. (2008) Different concentrations of Berberine result in distinct cellular localization patterns and cell cycle effects in a melanoma cell line. Cancer Chemotherapy and Pharmacology. 61(6):1007-18;

2007 - Gonçalo C. Pereira, Ana F. Branco, Júlio Matos, Sandro L. Pereira, Donna Parke, Edward L. Perkins, Teresa L. Serafim, Vilma A. Sardão, Maria S. Santos, Antonio J. M. Moreno, Jon Holy, and Paulo J. Oliveira. (2007) Mitochondrially targeted effects of berberine [Natural Yellow 18, 5,6-dihydro-9,10-dimethoxybenzo(g)-1,3-benzodioxolo(5,6-a) quinolizinium] on K1735-M2 mouse melanoma cells: comparison with direct effects on isolated mitochondrial fractions. Biochem. Pharmacol. 323(2):636-49.

SCIENTIFIC MEETINGS – Oral communication

2008 – Teresa L. Serafim, Claudia V. Pereira, Gonçalo Pereira, Nuno G. Machado, Donna Parke, Edward L. Perkins, Antonio J. M. Moreno, Jon Holy and Paulo J. Oliveira. Different concentrations of berberine result in distinct cellular localization patterns and cell cycle effects in a melanoma cell line. Annual Meeting of Center for Neurosciences and Cell Biology, Coimbra, Portugal, December 20-22th;

2008 – Teresa L. Serafim, Filipa S. Carvalho, M.P.M. Marques, Jorge Garrido, Nuno Milhazes, Fernanda Borges, Fernanda Roleira, Elisiário Tavares da Silva, Jon Holy, Paulo J. Oliveira. Pharmacological and toxicological activity of phenolic acids on breast cancer cell models. Annual Reunion of Portuguese Society of Pharmacology. Lisbon, Portugal, December 3-5th;

2008 – Teresa L. Serafim, Vilma A. Sardão, Júlio A. C. Matos, Gonçalo C. Pereira, Ana F. Branco, Sandro L. Pereira, Donna Parke, Edward L. Perkins, António J. M. Moreno, Jon Holy, Paulo J. Oliveira. Nuclear and mitochondrial effects of sanguinarine on mouse melanoma k1735-M2 cells. Annual Reunion of Portuguese Society of Pharmacology. Lisbon, Portugal, December 3-5th;

2007 – Teresa L. Serafim, Claudia V. Pereira, Gonçalo Pereira, Nuno G. Machado, Donna Parke, Edward L. Perkins, Antonio J. M. Moreno, Jon Holy and Paulo J. Oliveira. Different concentrations of berberine result in distinct cellular localization patterns and cell cycle effects in a melanoma cell line. Annual Reunion of Portuguese Society of Pharmacology, Coimbra, Portugal, December 5-7th;

2007 – Teresa L. Serafim, Filipa S. Carvalho, M.P.M. Marques, Jorge Garrido, Nuno Milhazes, Fernanda Borges, Fernanda Roleira, Elisiário Tavares da Silva, Jon Holy, Paulo J. Oliveira. Antiproliferative activity of ferulic and caffeic acid derivatives on tumor cell lines – Structure-function relationships and direct effects on mitochondria. Annual Reunion of Portuguese Society of Pharmacology, Coimbra, Portugal, December 5-7th;

2007 – Julio Matos, Teresa L Serafim, Vilma A. Sardão, Gonçalo C. Pereira, Ana F. Branco, Sandro L. Pereira, Donna Parke, Edward L. Perkins, António J. M. Moreno, Jon Holy, Paulo J. Oliveira. Sanguinarine cytotoxicity on mouse melanoma K1735-M2 cells: Role of nuclear and mitochondrial interactions. Annual Reunion of Portuguese Society of Pharmacology, Coimbra, Portugal, December 5-7th;

2007 – Gonçalo Pereira, Ana F. Branco, Júlio Matos, Sandro L. Pereira, Donna Parke, Edward L. Perkins, Teresa L. Serafim, Vilma A. Sardão, Maria S. Santos, Antonio J. M. Moreno, Jon Holy, and Paulo J. Oliveira. Mitochondrially-targetted effects of berberine on K1735-M2 mouse melanoma cells – comparison with direct effects on isolated mitochondrial fractions. Annual Reunion of Portuguese Society of Pharmacology, Coimbra, Portugal, December 5-7th.

SCIENTIFIC MEETINGS – Poster

2011 - Teresa L. Serafim, Filipa S. Carvalho, Gonçalo Pereira, Edward Perkins, Jon Holy, Dmytro A. Krasutsky, Oksana N. Kolomitsyna, Pavel A. Krasutsky and Paulo J. Oliveira. Cationic triterpenoid derivatives acting as Mitocans on breast cancer cells. Annual Scientific Meeting of the European Society for Clinical Investigation Crete, Greece. April 13-16th;

2010 - Teresa L. Serafim, Filipa S. Carvalho, Gonçalo Pereira, Edward Perkins, Jon Holy, Dmytro A. Krasutsky, Oksana N. Kolomitsyna, Pavel A. Krasutsky and Paulo J. Oliveira. Characterization of novel cationic triterpenoids as Mitocans in breast cancer. AICR - Saint Andrews, Scotland, April 7-9th;

2010 - Teresa L. Serafim, Filipa S. Carvalho, M.P.M. Marques, Jorge Garrido, Nuno Milhazes, Fernanda Borges, Fernanda Roleira, Elisiário Tavares da Silva, Jon Holy, Paulo J. Oliveira. Anti-Breast Cancer Activity of Phenolic Acid Derivatives. AICR - Saint Andrews, Scotland, April 7-9th;

2009 – Teresa L. Serafim, Filipa S. Carvalho, M.P.M. Marques, Jorge Garrido, Nuno Milhazes, Fernanda Borges, Fernanda Roleira, Elisiário Tavares da Silva, Jon Holy, Paulo J. Oliveira. Phenolic Acids Derivatives and their Biological Activity on Breast Cancer and Mitochondrial Bioenergetics. Advances in Breast Cancer Research: Genetics, Biology and Clinical Applications. San Diego, California, USA, October 13-16th;

2009 – Teresa L. Serafim, Claudia V. Pereira, Gonçalo Pereira, Nuno G. Machado, Donna Parke, Edward L. Perkins, Antonio J. M. Moreno, Jon Holy and Paulo J. Oliveira. Mitochondrial Interactions of Berberine – a Promising Anti-cancer Molecule. 18th Annual Short Course on Experimental Models of Human Cancer. The Jackson Laboratory, Bar Harbor, Maine, USA, August 21-27th;

2009 – Teresa L. Serafim, Filipa S. Carvalho, M.P.M. Marques, Jorge Garrido, Nuno Milhazes, Fernanda Borges, Fernanda Roleira, Elisiário Tavares da Silva, Jon Holy, Paulo J. Oliveira Cytotoxic effects of phenolic acids and derivatives on isolated mitochondrial fractions and tumor cell lines. International Courses on Toxicology, "Mitochondria: Between Life and Death", University of Coimbra, Portugal, May 5-8th;

2009 – Teresa L. Serafim, Claudia V. Pereira, Nuno G. Machado, Donna Parke, Edward L. Perkins, Antonio J. M. Moreno, Jon Holy and Paulo J. Oliveira. Berberine as a Potent Anti-cancer Molecule – Role of Mitochondrial Interactions. Chemistry in Cancer Research: A Vital Partnership in Cancer Drug Discovery and Development, New Orleans, USA, February 8-11th;

2009 – Teresa L. Serafim, Vilma A. Sardão, Júlio A. C. Matos, Gonçalo C. Pereira, Ana F. Branco, Sandro L. Pereira, Donna Parke, Edward L. Perkins, António J. M. Moreno, Jon Holy, Paulo J. Oliveira. Sanguinarine Inhibits the Proliferation of Metastatic Melanoma Cells by Causing Nuclear and Mitochondrial Alterations Chemistry in Cancer Research: A Vital Partnership in Cancer Drug Discovery and Development, New Orleans, USA, February 8-11th;

2008 - Teresa L. Serafim, Filipa S. Carvalho, M.P.M. Marques, Jorge Garrido, Nuno Milhazes, Fernanda Borges, Fernanda Roleira, Elisiário Tavares da Silva, Jon Holy, Paulo J. Oliveira. Biological Activity of Molecules Based on Phenolic Acids on Breast Cancer Cells. Meeting of Portuguese Society of Biochemistry, Azores, Portugal, October 22th-25th;

2008 – Teresa L. Serafim, Filipa S. Carvalho, M.P.M. Marques, Jorge Garrido, Nuno Milhazes, Fernanda Borges, Fernanda Roleira, Elisiário Tavares da Silva, Jon Holy, Paulo J. Oliveira. Antiproliferative Activity of Phenolic Acids on Breast Cancers cell models and Direct Effects on Mitochondria. International Courses on Toxicology, "Metabolic Toxicology: From Pathway to Organism", University

of Coimbra, Portugal, April 9-11th;

2008 - Teresa L. Serafim, Filipa S. Carvalho, M.P.M. Marques, Jorge Garrido, Nuno Milhazes, Fernanda Borges, Fernanda Roleira, Elisiário Tavares da Silva, Jon Holy, Paulo J. Oliveira. Antiproliferative Activity of Ferulic and Caffeic Acid Derivatives on Tumour cell Lines – Structure-Function Relationships and Direct Effects on Mitochondria. APOPTOSIS WORLD 2008, From Mechanisms to Applications, European Center, Luxembourg, January 23-26th.

INDEX

FIGURES INDEX

FIGURES INDEX

ABBREVIATIONS USED

3BrPA: 3-bromopyruvate
2DG: 2-deoxy-D-glucose
α-TOS: α-Tocopheryl succinate
Δψm: Mitochondrial Transmembrane Electric Potential

A

ADP: Adenosine Diphosphate
ADP/O: Ratio of the amount of ADP phosphorylated per oxygen consumed
AIF: Apoptosis Inducing Factor
Apaf-1: Apoptosis activating factor-1
APL: Acute promyelocytic leukemia
AMP: Adenosine Monophosphate
AMPK: 5' adenosine monophosphate-activated protein kinase
ANT: Adenine Nucleotide Translocase
APC: Allophycocyanin
As2O3: Arsenic trioxide
ATP: Adenosine Triphosphate
ATP5O: ATPase subunit-Fo
ATRA: All-trans retinoic acid

B

BIPL: Biomedical Image Processing Laboratory
BOP: (benzotriazol-1-yloxy) tris(dimethylamino)phosphonium hexafluorophosphate
bp: base pair
BrDU: Bromodeoxyuridine
BSA: Bovine Serum Albumin

C

CA: Caffeic Acid
Ca^{2+}: Calcium
CAPE: Caffeic acid phenyl ester
CD24: cell adhesion glycoprotein associated with cell differentiation
CD44: cell surface glycoprotein associated with cell migration
$CD44^{high}/CD24^{low}$: cell surface feature present essentially in stem-like cells
$CD44^{low}/CD24^{high}$: cell surface feature preferentially expressed by well differentiated cells
CD95/Fas: cell surface death receptor that lead to apoptosis
cDNA: complementary DNA
CDK: Cyclin-dependent kinases
CIII-Core2: Complex III, subunit Core2
CKI: Cyclin-dependent kinase inhibitor
CypD: Cyclophilin-D
Cytc*:* Cytochrome *c*
CM-H2DCFDA: Chloromethyl derivative of dichlorodihydrofluorescein diacetate, Redoxsensitive probe
CO_2: Carbon dioxide
COX: Cytochrome c oxidase
COX I: Cytochrome c oxidase, subunit I
COX II: Cytochrome c oxidase, subunit II
COX III: Cytochrome c oxidase, subunit III
COX IV: Cytochrome c oxidase subunit IV
CsA: Cyclosporin A
CV-alpha: ATPase, subunit F1α

D

DCA: Dichloroacetate
DECA: Dequalinium chloride
DISC: Death-Inducing Signaling Complex
D-loop: Displacement loop region
DLC: Delocalized lipophilic cations
DMEM: Dulbecco's modified Eagle's medium
DMSO: Dimethyl Sulfoxide
DNA: Deoxyribonucleic Acid
DTT: Dithiothreitol
Drp-1: Dynamin-related protein 1

E

E-310: Propyl gallate
E-311: Octyl gallate
ECF: Eosinophil chemotactic factor
EDTA: Ethylenediaminetetraacetic Acid
EDKC: N,N'-bis(2-ethyl-1,3-

dioxylene)kryptocyanine
EGCG: Epigallocatechin-3-gallate
EGTA: Ethylene Glycol Tetraacetic Acid
EI-MS: electron impact-mass spectrometry
ERK: Extracellular Signal-Regulated Kinase
ETC: Electron transport chain

F

FA: Ferulic acid
FeS: iron–sulfur cluster
FBS: Fetal Bovine Serum
FC3: Fetal Clone III
FCCP: Carbonylcyanide p-trifluoromethoxyphenylhydrazone
FH: fumarate hydratase
FITC: Fluorescein Isothiocyanate
FL1: flow cytometer green fluorescence detector
FL2: flow cytometer orange fluorescence detector
FL3: flow cytometer red fluorescence detector

G

GADD45: Growth Arrest DNA Damage 45
GAPDH: glyceraldehyde-3-phosphate
GLUT: glucose transporter
GLUT-1: glucose transporters 1
GSAO: 4-(N-(S-glutathionylacetyl) amino) phenylarsenoxide
GSH: Glutathione
GSK3β: Glycogen synthase kinase 3β

H

H2AXγ: DNA damage response pathway
H_2O: Water
HC: Hexyl Caffeate
HCA: Caffeoylhexylamide
HCl: Hydrochloric acid
HEPES: 4-(2-hydroxyethyl)-1-piperazineethanesulfonic acid
HF: Hexyl ferulate
HFA: Feruloylhexylamide
HIF-1: Hypoxia inducible factor
HK: Hexokinase
HK II: Hexokinase II
HSP90: Heat shock protein 90kDa

I

IAP: Inhibitor of Apoptosis Protein
IgG: Immunoglobulin G
IgG-AP: Immunoglobulin G-alkaline phosphatase

J

JNK: c-Jun N-terminal Kinase

K

kDa: kilodalton

L

LDH-A: Lactic Acid Dehydrogenase A

M

MAPKs: Mitogen-Activated Protein (MAP) Kinases
MDR: Multi-Drug Resistance
MFN1: Mitofusin 1
Mfn2: Mitofusin 2
$MgCl_2$: Magnesium chloride
MIM: Mitochondrial inner membrane
MnSOD: Manganese superoxide dismutase
MOM: Mitochondrial outer membrane
MPT: Mitochondrial permeability transition
mRNA: messenger RNA
MRP: Multiple drug resistance protein
mtDNA: Mitochondrial DNA
mTOR: Mammalian Target Of Rapamycin
MTs: Mitochondrial targeting sequences

N

NAC1: N-acetyl-L-cysteine
NADH: reduced form of Nicotinamide adenine dinucleotide
NADPH: reduced form of Nicotinamide adenine dinucleotide phosphate
NaOH: Sodium hydroxide
ND1: mitochondrially encoded NADH dehydrogenase 1
ND5: mitochondrially encoded NADH

dehydrogenase 5
ND6: mitochondrially encoded NADH dehydrogenase 6
nDNA: nuclear DNA
NDUFB8: NADH dehydrogenase [ubiquinone] 1 beta subcomplex subunit 8
NF-kB: Nuclear Factor-KappaB
NMR: Nuclear magnetic resonance

O

Omi/HtrA2: Omi stress-regulated endoprotease/High temperature requirement protein A 2
Opa1: Optic atrophy 1
OSW-1: (3 beta, 16 beta, 17 alpha-trihydroxycholest-5-en-22-one 16-O-(2-O-4-methoxybenzoyl-beta-D-xylopyranosyl)- (1-->3)-(2-O-acetyl-alpha-L-arabinopyranoside)
OXPHOS: Oxidative phosphorylation

P

PARP: Poly(ADP-ribose) polymerase-1
PBR: Peripheral benzodiazepine receptor
PBS: Phosphate Buffered Saline
PBS-T: Phosphate Buffered Saline with 0.1% Tween
PCR: Polymerase chain reaction
PDH: Pyruvade dehydrogenase
PDK: Pyuvate dehydogenase kinase
PDK II: Pyuvate dehydogenase kinaseII
PEITC: β-Phenylethyl isothiocyanate
PGC1α: Peroxisome proliferator-activated receptor-γ co-activator 1α
PI3K: Phosphoinositide 3-kinase
PKB: Promoted by the protein kinase
PMSF: Phenylmethylsulfonyl fluoride
PMT: Photomultiplier
PPIase: Peptidyl-prolyl cis–trans isomerases
pRb: Retinoblastoma protein
PS: Phosphatidylserine
PTEN: Phosphatase and Tensin Homolog
PTK´s: Protein tyrosinase kinase
PUM1: homolog of Pumilio, Drosophila 1
PVDF: Polyvinylidene fluoride

Q

QIAshredder: homogenizes cell or tissue lysates to reduce viscosity

R

RCR: Respiratory control ratio
RH123: Rhodamine 123
RLT: buffer for lysis of cells and tissues before RNA isolation
RNA: Ribonucleic Acid
RNAse: Ribonuclease
rRNA: ribosomal RNA
ROS: Reactive Oxygen Species
RPLP0: Ribosomal protein, large, P0
RT: Reverse Transcription
RT-PCR: Real-time polymerase chain reaction

S

Samc/Diablo: Second mitochondria-derived activator
SANG: Sanguinarine
SDH: Succinate dehydrogenase
SDS: Sodium Dodecyl Sulfate
SEM: Standard error of the mean
SIRT1: NAD-dependent deacetylase sirtuin-1
SRB: Sulforhodamine B
STAT-3: Signal transducer and activator of transcription 3

T

TAE: Tris/Acetate/EDTA
TBST: Tris-Buffered Saline Tween-20
TCA: tricarboxylic acid cycle
TIGAR: *T*P53-*i*nduced *g*lycolysis and *a*poptosis *r*egulator
TMRM: Tetramethyl Rhodamine Methyl Ester
TNF α: Tumor necrosis factor-α
TNFR1: Tumor Necrosis Factor Receptor 1
TBP: TATA-box binding protein
TPP+: Tetraphenylphosphonium cation
TRAIL: TNF Related Apoptosis

Inducing Ligand
Tsp-1: Thrombospondin
TSPO: Translocator protein (18kDa)

U

UQCRC2: Ubiquinol-cytochrome c reductase core protein 2

UV: Ultraviolet

V

VDAC: Voltage-Dependent Anion Channel

Abstract

Abstract

Cancer is the Disease of the past decades but also will be the Disease of our future, due to the progressive increase in the numbers of cancer-related deaths. Associated with the still often imperfect methods of measuring incidence and precocious detection, many of the current therapeutics are not selective leading to several and harmful side effects. The best approach for cancer treatment passes through the re-activation of apoptotic pathways in tumor cells, sparing normal cells. Indirectly activation of apoptosis was shown not to be enough in many situations, since resistant cancer cells frequently have the capacity to neutralize the death signaling that converge into mitochondria, the powerhouses and often death executioners of cells. Therefore, mitochondria, due to their unique structural and functional features, appeared as a target of several compounds that are aimed to sensitize tumors to apoptotic death. With this objective, a group of compounds with specific structural features and activity was developed, the so-called mitocans. The overall goal of the present work is to characterize groups of mitocans that would lead cancer cells to death by opening mitochondria, which, not unlike Pandora's Box, would open up and spread destruction into a desired target.

The first step in the work led us to detect selected mitochondrial alterations in a panel of human breast cancer cells, comparing them to non-tumor cells. This is a critical step since it has already been described that tumor behavior is dependent on mitochondrial physiology, which can be modulated by alterations in oxidative phosphorylation and by mitochondrial DNA alterations.

The next step in the work was the screening and characterization of the mechanism of action of possible mitocans phenolic acids, triterpenoids, berberine and sanguinarine. One of the strategies that is commonly used for anti-cancer drug delivery uses the fact that some cancer cells have a higher mitochondrial transmembrane potential ($\Delta\psi m$), the electrochemical gradient built across the inner membrane by the respiratory chain. In this context, some compounds used have positively-charged moieties, which is of the utmost importance for effectively targeting mitochondria, negatively charged in their inside. Also, the molecules used are phytochemical-based compounds. This class of compounds has been proposed as a promising and pragmatic

clinical approach: besides reducing cancer risk, these molecules constitute a wide family of natural compounds with a considerable range of important properties such as safety, low toxicity, and general acceptance as dietary supplements. The biological activity of the novel compounds in different biological models, including cell lines in monolayer, and isolated mitochondrial fractions were evaluated. Cells were grown in glucose media or in glucose-free galactose/glutamine media, since in the later case energy is produced only by oxidative phosphorylation and hence direct mitochondrial toxicity is more easily detected.

As for the first specific aim, we have characterized MCF-7 (adenocarcinoma; ER, PR and Herb2 positive), MDA-MB-231 (adenocarcinoma, ER, PR and Herb2 negative) and HS 578T (carcinosarcoma, ER, PR and Herb2 negative) breast cancer cell lines and compared primarily with non-tumor BJ fibroblasts. We have determined that differences between cells exist in what concerns to the $\Delta\psi m$, composition in proteins of the respiratory chain, intrinsic levels of pro- and anti-apoptotic proteins, among other differences. Also, the transition from a predominalty glycolytic to oxidative phosphorylation (OXPHOS) metabolism through manipulation of the media composition resulted in distinct alterations in cell behavior. Finally, the effects of classic mitochondrial poisons were different from cell to cell, demonstrating that distinct mitochondrial alterations may impact the way breast cancer cells react to mitocondrial-directed agents.

As for the screening of possible new mitocans, we initiated the study by investigating derivatives of the phenolic acids caffeic and ferulic acids. We observed that the increase of lipophylicity of these derivatives increase their toxicity towards breast cancer cells, especially against the estrogen-positive MCF-7 cell line; however, these compounds do not seem to have direct mitochondrial effects. Contrarily, lupane triterpenoids derivatives were shown to have direct effects on mitochondria from breast cancer cells, resulting in inhibition of cell proliferation and arresting the cell cycle.

As for the two benzophenanthrine alkaloids investigated, berberine possesses cytotoxicactivity against melanoma cells with several distinct mechanism, one of them being mitochondrial accumulation and toxicity at lower concentrations. Higher berberine concentrations accumulate in the nuclei and interfere with DNA synthesis. By its turn, sanguinarine cause apoptosis of melanoma cells at low micramolar

concentrations, involving p53 activation. Despite the fact that sanguinarine was primarily accumulated in the nuclei, mitochondrial depolarization was observed in a sub-set of cells that suffered sanguinarine-induced nuclear DNA damage. Caspase 3 and 9 activation were also observed after sanguinarine addition.

In conclusion, the present thesis proposes some molecules that act as a starting point for further refinement and development as anti-cancer agents, whose mechanism of action involves mitochondrially-mediated effects.

Keywords: Cancer, mitochondria, mitocans, phenolic compounds, triterpenoids, benzophenanthrine alkaloids, metabolism and chemotherapy.

Resumo

O Cancro é a Doença das decadas passadas mas também a Doenca das futuras, devido ao aumento progressivo de mortes associadas a esta doença. Os métodos de medição de incidência e detecção precoce são imperfeitos e estão de certa forma relacionados com a falta de selectividade das terapias, levando a efeitos secundários diversos e maléficos.

A melhor forma de abordar o cancro é através da re-activação das vias apoptóticas nas células cancerígenas, no entanto não interferindo com as células normais. A activação indirecta da apoptose já foi demonstrada de não ser eficaz em várias situações, onde células cancerígenas resistentes demonstraram ter uma elevada capacidade de neutralizar os sinais de morte que convergem para a mitocôndria, fonte de energia e por vezes executora de morte das células.

Portanto, com as suas características únicas estruturais e funcionais, as mitocôndrias aparecem como alvo preferencial de vários compostos para sensibilizar as células cancerígenas para morte.

Tendo este objectivo em mente, grupos de compostos foram desenvolvidos com actividades e características estruturais especificas, os designados *mitocans*. O objectivo principal do presente trabalho é a caracterização de grupos de *mitocans* que poderão levar as células cancerígenas à morte através da abertura da mitocôndria, não diferente do efeito da Caixa de Pandora, num determinado alvo, abriria e espalharia a destruição.

A primeira parte do trabalho levou-nos a detectar alterações mitocondriais num painel de linhas celulares de cancro da mama, comparando-as com células não-tumorais. Esta parte representa um momento importante, uma vez que já foi descrito que o comportamento tumoral está associado com a fisiologia mitocondrial, as quais podem ser moduladas por alterações na fosforilação oxidativa, bem como no DNA mitocondrial.

O passo seguinte do presente trabalho foi testar e caracterizar os mecanismos de acção de possíveis *mitocans* ácidos fenólicos, triterpenoides, berberina e sanguinarina. Uma das estratégias usadas para a introdução de fármacos anti-cancerígenos nas mitocôndrias é o facto de alguns tipos de células tumorais apresentarem elevado potencial transmembranar mitocondrial ($\Delta\psi m$), gradiente electroquímico gerado através

da membrana interna pela cadeia respiratória.

Neste contexto, alguns dos compostos usados apresentam carga positiva, característica de extrema importância para alvejar a mitocôndria com eficiência, uma vez que esta encontra-se carregada negativamente no seu interior. Também, as moléculas usadas são baseadas em compostos fitoquímicos. Esta classe de compostos fora proposta como uma abordagem clinica pragmática e promissora: para além de reduzirem a incidência do cancro, estas moleculas constituem uma vasta família de compostos naturais, com consideráveis e importantes propriedades tais como segurança, baixa toxicidade, e como suplementos alimentares.

A actividade biológica dos novos compostos foi avaliada nos diferentes modelos biológicos, incluindo linhas celulares em monocamada e fracções mitocondriais isoladas. Ainda, as células foram crescidas em meios contendo glucose ou contendo galactose e glutamina (sem glucose), estando no último caso o ATP a ser produzido maioritariamente pela fosforilação oxidativa e onde um efeito toxico directo ao nível mitocondrial será mais facilmente observavel.

No contexto do primeiro objectivo especifico, caracterizamos as linhas celulares de cancro da mama MCF-7 (adenocarcinoma; ER, PR e Herb2 positiva), MDA-MB-231 (adenocarcinoma, ER, PR e Herb2 negativa) e HS 578T (carcinosarcoma, ER, PR e Herb2 negativa) comparando-as com fibroblastos BJ, não-tumorais. Os resultados mostraram que existem diferenças entre as linhas celulares estudadas no que respeita ao $\Delta\psi m$, composição de proteínas da cadeia respiratória, entre outras alteracoes. A transição de metabolismo predominantemente glicolítico para fosforilação oxidativa (OXPHOS) através da manipulação da composição do meio de cultura resultou em alterações significativas no comportamento cellular. Finalmente, os efeitos de perturbadores clássicos mitocondriais foram diferentes de célula para célula, verificando-se que alterações distintas mitocondriais poderão influenciar o modo como reagirão as células cancerígenas de mama a agentes directos mitocodriais.

Na procura de possíveis mitocans, iniciámos o nosso estudo investigando derivados de ácidos fenólicos, nomeadamente dos ácidos cafeico e ferúlico. Observámos que com o aumento da lipofilicidade, os seus derivados aumentaram a sua toxicidade nas células cancerígenas de mama, especialmente nas células MCF-7 estrogénio-positivas; no entanto estes compostos não pareceram ter efeito direto na mitocôndria.

Contrariamente, os derivados de lupanos triterpenoides demonstraram ter efeitos diretos nas mitocôndrias das células cancerígenas de mama, resultando na inibição da proliferação e bloqueio do ciclo celular.

Quanto aos dois alcalóides da família das benzofenantrinas, a berberina possui uma actividade citotóxica nas células de melanoma através de diferentes mecanismos, sendo um deles de ser tóxica a baixas concentrações após de se acumular nas mitocôndrias. A elevadas concentrações, a berberina acumula-se no núcleo e interefere com a síntese de DNA. Por sua vez, a sanguinarina promove a apoptose das células de melanoma em concentrações na ordem dos micramolar, envolvendo a activação da p53. Apesar da sanguinarina ser acumulada primeiramente no núcleo, verificou-se despolarização mitocondrial num grupo de células que sofreram danos no DNA nuclear induzidos pela sanguinarina. Foram igualmente observadas a activação das caspases-3 e 9 após adição de sanguinarina.

Concluindo, a presente tese propõe algumas moléculas que podem servir como modelos para futuros refinamentos e desenvolvimentos de agentes anti-cancerígenos, cujos mecanismos de acção envolvem efeitos directos na mitocôndria cardiaca.

Palavras-chave: Cancro, mitocôndria, mitocans compostos fenólicos, triterpenoids, alcalóides benzofenantrinas, metablismo e quimioterapia.

I – Introduction

1. Introduction

1.1. Cancer

From the middle nineteenth until the first half of the twentieth century, cancer was seen as a normal cell population undergoing uncontrolled growth. The years passed and researchers collected more and more evidence on this subject and concluded that these particular cells could suffer alterations on their genome sequences through several distinct mechanisms, altering the structure and hence the way information is generated from the genome. Such alterations interfere with cellular growth programs and consequently lead to the appearance of large population of cells that no longer obey the rules governing normal tissue construction and maintenance (Weinberg, R., 2007). Cells appear to be motivated by only one objective: making more copies of themselves. The dysfunctional physiology observed in cancer is mainly a disorder of the safeguards that are normally responsible for determining when and where cells throughout the body will divide. This disorder results in the appearance of cancer in the human body, which sometimes requires years if not decades to develop in the adult (Siemann, D., 2010).

Early in this century, the six Hallmarks of Cancer were proposed as a signature of the disease which would help in future diagnosis, prognosis and treatment: limitless replicative potential, sustained angiogenesis, evasion of apoptosis, self-sufficiency in growth signals, insensitivity to antigrowth signals, tissue invasion and metastasis (Hanahan and Weinberg, 2000). Recently Hanahan and Weinberg (2011) reformuled their six hallmark signatures adding the reprogramming of energy metabolism and evading immune destruction.

Heredity and environment have been pointed out as the two obvious contributing factors for cancer incidence. World human populations can carry characteristic "susceptibility alleles" at different frequencies; however, the environment in which these people live may contribute to the modulation of cancer appearance rates. Cancer is revealed to be more common among people of certain cultures than in others (Aggarwal and Shishodia, 2006). For example, the most common cancers in Western countries are lung, colon, prostate and breast, while in India, head and neck and cervix cancers are prevalent. Interestingly, stomach cancer predominates in Japan (Aggarwal and Shishodia, 2006). Lifestyle, such as dietary choices and reproductive habits, but also the quality of water and air that are consumed, are environment factors that can

influence the disease incidence (Weinberg, R., 2007). However, diet seems to be one important modulator of cancer, with interestingly some natural compounds derived from plants acting as potential carcinogenic. We would think that this kind of molecules would be mostly beneficial and some would even act as potential chemotherapeutics, but actually the concentration achieved in the body (i.e. amount consumed), can determine the final outcome. Plants evolved thousands of chemicals in order to defend themselves from predation by animals. Consequently, a few are expected to have some reactive impact in our gastrointestinal tract.

Cancer can virtually originate from all cell types of the body, but the most common human cancers are of epithelial origin –carcinomas –, which are the cells that are in more close contact with different environmental agents. Carcinomas can be either adenocarcinomas, arising from specialized cells that secrete substances into the ducts or cavities, or squamous cell carcinomas, arising from epithelia that form protective cell layers. However, cancer can be also originated from other tissues, namely mesenchymal, hematopoietic and neuroectodermal (Weinberg, R., 2007).

The capacity to originate different types of cells is due to the presence of pluripotent cells derived from mammalian embryos. After their differentiation, embryos have their development potential progressively restricted. However, stem cells are found in the middle of differentiated cells presenting *in vitro* similar characteristics to pluripotent progenitors including the ability to self-renew and propagate indefinitely, although presenting differences in the transcriptional regulatory network (Ng and Surani, 2011). The deregulation of these pathways can be one of the mechanisms for carcinogenesis initiation (Liu et al, 2011), being possible to find differentiated cells and cancer stem-like cells in the same population. Several of the alterations allow cancer cells to efflux drugs, repair DNA-induced radiation damage and evade immunological recognition (Berridge et al, 2010).

The self-renewal capacity leads to widespread consensus that the vast majority of human tumors are monoclonal, *i.e.* a population of cells descended from single progenitor cells within a tumor, however, with the continual acquisition of new mutant alleles leads to heterogenic population therefore masking the true monoclonal origin (Shulman et al, 2006; Cabibi et al, 2006).

Cells are not categorized only as normal or highly malignant; in between, there

are several tissues in intermediate states. Normal cells have controlled programs for the homeostasis of diverse tissues, contributing to the survival of the organism. Anything that would be different from this goal can be considered anomalous. The great majority of primary tumors arising in humans is benign and is harmless to their hosts. Tumors, in general, grow faster than their normal counterparts; however, there are malignant cells that do not have necessarily a faster growth and cell cycle when compared with many normal cells in the body (Weinberg et al, 2010). Nevertheless, cancer cells have a highly disordered pattern of proliferation with little or no growth regulation, continuing to undergo cell cycles and thus continuing to proliferate under conditions that would force normal cells to halt proliferation. We can observe this effect in cells that are hyperplastic (Fearon, E., 1997). These cells have uncontrolled growth rates and they result into an excessive number of cells. But when a different type of cell is encountered in sites different from their origin displacing a layer of normal cells, this phenomenon is called metaplasia (Stappenbeck and Miyoshi, 2009). The degree of abnormality increases due to cytological alterations, i.e., the appearance of individual cells is no longer normal. Predisposing genomic lesions in various genes of these dysplastic cells confers a proliferative advantage over normal counterparts. At this point, a transitional state between normal and malignant cells can be considered. A further step onto malignancy is the invasion of underlying tissues. Tumors that start to form new types of tissue, whether they are benign or malignant, are called neoplasms. The cancer cells invade into surrounding tissue, colonize and populate the area in case a favorable microenvironment is found (Fearon, E., 1997). Cellular transformation is the result of oncogenic lesions jointly with inhibition of tumor suppressors, activated by genetic and epigenetic mutations. Many oncogenes will act by mimicking normal growth signaling in cancer cells, allowing them to escape from quiescent state (Hanahan and Weinberg, 2000).

The progressive growth of a tumor greatly increases the demand for oxygen and nutrients, resulting in the inability of tumor cells that are distant from blood vessels to be supplied. Hypoxic regions are developed within the tumor, which can also promote intermittent reactive oxygen species (ROS) bursts. It has been proposed that on of the main mechanisms for the metabolic remodeling seen in cancer cells is an adaptation to the novel enviroment, which is limited oxygen (Gatenby and Gillies, 2007). Cancer cells

achieved a way to adapt from aerobic to anaerobic glycolysis to survive in this new microenvironment, upregulating transporter proteins that extrude lactic acid from the cell into the surrounding extra-cellular area (Gatenby and Gawlinski, 2003). The molecular mechanism behind this switch is not completely understood, but aspects such as the availability of oxygen and nutrients, and tumor supressors that influence signaling via hypoxia-inducible factor 1 (HIF-1), phosphoinositide 3-kinase (PI3K), and mammalian target of rapamycin (mTOR) pathways, can be involved. Moreover, malignant cells will survive under hypoxic conditions due to the modulation of oncogenic poteins, such as MYC, p53, STAT-3 and RAS, that will have a crucial role in modulating the expression of genes of mitochondrial proteins and consequently their function in cancer cells (Gogvadze et al, 2010; Ralph et al, 2010). c-Myc, ras or scr can cause an elevated expression of glucose transporters (GLUT), which are associated with tumor invasiveness and metastasis, while the overexpression of lactate dehydrogenase A (LDH-A) is attributed to c-Myc only (Chen et al., 2010). Tumors in which oncogene Myc is involved are particularly sensitive to the amount of glutamine and therefore, Myc protein appears to be regulated by genes associated with glutamine metabolism (Heiden et al, 2009).

Furthermore, succinate, which accumulates due to tricarboxylic acid (TCA) cycle impairment, acts as a signaling molecule and triggers the activation of HIF-1 (Selak et al., 2005). HIF-1 will promote upregulation of all enzymes involved in glycolysis, modulating the expression of aldolase, phosphoglycerate kinase, phosphofructokinase, pyruvate kinase and LDH-A, at the same inhibiting pyruvate conversion to acetyl-CoA and mitochondria biogenesis. Due to the lower energy efficacy of aerobic glycolysis, glucose uptake verified in tumors is higher than in normal tissues (Vaupel et al, 1989).

Curiously, when new vessels are formed in a later state and oxygen is avaliable in higher amounts, cancer cells still prefer to use aerobic glycolysis, which not only provides a survival advantage over non-transformed cells but also ensures the persistence of the most successful cancer cells (Gatenby and Gillies, 2004). This phenomenon is widely explored in cancer biology and was termed the Warburg effect, from Otto Warburg, who initially identified that cancer cells would rather use glycolysis than oxidative phosphorylation to obtain most of their energy (Warburg et al, 1926). Recently, Berridge et al. (2010) has discussed the fact that not all cancer cells

preferentially use glycolysis, and that this switch may be related to specific cells or tissue types, with this metabolic flexibility being important for certain tumors to grow and metastasize. Tumor microenvironment can also dictate the type of metabolic pathway to use in cells, which, in turn, give the ability the tumor for self-renewal.

Increase motility facilitates the movement of the cells through layers of endothelial cells surrounding blood vessels and allows cells to somehow secret into the vascular system destabilizing factors and accessing the circulation. Cancer is thought to be a homogeneous cell population that adapt to a new environment, but actually cancer cells grow in a microenvironment of their own (Berridge et al, 2010), surrounded by an extracellular matrix, blood vessels, immune cells, and other supporting structures. Both epithelial malignancy transformation and host stromal activation can occur simultaneously, with consequent inducing of angiogenesis, fibroblast activation and proliferation and recruitment of inflammatory mediators (Tlsty and Hein, 2001) (Fig.1).

After a primary tumor is settled, cancer cells seed new tumor colonies at distant sites in the body through the process of metastasis. Besides uncontrolled cell proliferation and aberrant cell cycle checkpoints, cancer cells also lose contact-inhibited growth regulation. Cells alter their adhesion molecules and rearrange their extracellular matrix allowing them to become more motile. These cells invade vessels of circulatory blood and lymph systems traveling into a distant organ to establish a secondary tumor. It is generally accepted that cells with metastasis ability are those with invasive and migratory capacity (Hughes et al, 2008). Metastasis from malignant tumors is responsible for 90% of all deaths. Prostate tumor metastases are found in bones, while colon carcinomas metastasize to the liver. Breast cancer spreads into diverse body tissues, such as the brain, liver, bones and lungs (Weinberg, R., 2007) (Fig.1).

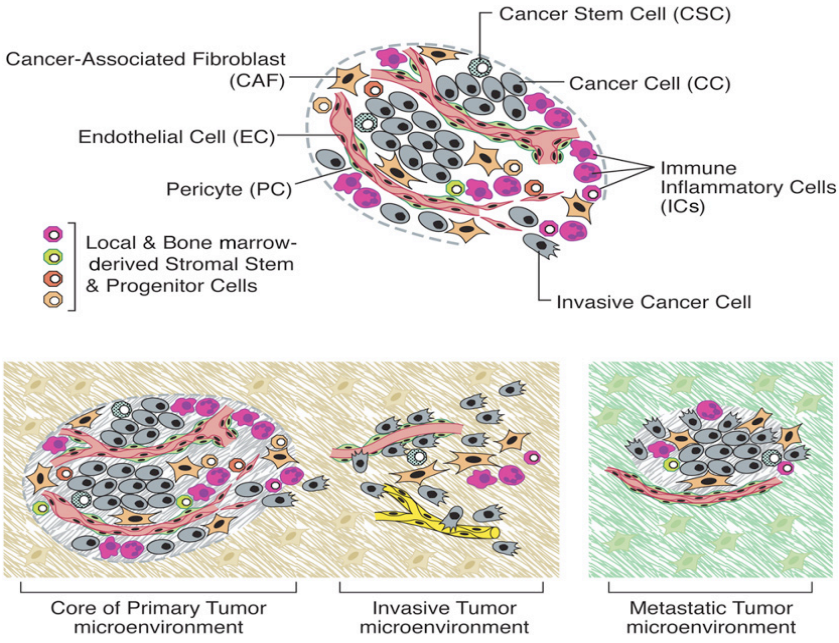

Fig.1 - The tumor microenvironment components (upper); the different types of tumor microenvironment (lower) (adapted from Hanahan and Weinberg, 2011).

From cancer initiation to cancer development and settlement in sites distant from the origin, all leads researchers to a wide spectrum of research. Investigators tend to focus in one determined area of cancer biology, from genetics to the microenvironment, in order to find new strategies to overcome this disease.

There are no doubts that mitochondria have certainly a role in cancer progression, most specifically in the metabolic shift that occurs, as their physiology is linked to energy metabolism (Hanahan and Weinberg, 2011). In the present thesis, we will approach cancer through a mitochondrial perspective, since these organelles can be involved in cancer initiation and development, besides the importance of their vital cellular functions, such as cell energy production and cell survival/death mechanisms. We believe that on of cancer Aquilles' heel can be mitochondria. Thus, in the following sub-chapter we will briefly address the current knowledge of mitochondrial complicity in cancer.

1.2. Mitochondria and Cancer

Otto Warburg observed in the 1920s that tumors have elevated levels of glucose consumption and lactate production in the presence of oxygen, a phenomenon that was termed aerobic glycolysis or Warburg effect. It was initially postulated that due to possible irreversible defects in mitochondrial respiration in cancer cells, including impaired oxidative phosphorylation (OXPHOS), increased glycolysis would be observed as a mechanism to counteract an ATP deficit (Weinberg et al, 2010). With more studies on the role and function of mitochondria, initiated with Mitchell and Moyle (1967), together with the discovery of genes that could promote cancer (oncogenes), or tumor suppressor genes and other advances in tumor biology, the study of the role of metabolism in cancer was lagging behind. In the 90s, a renaissance of mitochondrial biology studies was observed, with landmark papers where causative links between defects in the mitochondrial genome and human diseases were proposed (Wallace et al, 1988; Holt et al, 1988). Not without surprise, an increased interest in these organelles in cancer etiology was soon growing (Armstrong, 2007).

Today, there are controversial opinions about the importance of mitochondrial alterations in cancer, with most researchers defending that mitochondria are fully functional in most tumors, while a few argue that the decrease in mitochondria metabolism and respiratory rate are characteristic of tumor development (Weinberg et al, 2010). It was shown that although in a majority of cancer cells, glycolysis accounts for the most percentage of ATP generation (Lopez-Rio et al 2007), mitochondrial ATP production in other tumors is entirely similar to a non-tumor cell. Tumor cells that show mitochondrial dysfunction are those particularly aggressive and rapidly showing a rapid growth (Gogvadze et al, 2010). These tumors normally present mutations in succinate dehydrogenase (SDH) or fumarate hydratase (FH), enzymes from the tricarboxylic acid (TCA) cycle (Weinberg et al, 2010). This downregulation of some mitochondrial proteins, including OXPHOS components, in cancer cells seems to be achieved by distinct mechanisms (Feichtinger et al, 2010).

To better approach this subject, the different mitochondrial alterations found in cancer cells were divided in the following sections: a) mitochondrial structure and function, b) cell death and c) mitochondrial DNA.

1.2.1. Mitochondrial Structure and Function

With apparent origin from a proteobacterium that invaded a eukaryotic cell, the mitochondrion is surrounded by two membranes, the outer membrane (MOM) involving the entire contents of the organelle and the inner membrane (MIM), with a much bigger surface, forming a series of invaginations, known as cristae, and which is enriched in the distict lipid cardiolipin (Modica-Napolitano et al, 2007; Armstrong et al, 2007).

During normal physiology, the MOM is considered freely permeable to solutes and small metabolites (approximately 5 kDa.), due to the presence of the abundant protein voltage-dependent anion channel (VDAC), which allows the diffusion of such molecules (Karbowski and Youle, 2003). MOM rupture due to excessive osmotic influx can be lethal, not only by releasing caspase-activating molecules and caspase-independent death effectors as described below, but also by initiating metabolic failure of mitochondria. In contrast, the MIM is impermeable to the majority of ions, including protons. Membrane selectively is important for maintaining the proton gradient that is required for OXPHOS (Galluzzi et al, 2007). It is at the MIM that ATP synthesis occurs, through electron transfer coupled to proton ejection.

Mitochondria are essential organelles for cell survival and growth. All nucleated cells have mitochondria and these are the main source of cellular ATP produced via OXPHOS (Taylor and Turnbull, 2007). In normal conditions, energy generated by this pathway is used to produce ATP for cellular activity. Electrons are transferred from carbohydrates and fats via nicotinamide adenine dinucleotide (reduced form) to complex I (NADH dehydrogenase or NADH ubiquinone oxidoeductase), major entrance point of electrons in the respiratory chain, or from succinate to complex II (succinate dehydrogenate or succinate ubiquinone oxidoreductase), that directly connects the tricarboxylic acid cycle to the respiratory chain (Dudkina, 2010).

The electrons are used to reduce a lipophilic quinone, known as ubiquinone, to ubisemiquinone and then to ubiquinol. Electrons are transferred from ubiquinol to complex III (ubiquinone cytochrome c oxidoreductase), then electrons flow through cytochrome c (cytc) to complex IV (cytc oxidase, COX) where they reduce oxygen to water. Protons are pumped from the matrix to the inter-membrane space, coupled to electron transport at complexes I, III and IV, creating an electrochemical gradient,

composed from an electric component (Δψm), being negative inside, and from a pH component (ΔpH), alkaline in the matrix. Protons that are pumped to the intermembrane space can then re-flow through the ATP synthase proton channel, driving ADP phosphorylation to generate ATP (Chen et al, 2009) (Fig.2).

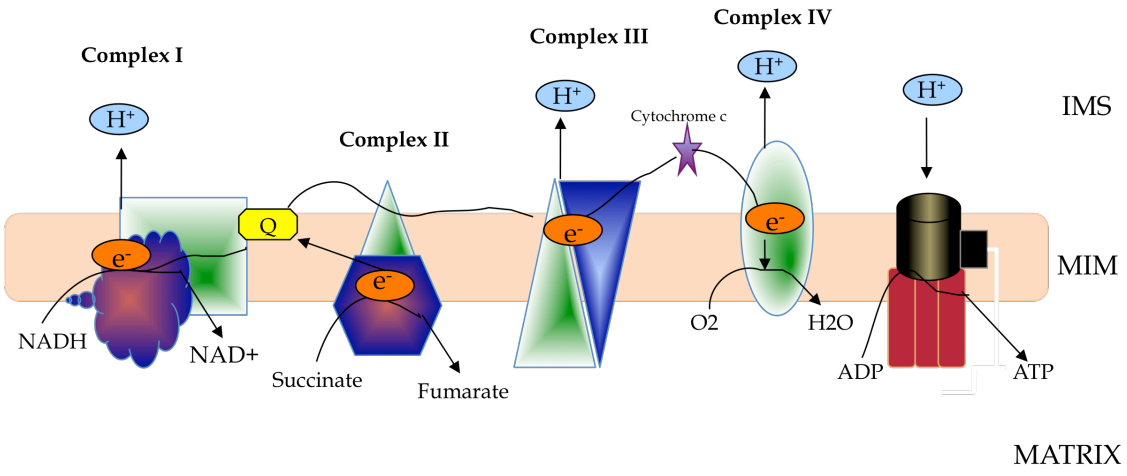

Fig.2 - Mitochondrial electron transfer system. The figure represents the different components of mitochondrial oxidative phosphorylation, including the respiratory chain.

The adenine nucleotide translocase (ANT) will facilitate the exchange of ATP with ADP from the cytosol. The electron transport chain (ETC) is coupled with the phosphorylation system, in order to maximize mitochondrial ATP production and minimize heat production (Brandon et al, 2006; Alirol et al, 2006). Leakage of electrons can occur from complexes I or III. These unpaired electron can be captured by molecular oxygen to form superoxide radical, which in turn can be converted to other forms of reactive oxygen species such as hydrogen peroxide or even react with nitric oxide forming other reactive species. In this context, it is important to note that mitochondrial activity is not restricted to ATP production for metabolic demands. Mitochondria are also the major source of reactive oxygen species (ROS), which are involved in the regulation of many physiological processes such as cancer cell proliferation, mitogenic signaling, cell survival, disruption of cell death signaling, epithelial-mesenchimal transition, metastasis and chemoresistance (Chen et al., 2010). At the same time, excessive ROS production can be harmful to the cell, affecting proteins, lipids and DNA. In fact, ROS can exceed the capacity of the cell antioxidant defenses, resulting in

"oxidative stress" and leading to cell injury or more dramatically to cell death (Trachootham et al, 2009). The cellular antioxidants that ensure that only nontoxic levels of ROS are produced include manganese superoxide dismutase (MnSOD) and mitochondrial GSH-dependent peroxidase. Besides these enzymes, p53 can also have a role in regulating ROS production, since when p53 is highly active, it may lead cells to apoptosis via ROS generation (Ralph et al, 2010). Interestingly, a lower than normal generation of mitochondrial ROS was recently correlated to the intrinsic chemotherapy resistance of cancer stem cells (Diehn et al, 2008). Furthermore, elevated mitochondrial oxidative stress, in conjugation with matrix calcium overload, can lead to increased MIM permeabilization, through a phenomenon called the mitochondrial permeability transition pore (MPT pore) (Gogvadze et al, 2008). The MPT pore is a dynamic molecular complex, whose precise structure is not yet well understood, due to the fact its constituents exist in multiple isoforms and functionally related proteins can substitute each other (see below). One possible regulatory component of the MPT pore is hexokinase (Pedersen et al., 2002). The first significant insight into a possible cause for aerobic glycolysis was the different expression of hexokinase, isoforms IV and II in normal and tumor hepatic cells, respectively. Hexokinase II (HK II) uses glucose that is transported into cells by GLUT transporters. HK II can bind the Voltage-dependent Anion Channel (VDAC) at the outer mitochondrial membrane. This interaction can be promoted by protein kinase B (PKB), also known as AKT kinase. Interestingly, AKT can inhibit at the same time this interaction via glycogen synthase kinase 3β (GSK3β), which mechanism can be activated by the common loss of function of phosphatase and tensin homolog (PTEN) (Dromparis et al, 2010). The binding of hexokinase II to VDAC stabilizes the MPT pore or other forms ou MOM permeabilization, which can block the induction of apoptosis, due to an antagonist effect to pro-apoptotic proteins action (Pedersen et al., 2002; Gatenby and Gillies, 2004).

During aerobic glycolysis, the ANT transports adenosine triphosphate (ATP) to the VDAC-HKII complex, supplying a phosphate group for the phosphorylation of glucose (Mathupala, 2006; Brandon et al, 2006). The chaperone Cyclophilin D (CyPD) is proposed to be bind to the ANT during MPT pore formationand opening. Cyclophilins constitute a group of peptidyl-prolyl cis–trans isomerases (PPIase) with highly conserved protein sequences, which are important for protein folding (Gothel and

Marahiel, 1999). It seems unlikely that the protective effect of CyPD on apoptotic cell death is due to binding of CyPD to ANT. Recently, CyPD was shown to be specifically up-regulated in human tumors of the breast, ovary, and uterus (Schubert and Grimm, 2004). The authors suggested that CyPD is a new type of apoptosis inhibitor, which is effective at alevel which is functionally different from that of the previously known inhibitors of the Bcl-2 family.

Overall, the coordination of these proteins results in a rapid and efficient production of glucose-6-phosphate that serves as precursor for glycolysis, but also for biosynthesis of key metabolites essential for cancer cell growth and proliferation, such as pentose phosphate pathway and mitochondrial tricarboxylic acid cycle (Mathupala et al, 2006). Thus, VDAC-bound hexokinase II can use mitochondrial ATP to rapidly phosphorylate glucose to glucose-6-phosphate and hence not act as a limiting step in the initial stages of glucose metabolism (Brandon et al, 2006). Elevated intracellular glucose concentrations lead the cell to redirect pyruvate (the final product of glycolysis) toward lipid synthesis, which is necessary for membrane assembly. Moreover, pyruvate can also be converted to lactate by lactate dehydogenase (LDH) in the cytosol and consequent cause extracellular acidification after extrusion, instead of what occurs in normal cells, where pyruvate is imported into mitochondria to enter the TCA cycle (Fulda et al, 2010b). In normal cells, the oxidation of pyruvate in the mitochondria leads to the production of NADH and succinate, which will fuel the electron transport chain (ETC) in two different sites (Alirol et al, 2006).

The tumor suppressor p53 was also shown to be involved in cell metabolism in addition to its regulation of cell proliferation (Dromparis et al, 2010). The p53 association with cancer metabolism is by the control of metabolic genes, whose regulation can alter the use of glucose (Heiden et al, 2009). The loss of p53 function contributes to increase of glycolysis via defective transactivation of TIGAR, an isoform of 6-phosphofructo-2-kinase, with ability to inhibit glycolysis and generation of ROS (Dromparis et al, 2010). Moreover, during the development of some types of tumors, especially during hypoxia, p53 response can be silenced or altered which impacts how cells respond to DNA damage. The p53 can accelerate the development of nearby capillary network and contribute to minimize hypoxia, through the consequent inactivation of thrombospondin (Tsp-1) a potently anti-angiogenic molecule. p53 has the ability to

temporarily arrest the cell cycle or activate the apoptotic program depending on the severity of cellular stress and efficiency of cells to repair defects that have been detected. While p53 circuitry monitors the internal well-being of the cell and permits cell proliferation and cell survival, when functioning properly, retinoblastoma protein (pRb) circuitry deals with the relations between the cell and the outside world. pRb together with p53 play important role in normal cell physiology, for example the control of cell cycle, and in cancer development (Heiden et al, 2009).

1.2.2. Cell Death

Malignant cells have several metabolic modifications, together with the ability to evade cell death. Next, we will review the different mechanisms of cell death and how are they altered in cancer cells.

1.2.2.1. Apoptosis

Apoptosis is an evolutionarily conserved and genetically regulated process of critical importance for embryonic development and maintenance of tissue homeostasis in the adult organism (Viktorsson et al., 2005).

A possible consequence of the glycolytic shift in tumor is their resistance to apoptotic cell death. The lower susceptibility to apoptosis includes a decreased ability of tumor mitochondria to undergo MOM permeabilization, which can impede the therapeutic efficacy of anticancer drugs.

Apoptosis develops in different stages: 1) an initiation phase, which depends on the nature of the lethal signal; 2) a decision phase, characterized by equilibrium between pro- and anti-apoptotic molecules levels, which is decisive for cell destiny; 3) and a common degradation phase, when the cell ceases its function (Constantini et al, 2000). A typical phenotype consists in a progressive shrinkage of cells and formation of apoptotic bodies, as well as nuclear (chromatin condensation and nuclear fragmentation) and plasma membrane (phosphatidylserine (PS) exposure) alterations. PS exposure functions as a signal for macrophages, preceding the clearance of apoptotic cell, avoiding inflammation (Fadok et al, 2000).

Apoptosis can occur through several pathways, but two of them are more

described: the extrinsic pathway, consisting in the regulation of death receptors located on the cell surface, which transducer death signals from the extra-cellular media to the inside. The second pathway is termed the intrinsic pathway, where death signals originate from inside the cells, with a special emphasis on mitochondria (Gogvadze et al, 2008), where bcl-2 family members have an important role in initiating the programmed cell death (Galluzzi et al, 2007). The pro-apoptotic BH3-only family members (such as Bid, Bad, Bim, Noxa and Puma) activate Bax and/or Bak. The balance between anti-apoptotic (Bcl-2, Bcl-xl, Bcl-w and Mcl-1) and pro-apoptotic protein levels is crucial for the cell fate. Bax can form pores in mitochondrial membrane in response to apoptotic stimuli and cytochrome c is released activating the caspase cascade, while Blc-2 and counterparts can antagonize cytochrome c release. Abnormalities in the expression of Bcl-2 and caspase family members have been documented in many cancers (Vinothini et al, 2010).

In the extrinsic pathway (Fig.3), a cell death signal is transduced within cells, either by the activation of the receptor-mediated process (absence of the corresponding ligands), or by the ligand-induced activation of receptors such as TNFR1, Fas, CD95/Fas (the receptor of CD95L/FasL) and of the tumor necrosis factor-α (TNF-α) receptor -1 (Orrenius, S., 2007). In some cases, activated TNF receptors have been demonstrated to promote a different signalosome through NF-kB activation, leading to a release of inflammatory cytokines and to anti-apoptosis responses. TNF can also target angiogenesis, inducing tumor necrosis, overall having a antiproliferative activity. If coupled to pro-apoptotic processes, death-inducible signaling complexes (DISC) are formed and cause activation of pro-caspase-8 (Nguyen and Hussain, 2007).

It has been demonstrated that caspase-8 can activate pro-caspase-3, which then cleaves target proteins (Galluzzi, et al, 2007). Also, in several cell types, caspase-8 first cleaves Bid (a Bcl-2 family protein), which in turn, is directed to mitochondria or induces translocation, oligomerization and insertion of Bax and/or Bak, another Bcl-2 family member.

As described, mitochondrial permeabilization then follows, which leads to the release of several proteins from the mitochondrial inter-membrane space, including cytochrome c, Omi/HtrA2 (Omi stress-regulated endoprotease/High temperature requirement protein A 2) and Smac/Diablo (second mitochondria-derived activator),

which indirectly favors the caspase cascade by antagonizing the activity of the inhibitor of apoptosis proteins (IAPs), an endogenous caspase inhibitor, as well as caspase-independent death effectors such as the apoptosis-inducing factor (AIF) and endonuclease G. A cytosolic complex is formed in the presence of dATP, comprising cytochrome c, the apoptosis activating factor-1 (Apaf-1) and pro- caspase-9, resulting in caspase-9 activation, which triggers caspase-3 activity and signal amplification (Orrenius, S., 2007). AIF, endonuclease G and HtrA2/Omi are then directly translocated to the nucleus, triggering chromatin condensation and the appearance of high-molecular weight chromatin fragments (Don and Hogg, 2004).

On the other hand, the intrinsic pathway (Fig.3) can also be characterized by the initial role of subcellular compartments such as the nucleus, lysosome, the endoplasmic reticulum, or cytosol, originating death-promoting stimuli that will act (directly or indirectly) on mitochondria. Permeabilization of the mitochondrial outer membrane (MOM) can occur, leading, as described above, to the release of intermembrane space proteins, including caspase activators such as cytochrome c.

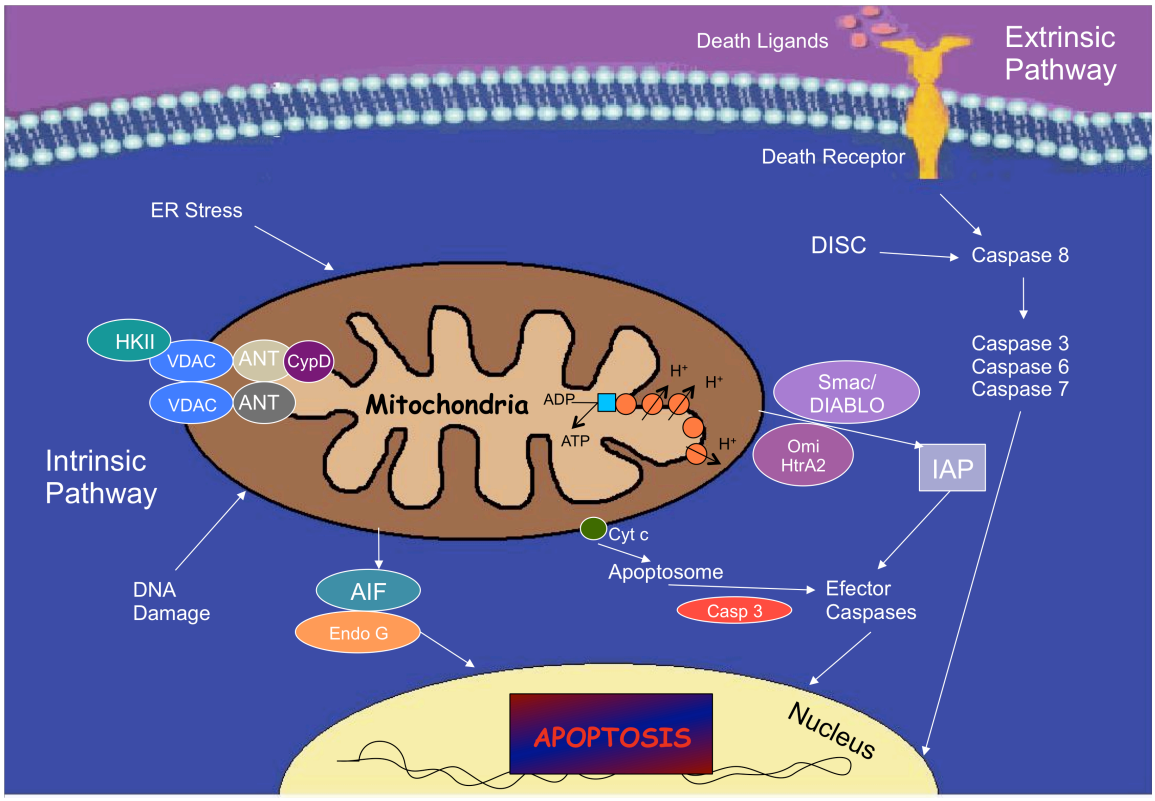

Fig.3 - Extrinsic and Intrinsic pathways of Apoptosis. The extrinsic pathway is mediated by death receptors, while the intrinsic pathway is mostly mediated by mitochondria.

Bcl-2 and Bcl-xL are capable of rescuing cells from death, preventing the permeabilization of MOM, for example by sequestering activated Bax and Bak, and inhibiting the release of proteins from the inter-membrane space (Cory et al, 2003). Moreover, p53 in cytoplasm appear to have a pro-apoptotic effect by releasing Bax from Bcl-2 family members interaction. Interestingly, studies have demonstrated that Bcl-2 proteins are strongly expressed in human breast cancer cells; in particular, Bcl-xL expression confers resistance to chemotherapy-induced apoptosis (Williams et al, 2005). Moreover, Bax/Bak pores can be formed and release cytochrome c after ROS-stimuled production oxidase cardiolipin (Ott et al., 2002).

As mentioned above, the intrinsic pathway for apoptosis can also be triggered by the induction of the mitochondrial permeability transition (MPT) (Fig.4). In healthy cells, the MPT can cause the collapse of $\Delta\psi m$ by forming a channel at mitochondrial inner membrane, leading to osmotic swelling of the mitochondrial matrix, burst of the outer membrane and release of apoptotic proteins (see above) (Hajnóczky, et al, 2006). As described previously, the MPT pore is composed by the VDAC at the outer membrane, by the ANT at the MIM and Cyp D in the mitochondrial matrix (Kroemer et al, 2007). Additional proteins that are thought to compose or at least regulate the MPT pore include the peripheral benzodiazepine receptor (PBR or TSPO) that is located in the outer membrane and hexokinase (HK), which, as already described, binds to mitochondria at points of contact between the MOM and MIM (Toogood, P., 2008). The PBR seems to be overexpressed in several cancers and has been also described to interact with the MPT through the VDAC, but also by blocking Bcl-2, Bcl-xl and MCL-1 proteins effect and can be overexpressed in several cancers (Fulda and Debatin, 2006).

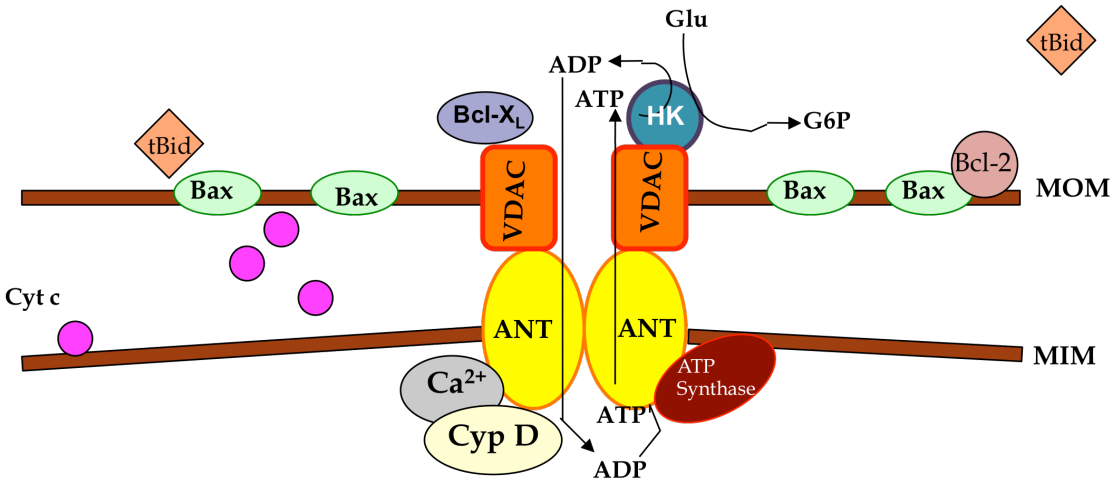

Fig.4 - Mitochondrial membranes dynamic in apoptosis. Oligomerization of Bax can be mediated by pro-apoptotic protein Bid (tBid) (on the right). MPT pore is a multimeric complex, composed of VDAC located in the MOM, ANT, an integral protein of the MIM, and a matrix protein, Cyp D; also the interaction with VDAC allows hexokinase (HK) to use exclusively intramitochondrial ATP to phosphorylate glucose, thereby maintaining high rate of glycolysis; the anti-apoptotic protein Bcl-X_L prevents tBid-induced closure of VDAC and apoptosis by maintaining VDAC in open configuration allowing ADT/ATP exchange and normal mitochondrial functioning (in the center). Bcl-2, Bcl-X_L, Mcl-1, and Bcl-w, interact with the pro-apoptotic proteins, Bax and Bak, to prevent their oligomerization (on the left)(adapted from Gogvadze, 2010).

Other important proteins involved in apoptosis regulation are involved in the processes of mitochondrial fusion and fission (Armstrong et al, 2007). In mammals, proteins that regulate fusion are Opa1, mitofusin 1 (Mfn1) and mitofusin 2 (Mfn2), while one that regulate mitochondrial fission is dynamin-related protein 1 (Drp-1) (Cereghetti and Scorrano, 2006). Whereas usually mitochondria appear as a contiguous network, during apoptosis, mitochondria can change their shape, including by undergoing fragmentation (Frank et al, 2001). In cancer cells, the expression of these mitochondria-shaping proteins is altered. For example, in nonsmall- cell adenocarcinoma of the lung and in other cancer cell lines Mfn1 is upregulated. It is also suggested a relationship between BH3-only proteins and fragmentation promoted by pro-fission proteins such Drp-1 (Germain et al., 2005).

Mitochondrial membrane permeabilization is considered to be a "point of no return" (Debatin et al, 2002), leading cells to death by apoptosis or necrosis, which makes this organelle as a target choice in therapy (Mathupala et al, 2006). Thus, for the

regulation of apoptosis the balance between anti- and pro-apoptotic proteins is fundamental (Gogvadze et al, 2010).

1.2.2.2. Autophagy

Autophagy is a mechanism in which parts of the cytoplasm are engulfed in double-membraned vesicles and later hydrolized (Gozuacik and Kimchi, 2004). Autophagy can be triggered as a cell defense in acute stress, such as during nutrient deficit, but also can be involved in cell death. Autophagy can prevent cells from accumulating misfolded proteins, mediating neuroprotection when preventing neurons from cell death. However, it is still largely unknown how this mechanism is actually associated with cell death, i.e., whether autophagy is an independent system or a consequence or mediator of cell death (Kroemer et al, 2007). A correlation between reduced autophagy and cancer development has been observed, where proteins involved in autophagy are deregulated. Thus, autophagy may have a role as safeguard mechanism that would control the appearance of aberrant cells. However, in certain cancer cells, it is also observed that in the presence of anticancer agents that trigger autophagy, cells will first try to evade cell death induced by the drug. Ifsucceding, the cell will survive, otherwise the cell will activate cell death mechanisms (Gozuacik and Kimchi, 2004).

1.2.2.3. Necrosis

The pool of intracellular energy determines whether the cell will die by apoptosis or necrosis. Cell death normally starts as apoptosis, but during the process apoptosis can shift to a necrotic phenotype, when caspases are inhibited. Necrosis was thought to be an accidental cell death, occurring in a short period after it activation. However, it was recently verified that the necrotic process is actually determined by the cell, and not only by the stimulus, being subjected to regulation. It was demonstrated that the inhibition of ATP/ADP exchange, mediated by ANT regulation by kinase receptor interacting protein (RIP), was determinant for necrosis cell death Temkin et al, 2006). Necrosis is a form of death with loss of control of ionic balance, uptake of water and cell swelling that leads to plasma membrane rupture and the release of damaged organelles. Consequently, necrosis causes the recruitment of immune cells and promotes local

inflammation, which has been associated with tumor growth (Demaria et al, 2010).

1.2.2.4. Mitotic Catastrophe

During mitosis, a type of cell death called mitotic catastrophe can also occur. Mitotic catastrophe results in general from errors in cell cycle checkpoints (Castedo et al, 2004). Aberrant chromosome segregation can occur due to failure of cell cycle arrest, ending to apoptosis pathway, where mitochondrial permeabilization is also observed. Thus, mitotic catastrophe is seen as a mechanism that acts against undesirable aneuploidization, which could lead to oncogenesis. Proteins such as p53, survivin, caspases and bcl-2 family members are involved in this type of cell death (Kroemer et al, 2007).

1.2.3. Mitochondrial DNA and its relationship with cancer

Mitochondria are the only organelles that have their own genetic material (mtDNA) and have a replication system independent from nuclear DNA replication (Chen et al, 2010). Of the total cellular DNA content, mtDNA represents less than 1%. mtDNA does not contain introns or histones and is very susceptible to deleterious oxidative damage (Modica-Napolitano et al, 2007). However, the mitochondrial protein pool is assembled from both nuclear (nDNA) and mitochondrial DNA (mtDNA) genes. Whereas mtDNA-encoded subunits correspond to catalytic enzymes, nDNA-encoded subunits have functional and structural activities. Thus, the coordination of the expression of nDNA-and mtDNA-encoded genes is essential for normal mitochondrial physiology (Chen et al, 2009). mtDNA is fairly small (16,569 bp), codes for 37 genes, including 13 polypeptides of respiratory chain, 22 transfer RNAs and 2 rRNAs. mtDNA is composed by two strands, a guanine-rich heavy strand and a cytosine-rich light strand (Fig.5). Every mitochondrion contains between 2 to 20 copies of mtDNA and the copy number of mitochondrial genome per cell is around 1000 copies in average, ranging from hundreds to more than 10,000, depending on the cell type (Taylor et al, 2007).

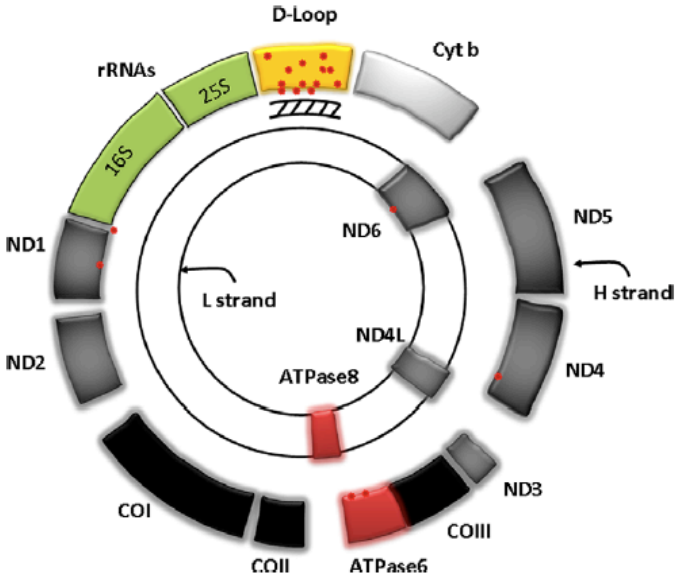

Fig.5 - Mitochondrial genome map. Mitochondrial-encoded genes are represented in their locations in mtDNA. The red dots indicate the location of common mutations detected in mtDNA from tumor samples (adapted from Ralph, 2010).

mtDNA has a very high mutation rate, due to the proximity to the respiratory chain and consequently exposure to ROS production sites and importantly the lack of histones and decreased capacity for DNA repair (Taanman, J, 1999). Higher frequency of mtDNA mutations in somatic mammalian cells compared to mutations in nuclear DNA, is reflected and correlated with cancer development (Sutton, S., 2005), such as in breast cancer, prostate cancer and thyroid cancer (Carter et al, 2005; Petros et al, 2005). In fact, mutations and deletions in mitochondrial or nuclear DNA, lead to dysfunction of mitochondrial respiratory chain, resulting in inefficient ATP production, ROS production and oxidative cell damage, which are conditions that in theory favor tumorigensis (Diaz et al, 2002). However, some cancers can also contain mutations in nuclear-encoded mitochondrial genes, as example, coding for SDH (complex II). mtDNA is, in most of the cases, maternally inherited, so cancer mutations can either arise from the female germline (associated with cancer predisposition) or arise from mutations in tissues (Brandon et al, 2006).

Moreover, higher mtDNA content was found in papillary thyroid carcinomas, during endometrial cancer development, primary tumors of head and neck squamous

cell carcinoma, while mtDNA content is decreased in breast tumors relative to normal controls (Modica-Napolitano et al, 2007). It is thought that the decrease of copy number is essentially due to mutations in the displacement loop (D-loop) region, where mutations are higher especially in later stages of cancer development, while the increase could be attribute to mutations in genes encoding oxidative phosphorylation (Kim et al, 2004).

From the above sections, one can have a basic understanding of mitochondrial physiology and how that can change in cancer. Whereas these alterations are causally linked with cancer or are merely a small component of a larger metabolic remodeling, is still under debate, although the latter appears to be more likely. Whatever the mechanism is, it is clear that mitochondria can be important targets in cancer therapy. Therefore, the design and synthesis of effective pharmaceutical agents that would directly target mitochondrial alterations and decrease tumor size can be achieved. Also, the differential metabolism used by normal and cancer cells can provide knowledge to discover new drugs with no side effects on normal cells.

In the next section we will discuss different strategies and some promising therapeutics to preferentially target cancer mitochondria.

1.3. Mitochondria and therapeutic anti-cancer strategies

Distinct approaches to control cancer are available, such as surgery, radiotherapy, and hormone and biological therapies, etc. However, in many cases, those methods are not enough, so chemotherapy is usually another tool to eradicate cancer, by using drugs alone or in combination. Unfortunately, the low specificity and the fact that the drugs used currently have some uncomfortable side effects lead us to research for new selective drugs.

Mitochondria play a critical role in the process of cell death and moreover that mitochondria are altered in malignant neoplasia promoted a radical change in cell death research. Guchelaar et al. (1997) and Decaudin et al. (1998) were the first to point out mitochondria as a potential target for anticancer drugs, proposing the modulation of extrinsic and intrinsic regulators and finding strategies to develop chemotherapeutics that would act on mitochondria, respectively (Weissig and D'Souza, 2010). A new term, mitocan, was coined to all compounds that would exert their action by targeting mitochondria. Nowadays, the vast majority of conventional anti-cancer drugs indirectly exploit apoptosis by the activation of intrinsic pathways in order to exert their cytotoxic action, using multiple activation routes (e.g. p53 or death receptors) (Dias and Bailly, 2005). However, many of these agents fail due to disruption of endogenous apoptosis-inducing pathways in tumor cells (Weissig and D'Souza, 2010).

The first goal in chemotherapy administration is reached when the drug is selectively accumulated in the tumor. After systemic administration, the drug needs to reach the tumor mass, which is composed by different types of cells (as described in 1.1). Furthermore, the drug needs to get in the tumor cell and reach mitochondria. Although at first sight it may simple, the drug must pass through many biological membranes. Inside the cancer cell, two major factors determine the fate of low-molecular-weight anticancer molecules, the nature of the drug and intracellular environment (Li et al, 2011). Drug accumulation in mitochondria is another step to take into account in drug delivery process and it is also extremely complex. The selective accumulation of promising anticancer molecules inside mitochondria of tumor cells, thus sparing normal cells, is a key point in the design of novel molecules (Modica-Napolitano and Aprille, 2001). The growth of mitochondria-based strategies, either by chemical conjugation or

targeting transporters has demonstrated promising efficacy, however their specificity is still discussed. Thus, new agents can specifically target cancer cells when fused with peptides that could recognize cancer-cell-specific surface receptors or internalized through the plasma membrane due to the biological activity of the molecule. Furthermore, if the agent has a lipophilic cationic moiety, its accumulation by polarized mitochondria, which are negatively charged in the matrix, will increase (Fulda et al, 2010b). Thus, the extent to which a drug might interact or even bind to subcellular components, such as membranes and cell organelles, depends on the physicochemical properties of the drug.

1.3.1. Mitochondriotopic delivery molecules

In order to reduce undesirable side effects, which may result from the drug being accumulated in wrong tissues or in normal cells, or even in wrong organelles, efficient mitochondria-specific delivery systems are being proposed (Fig.6).

In fact, specific delivery of drugs into tumors, based on Ehrlich's 'Magic Bullet' is the goal of many researcher groups. To specifically target mitochondria, distinct approaches can be found, including delocalized lipophilic cations (DLcs), mitochondrial targeting sequence (MTs)-containing polypeptides, synthetic peptides and amino-based transporters, and vesicle-based carriers.

The simplest ones are delocalized lipophilic cations (DLCs), which are based on small membrane-permeable cationic molecules with delocalized positive charge. These compounds basically cross mitochondrial membranes due to their electrophoretic attraction to the mitochondrial matrix, and efficiently accumulate within mitochondria, in accordance with the Nernst equation (Murphy, M., 1997; Kurtoglu and Lampidis, 2009). DLC molecules selectively target those cancer cells with higher $\Delta\Psi m$ compared to normal cells (Armstrong, J., 2007). DLCs can act as mitochondrial transporters and delivery both small and large molecules, but with some limitations, once normally DLCs are used at high concentrations and with large polar coupled-molecules (Ross et al, 2004; Kelso et al, 2001; Mukhopadhyay et al, 2005). However, cardiac toxicity can occur with DLCs, due to the enhanced accumulation of DLCs by myocardial cells (Zhang et al, 2011). Examples of DLCs include rhodamine 123 (Rh123), the rhodamine analogue MKT-077, the cationic cyanine dye EDKC, Dequalinium chloride (DECA) and

tetraphenylphosphonium (TPP^+)-conjugated compounds.

Mitochondrial proteins encoded by the nucleus carry amino-terminal mitochondrial targeting sequences (MTSs) of 20-40 amino acids that will be recognized by receptors at the MOM. ATP and mitochondrial $\Delta\Psi m$ can be involved with the import of MTS-containing polypeptides, which is mediated by several translocases, which provide the recognition, translocation and membrane insertion of precursor proteins. Thus, MTS transporting process can become a potential delivery system to selectively introduce inside cancer cells mitochondrial therapeutic agents (Zhang et al, 2011).

Moreover, a variety of amino acid- and peptide based mitochondrial transporters are also in use. The peptide strategy is based on endossomal or lypossomal sequestration, after direct cell uptake. This is a brand new action plan, with very good expectancy, since these peptides are easy to synthesize, to deliver and present excellent biocompatibility. As example is the proapoptotic peptides with two functional domains developed by Ellerby et al. (1999), where the proapoptotic peptide will be able to target mitochondria and at the same time present no toxicity to normal cells.

Unfortunately, many of these strategies can fail if the compound does not reach tumor cells. In fact, several potent anticancer candidates have been shelved due to have low solubility and low membrane permeability. It is not easy to design a drug that would combine all essential physicochemical properties of biovailability and high pharmacological activity (Weissig and D'Souza, 2010). Thus, the development of lipossomes as drug delivery systems, based on phospholipid vesicles able to encapsulate water-soluble drugs in their aqueous inner space, and also soluble polymer carrier systems strategies have been in use and revealed to overcome those issues. From these systems, examples are dequalinium-based liposome vesicles (DQAsomes), dicationic mitochondriotropic compounds and the new MITO-Porter (Yamada and Harashima, 2008; D'Souza and Weissig, 2009).

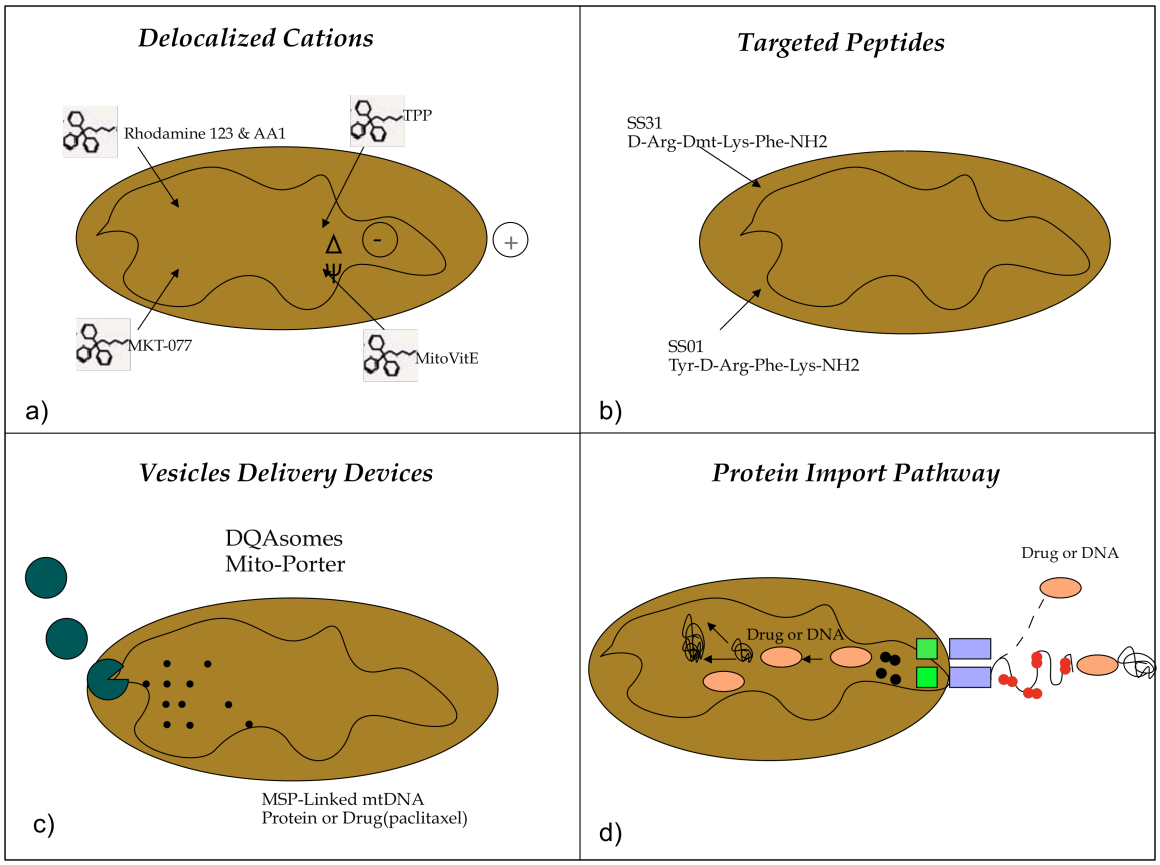

Fig.6 - Mitochondriotopic delivery systems.(a) Mitochondria accumulate delocalized lipophilic cations (DLCs) because of the higher transmembrane electric potential across their inner membrane (negative on the inside); (b) Szeto–Schiller (SS) peptides selectively partition into the inner mitochondrial membrane independent of the $\Delta\psi m$ and possess intrinsic antioxidant and cytoprotective properties; (c) Dequalinium is a dicationic mitochondriotropic compound that self-assembles and forms vesicle-like aggregates called DQAsomes and Mito-Porter; (d) Mitochondria can be targeted by linking a MSP to a non-mitochondrial protein to create a chimeric protein that is taken up into the mitochondrial matrix via the protein import pathway (adapated from Armstrong, 2007).

1.3.2. Mitochondrial targets and Mitocans

The mechanism by which mitochondrial drugs trigger apoptosis depends on the molecular mitochondrial target site. Newer and more specific therapies have become more prevalent in the treatment of specific cancers as the molecular mechanisms of carcinogenesis become better characterized.

Next, we will review a few of the new mitochondrially-targeted compounds that show the greatest promise as chemotherapeutics. The compounds can be subdivided in

different targets of action.

Although not technically mitocans, some compounds will target different steps of the glycolytic pathway, affecting preferentially those tumors that rely on glycolysis. Inhibition of glycolysis can lead to increased tumor susceptibility to common anti-cancer agents ((Gogvadze et al, 2010). For example, ATP depletion and consequent cell death is verified when the hexokinase inhibitor 3-bromopyruvate (3BrPA), a glucose analog 2-deoxy-D-glucose (2DG) and dichloroacetate (DCA) were used together.

3BrPA, is a lactic acid analog known for its alkylating property. 3BrPA selectively targets hepatocellular carcinoma cells *in vitro* (Ko et al, 2001). *In vivo,* 3BrPA was shown to suppress metastic lung tumors with no apparent side effects (Ko et al, 2001). This compound suppressed glycolysis, inhibited the activity of hexokinase, by interfering with VDAC-hexokinase interaction and suppressed mitochondrial respiration, but also interfering with succinate dehydrogenase activity (Ko et al, 2001).

3BrPA has also been used in combination with other chemotherapeutics, such as [Cu(isaepy)2], a DLC-like molecule that affects mitochondrial oxygen consumption and produce ROS leading to cell death (Filomeni et al, 2011). Moreover, *in vivo* antitumor effect in hepatic and pancreatic cancer was observed in combination with the heat-shock protein, 90 kDa (HSP90) inhibitor geldanamycin (Fulda and Kroemer, 2010).

2-deoxy-D-glucose, in turn, is a non-metabolizable glucose analogue, that was used in human lymphoma cells to inhibit glucose metabolism and in combination with TNF was shown to lead to apoptosis (Gleiss et al., 2002). 2DG suppresses intracellular ATP, potentiates phosphatidylserine exposure induced by Fas, suggesting this way that intracellular ATP is related to the externalization of PS in apoptosis (Gleiss et al., 2002). Certain pancreatic tumors, with specific GLUT-1 expression profiles, were shown to be susceptible to 2DG, due to great accumulation of this drug (Maher et al, 2004). 2DG was used also as adjuvant in combination with electron transport chain blockers showed to be particular effective in colon cancer cells (Boutros and Almasan, 2009).

Dichloroacetate (DCA), structurally similar to pyruvate, stimulates oxidative phosphorylation through inhibition of pyuvate dehydogenase kinase (PDK), hence activating pyruvate dehydrogenase (PDH) and shifting metabolism from glycolysis to glucose oxidation. Gammer and coworkers (2010) recently observed that DCA depolarized mitochondria, increased mitochondrial ROS generation leading to cell death

of glioblastoma multiforme cells, both *in vitro* and *in vivo*, by targeting PDK II, which is highly expressed in this type of cancer.

In other studies, DCA showed to have larger activity in cells with defective mitochondria, presenting effective synergistic effect with other mitocans (Stockwin et al, 2010). Unfortunately, DCA does not have a selective activity, acting on both cancer and normal cells, although DCA has also been used to treat mitochondrial diseases (Stockwin et al, 2010). Therefore, for cancer cells with functional mitochondria this might not be enough, suggesting that DCA may benefit only a selected sub-set of patients (Stockwin et al, 2010).

1.3.2.1. Disturbing Adenine Nucleotide Translocator (ANT) function

Drugs targeting the adenine nucleotide translocator (ANT) have also been reported to induce mitochondrial apoptosis and cell death. Examples include berberine, lonidamine and arsenites. **Lonidamine,** an indazole carboxylate, and **arsinite** (such as arsenic trioxide and GSAO) are agents that appear to have similar cellular actions, inducing the MPT by directly affecting the ANT. This MPT inducing action can be inhibit by the ANT's ligands, ATP and ADP, as well by Bcl-2 (Belzacq et al, 2001). More, Lonidamine is viewed as inhibitor of aerobic glucose utilization and can also interact directly with hexokinase (Don and Hogg, 2004). Arsenic trioxide (As_2O_3) triggers cancer cell death by inhibiting thioredoxin reductase and promoting oxidative stress (Toogood, P., 2008). In traditional Chinese medicine, arsenic trioxide was commonly used, and recently its therapeutic effects in acute promyelocytic leukemia (APL) were also proposed. As_2O_3 has also been used in combination with all-trans retinoic acid (ATRA) showing a synergistic effect in APL mouse models (Marchetti et al, 1999). ATRA is a natural derivative of vitamin A, which known to stimulate the expression of retinoic acid receptor-responsive genes (Marchetti et al, 1999). This compound suppresses mitochondrial respiration, decreases $\Delta\Psi m$ and triggers ANT-dependent MPT and cell death independent from nuclear receptor binding, suggesting another potential mechanism of action is involved (Notario et al, 2003). The potentials of As_2O_3 and ATRA in the treatment of other cancers are also being explored (Zhang et al, 2001).

A glutathione-coupled trivalent arsenical compound (**GSAO)** was observed to induce apoptosis in angiogenic endothelial cells *in vitro* and *in vivo*, with these cells and

it happens once these cells presenting a large mitochondrial population. It was suggested that proliferating cells would be target as well, due to their higher mitochondrial calcium levels and elevated respiration rates, however low toxicity towards these cells was observed (Don, A., 2003). GSAO can inhibit ATP/ADP transport by interacting with the ANT, by cross-linking two of the three matrix facing cysteine thiols. This will lead to ATP depletion, ROS generation, mitochondria depolarization and apoptosis (Don, A., 2003; Don and Hogg, 2004). Angiogenic cells can often circumvent many therapies, however these cells have decreased capacity to buffer the arsenical moiety by expressing low MRP1/2, but also due to altered glutathione levels. GSAO is currently in clinical trials in cancer patients and promising results are anticipated (Cadd et al, 2006; Dilda et al, 2008).

1.3.2.2. Targeting mitochondrial respiratory chain

Modulation of mitochondria by agents that interfere with mitochondria respiration, or uncouple oxidative phosphorylation, was found to cause cell death. Numerous inhibitors of mitochondrial respiratory chain have been used for a long time as tools to better understand mitochondrial respiration, however, in general, these mitochondrial poisons are toxic *in vivo*, due to their non-specific activity. These classic mitochondrial poisons include rotenone (complex I), antimycin A (complex III), cyanide (complex IV), oligomycin (ATP-synthase) and protonophores, such as FCCP (Don and Hogg, 2004). Other molecules, presenting lower toxicity have been developed. **α-Tocopheryl succinate** (α-TOS) is vitamin E analog capable of preferentially targeting mitochondria in cancer cells, inducing morphological changes and causing growth inhibition in mouse melanoma cells (Prasad and Edwards-Prasad, 1982). α-TOS has been shown to be tumor-selective due to its ester structure, since the hydrolysis of α-TOS to α-tocopherol in normal cells is increased, the same not occuring in cancer cells (Jia et al, 2008). Moreover, it was shown that this compound induces cell death by targeting ubiquinone-binding site at complex II, causing leakage of electrons, stimulating ROS generation and killing malignant cells at non-toxic concentrations to normal cells (Dong et al, 2009; Ottino and Duncan, 1997). α-TOS facilitates the translocation of Bax from the cytosol to mitochondria and subsequent cytochrome c release (Yu et al, 2003). α-TOS also induces apoptosis in proliferating endothelial cells, through the accumulation of

ROS and thereby suppressing angiogenesis *in vitro* and *in vivo* in breast cancer models (Dong et al, 2007).

Another compound, which has been described to target the respiratory chain, is **resveratrol**. Resveratrol is a natural compound, a polyphenolic phytoalexin, found in the skin of red grapes, berries and peanuts, with chemotherapeutic and chemopreventive properties (Jang et al., 1997). Resveratrol can induce the redistribution of Fas/CD95 and TRAIL receptors in lipids rafts in colon carcinoma cells (Delmas et al., 2004). Moreover, resveratrol can lower ROS production by competing with coenzyme Q and consequently decreasing complex III activity (Zini et al, 1999). Recently, it was observed that nitric oxide production, caspase activation and p53 were necessary for the mechanism of action of resveratrol (Kim et al, 2009). Resveratrol has recently been found to improve mitochondrial function by activation of peroxisome proliferator-activated receptor-γ co-activator 1α (PGC1α), which in turn stimulates sirtuin 1 (SIRT1) (Lagouge et al, 2006). Structure-activity studies showed that resveratrol inhibits mitochondrial ATP synthesis by binding to F1-ATPase, contributing to cell death (Gledhill et al, 2007). Resveratrol specifically targets mitochondria when coupled to the lipophilic triphenylphosphonium cation (TPP+) (Biasutto et al, 2008). Resveratrol is currently under clinical evaluation for colon cancer and multiple myeloma treatments (Fulda and Kroemer, 2010).

1.3.2.3. Targeting mitochondrial membrane polarization and physiology

Rhodamine 123 and analogs are preferentially accumulated in mitochondria, due to the presence of an esterified carboxyl group and a positive charge, without interfering with lipophilic structure of parental molecule (Kurtoglu and Lampidis, 2009). Cells with high mitochondrial membrane potential exposed to rhodamine123 and analogs will accumulate more of this compound and be more susceptible to the compound, when comparing with cells presenting lower $\Delta\Psi m$ (Zinkewich-Péotti and Andews, 1992). Rhodamine 123 has also been used in conjugation with other compounds, such as 2DG, in the treatment of human breast carcinoma. The two compounds together inhibit the growth of cancer cells, whereas no toxicity was observed in normal cells. A similar effect was observed in *in vivo* studies, suggesting that the disturbance of OXPHOS and glycolysis pathways in tumor cells can be an opening for an effective treatment (Kurtoglu and Lampidis, 2009). **OSW-1** is chemically

synthesized from steroids found in the bulbs of *Ornithogalum saudersiae*. OSW-1 is extremely potent for cancer cells in the sub-nanomolar range, having no effects in non-tumor cells (Zhou et al, 2005). The mechanism responsible for such selectivity could be due to alterations in mitochondrial structure and calcium regulation in cancer cells. This compound exhibited a unique mechanism of action, having significant effect in mitochondrial membranes and cristae, due to calcium overload, which leads to apoptosis of pancreatic and leukemia cancer cells (Zhou et al, 2005). To demonstrate that mitochondria is a target for OSW-1, a study was performed where leukemia cancer cells lacking mitochondrial DNA and with defective respiration, were shown to be resistant to the treatment (Zhou et al, 2005).

$_D$(KLAKKLAK)$_2$ is a pro-apoptotic peptide, which mechanism of action consists in disrupting mitochondrial membrane, which releases cytochrome c and activating the caspases cascade and triggering apoptosis. The drug inhibit the cell growth of endothelial cells, such as the MDA-MB-435 cells that at their membrane surface present the integrin αVβ3 receptors. (Smolarczyk et al., 2006). To better direct this agent to mitochondria, a Triphenylphosphonium moiety was added to the structure, increasing the biological activity of the peptide as citotoxic agent (Kolevzon et al, 2011).

1.3.2.4. Mitochondrial DNA as a target

A type of vitamin K, **vitamin k3**, is a synthetic compound that has been described to inhibit DNA polymerase (pol)ϒ, thus perturbing mitochondrial DNA replication, and promoting ROS generation leading to apoptosis (Sasaki et al, 2008). However, vitamin k3 can interfere with calcium homeostasis and decreases glutathione levels as well (Di Monte et al, 1984). Recently, it was found that vitamin k3 can bind at the colchicines binding site of tubulin and inhibit microtubule polymerization (Archarya et al, 2009). *In vitro* studies demonstrated that vitamin k3 displayed antitumor activity in pancreatic and breast cancer cells (Zhang et al, 2011).

Ditercalinium is another agent that targets mtDNA target which is preferentially accumulated in mitochondria, inhibiting their replication (REF). After treatment with ditercalinium, ultrastrutural studies showed a depletion of mtDNA and loss of mitochondrial cristae. Similarly to vitamin k3, ditercalinium inhibits human DNA polymerase ϒ activity (Zhang et al, 2011).

1.3.2.5. Anti-cancer agents that modulate cancer redox environment

Several natural compounds show to be able to selectively kill cancer cells with mitochondrial dysfunction (Chen et al, 2010). Furthermore, oncogene products modulate MOM permeability by regulating Bcl-2 family proteins, which modulate the bioenergetic metabolite flux and putative components of the MPT pore. In this regard, phenolic acids may act through similar mechanisms (see chapter 4.2). In fact, several authors have reported that **CAPE** (caffeic acid phenyl ester) is cytotoxic towards tumors, but not against normal cells, through a mitochondrial-mediated mechanism involving an altered Bcl-2 protein expression (Jin et al, 2008). A number of other experimental chemotherapeutic agents have the opposite effect, acting on mitochondrial lipids and proteins and inhibiting MPT pores opening through direct binding to certain protein components (Green and Kroemer, 2004). A general rule is that antioxidants act as MPT inhibitors, decreasing or hindering oxidative stress which is responsible for the oxidation of proteins of the pore complex that is a prime cause for the consequent MIM permeabilization (Zamzami and Kroemer, 2001)..

On the other side, cancer cells can upregulate cellular antioxidant capacity, as a response to ROS production induced by chemical agents, becoming these cells more resistant (Chen et al, 2010). Thus, there are compounds capable to overcome such resistance, namely **β-Phenylethyl isothiocyanate** (PEITC). It was suggested that this compound, with low toxicity towards normal cells, has potent anticancer activity, which mode of action involve a ROS-mediated mechanism (Chen et al, 2010). Moreover, PEITC effectively kills cancer cells resistant to standard agents such as fludarabine, cisplatin and gleevec (Trachootham et al., 2008). PEITC will deplete cellular GSH and inhibits the redox-modulation enzyme glutathione peroxidase antioxidant system that cancer cells depend on to maintain redox balance (Trachootham et al., 2009). Recent studies also show that PEITC target irreversibly certain thiol proteins such as peroxiredoxin 3 and tubulin.

Honokiol, a polyphenol from cones, bark and leaves of *Magnolia grandifloris*, was reported to act as scavenger of hydroxyl radicals and lipids peroxides, and also to have an inhibitory effect on NADPH oxidase. Contrarily, other research group describe that honokiol induces ROS in various cell lines (Chen et al, 2010). This can be justified by the

fact it may function as an antioxidant or pro-oxidant depending on the redox environment or even the concentration. The mechanisms of action associated to honokiol include the induction of apoptosis through mitochondria perturbation and endoplasmic reticulum stress, interaction with pRb leading to cell cycle arrest and inhibition of the E2F1 transcriptional activity, among others (Hahm and Singh, 2007). Honokiol was showed to interfere with the MPT pore, more specifically with cyclophilin D to promote cell death. On the other hand, honokiol can also interfere with mitochondria through Bcl-2 family proteins (Yang et al, 2002). Recently, honokiol showed to inhibit breast cancer cell migration through targeting nitric oxide levels and cyclooxygenase-2 (Singh and Katiyar, 2011).

Gallic acid and its esters are presently used as antioxidant aditives in both food and pharmaceutical industry – propyl gallate (E-310) and octyl gallate (E-311) – since they are known to protect against oxidative damage induced by reactive oxygen, nitrogen and sulphur species (Masaki et al, 1997). Gallic acid derivatives have been described to cause apoptosis in tumor cell lines, to inhibit lymphocyte proliferation and to inhibit protein tyrosinase kinase (PTK´s) activity (Palacios et al, 2001). The derivative epigallocatechin-3-gallate (EGCG) was able to promote apoptotic cell death in various malignant-B-cell lines, where ROS may play a key role. It was observed that malignant cells have increased ROS after treatment with EGCG, while a decrease was observed in normal cells. The difference may be explained by the fact that normal cells present a higher content in catalase (Yamamoto et al., 2003).

1.3.2.6. Other targets

Other mitochondrial interacting proteins are also target of interesting molecules that would lead to tumor grow inhibition. **Curcumin** is a phenolic derivative present in plants formed by two ferulic acids linked by a methylene group, in a diketone structure. The compound is the active ingredient of turmeric (Curcuma longa) used as a traditional herbal medicine in South Asia for thousand years, displaying anti-inflammatory, antioxidative and anticarcinogenic properties, with an immense potential in cancer cancer chemotherapy because of its effect in cell growth regulatory mechanisms. Analysis of its structure revealed that the presence of the beta-diketone moiety and phenolic groups in the structure have a direct contribution on its antioxidant behavior

(Kikuzaki et al, 2002). Curcumin exhibits growth inhibitory activity against prostate, colon and breast cancer (Curini et al, 2006). Some studies evidence a selective growth-inhibiting effect of curcumin on transformed cell lines, as compared to non-transformed cell lines (Leu and Maa, 2002). It was also previously demonstrated that the anticarcinogenic action of curcumin in colon have the involvement of the phenolic groups and the conjugated bonds in the central seven carbon chain (Wahl et al, 2007). Moreover, curcumin also affects various cell cycle proteins and checkpoints, leading to the down-regulation of some cyclins and cyclin-dependent kinases, as well as to up-regulation of cdk inhibitors, and to inhibition of DNA synthesis (Karunagaran and Kumar, 2007). Of special relevance is the fact that curcumin can also induce apoptosis by targeting mitochondria, affecting p53-related signaling and blocking NF-kB activation, in a similar fashion to caffeic acid (Devasena et al, 2003). Prostate cancer cells can sensitized with curcumin on TRAIL treatment, inducing both the extrinsic and the intrinsic pathways for apoptosis, which suggests that curcumin is a beneficial adjunct against chemoresistance to standard therapeutic drugs (Manach et al, 2005). Moreover, it was recently suggested that this compound would be a good compound for cancer cells with mitochondrial dysfunction and increased ROS generation (Subudhi et al., 2008).

Triterpenoids are another group of natural compounds with chemotherapy potential. **Betulinic acid**, a pentacyclic triterpene, was reported to induce apoptosis in a variety of tumor cells p53-indendent, which show absence of the MPT and ROS generation (Fulda and Debatin, 2005; Elrod, 2008). Betulinic acid seems to interact and modulate Bcl-2 family members in different types of cancer (Fulda, S., 2009). Moreover, betulinic acid was shown to be an activator of NF-kB in several cancer cell lines. Normal cells and tissue present a significant resistance to betulinic acid (Fulda, S., 2009) (for more information see chapter 4.4).

HSP90 is not normally present in mitochondria of normal cells; however, this chaperon can be found in mitochondria of cancer cells, due to a possible induction by RAS and AKT oncogenes. HSP-90 is an ATPase-directed molecular chaperone that has the role to supervise protein folding during cellular stress response, and the interacted molecules are involved in cell proliferation and cell survival (Plescia et al, 2005). The molecular chaperone Hsp90 provides an attractive target for therapeutic intervention in cancer. **Shepherdin** is a novel peptidomimetic that is easily accumulated in

mitochondria, and that is antagonist of the complex between Hsp90 and survivin (cell cycle-regulating protein), plus other additional client proteins such as TRAP-1. Shepherdin inhibits Hsp90 chaperone activity via an ATP competition mechanism and kills cancer cells by inducing the MPT. Shepherdin showed no toxicity for brain and liver mitochondria of human cancers xenografts (Plescia et al, 2005; Kang et al, 2007).

Gamitrinib was conceived by coupling a HSP90 inhibitor to lipophilic cationic moieties. Gamitrinib targets specifically mitochondria of cancer cells, by antagonizing the ATPase activity of HSP90. It was shown that Gamitrinibs causes the death of cancer cells and suppress tumor growth *in vivo*, with no apparent effects on normal counterparts (Fulda and Kroemer, 2010).

Being aware that mitochondria are the center of apoptosis regulation and energy metabolism, these organelles should therefore be considered as a target to the search of novel anticancer molecules (Biasutto et al, 2010). The term Mitocan was first suggested by Ralph et al. (2010), to designate agents with anticancer activity that induces cell death in malignant cells through direct mitochondrial perturbation. Although mitocans present an excellent *in vitro* interaction with mitochondria, the results may not be so straightforward *in vivo*. Mitocans are widely distributed in the cell and only a portion of the initial pool actually accumulates in mitochondria. Recent findings by Morrison et al. (2009) propose that mitocans can efficiently target cancer stem cells. This way resistant neoplastic disease can be controlled in the near future. Thus, the success of cancer control will pass through the induction of apoptosis by directly disrupt mitochondrial function and/or membrane integrity. A better understanding of the mitochondria role in cancer will lead to the discovery of new therapeutic strategies and therefore to the objective of killing or controling tumor development with the fewer side effects possible (Gogvadze et al, 2008).

II - Aims

2. Aims

Whether mitochondria are a primary mediator of the tumorigenesis or a partner in a long chain of events that lead to the whole process, the unequivocal truth is that mitochondrial alterations can be explored for the design of more suitable and selective anti-cancer therapies. Despite all the work done so far (Chen et al, 2010; Gogvadze et al, 2010), there is still ample room for novel insights on this question. For example, do specific mitochondrial alterations result in well-defined susceptibility to mitochondrial agents, otherwise known as mitocans? Another eternal question regards the screening of several possible candidates for mitocans and investigate whether one of them is a possible candidate for drug development.

The general goal of the present thesis is the understanding of involvement of mitochondria in cancer development and treatment, in an attempt to find strategies to overcome the several alterations that reduce the susceptibility to mitochondrial-mediated cell death pathways.

Therefore, to reach the proposal goal, the following objectives were pursued:

1. Characterize mitochondrial physiology in several breast tumor in order to assemble more information of possible vulnerable mitochondrial alterations in tumor cell lines that can be explored in therapy (section 4.1);
2. Evaluate several possible mitocans and their interaction with two distict types of cancer: breast and melanoma. Three distinct families of compounds were explored: phenolic compounds (section 4.2) on breast cancer cell lines, benzophenanthrine alkaloids berberine and sanguinarine on melanoma cell lines (section 4.3) and triterpenoid derivatives (section 4.4).

III - Material & Methods

3. Material and Methods

3.1. Common reagents

The following reagents Adenosine 5′-diphosphate (ADP), acetate, agarose, albumin from bovine serum (BSA), ammonium persulfate (APS), Bradford reagent, brilliant blue G, calcium chloride ($CaCl_2$), dimethyl sulfoxide (DMSO), DL-Dithiothreitol (DTT), ethylenediaminetetraacetic acid (EDTA), Ethylene glycol-bis (2-aminoethylether)-*N,N,N′,N′*-tetraacetic acid (EGTA), Ethidium bromide, glutamate, glycerol, glycine, malate, β-mercaptoethanol 98%, mesoxalonitrile 4-trifluoromethoxyphenylhydrazone (FCCP), oligomycin, phenylmethylsulfonyl fluoride (PMSF), protease Inhibitor Cocktail (containing 1mg/ml of leupeptin, antipain, chymostatin and pepstatin A), propidium iodide, RNAse, rotenone, sucrose, sodium azide, sodium chloride (NaCl), sodium dodecyl sulfate (SDS), succinic acid minimum 99%, Sulforhodamine B sodium salt (SRB), trizma base, Tris pH 8.8, Tris pH 6.8 and trypan-blue solution were obtained from Sigma-Aldrich Chemical Co. (Saint Louis, MO, USA). The reagents acetic acid, ethanol, hydrochloric acid (HCl), magnesium chloride ($MgCl_2$), methanol, perchloric acid, phosphoric acid, potassium chloride (KCl), potassium phosphate monobasic (KH_2PO_4), sodium hydrogencarbonate ($NaHCO_3$), sodium sulfate ($NaSO_4$) and sodium hydroxide (NaOH) were also obtained from Merck (Whitehouse Station, NJ, USA).

Acrylamide, Laemmli buffer, PVDF membranes and *N,N,N′,N′*-Tetramethylethylenediamine (TEMED) were obtained from BioRad (Hercules, CA, USA). The ECF detection system was obtained from Healthcare Life Sciences (Buckinghamshire, UK). RNase-Free Water was from Qiagen (Valencia, CA, USA).

The fluorescent probes Tetramethyl rhodaminemethylester (TMRM), calcein-AM, ethidium homodimer and Hoechst 33342 were obtained from both Molecular Probes (Eugene, OR, USA).

All reagents and chemical compounds used were of the greatest degree of purity commercially available. In the preparation of every solution, ultrapure distilled water (conductivity < 18 μS.cm-1), filtered by the Milli Q from a Millipore system, was always used in order to minimize as much as possible contamination with metal ions.

3.2. Cell lines

Human breast cancer cell lines used were MDA-MB-231 (92020424, ECACC, United Kingdom), MCF-7 (86012803, ECACC, United Kingdom) and HS578T (HTB-126, ATCC, Manassas, VA, USA). The normal human breast cell line was HS578Bst (HTB-125, ATCC, Manassas, VA, USA) and the normal human fibroblast BJ cell line (CRL-2522, ATCC, Manassas, VA, USA). Cells were cultured in glucose medium composed by Dulbecco's modified Eagle's medium (DMEM; D5648) supplemented with sodium pyruvate (0.11g/l), sodium bicarbonate (1.8g/l) and 10% Fetal bovine serum (FBS) and 1% of antibiotic penicillin-streptomycin 100x solution in an atmosphere of 5% CO_2 at 37°C. Cells were also cultured in galactose/glutamine medium, which was composed by DMEM (D5030) supplemented with galactose (1.8g/l), L-glutamine (0.584g/l), sodium pyruvate(0.11g/l), sodium bicarbonate (1.8g/l) and 10% FBS and 1% of antibiotic penicillin-streptomycin 100x solution in an atmosphere of 5% CO_2 at 37°C. All the reagents used were from Sigma-Aldrich (Saint Louis, MO, USA).

The melanoma cell lines used were mouse K1735-M2 (the kind gift of Dr Lillian Repesh, Department of Anatomy, Microbiology, and Pathology, University of Minnesota School of Medicine, Duluth, MN, USA) and human WM793 vertical growth phase (the kind gift of Dr Meenhard Herlyn, Wistar Institute, Philadelphia, PA, USA). Melanoma cell lines were grown in DMEM (GIBCO, Grand Island, NY, USA) and 10% Fetal Clone III (FC3; HyClone, Logan, UT, USA) in a 5% CO2 atmosphere at 37°C.

Cells were passaged by trypsinization, 0.25% trypsin-EDTA were purchased from Gibco (Carlsbad, CA), using standard methods; all experiments were performed with cultures in log-phase growth.

3.3. Common methods

3.3.1. Cell Proliferation Measurement

Cell proliferation assays were conducted in order to evaluate the effect of the test compounds on tumor and non-tumor cell lines, following the protocol described previously by our laboratory (Pereira et al, 2007). Compounds wee added to each well of 48-well plate one day after cell seeding. Vehicle controls were also performed. Cells were harvested and cell density was determined by the sulforhodamine B (SRB) assay.

After SRB labelling, absorbance was measured in a spectrophotometer at 540 nm. The amount of released dye is proportional to the number of cells present in the sample, and is a reliable indicator of cell proliferation (Skehan et al, 1990).

3.3.2. Western blotting

3.3.2.1. Antibodies used

For Western blotting, primary antibodies used were NADH dehydrogenase (ubiquinone) 1 beta subcomplex, 8 (NDUFB8; 1:1000 dilution), iron–sulfur cluster (FeS; 1:1000); Cytochrome b-c1 complex subunit 2 (CIII-Core2; 1:1000), Cytochrome c oxidase subunit 2 (MT-COXII; 1:1000), Complex V, F1-alpha (CV-alpha; 1:1000), Cyclophilin D (Cyp D; 1:1000), Porin (1:1000) and Cytochrome c (Cyt c; 1:1000) from Mitosciences (Eugene, OR, USA); Mitofusin 1 (MFN1; 1:500), Complex V, Fo-ATPase (ATP5O; 1:1000) and voltage-dependent anion channel (VDAC; 1:1000) from Abcam (Cambridge, MA, USA); Adenine nucleotide translocase (ANT; 1:200) from Santa Cruz Biotechnology (San Diego, CA, USA). Cytochrome c oxidase subunit IV (COX IV; 1:1000), Hexokinase II (1:1000), heat-shock protein 90 (HSP90; 1:1000), human anti-Bax (1:1000), mouse anti-Caspase-8 (1C12; 1:1000), human rabbit anti-Caspase-9 (1:1000), rabbit anti-p53 (7F5; 1:1000), rabbit anti-Bcl-xl (54H6; 1:1000), rabbit Bcl-2 (50E3; 1:1000) and Apoptotic protease activating factor 1 (APAF-1; 1:500) from Cell Signaling (Beverly, MA, USA); mouse anti-β-Actin (A5441; 1:500) from Sigma (Saint Louis, MO, USA). The secondary antibodies used were goat anti-rabbit IgG-AP (sc-2007; 1:5000) and goat anti-mouse IgG-AP (sc-2008; 1:5000), both from Santa Cruz Biotechnology (San Diego, CA, USA).

3.3.2.2. Collection of total extracts from cells

For Western blot analyses, around $1.0x10^6$ cells were collected, including floating cells, ressuspended and added to lysis buffer (20 mM HEPES/NaOH, pH 7.5, 250 mM sucrose, 10 mM KCl, 2 mM $MgCl_2$, 1 mM EDTA) supplemented with 2 mM dithiothreitol (DTT), 100 mM phenylmethylsulfonyl fluoride (PMSF) and a protease inhibitor cocktail. Afterwards, extracts were sonicated and stored at -80C.

3.3.2.3. *Western blot procedure*

The protein concentration in cellular and mitochondrial extracts was determined by the Bradford assay, bovine serum albumin (BSA) as a standard. Fifty micrograms of total protein extract was separated by electrophoresis in a 12% SDS-PAGE gel, after denaturation at 95ºC for 5 min in Laemmli buffer, and electrophoretically transferred to PVDF membranes. After blocking with 5% milk or BSA, depending on antibody information, in TBST (50mM Tris-HCl, pH 8; 154mM NaCl and 0.1% Tween 20) for 3 hours at room temperature, membranes were incubated overnight at 4°C with specific antibodies. Membranes were washed three times with TBST for 5 minutes and incubated for 1 hour with respective secondary antibodies.

Afterward, membranes were reacted with the ECF detection system (Healthcare Life Sciences, Buckinghamshire, UK) and visualized using an enhanced chemiluminescence detection system (VersaDoc, from Bio-Rad). Densities for each band were calculated with the Quantity One Software (Bio-Rad).

3.3.3. Cell Cycle Analysis

Cell cycle progression was analyzed by using flow cytometry (Serafim et al, 2008). Cells in log-phase growth were treated with different concentrations of the tested compounds for various lengths of time. Adherent and floating cells were then collected and fixed with cold 70% ethanol and stored overnight at -20ºC. After washing and ressuspending in PBS-T (132 mM NaCl, 4mM KCl; 1.2mM NaH_2PO_4, plus 0.1% Tween) samples were incubated at 37ºC in 0.5 ml PBS-T with 20µg/ml RNAse for 45 min, and with Propidium Iodide at 37ºC, for a further period of 30 min. The percentage of cells in the different cell cycle phases was quantified in a flow cytometer (Becton-Dickenson FACScalibur), using Modfit LT software (Verity Software House, Topsham, ME, USA).

3.3.4. Vital Epifluorescent microscopy

For experiments involving phenolic and triterpenoids compounds the images were obtained using a Nikon Eclipse TE2000U epifluorescence microscope. Cell lines were seeded in 6-well plates with a glass coverslip per well, at a density of 5-10x10^4 and allowed to attach for 24 hours. Cells were then treated with either the test compound solutions or the vehicle for the desired time. 30 minutes prior the end of the exposure

time, the cultures were incubated with TMRM (100 nM) in a phosphate buffered saline solution (PBS: 132 mM NaCl, 4mM KCl, 1.2mM NaH_2PO_4) solution supplemented with 10% FBS. In phenolic acids assays, cells with labeled with Hoechst 33342, 1 mg/mL, in order to label nuclei and detect apoptotic chromatin condensation.

3.3.5. Total RNA Extraction

To extract total RNA, about $1x10^6$ cells were collected, and disrupted in 350µl of Buffer RLT from QIAGEN (RNeasy Protect Mini Kit). The suspension was homogenized, added to QIAshredder Spin Columns and centrifuged for 2 min at the highest velocity. Another centrifuge of 5min at 3000-5000xg was performed and supernatant transfer to RNeasy Mini Spin Columns with 350µl of ethanol 70%. A sequence of centrifugations was performed as described by the vender (RNeasy Mini Handbook from QIAGEN). Total RNA bound to the membrane and was then eluted in RNase-free water.

3.3.6. Determination mitochondrial gene expression

From previous RNA extracts, Reverse Transcription (RT) reaction was performed to obtain cDNA. This reaction was carried out before real-time PCR, where oligo-dT primers for RT and for PCR gene-specific primers were used. For real-time PCR a mix with 5µl of 2x GoTaq Master Mix solution (Promega, Inc.), 0.5µl of 5µM primer set (forward and reverse) and 3.5µl RNase-Free Water was prepared. To each well 10µl of prepared mix and 10ng of cDNA was added. A 1.5% TAE-agarose gel was prepared to run the products and after stained with ethidium bromide. 7900HT Fast Real-Time PCR System from Applied Biosystems by Life Technologies (Carlsbad, CA USA) was used for quantitative real-time PCR.The mitochondrial set of primers used, but also the nuclear encoded reference gene (*), were:

Primer	Sequence	MW
MT-ND1	F: 5'-ACGCCATAAAACTCTTCACCAAAG-3′	31.4
	R: 5'-TAGTAGAAGAGCGATGGTGAGAGCTA-3′	31.0
MT-ND5	F: 5′-AGTTACAATCGGCATCAACCAA-3′	29.5
	R: 5′-CCCGGAGCACATAAATAGTATGG-3′	29.6
MT-ND6	F: 5'-TGGATATACTACAGCGATGGC-3′	43.7
	R: 5'-AACCACCACCCCATCATAC-3′	58.4
MT-COXI	F: 5'-CTGCTATAGTGGAGGCCGGA-3′	33.8
	R: 5'-GGGTGGGAGTAGTTCCCTGC-3′	37.1
MT-COXIII	F: 5′-CCAATGATGGCGCGATG-3′	44.1
	R: 5′-CTTTTTGGACAGGTGGTGTGTG-3′	28.1
MT-CYB	F: 5'-CCAACATCTCCGCATGATGAAAC-3′	36.6
	R: 5' GTGGGCGATTGATGAAAAGG-3′	29.7
GAPDH*	F: 5′-GAAGGTGAAGGTCGGAGT-3′	42.8
	R: GAAGATGGTGATGGGATTTC-3′	36.8

The primers were ordered from IDT, Coralville, IA. The following experimental protocol was used: denaturation program (95^{o}C for 2min), amplification and quantification program repeated 35 times (95^{o}C for 30 s, 50^{o}C for 30s, 72^{o}C for 1min), melting curve program (72^{o}C with final heating rate of 0.1C/s and a continuous fluorescence measurement), and finally a cooling step to 40^{o}C. The crossing points for each transcript based on standard curves were mathematically determined.

3.3.7. Detection of CD24 and CD44 cell surface markers on breast cancer cells

Cell differentiation status was analyzed using cell surface markers CD24 and CD44 antibodies (BD Biosciences, Franklin Lakes, NJ, USA). Cells were trypsinized, washed once with cold buffer of PBS with 0.2%BSA and 0.1% sodium azide. After centrifugation at 300xg for 3 minutes, cells were ressuspended in a volume of 50µl with a final cell count of about 5x10^{5} cells per tube. To each cell pellet 10µl of antibody plus 40µl

of buffer solution was added and resulting samples were incubated for 30 minutes at 4°C in the dark. Cells were washed twice with 1ml of buffer and centrifuged at 300xg for 5 minutes. Samples were ressuspended in 1ml of buffer and analyzed by flow cytometry (Becton-Dickenson FACScalibur). The antibodies used are fluorochrome-conjugated, where CD24 is conjugated with FITC, detected at FL1, and CD44 is conjugated with APC, detected at FL3. Separate controls with FITC and APC added individually were performed.

3.3.8. Animals

Male Wistar-Han rats (10 weeks old) were housed in our accredited animal colony (Laboratory Research Center, Faculty of Medicine, University of Coimbra). Animals were group-housed in type III-H cages (Tecniplast, Italy) and maintained in specific environmental requirements (22 °C, 45-65 % humidity, 15-20 changes/hour ventilation, 12 h artificial light/dark cycle, noise level < 55 dB) and free access to standard rodent food (4RF21 GLP certificate, Mucedola, Italy) and acidified water (at pH 2.6 with HCl to avoid bacterial contamination). This research procedure was carried out in accordance with European Requirements for Vertebrate Animal Research and according to the ethical standards for animal manipulation at the Center for Neuroscience and Cell Biology.

3.3.9. Isolation of Rat Liver Mitochondria

Mitochondria were isolated from the livers of male Wistar rats by conventional differential centrifugation (Rolo et al, 2000). Livers were harvested and homogenized with buffer medium containing 250 mM sucrose, 10 mM HEPES (pH 7.4), 1 mM EGTA and 0.1% BSA lipid-free. The pH was adjusted to 7.2, EGTA and BSA being omitted from the final washing medium. The protein content was determined by the biuret method, using BSA as a standard (Gornall et al, 1949).

3.3.10. Oxygen Consumption

A Clark-type oxygen electrode connected to a suitable recorder in a 1 mL thermostated, water-jacketed and closed chamber was used to measure the oxygen consumption of isolated liver mitochondria (Oliveira et al, 2000). Mitochondria were

suspended at a concentration of 1.5 mg/mL in respiratory medium comprising 135 mM sucrose, 65 mM KCl, 2.5 mM $MgCl_2$, 5 mM KH_2PO_4, 5 mM HEPES (pH 7.2). The phenolic compounds were pre-incubated with mitochondria for 2 minutes before respiratory substrate. The respiratory substrates – glutamate/malate (5mM) or succinate (5mM) plus rotenone (3mM) – were added to the system to energize mitochondria, while ADP (83.3 nmol/mg protein) was used to induce state 3. In order to uncouple respiration and measure the maximal electron transfer rate through the respiratory chain, FCCP (1 μM) was added. The respiratory control ratio (RCR) is a measure of oxidative phosphorylation coupling and is calculated as the rate between state 3 and state 4. The ADP/O ratio represents the oxygen consumed during state 3 respiration and is an indication of the efficiency of the phosphorylative system (Chance et al, 1963).

3.3.11. Measurement of Mitochondrial Transmembrane Potential

The mitochondrial transmembrane potential ($\Delta\Psi$) was monitored indirectly, through the activity of the lipophilic cation tetraphenylphosphonium (TPP+), using a TPP+ selective electrode as previously described (Oliveira et al, 2001). Mitochondrial protein (1.5 mg) was suspended in reaction medium composed of 125 mM sucr.ose, 65 mM KCl, 5 mM KH_2PO_4, 2.5 mM $MgCl_2$ and 5 mM Hepes (pH 7.4, 30^{o}C), and supplemented with 3 μM TPP^+. Phenol compounds were added to mitochondria for 1 min, followed by 10 mM glutamate/malate or 10 mM succinate (plus 3μM rotenone). In order to initiate state 3, ADP (83.3 nmol/mg protein) was added. Assuming a Nernst distribution of the ion across the membrane electrode, the equation proposed by Kamo et al. (1979) yielded the values for transmembrane electric potential.

3.3.12. Induction of the mitochondrial permeability transition pore

The induction of the mitochondrial permeability transition (MPT) pore leads to mitochondrial swelling, which can be followed by the alterations in pseudo-absorbance of the mitochondrial suspension (Oliveira et al, 2004). The turbidity of the mitochondrial suspension was measured at 540nm in a JASCO V-560 spectrophotometer. Mitochondrial protein (1.5 mg/ml) was incubated at 30 ^{o}C, in a reaction medium containing 200 mM sucrose, 10 mM Tris-MOPS (pH 7.4), 10μM EGTA, 1 mM KH_2PO_4, 1.5 μM rotenone and 2.5 mM succinate, both in the absence and in the presence of the

phenolic compounds to be tested. Mitochondrial swelling was induced when calcium (20 μM) was added to the system, about 60 seconds later. As a control, cyclosporin A (1 μM), the specific MPT pore inhibitor (Broekemeier et al, 1989) was pre-incubated with the mitochondrial preparation in the presence of the highest concentration of the test compound observed to induce mitochondrial swelling.

3.4. Synthesis and Characterization of the Test Compounds

For the present work, three distinct classes of test compounds were used: phenolic compounds (Fig.7), triterpenoids (Fig.8) and benzophenanthrine alkaloids (Fig.9).

Transformation of the original parent compounds included modification of the liposolubility by altering the side chain either by amidation or esterification with alkyl substituents of different lengths and charge. The phenolic cinnamic derivatives were identified by both nuclear magnetic resonance (NMR) and electron impact-mass spectrometry (EI-MS) (data not shown). Synthesis of the phenolic compounds was performed at the Molecular Physical-Chemistry Research Unit, Faculty of Life Sciences, University of Coimbra; Pharmaceutical Chemistry Group, Faculty of Pharmacy, University of Coimbra, Portugal and at the Department of Chemistry and Biochemistry, Faculty of Sciences, University Porto, Portugal (Fig.7).

Triterpenoids used were synthesized using as basic natural pecursors betulin and betulinic acid at the National Resources Research Institute at University of Minnesota, Duluth, USA (Fig.8). Betulin was isolated from the extract of outer birch bark of *Betula papyifera* and Betulinic acid were converted to dimethylaminopyridine (DMAP) derivatives through intermediate acylation of corresponding hydoxy groups with bromoacids and chloroacids. Both protocols, isolation and synthesis, follow as described in Holy et al. 2010. All the compounds prepared were completely characterized by melting point, infrared (IV), nuclear magnetic resonance (1H NMR and 13C NMR) and mass spectrometry (MS) (data not shown).

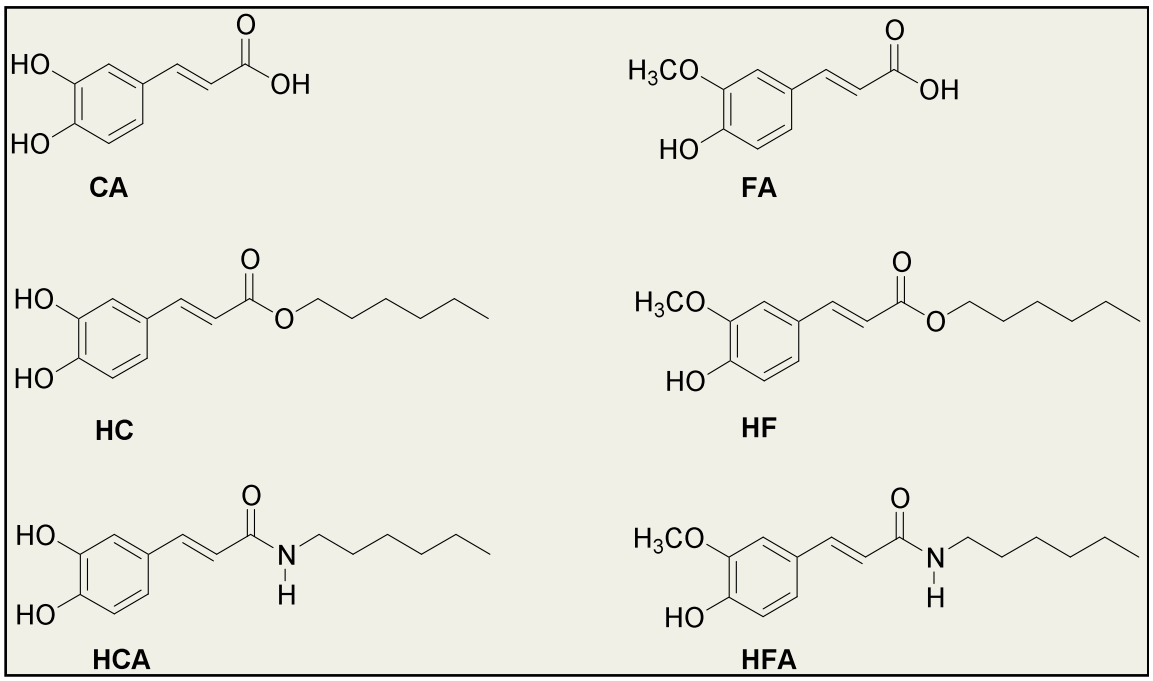

Fig.7 - Chemical structure of hydoxycinnamic parent compounds and derivatives. CA: Caffeic Acid, mw 180.7; FA: Ferulic Acid, mw 194.19; HC: Hexyl caffeate, mw 264.322; HF: Hexyl ferulate, mw 278.35; HCA: Caffeoylhexylamide, mw 263.34; HFA: Feruloylhexylamide, mw 277.35.

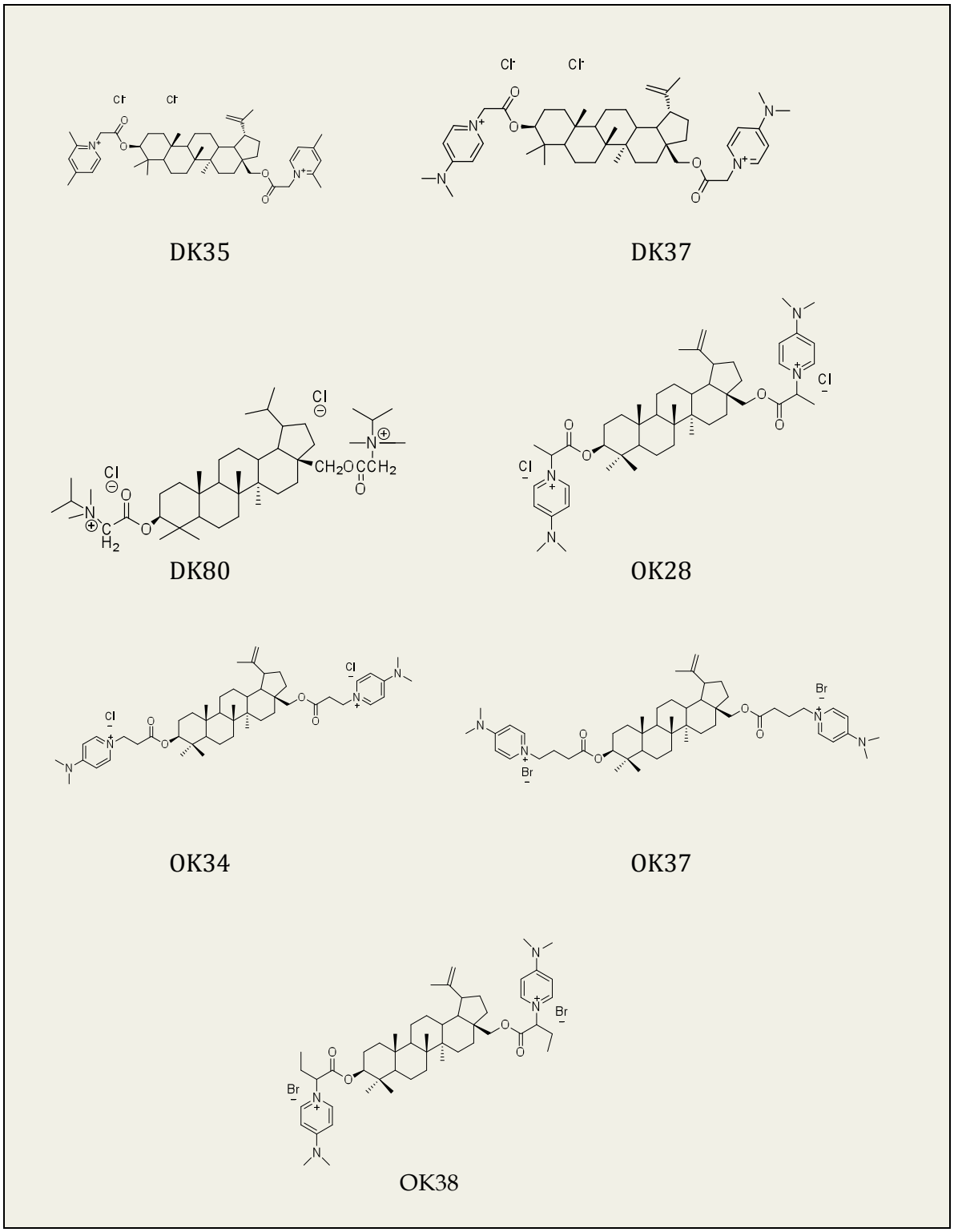

Fig.8 - Chemical structure of Triterpenoids compounds: betulin and betulinic acid derivatives (DK35 mw 809.986; DK37 mw 840.016; DK80 mw 801.084; OK28 mw 868.07; OK34 mw 868.07; OK37 mw 985.02 and OK38 mw 985.02).

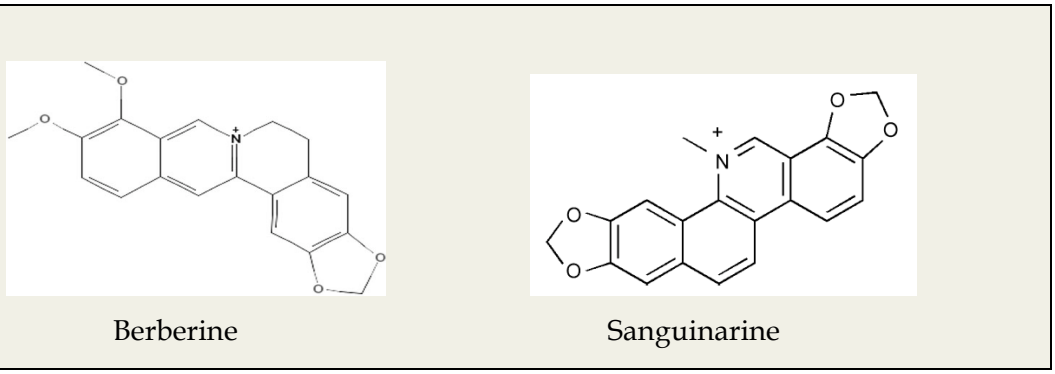

Fig.9 - Molecular structures of Berberine (mw 371.81) and Sanguinarine (mw 367.78). Both compounds were acquired from Sigma Chemical Co. (St Louis, MO, USA; Sintra, Portugal).

3.5. Characterization of breast cancer cells

3.5.1. Analysis of mitochondrial D-loop

Total DNA was extracted from cells using ZymoBead Genomic DNA Kit (CA, USA). The technique consists in using beads to capture DNA, at which follows a sequence of centrifugations and washing steps to obtain purified DNA.

Each DNA sample underwent PCR amplification for D-loop region using primer set Mitout-F (5′- cccaactaaatactaccgtatgg -3′), Mitout-R (5′-ggctcaggcgtttgtgtatgat -3′), Mitin-F (5′-ctgagccttttaccactccag-3′) and Mitin-R (5′-ggtgattgatactcctgatgcg-3′), using the cycle conditions described in Wheelhouse et al. (2005). Mitin primer has only product of 142bp, which represents wild-type mtDNA (no deletions), while Mitout primer has 214bp PCR product correspondent of altered mtDNA. For D-loop analysis a mix with 5µl of 2x GoTaq Master Mix solution (Promega, Inc.), 1µl of 2µM primer set (forward and reverse) and 3µl RNase-Free Water was prepared. To a final volume of 10µl prepared mix 10ng of cDNA was added. Finally, PCR products were run on a 2% of agarose gel, and stained with ethidium bromide and visualized at UV light.

3.5.2. Fluorescent phagokinetic migration assay

Cell motility was evaluated according the protocol optimized by Windler-Hart et al. (2005). Briefly, the breast cancer cells were plated in tissue culture plates pre-treated with 50µg/ml poly-D-Lysine (30 min at room temperature) and coated with 1µM diameter red fluorescent carboxylate-modified microspheres (Fluospheres carboxylated-

modified microspheres from Invitrogen F8821, 0.005% suspendend in PBS) for 2 hours at room temperature. After coating with the fluorescent beads, tissue culture plates were rinsed twice with PBS and cells were plated at a density of 7 cells/mm^2 in DMEM supplemented with 10% FBS, in presence of glucose or galactose. After incubation period (18-20 hours) cells were fixed and stored in 4% paraformaldehyde in PBS at 4ºC. Cell motility was evaluated microscopically, using an epifluorescence Nikon Eclipse TE2000U microscope equipped with 10X Plan Fluor 0.6NA phase contrast objective and by flow cytometry using a Becton-Dickenson FACScalibur flow cytometer with FL2 fluorescence sensor. For flow cytometry, cells were harvested by tripsinization and spun at 250xg for 5 min at room temperature. Cells were also rinsed with PBS and fixed and stored in 4% paraformaldehyde in PBS at 4ºC until analyzed. Images from microscopy were obtained using Metamorph software (Universal Imaging, Downingtown, PA). The average of cells fluorescent intensity was calculated using the cytometer CellQuest software package.

3.5.3. Evaluation of Mitochondrial Membrane Potential of Cell Lines

Vital confocal microscopy (LSM 510 Meta, Carl Zeiss) and flow cytometry were the two techniques to evaluate the differential of mitochondrial membrane potential of the cell characterization study. For microscopy cells grown in galactose and glucose media were seeded in 6-well plates with a glass coverslip per well, at a density of 5-10x10^4 and allowed to attach for 24 hours. 30 minutes prior the end of the exposure time, the cultures were incubated with TMRM (100 nM) in a microscopy solution (120mM NaCl; 3.5mM K; 0.4mM KH_2PO_4; 20mM HEPES; 5mM $NaHCO_3$; 1.2mM $NaSO_4$ and 10mM pyruvate at pH 7.4) supplemented with 1.2 mM $MgCl_2$, 1.3mM $CaCl_2$ and 5% FBS.

For flow cytometry, cells were treated under the same condition as for microscopy, including media and cell diluition. 30 minutes prior flow analysis, cells were trypsinised and ressuspended and incubated, at 37C and 5%CO2, in 500µl of microscopy solution with 5%FBS and 100nM TMRM. The median cell number was quantified in flow cytometer (Becton-Dickenson FACScalibur, ME, USA).

3.5.4. Intracellular Adenine Nucleotides

For the evaluation of intracellular concentration of adenine nucleotides, the media was removed and cells were collected in perchloric acid solution. By centrifugation supernatant, with adenine nucleotides, was separated from the pellet, the cells. The supernatant was neutralized and analyzed by reverse-phase high performance liquid chromatography, to quantity adenine nucleotides. The chromatographic apparatus was Beckman-System Gold (Beckman Coulter, Fullerton, CA), consisting of a 126 Binary Pump Model and a 166 Variable UV detector, computer-controlled. Detection was performed by an ultraviolet detector at 254 nm and the column was a Lichrospher 100RP-18 (5 μm) from Merck (Dramstadt, Germany). Samples were eluted with 100 mM phosphate buffer (KH_2PO_4), pH 6.5, and 1% methanol with a flow rate of 1.1 ml/min. NaOH 1M was added to the pellet and protein concentration was measured by the Bradford assay, using BSA as a standard. Energy charge was calculated as ([ATP] + 0.5 [ADP])/([ATP] + [ADP] + [AMP]).

3.6. Investigation on Mitocans

3.6.1. Triterpenoids

3.6.1.1. Microarray Gene Expression Analysis

HS578T cells were exposed to 0.5μg/ml of OK34 for 48 hours and collected afterwards. The protocol described previously for RNA extraction was followed and RNA concentration determined. RNA purity was verified using Agilent Technologies, Eukaryote Total RNA Nano assay.

The microarray hybridization was done at the Biomedical Image Processing Laboratory (BIPL) of the University of Minnesota, USA, using the Human Genome U133 Plus 2.0 Chip (Affymetrix, Inc.), which contains about 47 000 transcripts, from nuclear encoded genes.

Experiments were done in triplicate. Raw data files were imported into JMP Genomics (SAS; RTP, NC) for quality control, normalization and analysis including hierarchical clustering. Pathway analysis was performed on the significant data sets using Ingenuity Pathway Analysis (Ingenuity; Redwood City, CA).

3.6.1.2. Combination Effect of Chemotherapeutics

HS578T breast cancer cells were exposed to triterpenoids alone or in conjugation with commercial compounds, including Taxol, Doxorubicin and Cisplatin. $1x10^4$ cells/ml were seeded in 48-well plate and 24 hours later were incubated with the compounds for three days at 25% of inhibitory cell growth concentration of each drug. Cell density analysis by SRB was performed as mentioned above.

3.6.2. Benzophenanthrine Alkaloids

3.6.2.1. Collection of mitochondrial extracts from K1735-M2 cells

For subcellular fractionation, cells were harvested as described above and resuspended in homogenization buffer (250 mM sucrose, 20 mM K^+, HEPES pH 7.5, 10 mM KCl, 1.5 mM $MgCl_2$, 0.1 mM EDTA, 1 mM EGTA) supplemented with 1 mM DTT, 100 mM PMSF and protease inhibitor cocktail (containing 1 mg/ml of leupeptin, antipain, chymostatin and pepstatin A). Cell homogenization was performed in a Potter–Elvehjem homogenizer with Teflon pestle. The homogenate was subjected to sedimentation at 220x g during 5 min at 4°C. The supernatant, containing mitochondrial fraction, was centrifuged again at 14,000x g during 10 min at 4 °C. The pellet, corresponding to the mitochondrial fraction was resuspended in 50 ml of homogenization buffer. Samples were stored at -80°C until used. Protein contents were determined by the Bradford method.

3.6.2.2. Caspase-like Activity Assay

Total cellular extracts were collected as described above (3.9.1.) and protein contents were assayed using the Bradford method. To measure caspase 3 and 9-like activity, aliquots of cell extracts containing 25 mg (for caspase 3) or 50 mg (for caspase 9) were incubated in a reaction buffer containing 25 mM HEPES (pH 7.4), 10% sucrose; 10 mM DTT, 0.1% CHAPS and 100mM caspase substrate (Ac-DEVD-pNA for caspase 3 or Ac-LEHD-pNA for caspase 9, purchased from Calbiochem, NJ, USA) for 2 h at 37 8C. Caspase-like activities were determined by following the detection of the chromophore p-nitroanilide after cleavage from the labelled substrate Ac-DEVD-p-nitroanilide or Ac-

LEHD-p-nitroanilide. The method was calibrated with know concentrations of p-nitroanilide (purchased from Calbiochem, NJ, USA).

3.6.2.3. Measurement of berberine and sanguinarine cellular uptake

For time-course studies, berberine (100μM) was added to dishes of K1735-M2 cells 360, 300, 240, 180, 120, 60 and 30 min prior to harvesting by trypsinization. Cells were resuspended in PBS-5% FC3, and immediately measured with a Becton-Dickenson Flow cytometer, using the FL1 filter set. For dose-response studies, a range of berberine concentrations (12.5–150μM) was added to dishes of K1735-M2 cells 2.5 h prior to trypsinization, resuspension in PBS-5% FC3, and measurement with the flow cytometer. The same protocol was used for sanguinarine, where cells were exposed for 150 min with 1.25, 2.5, 5, 10 and 20 μM of SANG. For all samples, approximately 15 min were elapsed between removal of compound-containing culture media and the measurement of berberine and sanguinarine fluorescence intensities.

3.6.2.4. Quantification of cell death by flow cytometry

After alkaloid (Berberine or Sanguinarine) or DMSO (vehicle-only control) treatment, cell culture media was collected from the samples and saved. Cells were trypsinized, and added back to the collected media in order to collect both adherent cells as well as non-adherent (dead and dying) cells floating in the media. Cells were collected by centrifugation and resuspended in PBS containing 5% fetal bovine serum. Components of the live/dead kit (calcein-AM and ethidium homodimer) were added according to manufacturer's instructions, and cells incubated at 37°C for 15 min. The FL1 (calcein, green) signal and FL3 (ethidium, red) signal were measured with a Becton-Dickenson FACScalibur Flow cytometer. The red-fluorescing cells were separated from the green- fluorescing cells and counted using the cytometer Cell Quest software package.

3.6.2.5. M-phase Quantitation

To quantify the percentage of cells in M-phase, K1735-M2 cells were seeded onto glass coverslips and grown in the presence of 100 μM berberine (or an equivalent amount of DMSO only) for 24 h. Cells were then fixed in freezer-temperature absolute

methanol, and subsequently immunolabeled using a monoclonal antibody to β-tubulin (E7; Developmental Studies Hybridoma Bank, Iowa City, IA, USA), followed by a goat-anti-mouse-Texas Red secondary-antibody (Jackson Immunoresearch, Malvern, PA, USA). Chromatin was counterstained by adding Hoechst 33258 to the secondary antibody at 5 μg/ml.

Cells were examined by epifluorescence microscopy to identify M-phase cells, which were easily identifiable as rounded cells containing mitotic spindles and condensed chromatin. For quantitation, random fields of view were selected, and both the total number of cells and the number of M-phase cells counted. At least five fields of view were counted for each sample, with a total of 500 cells counted per sample.

3.6.2.6. BrdU Labeling

At various time points after the addition of berberine (or DMSO vehicle only), cells were pulse-labeled with 10 μM bromodeoxyuridine (BrdU; Sigma Chem. Co.) for 30 min and then fixed in cold (-20°C) absolute methanol. For BrdU labeling, cells were rehydrated with PBST and treated with 2 N HCl for 20 min at room temperature. Cells were then washed five times with PBST, and incubated in PBST containing 0.5% non-fat powdered milk for 30 min at 37°C. Cells were immunolabeled and counterstained with Hoechst as described above, using a labeled anti-BrdU antibody (G3G4, Developmental Studies Hybridoma Bank).

Evaluation of mitochondrial effects of berberine K1735-M2 and WM793 cells were seeded in 35 mm glassbottom petri dishes as described above, and subsequently treated with either 25 μM berberine or vehicle only (0.1% DMSO) for 6 h. Hoechst 33342 and tetramethylrhodamine methyl ester were added to 2 μg/ml and 100 nM, respectively, and the dishes incubated for 30 min prior to examination by epifluorescence microscopy. All TMRM images from control and berberine-treated samples were taken at the same exposure times and processed identically in order to compare fluorescence intensities.

3.6.2.7. Identification of intracellular berberine localization by confocal microscopy

Cells treated with berberine were seeded into 35 mm glass-bottom petri dishes (MatTek Inc., Amherst, MA, USA) at a density of $1x10^4$/ml, and allowed to recover for

24 h prior to use. A range of concentrations of berberine and was added to the dishes; after 2 h, the dishes were removed from the incubator and placed on the stage of a Nikon C1 laser-scanning confocal microscope. Laser excitation and photomultiplier (PMT) gain were set at values to best visualize the range of fluorescence emitted by cultures treated with 12.5–150μM berberine. Berberine fluorescence was imaged using a Spectra Physics Krypton-Argon Model 163C polarized laser (40 mW at 488 nm) and a 545 nm dichroic long pass, with a 605/75 band pass for the red channel (PMT 2). All pictures were obtained and processed using identical settings in order to directly compare differences in fluorescence intensity or localization patterns.

3.6.2.8. Vital Epifluorescent Imaging for sanguinarine toxicity and localization

Sanguinarine accumulation was studied by using the compound self-fluorescence, and analysing cells under a Nikon Eclipse TE2000U epifluorescence microscope using the fluorescein filter. A short time of exposure was used as SANG selffluorescence decayed rapidly with light exposure. 100 nM TMRM was incubated with cells 30 min before the end of the exposure time. Before the ending the drug exposure time, cells in glassbottom dishes were incubated with TMRM (100 nM), Hoechst 33342 (1 mg) and calcein-AM (300 nM) for 30 min at 37 8C in the dark. Due to the very low fluorescence of the probes in the extracellular media, the images were collected without replacing the cell culture media. The images were obtained using a Nikon Eclipse TE2000U epifluorescence microscope.

3.6.2.9. Determination of Mitochondrial DNA Copy Number

Total genomic nuclear and mtDNA from K1735-M2 cells was isolated using the GenElute Mammalian Genomic DNA Miniprep Kit (Sigma-Aldrich). Standard curves were generated from the control DNA sample using serial dilutions. Quantitative real-time PCR using the LightCycler system (Roche Diagnostics, Indianapolis, IN) was performed, and the following reaction components were prepared: 3.6 μl of water, 0.2 μl of forward primer (0.2 μM), 0.2 μl of reverse primer (0.2 μM), and 5.0 μl of LightCyler (Roche Diagnostics).

LightCycler mixture (9 μl) was filled in the LightCycler glass capillaries, and 1 μl of DNA sample (2 ng) was added as PCR template. 5COXI and 3COXI are mtDNA

primers (Thundathil et al., 2005), and MuRTGADD45a (5'-ACCCCGATAACGTGGTACTG-3') and MuGADD45R (5'-TGACCCGCAGGATGTTGATG-3') are mouse GADD45 genomic DNA primers that sit in exon 3. Capillaries were closed, centrifuged, and placed into the LightCycler rotor. The following LightCycler experimental run protocol was used: denaturation program (95°C for 30 s), amplification and quantification program repeated 50 times (95°C for 5 s, 60°C for 20 s, 72°C for 20 s), melting curve program (95–45-95°C with a final heating rate of 0.1°C/s and a continuous fluorescence measurement), and finally a cooling step to 40°C. The crossing points for each transcript based on the standard curves were mathematically determined.

3.6.2.10. Determination of Oxidative Stress in Live Cells

Vital imaging of oxidative stress in K1735-M2 was determined according to the protocol by Sardao et al. (2007). Cells seeded in glass-bottom dishes were incubated with 7.5 mM CMH2DCFDA (Molecular Probes, Invitrogen, Carlsbad, CA) for 1 h at 37°C in the dark. Media was then replaced by new pre-warmed DMEM and cells were returned to the incubator for another hour. Media was then again replaced by 2 ml of Krebs buffer (1mM $CaCl_2$; 132mM NaCl; 4mM KCl; 1.2mM Na_2HPO_4; 1.4mM $MgCl_2$; 6mM glucose; 10mM HEPES, pH 7.4). Cells were observed by epifluorescence microscopy using a Nikon Eclipse TE2000U microscope (fluorescein filter) and images were obtained using Metamorph software (Universal Imaging, Downington, PA).

3.6.2.11. Immunocytochemistry for Phosphorylated H2AX Histone (H2AXγ)

K1735-M2s grown on glass coverslips were treated with 2 mM SANG; controls received an equivalent amount of DMSO (vehicle only). After a 16 h exposure, cells were loaded with Mitotracker Red, 1:10,000 dilution from a 1 mM stock solution (Molecular Probes, Invitrogen, Carlsbad, CA) which was added directly to the culture medium for 45 min. Cells were then fixed in 2% paraformaldehyde in PBS for 5 min at room temperature, and subsequently transferred to ice-cold methanol and stored in a freezer overnight. After rehydration in PBST, coverslips were blocked with 1% powdered milk in PBS-T for 30 min at 37°C, and incubated in a mouse monoclonal antibody to phosphorylated histone H2AX (H2AXγ; Upstate, Cell Signalling, Piscataway, NJ) for 1 h

at 37°C.

Following three PBS-T washes, cells were incubated in goat anti-mouse IgG conjugated to fluorescein (1:10,000, Jackson Immunoresearch) (Cell Signalling, Piscataway, NJ) and Hoechst 33258 (5 mg/ml) for 1 h at 37°C, washed again in PBS-T, and mounted in anti-fade medium (90% glycerol, 10% CAPS buffer, pH 9.0, and 0.1% phenylenediamine).

3.7. Statistics

Data was loaded to GraphPad Prism 4.0 program (GraphPad Software, Inc.), all results being expressed as means ±SEM, and analysed by t-student to compare two groups, one-way ANOVA with Bonferroni multiple comparison post-test to compare groups with one independent variable, while for two independent variables, two way ANOVA was used. Values with $p<0.05$ were considered as statistically significant.

IV - Results

4. Results

4.1. Characterization of mitochondrial physiology in breast cancer cell lines

4.1.1. Background and Objective

Proliferative cells normally generate a significant portion of their ATP via glycolysis, regardless the amount of oxygen present or mitochondrial integrity. Even if glycolysis is less efficient in generating ATP, it does it at faster rates than oxidative phosphorylation (Heiden et al., 2009). Therefore, glycolysis seems to provide metabolic advantages to cancer cells, with mitochondria having now a critical role of providing TCA cycle intermediates to synthesize new lipids and nonessential amino acids (DeBeradinis et al., 2008). Different research groups have described an up-regulation of glucose transporters, glycolytic enzymes, trans-activation of pyruvate dehydrogenase kinase 1, and consequent down regulation of oxidative phosphorylation (OXPHOS) mediated by inhibition of pyruvate dehydrogenase in cancer cells (Papandreou et al., 2006). Knowing the important role of mitochondria in certain cellular functions, such as cell death regulation, it is not surprising that these organelles have been implicated in cancer (Fulda et al, 2010). Thus, comparatively to normal cells, it is suggested that cancer cells present differences in terms of mitochondrial physiology that can contribute to the general metabolic remodeling observed in cancer cells (Rossignol, 2004).

The objective of the present chapter was to characterize several commercial human breast cancer cell lines in terms of mitochondrial physiology trying to establish a rationale on how such alterations can impact cancer cell resistance to chemotherapeutics and overall aggressive behavior. For the present objective, the human breast cancer cell lines MCF-7 (adenocarcinoma; ER, PR and Herb2 positive), MDA-MB-231 (adenocarcinoma, ER, PR and Herb2 negative) and HS 578T (carcinosarcoma, ER, PR and Herb2 negative) were studied (Neve et al, 2006) and compared with a normal fibroblast cell line (BJ).

4.1.2. Results

4.1.2.1. Alterations in mitochondria structure and ATP content are observed in cancer cells

We started by assessing mitochondrial transmembrane potential, since it has been reported that mitochondria in some types of cancer have an intrinsic higher transmembrane electric potential than normal cells (Chen L, 1988). From our data, we confirmed a higher membrane potential in cancer versus normal cells, although only MCF-7 cells showed a statistically significant difference (Fig.10A). When measuring intracellular [ATP]/[ADP] ratios, no differences were observed for MCF-7 and MDA-MB-231 breast cancer cells when compared with normal BJ cells (Fig.10B), with only HS578T cell line showing a lower ratio comparatively to non-tumor cells. Nevertheless, the energy charge, calculated as [ATP] + 0.5 [ADP])/([ATP] + [ADP] + [AMP], did not differ among cell lines: BJ (0.863 ± 0.024), MCF-7 (0.877 ± 0.031), HS 578T (0.709 ± 0.025) and MDA-MB-231 (0.803 ± 0.016). Further analysis of mitochondria network morphology by TMRM-labeling imaged by confocal microscopy (Fig.10C) revealed that while in BJ fibroblasts, mitochondria appear to be organized as a filamentous network, morphology is more diverse in cancer cells, although predominant perinuclear clusters are visible.

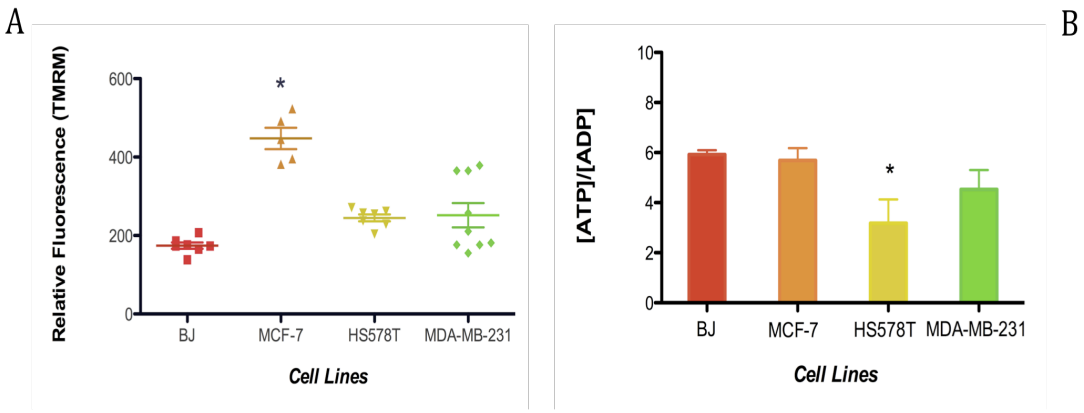

C

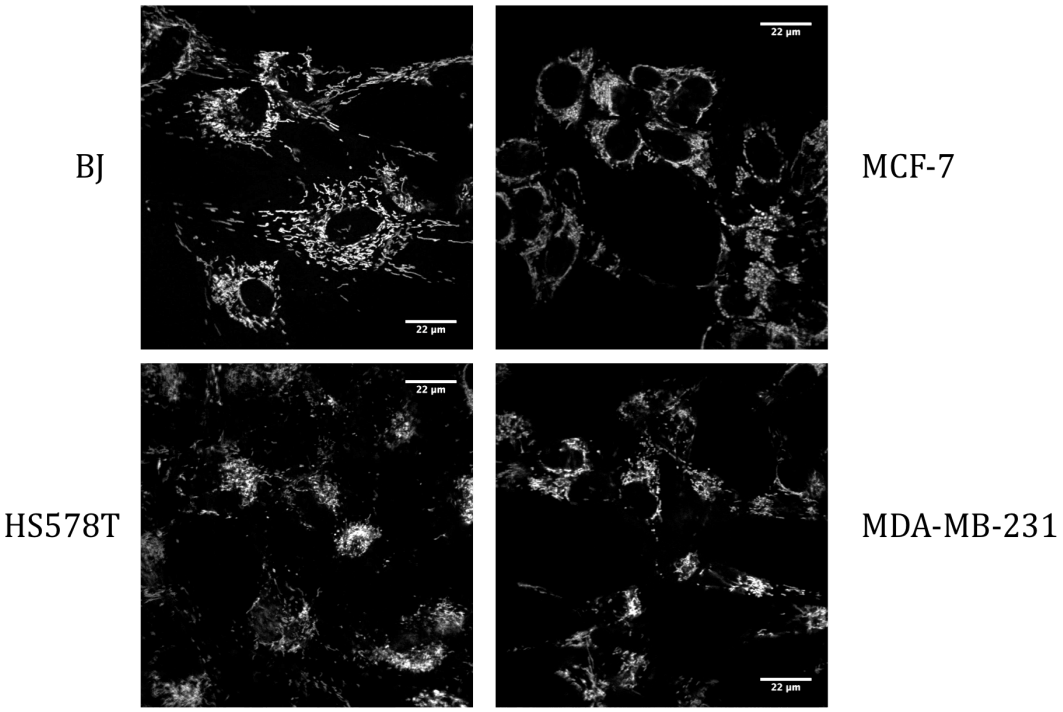

Fig.10 - The mitochondrial physiology in breast cancer cells. (A) FACS analysis of mitochondrial membrane potential of normal human fibroblasts BJ, and breast cancer MCF-7, HS578T and MDA-MB-231 cell lines cultured in glucose medium. Data shown are means ± S.E.M. of seven independent experiments. (*) Significant difference compared to BJ cell line ($p< 0.05$). **(B)** Base line [ATP]/[ADP] ratio of the cell lines studied. The results are representative of four separate experiments. (*) Significant difference compared to BJ cell line ($p< 0.05$). **(C)** Confocal micrographs showing the mitochondrial network of the different cell lines, where mitochondria were labeled by the polarization-dependent probe TMRM.

4.1.2.2. Cell type-dependent alterations in mtDNA and oxidative phosphoulation proteins

Morphology and functional mitochondrial differences can also involve differential expression of mitochondria respiratory chain complexes. By western blotting, we detected that nuclear encoded proteins, such as UQCRC2 (complex III) and ATP synthase-F1α are less present in HS578T, while the most surprising result was the fact that the ATPase-Fo subunit had a lower content in all three cancer cells studied (Fig.11). Only NDUFB8, a complex I subunit, did not show any variation between the cells studied, while FeS, a complex II subunit, was shown to be more expressed in MDA-MB-231. HS 578T cells were also shown to have lower content of mitochondrial encoded COX II (cytochrome c oxidase, subunit II), but no significant variations were detected in the only subunit encoded by the nuclei, COX IV (cytochrome c oxidase subunit IV).

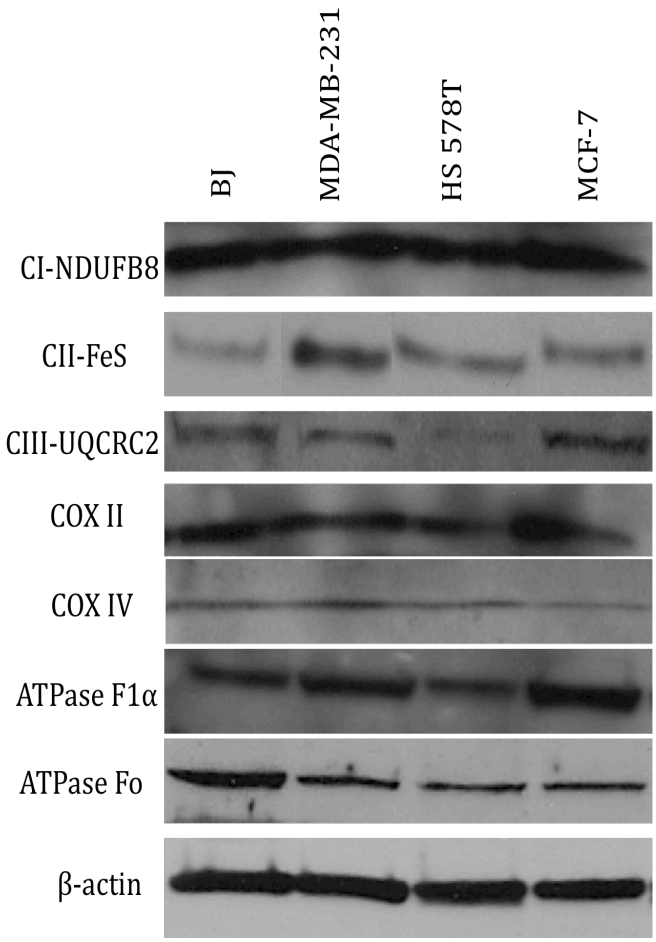

Fig.11 - Detection by Western Blotting of mitochondrial phosphorylation oxidative chain proteins. Western blotting was used to detect NDUFB8 (subunit of complex I), FeS (subunit of complex II), UQCRC2 (subunit of complex III), COX II (complex IV, subunit II), CV-F1α (ATPase, subunit F1α) and ATP5O (ATPase subunit Fo) in total fractions from BJ fibroblasts and breast cancer MDA-MB-231, MCF-7 and HS 578T cell lines. β-actin was used as loading control. The results are representative of 4 separate assays.

We further analyzed mitochondrial DNA (mtDNA)-encoded proteins by qRT-PCR, and we found out that transcripts for complex I ND5 and ND6 subunits were more present in MCF-7 cells, while COX I transcripts were lower for MDA-MB-231 and COX III for HS 578T cells (Fig.12).

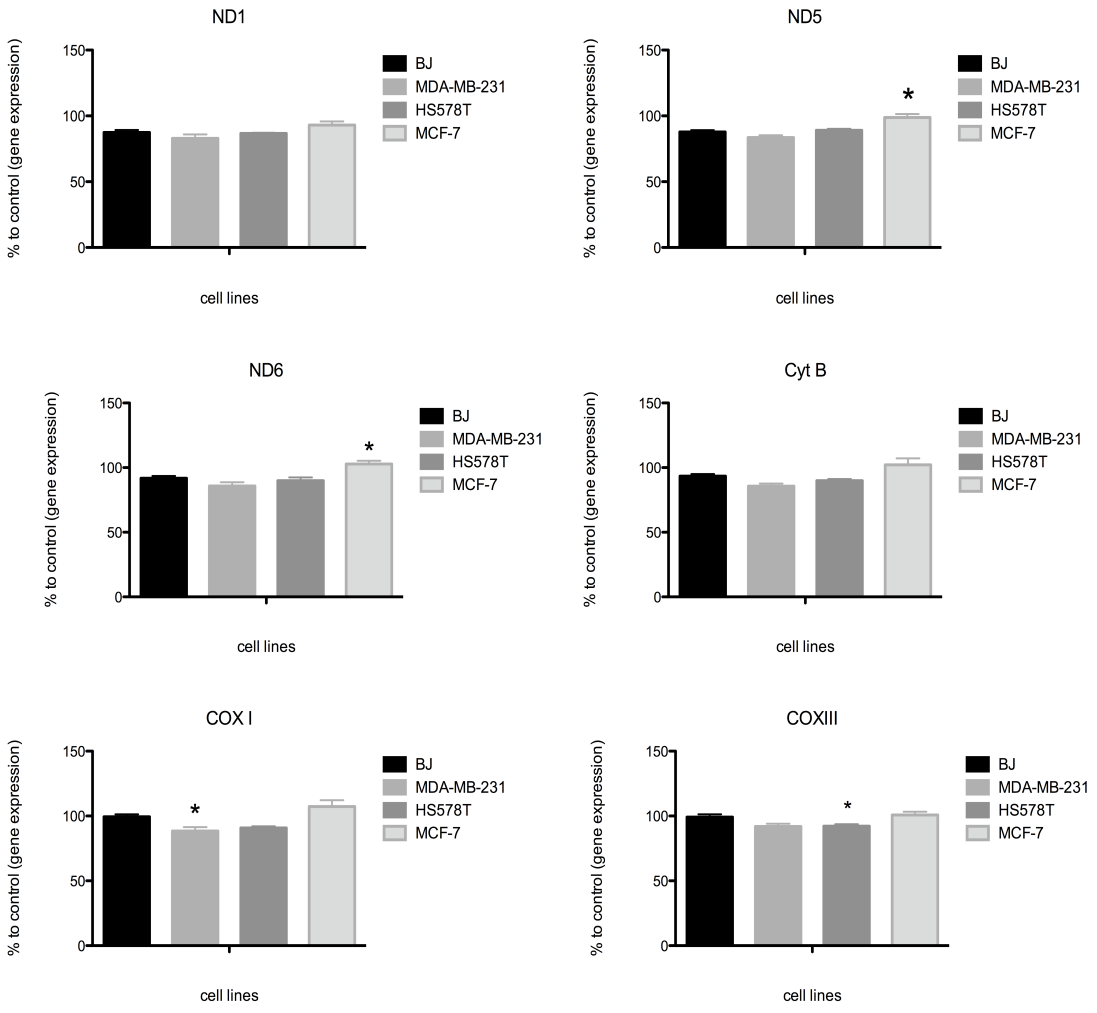

Fig.12 - Differences in mitochondrial mRNA expression. mRNA from mitochondria DNA, namely MT-ND1 (complex I), MT-ND5 (complex I), MT-ND6 (complex I), MT-CytB (complex III), MT-COXI (complex IV) and MT-COXIII (complex IV) were measured from all cell lines in study, BJ, MDA-MB-231, MCF-7 and HS578T, determined by Real-time PCR. mRNA of nuclear encoded gene GAPDH was used to normalize variability in template loading. The graph bars correspond to the average of four independent experiments, with standard error of the mean ± S.E.M. (*) Significant difference from BJ cell line ($p < 0.05$). The results are expressed as a percentage of the control (BJ) cells.

mtDNA contains a very instable region, where mutations have been found in cancer cells (10). This region is named displacement loop (D-loop) and is a major control site for mtDNA replication (Wheelhouse et al, 2005). We did not identify the 4977bp common deletion (determined by the presence of a 214bp band) in the D-loop region (Fig.13).

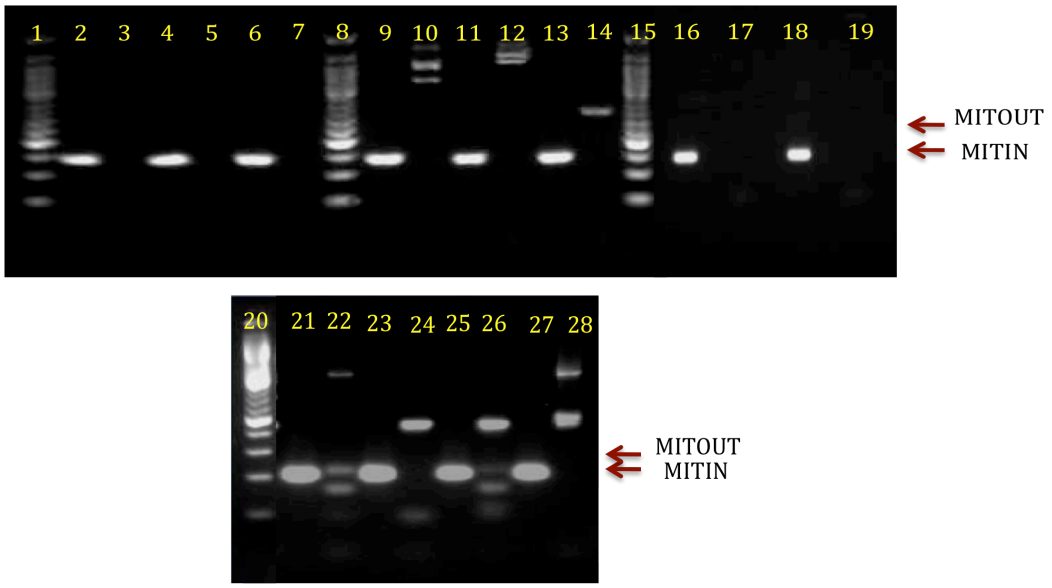

Fig.13 - Cancer cells show no alterations in D-loop region. Frequency of PCR products derived from using MITIN (142bp) and MITOUT (214bp) primers: (2, 4, 6 – MITIN and 3, 5, 7 – MITOUT) normal BJ cell line; (9, 11, 13 – MITIN and 10, 12, 14 – MITOUT) MDA-MB-231; (16, 18 – MITIN; 17, 19 – MITOUT) HS 578T and (21, 23, 25, 27 –MITIN and 22, 24, 26, 28 –MITOUT) MCF-7 breast cancer cells. (1, 8, 15, 20) correspond to 50bp ladder.

4.1.2.3. Analysis of proteins involved in the mitochondrial apoptotic pathway

As mentioned before (chapter I), one of the hallmarks of cancer is evasion from apoptosis (Hanahan and Weinberg, 2011). By western blot, it is seen that Bax protein is less present in samples from breast cancer cells, while Bcl-2 showing no significant alterations in two of the breast cancer cells studied, namely MDA-MB-231 and HS578T cells (Fig.14).

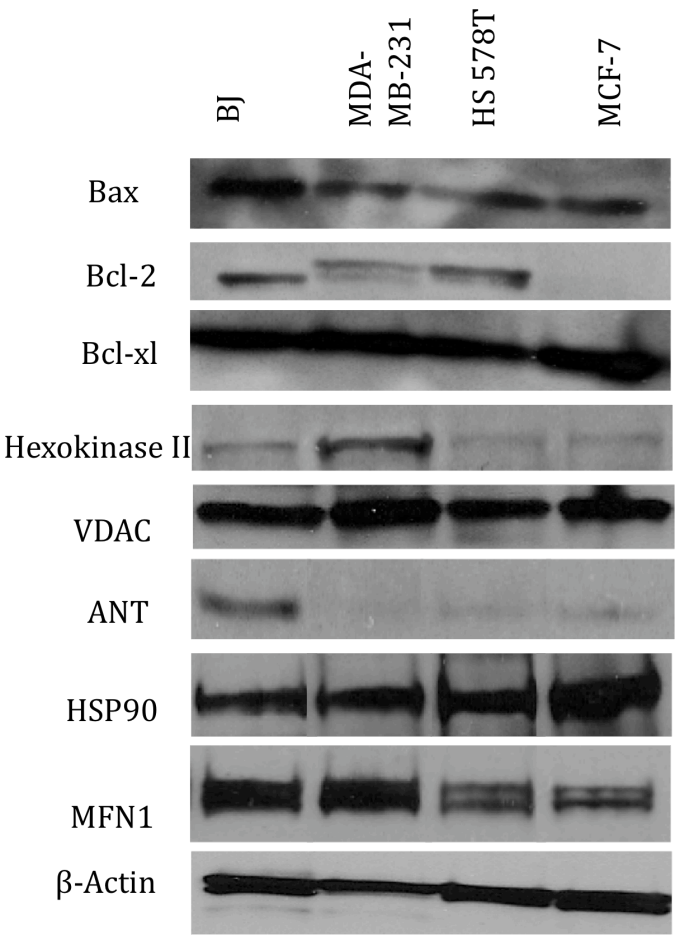

Fig.14 - Detection by Western blotting of proteins involved in cell death. Western blotting measurement was performed to detect protein associated with cell death such as Bax, Bcl-2, Bcl-xl, Hexokinase II, VDAC, ANT, HSP90 and MFN1 and normalized with β-actin of the three breast cancer cell lines and BJ normal cells. The results are representative of three-four independent experiments.

Interestingly, Bcl-2 protein was not detected in MCF-7 cells, however, an analog protein, Bcl-xl, was found to be present in higher levels in MCF-7 cells, with the same occurring in MDA-MB-231 cells (although in a lower extent). Moreover, hexokinase II and VDAC, both proteins that are describe to interplay in the MOM, were detected in higher levels in MDA-MB-231 cells. Interestingly, a lower amount of ANT was observed in those cells, when compared with BJ fibroblasts. Two other proteins were analysed. One of them, MFN1, is involved in the process of mitochondrial fusion (Huang et al, 2011), while HSP90, a mitochondrial chaperon is involved in the protection against

oxidative stress and apoptosis in cancer cells (Kang et al, 2007). HS578T and MCF-7 cells had a deceased content in MFN1, while HSP90 presented higher levels in all cancer cell lines studied, especially in MCF-7.

4.1.2.3. Mitochondrial adaptation in galactose/glutamine media – the shift to OXPHOS

Cancer cells are metabolic adapted to use glycolysis to obtain energy, even in the presence of O_2 (Koppenol et al, 2011). Thus, a set of experiments was performed to evaluate the re-adaptation to OXPHOS metabolism in the different cell lines, by replacing glucose for galactose and supplementing the media with glutamine. Contrarily to glucose experiments, cells grown in galactose/glutamine media showed larger alterations in terms of their mitochondrial membrane potential. Normal cells seem to maintain roughly the same mitochondrial membrane potential after the transition from glucose and galactose/glutamine media, while cancer cells showed a dramatic decrease in this parameter, especially HS578T and MDA-MB-231 cell lines (Fig.15A).

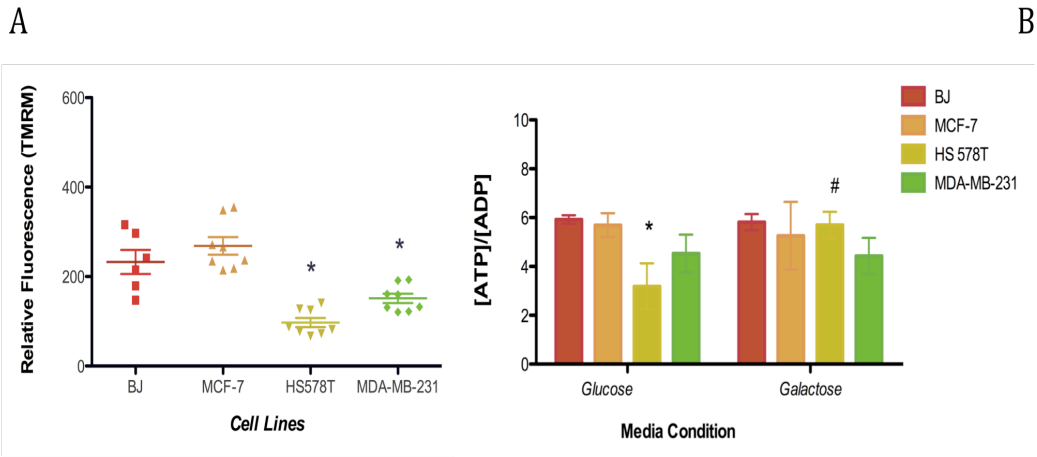

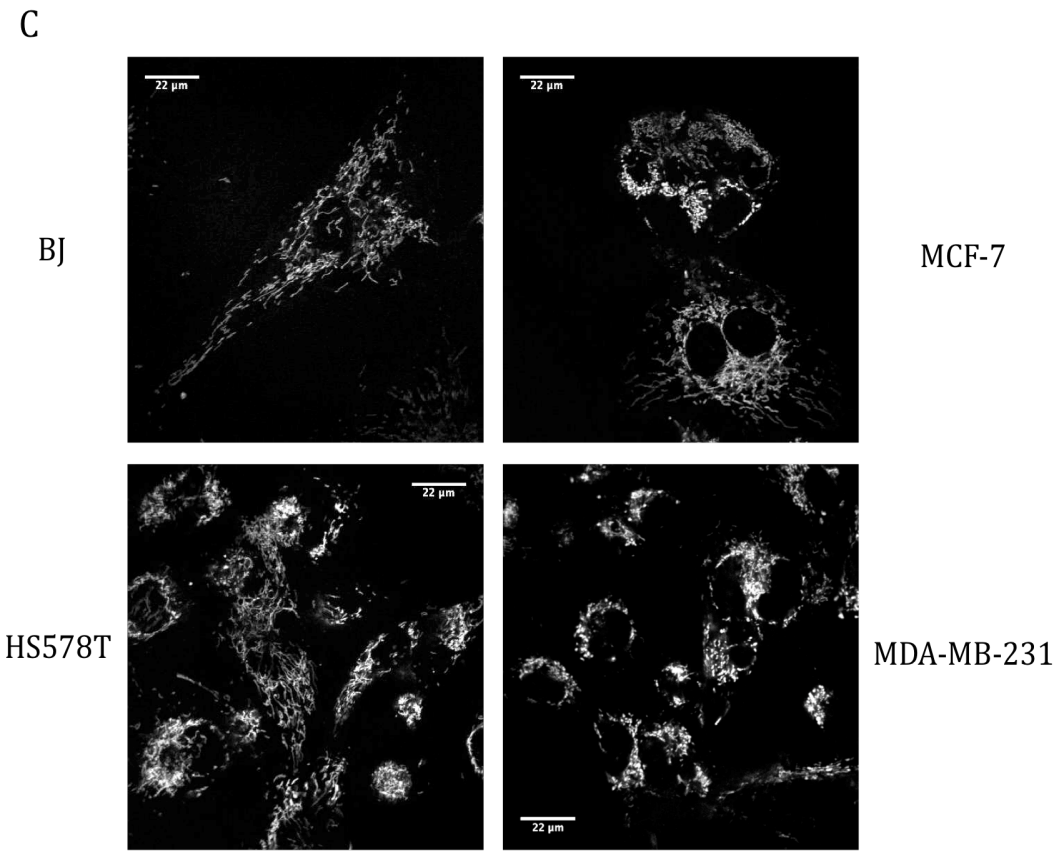

Fig.15 - Transition of breast cancer cells to glucose-free, galactose/glutamine media. **(A)** Mitochondrial membrane potential was measured by flow cytometry in breast cancer cells and normal fibroblast BJ when cultured in galactose. **(B)** [ATP]/[ADP] ratio of cell lines, when cultured in glucose and galactose. The results are representative of four separate experiments. (*) Significant difference from BJ cell line in glucose ($p < 0.05$), (#) significant difference between cells grown in glucose and galactose media. **(C)** Confocal micrographs showing the mitochondrial network of the different cell lines grown in galactose, where mitochondria were labeled with TMRM probe.

Furthermore, the mitochondrial network appearance is also altered with a more general filamentous network spreading all over the cell, with clear and inter-connected reticulum. The effect is more observed in HS578T cells (Fig.15C). Both cancer and normal cells basically maintained their intracellular [ATP]/[ADP] ratio (Fig.6B), with energy charge, once more, being equivalent in all cells: BJ (0.675 ± 0.047), MCF-7 (0.674 ± 0.014), HS 578T (0.702 ± 0.019) and MDA-MB-231 (0.746 ± 0.020). The only difference found in the [ATP]/[ADP] ratio was found in HS578T cells, that had now a higher [ATP]/[ADP] ratio vs. non-tumor BJ fibroblasts (Fig. 15B).

4.1.2.4. Cell motility in glucose vs. galactose/glutamine media

To determine whether cancer cells alter their motility behavior when transitioning from glucose to galactose/glutamine media (i.e., by remodeling back their metabolism to a predominantly OXPHOS metabolism), we performed the fluorescent phagokinetic migration assay. Using fluorescent microscopy, the motility of breast cancer cells was visualized as the microsphere-free paths generated (Fig. 16A). Differences in motility among breast cancer cells grown in galactose/glutamine medium were observed: an increase of motility in HS 578T cells and in MDA-MB-231 cells was measured, when compared with the same cells grown in glucose medium. In order to quantify cells migration capacity, cells were analyzed by flow cytometry, where it is expected that the accumulation of microspheres during migration, will be correlated both with increased total cell fluorescence and granularity as measured by side scatter. Microscopy observations were confirmed, with a significant increase in HS578T cell migration detected. Moreover, it was also interesting to verify that HS 578T cells were the most motile cells among all studied (Fig.16B).

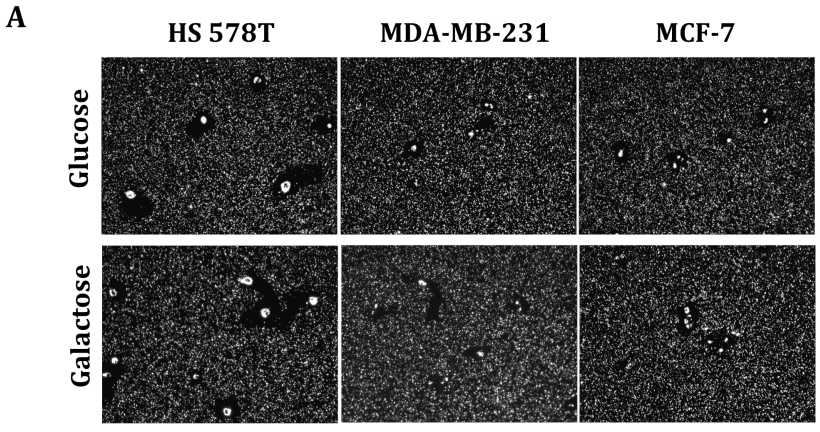

B

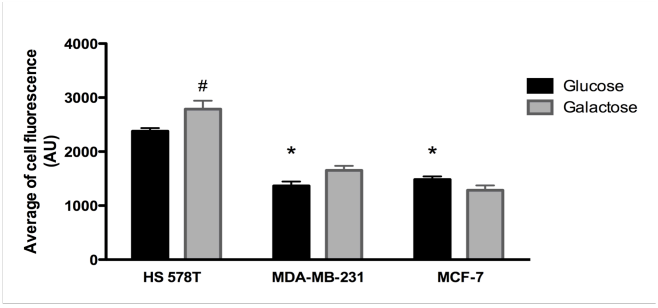

Fig.16 - Cell motility based on fluorecent phagokinetic assay. **(A)** Micrographs of breast cancer cells migration using fluorescent microspheres, when cells were cultured in galactose and glucose media. HS578T cells exhibit greater motility comparatively to the other cells (cleared area/cell) **(B)** Quantitative evaluation of fluorescence intensity of individual migrating cells by flow cytometry. The data reported is the average of four independent experiments with standard error of the mean ± S.E.M., (*) significant difference to HS 578T and (#) significant difference between media condition ($p < 0.05$).

4.1.2.5. Stemness markers in breast cancer cells grown in glucose vs galactose/glutamine media

The expression of $CD44^{high}/CD24^{low}$ is attributed to both human cancer stem-like cells and normal mammary epithelial stem cells, while the opposite expression pattern, $CD44^{low}/CD24^{high}$, is characteristic of differentiated mammary cells (Al-Hajj et al., 2003). When grown in glucose medium, both HS 578T and MDA-MB-231 cells have a strong stem-like sub-population; instead, MCF-7 cells have a predominant differentiated sub-population (Fig.17A).

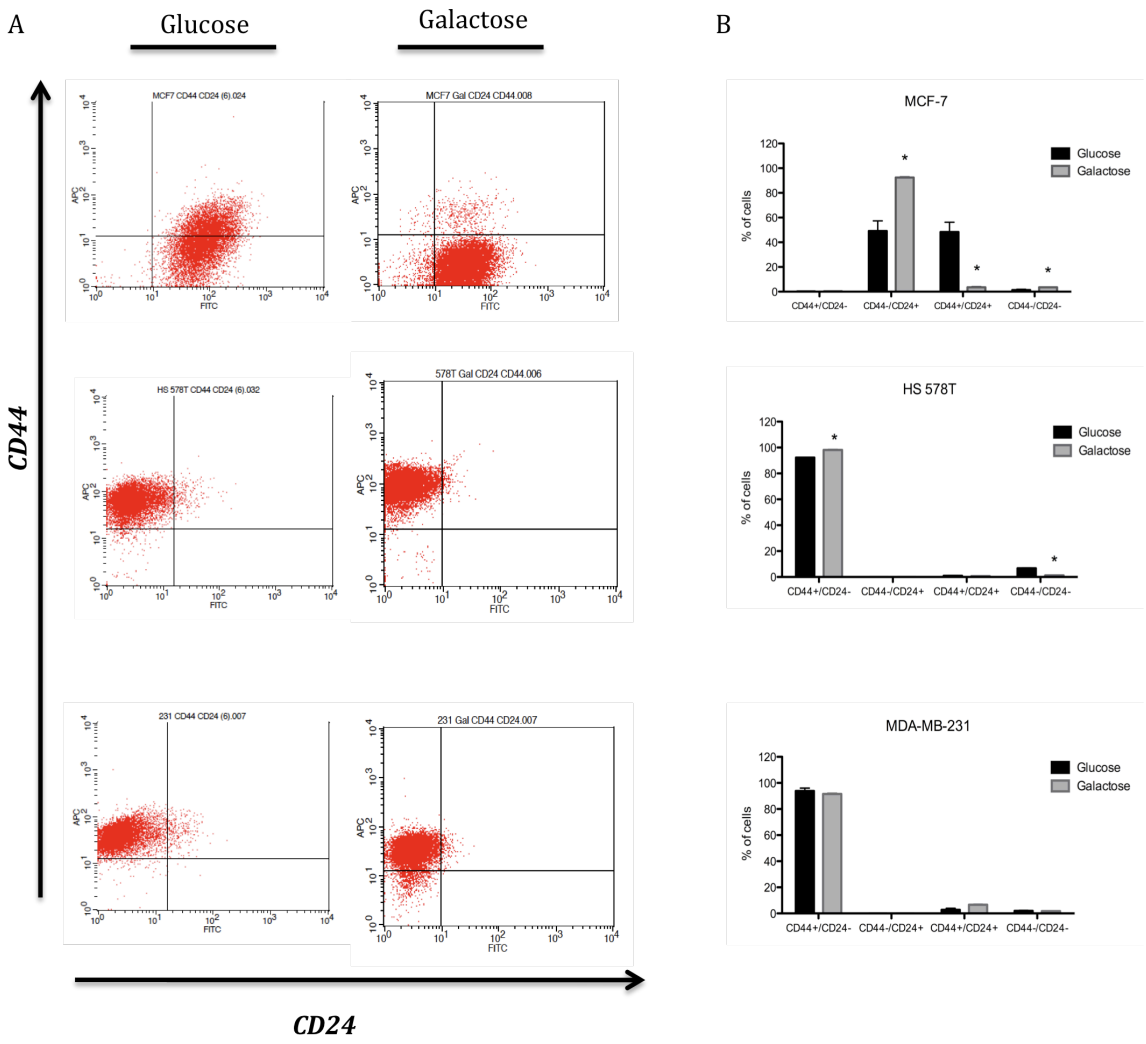

Fig.17 - Cell-surface markers CD44 and CD24 define cell subpopulations. **(A)** Representative FACS analysis of CD44/CD24 cell surface markers of breast cancer cells cultured in glucose and galactose media. **(B)** Percentage of $CD44^{high}/CD24^{low}$ stem-like cells and $CD44^{low}/CD24^{high}$ differentiated cells cultured in glucose and galactose/glutamine media. The results are representative of four separate experiments, with (*) as significant difference between condition media ($p< 0.05$).

Surprisingly, when cells are forced to use OXPHOS in place of glycolysis as the major source of ATP, a few differences existed in each cell line sub-populations. One interesting observation was that all cell lines appear to be more homogenous, expressing preferentially one type of cell surface marker, i.e., MCF-7 cells in glucose have two major sub-populations of cells, while in galactose, a more differentiated population was observed. HS 578T and MDA-MB-231 revealed a higher content in cancer stem-like cells, which was not greatly affected after the transition to galactose/glutamine media (Fig.17B).

4.1.2.6. Toxicity of mitochondrial poisons on human breast cancer cell lines – effects of metabolic manipulation

Finally, different golden-standards for mitochondrial poisons such as complex I inhibitor rotenone, complex V inhibitor oligomycin and the protonophore FCCP, besides the phytochemical berberine, which acts on complex I and on the ANT (Pereira et al, 2007, Pereira et al, 2008), were tested on cells grown in glucose vs galactose/glutamine media for 24 hours. The objective was to find out whether different breast cancer cell lines, presenting specific mitochondrial alterations, would be equally susceptible to compounds that cause cell death through mitochondria mechanisms (Fig.18). Cell proliferation experiments were performed by using the SRB assay, as described in Material and Methods (chapter III).

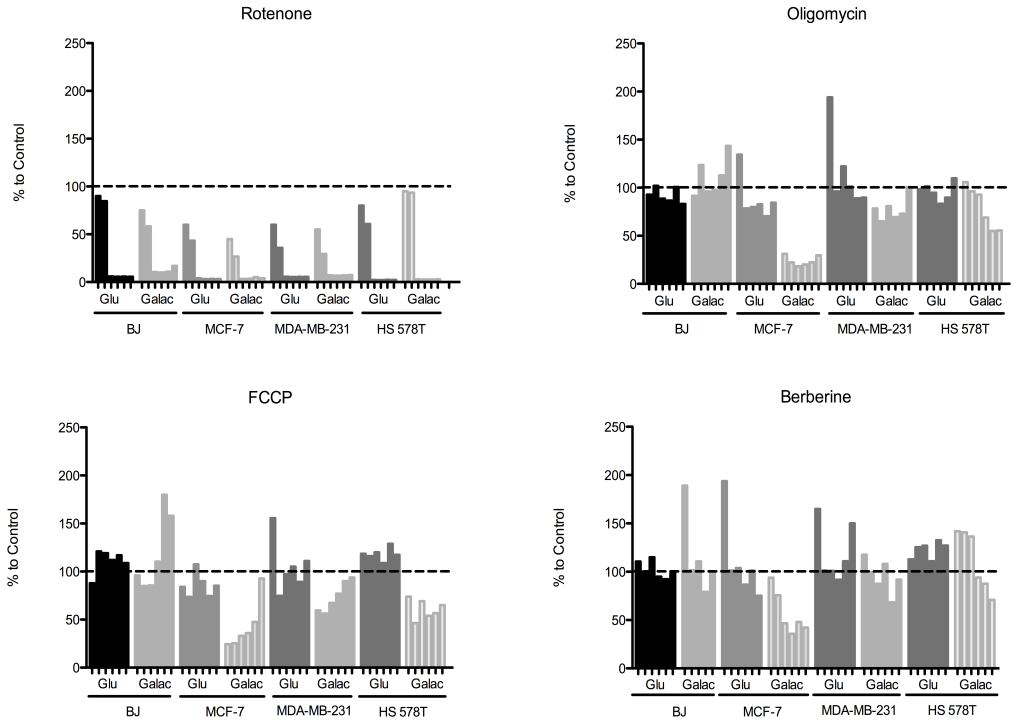

Fig.18 - Mitochondrial poisons affect cancer cells proliferation. Cells cultured in glucose and galactose/glutamine media were incubated with the different mitochondrial poisons for 24 hours at different concentrations. Cells were exposed to concentrations from 0.125-4µM rotenone (A), 0.125-4µg/ml oligomycin (B), 0-125-4µM FCCP (C) and 1.25-40µM berberine. Sulforhodamine B method (SRB) was performed to evaluate the cell proliferation inhibition. The results are expressed as percentage of the control, non-treated cells. The experiments were performed twice.

Proliferation of non-tumor BJ fibroblasts was dramatically inhibited by rotenone (Fig.18A), regardless of the culture media used, especially for concentrations above 0.5μM. Interestingly, none of the other mitochondrial poisons used, did affect BJ fibroblast proliferation. Contrarily, breast cancer cells showed to be much more sensitive to mitochondrial poisons tested, especially when forced to use OXPHOS for ATP production (i.e. in galactose/glutamine medium). Overall, the MCF-7 cell line was the most affected by the mitochondrial poisons. In the presence of rotenone, the cell mass is reduced to 50% in glucose medium and less than 50% in galactose/glutamine medium for 0.125 μM and 0.5μM, while for higher concentrations lead cells to die. In the presence of oligomycin (Fig.18B) and FCCP (Fig.18C), MCF-7 cells cultured in glucose suffer an inhibition in cell proliferation, whereas in galactose/glutamine medium, cell number is reduced to 25%. Although for the highest concentrations of FCCP, a decrease in the toxicity of this molecule in cell proliferation was observed, this may be explained by precipitation in the aqueous media. For the berberine concentrations used (Fig.18D), only cells growing in galactose/glutamine medium suffer an inhibitory effect on their proliferation. MDA-MB-231 and HS578T cells showed similar patterns of cell proliferation inhibition with the poisons used, however, a greater effect was observed in HS578T cells. One general observation is that For instance, the mitochondrial poisons did have a very residual effect on cell proliferation when in glucose media. In galactose/glutamine conditions, the results were very dissimilar. MDA-MB-231 cells had a 25% reduction comparatively to control (no treated cells, taken as 100%) when treated with oligomycin and FCCP and for the higher concentrations (20 and 40 μM) of berberine. When using HS578T cells, their number is reduced to 50% with FCCP, the same result occurring for higher concentrations (2 and 4 μM) of oligomycin and with a 25% decrease in cell numbers for the highest concentrations (20 and 40 μM) of berberine.

4.1.3. Discussion

Breast cancer is a remarkably heterogeneous disease; however, tumors can have recurrent patterns of metabolic, genomic and biological abnormalities (Oakman et al, 2010). Metabolic remodeling is typical of most tumors and mitochondrial alterations can alter the resistance to chemotherapy. Although mechanisms for metabolic remodeling

have recently been described and characterized (Ferreira L, 2010), the completion of more detailed studies on the alterations of the cellular metabolism, and particularly mitochondrial physiology of breast cancer cells will help the discover of new drugs that target cell metabolism more efficiently. Therefore, it is crucial to identify those patterns to enable progression in finding the best therapy.

Cell lines models have been used to advance our understanding of cancer for many decades, since the recurrence of aberrations accumulated over multiple passages *in vitro* culture cells is discarded, and cells may have stable genomic and expression patterns (Neve et al, 2006). Thus, for this work we selected three different breast cancer cell lines, namely MDA-MB-231, HS578T and MCF-7, but also normal non-transformed BJ fibroblasts. MDA-MB-231 and HS578T are considered "triple negative" cells, as they are do not stain for estrogen receptor (ER), progesterone receptor (PR) and human epidermal growth factor receptor 2 (HER2), a clinical tumor type grouping. In the same analysis, MCF-7 cells showed to be positive for the three receptors thus is designated as "triple positive" cell line (Oakman et al, 2010). These characteristics have been associated with their aggressiveness, where triple negatives are correlated to poor prognostic. Despite being triple-negative, MDA-MB-231 and HS578T respond differently to chemotherapeutic studies (chapter 4.4.). More, cancer cell mitochondria have been described to be structurally and functionally different from normal non-transformed cells (Fulda et al, 2010). For these reasons, we were interested in analyzing the three types of breast cancer cells to evaluate and characterize them by their specific mitochondrial alterations, including proteins involved in OXPHOS, intrinsic apoptotic pathway, bioenergetic re-adaptation to a predominantly oxidative metabolism and how this adaptation can alter their aggressiveness and resistance to cell death. Thus, the present section provides a good starting point to select mitochondrial alterations that can be used to develop new agents aimed at those same mitochondrial differences.

Mitochondrial membrane potential has been associated with tumorigenicity and cell differentiation status (Ye et al, 2010). In the present research, despite all the cancer cells showed to have a mean higher $\Delta\psi m$ than BJ fibroblasts, only MCF-7 cells had a statistically significant difference (Fig 10A). This result is in concordance with Ye, et al (2010), where an increase in $\Delta\psi m$ in matured/differentiated cells was observed. Reasons that could be involved in higher $\Delta\psi m$ include mitochondrial membrane alterations,

decreasing proton influx, or a decreased activity of the ATP synthase, among other causes (Solaini et al, 2010). Moreover, in normal situation, cells maintain their Δψm under a certain threshold to avoid the formation of ROS, while in cancer cells, incomplete oxidative phosphorylation may lead to higher Δψm and enhanced ROS production by the respiratory chain.

No differences were observed in either [ATP]/[ADP] ratio or energy charge among cells, except for HS578T cells, found to have a lower [ATP]/[ADP] ratio comparatively to the others (Fig. 10B). It could be explained by several factors including a decreased rate of mitochondrial ATP production or even a greater ATP usage for proliferation. In fact, proliferating cells stimulate both oxidative phosphorylation and glycolysis leading to an increased [ATP]/[ADP] ratio (Mezhybovska et al, 2009). What is interesting is that despite the possible metabolic remodeling in breast cancer cells, with the exception of HS578T, the two remaining breast cancer cells studied were able to maintain [ATP]/[ADP] ratio similar to BJ fibroblasts. This can also give some clues whether metaboling remodeling and mitochondrial alterations causes a real impact on intracellular energy charge or are instead aimed at activating pathways that may lead to biosynthetic processes.

Alterations in the content of mitochondrial oxidative phosphorylation proteins were observed. All breast cancer cells showed decreased ATPase-Fo content, which was the most consistent alteration (Fig.11). Interestingly to notice was the decrease of expression of COX subunits, detected once more by Western blotting and qRT-PCR (Fig.11 and 12), for both triple negative cells. The COX subunits studied represent the catalytic and regulatory cores of the protein (Chen et al, 2009). Accordingly with our results, both COX I and COX III are overexpressed in well-differentiated cells and such characteristic seems to be lost during cancer-malignancy progression (Heerdt et al, 1990). Studies suggest that under hypoxic conditions, COX subunit I (COX I), responsible for COX activity under aerobic conditions, is downregulated and COX II is increased for an optimization of COX activity (Fukuda et al, 2007). Hence, Gogvadze et al. (2010) suggested that switching between COX subunits allow cells to adapt to the different environment conditions, such as hypoxia or normoxia, in the name of an efficient respiration.

Interestingly was the observation of increased mitochondrial-encoded complex I

subunit transcripts in MCF-7 cells. Being aware that in the cell culture medium, some components that can activate estrogen receptors are present, Chen and Yager (2004) showed that in estrogen-dependent MCF-7 cells, estrogen receptors localized in mitochondria would enhance the levels of mtDNA-encoded transcripts.

Despite the fact that some of results regarding transcripts were in concordance with previous works, it is important to mention that choosing glyceraldehyde-3-phosphate (GAPDH) for our reference gene was probably not a good choice. GAPDH was shown to be upregulated in tumor progression, especially when glycolysis is activated, as well shown to be estrogen-regulated, having its expression increased in MCF-7 cells (Cuezva et al, 2002; Lyng et al, 2008). Therefore, another reference gene should be used to confirm the results obtained. We hereby suggest for breast cancer cells using TATA-box binding protein (TBP), Ribosomal protein, large, P0 (RPLP0) and homolog of Pumilio, Drosophila, 1 (PUM1) as a group of genes for reference, or PUM1 as a single one (Lyng et al, 2008).

The alterations observed in protein content and mRNA have no clear translation for mitochondrial physiology. The only exception may well be the decreased Fo ATPsynthase subunit in all breast cancer cells. This fact may result into decreased ATP production and increased $\Delta\psi m$ (see above), and collaborate in the aerobic glycolytic phenotype.

Even with no apparent effects on mitochondrial function, it is interestingly to note that somatic mtDNA alterations seem to occur in the non-coding D-loop regions (Ma et al., 2009). Mutations within D-loop region include a variety of types, such as gastric, breast, oesophageal and thyroid (Wheelhouse et al, 2005). However, some cancers types, such as hepatocellular carcinoma (Kotake et al, 1999), oesophageal (Tan et al, 2009) and oral carcinogenesis (Lee et al, 2001), commonly have deletion of 4977bp in this region. In the present study we verify that none of the cells analyzed presented such deletion (Fig.13).

One of the hallmarks of cancer cells is evasion from apoptosis. In the present work we observed that breast cancer cells have a decreased content in the pro-apoptotic protein Bax, with MCF-7 cells presenting an absence of the pro-survival protein Bcl-2, most likely compensated by increased Bcl-Xl. Moreover, MCF-7 cells had increased heat shock protein 90 (HSP90) and decreased mitofusin 1 (MFN1) when compared with other

cell lines investigated (Fig.14). In fact, cancer cells have been already described to have a higher content in HSP90, which has been linked to increased ATPase activity, and also to increased cell survival, by involving adaptation to unfavorable environments and inhibition of mitochondria-initiated apoptosis (Kang et al, 2007). MFN1, by its turn, controls the outer mitochondrial membrane fusion and has been shown to interact with pro-apoptotic Bcl-2 family members Bax and Bak to increase mitochondria fusion in healthy cells and inhibit cell death due to MOM permeabilization (Thomas and Cookson, 2009). The result obtained is interesting since it has been reported that mitochondrial fusion is normally anti-apoptotic (Brooks et al, 2011). Nevertheless, a decrease in MFN1 may be compensated by increased MFN2 (which was not measured in this work) and also contribute to increase mitophagy (Gegg et al, 2010), eliminating mitochondria that are not being used by the cell, generating in the process more building blocks for cell proliferation. MDA-MB-231 cells were shown to have higher levels of of hexokinase II and VDAC when comparing with other cell lines analyzed, suggesting a typical phenotype of glytolytic dependent cells (Fig.14), since these two enzymes have been shown to associate at the MOM to promote increased glycolytic flux and increased protection of mitochondria against chemotherapy (Pedersen et al, 2008). All together, the results suggest different mechanisms acquired by breast cancer cells to resist cell death and which may also participate in the general process of metabolic remodeling.

We further investigated whether mitochondria from the breast cancer cells studied had irreversible defects by up-regulating OXPHOS through cells from the regular glucose-containing media to glucose-free media supplemented with galactose and glutamine. In this media, galactose is used for nucleic acid synthesis and glutamine is consumed by mitochondria to generate 98% of ATP used for growth (Rossignol et al., 2004; Smolkova et al, 2010). Cancer cells required a variable lag-phase to re-start proliferating, which may be due to the alterations required in the OXPHOS system. Nevertheless, all cells were able to remodel their metabolism back to a predominant OXPHOS phenotype showing that mitochondrial alterations are not irreversible, in agreement with previous works (Rossignol et al., 2004). In agreement, Smolkova, et al (2010) detected a significant increase of oxidative phosphorylation proteins of HS578T cancer cells cultured in glucose-deprived galactose/glutamine medium. In fact, an

increase of the [ATP]/[ADP] ratio in HS578T cells when cultured in galactose media was observed (Fig.15B). Further, TMRM vital imaging, was used to characterize the structure of mitochondrial reticulum, since it is accumulated as a function of $\Delta\psi m$. We verify a rearrangement of mitochondria structure when OXPHOS was stimulated by using the glucose-free/galactose-glutamine media. The mitochondrial network expanded all over the cell, forming a more reticulated and thinner net (Fig.15C), contrarily to glucose medium-cultured cells, where clustered perinuclear network was formed (Fig.10C). Rossignol et al (2004) and coworkers showed increased mitochondrial activity in HeLa cells grown in galactose medium, including an increase of cristal membrane, that is thought to be related with the increase synthesis of respiratory chain complexes. This ramification may be important to supply ATP to all parts of the cell. Again, results from this and other works show that the Warburg effect, i.e., a metabolic remodeling that results in higher aerobic glycolysis does not result from irreversible mitochondrial defects, instead of a rearrangement of metabolism consistent with a faster need for ATP and building blocks for biosynthesis (Cairns et al, 2011).

The process of tumor invasion and subsequent metastasis represents the most lethal aspect of cancer. Solid breast tumors contain a distinct population of cells designated "cancer stem cells" with the capability to sustain tumor formation and growth (Al-Hajj et al, 2003). These cells express $CD44^{high}/CD24^{low}$ surface markers and have the capacity for self-renewal and enhanced invasive properties ((Sheridan et al, 2006). Two questions arose during this work: a) how are the cells investigated in the present work characterized in terms of stem vs. differentiation markers? Also, does OXPHOS re-activation alter the relative sub-populations? Contrarily to what we were expecting, this change promoted the increase of $CD44^{high}/CD24^{low}$ sub-population in triple-negative cells. Our results confirm that CD24 protein is expressed on more differentiated and luminal-like cells, MCF-7 cells, whereas CD44 is expressed on more progenitor-like and basal-like cells, MDA-MB-231 and HS578T cells (Fig.17). Cells with $CD44^{high}/CD24^{low}$ phenotype express genes involved in angiogenesis and cell motility (Shipitsin et al, 2007). Moreover, we also verified that cells expressing $CD44^{high}/CD24^{low}$, MDA-MB-231 and HS578T, were more motile than MCF-7 cells (Fig.16). Similar results were obtained by other investigators, where they observed more invasiveness by HS578T cells and higher motility capacity of MDA-MB-231 cell line, while MCF-7 cells

were found to be weakly invasive and migratory (Hughes et al, 2008). These results are in concordance with a large sub-population of stem-like cells that was observed with CD44 and CD24 markers in cells grown in glucose-free medium. Also, it is curious to note that HS578T cells increase their motility upon re-activation of OXPHOS, when cultured in galactose media. This is another clear evidence that intact mitochondrial function is important for an aggressive phenotype and maybe that shutting down mitochondrial ATP production in some cancer cells is a price to pay for shunting resources to biosynthesis.

Another observation from this work is that inhibition of glycolysis *per se* (here mimicked in a glucose-free media) may not a good strategy to control cancer stem-like cells, since these cells can become more aggressive.

A question has to do with the susceptibility of breast cancer cells in different metabolic states (aerobic glycolysis vs. OXPHOS) to different classic mitochondrial inhibitors, with the objective of testing the hypothesis that different mitochondrial alterations can impact how mitochondrial-specific chemotherapeutics (mitocans) effectively kill cancer cells. For this objective, rotenone, oligomycin, FCCP and berberine and were tested (Fig. 18). Rotenone was shown to have a large impact on cell proliferation, especially on MDA-MB-231 and MCF-7 cells. Rotenone is an inhibitor of complex I of mitochondrial respiratory chain, resulting in the generation of reactive oxygen species (ROS) (Koopman et al, 2010), which may synergize with blockade of the respiratory chain to kill cancer cells. It has been already demonstrated that rotenone induces apoptosis in MCF-7 cells (Li et al, 2003) perhaps through ROS and JNK/p38 MAPKs activation (Deng et al, 2010). The same did not happen to HS578T cells, which may be due to the fact that ROS production is counteracted by internal antioxidants, such as manganese superoxide dismutase (MnSOD). In fact, it is known that some breast cancer stem cells have higher levels of antioxidants than their non-tumorigenic progeny (Fulda et al, 2010). However, this is something that must be verified in future works.

Cells were usually more susceptible to mitochondrial poisons when in galactose media, which agrees with previous works (Marroquin et al, 2007). When cells were incubated with oligomycin, which blocks oxidative phosphorylation by inhibiting ATP synthase, we verify that MCF-7 cells were the most affected, when compared with other cell lines. Besides inhibition of ATP synthesis, a possible mechanism by which

oligomycin inhibit MCF-7 cells growth could be by hyperpolarizing mitochondrial membrane potential, leading to an increase of electrons leakage and resulting on ROS generation (Mizumachi et al, 2008). Interestingly, normal BJ fibroblasts did not seem to be as affected in the same way as cancer cells, probably due to the fact that they contained more Fo subunits (Fig.11). Similar result was observed with FCCP, with normal cells not being affected. FCCP is protonophore which dissipates mitochondrial membrane potential and to uncouple respiration. The results with FCCP raise some doubts and must be repeated for confirmation. Berberine, another mitochondrial poison (Serafim et al., 2008), targets the respiratory chain and interferes as well at mitochondrial phosphorylative system (Pereira et al., 2007), especially with the ANT (Pereira et al., 2008). Here we verify that MCF-7 cells in galactose show once more to be the most sensitive to yet another mitochondrial poison. One interesting observation is that berberine targets the ANT as well (Pereira et al., 2008), which was virtually undetected in the three tumor cells studied. Although the proliferation assays still need to be concluded, one interesting possibility is that berberine may target the ANT on cancer cells, which would exist in a limited number of units, below a reserve threshold, and thus be more susceptible to chemical agents. The results suggest that normal cells may not be as susceptible to mitochondrial poisons as their tumor counterparts, which has in fact been described before (Fulda and Kroemer).

In the present section, we observed that the three breast cancer cell lines used have alterations in mitochondrial physiology, which may lead to different phenotypes and response to different metabolic conditions. Cancer cells with mitochondrial dysfunction are particularly aggressive with rapid growth (Simonnet et al, 2002). From the results presented, MCF-7 cells were more susceptible to different treatments. Thus, our results suggest that MCF-7 cancer-like cell types could be easier eliminated using cationic mitocans. The fact that MDA-MB-231 cells have a higher content in HKII and VDAC suggests that these two proteins, which can associate, as described, may be a good target. One possibility would be to use 3-bromopyruvate, which is known to target complexes between HKII and VDAC and cause cancer cell death (Chen et al, 2009b).

The findings here also indicate that targeting glycolysis only, will not be sufficient as an anti-cancer therapy, with secondary approaches needed, including agents that specifically target the mitochondrial machinery in cancer cells. The better

knowledge of the pathophysiological differences between mitochondria in cancer cells and their normal counterparts will be a tool for increasing the level of selectivity of mitochondrially-targeted anticancer agents. Hopefully, it will be possible one day to metabolically characterize each patient and offer individualized treatment by considering the mitochondrial differences among cells.

4.2. Opening Pandora's Box: testing new chemotherapeutics

In this section, we are using three distinct families of possible Mitocans, in order to dig deeper in their possible mechanisms of action, not only to confirm that they do act as direct modulators of mitochondrial function (i.e.mitocans), but also to test their efficacy against cancer cells. The three families of compounds, triterpenoids, phenolic acids and alkaloids have no apparent relationship among each one, but they were used as a result from the multiple collaborations our research group has in Portugal and in the USA. Two distinct types of cancer were studied, breast and melanoma, each one presenting a large degree of mortality if undetected. We have used different markers of cell and specifically mitochondrial dysfunction to study whether any of these compounds can be the beginning of the development of a novel next generation anti-cancer agent.

4.2.1. Citotoxicity of new lipophilic Caffeic and Ferulic acid Derivatives

4.2.1.1. Background and Objectives

Diet-associated phenolic compounds, including hydroxycinnamic and hydroxybenzoic acids, are often described as potential antioxidants and consequently inhibitors of deleterious oxidative processes related with cardiovascular and inflammatory diseases and cancer (Czuba et al, 1992; Fresco et al, 2006; Fresco et al, 2010). A large body of scientific evidence suggests that phenolic compounds can act as chemopreventive and/or chemotherapeutic agents (Huang et al, 2010; Lee et al, 2006; Serafim et al, 2008b). Specifically, hydroxycinnamic acids and derivatives are known to display relevant antioxidant properties as well as biological activity towards several tumor cells, with their growth-inhibitory potency being strongly dependent on their structural characteristics (Fiuza et al, 2004; Marques et al, 2006). For example, it has been demonstrated that caffeic acid phenethyl (CAPE) and benzyl/alkyl esters, have been shown to display selective antiproliferative activity against some types of cancer cells (Bravo L, 1998; Kelloff G, 2000). It is also recognized that hydroxycinnamic acids and derivatives can inhibit key proteins in signal transduction pathways (such as MAP-kinases or AP-1) or pathways downstream from the transcription factor NF-kB and modulate cell-cycle regulation and apoptosis (Fresco et al, 2006; Serafim et al, 2008b).

Despite all the interesting biological effects of hydroxycinnamic acids and despite being dietary components, their bioavailability presents some limitations: although working well in aqueous media, their hydrophilic nature is usually a restriction for lipophilic systems protection (Gao and Hu, 2010; Crozier et al, 2009). In order to develop new and more effective phenolic agents suitable for chemopreventive and/or chemotherapeutic purposes caffeic and ferulic acid ester and amide derivatives with increased lipophilicity conferred by an additional alkyl chain (Fig. 7), were screened in terms of cytotoxicity on three different human breast cancer cell lines, namely MCF-7, HS578T and MDA-MB-231, and on a non-transformed human fibroblast cell line (BJ), which was used as a non-tumor cell control. The parent compounds, caffeic and ferulic acids were also used for comparative purposes. The study was accomplished by investigating proliferation, cell cycle and cell death effects of the test compounds. It is important to note that the antioxidant properties and partition coefficients of the compounds under study were previously assessed (Roleira et al, 2010).

Among several possible mechanisms for tumor cell cytotoxicity caused by phenolic acids, direct effects on mitochondria can also be envisioned. Mitochondria are involved in several energy and metabolic-linked processes, in the generation of reactive oxygen species (ROS) and in several disease-initiated processes (Shaw and Winge, 2009); in fact, the role of mitochondria in carcionogenesis (Weinberg and Chandel, 2009) and anti-cancer therapy (Gogvadze et al, 2010) has also been explored in detail, with this organelle being considered an attractive target of different chemotherapeutics with the ultimate objective of eliminating cancer cells (Ralph and Neuzil, 2009). In order to investigate whether the test compounds could directly impact mitochondrial physiology and cause a pro-apoptotic increase in membrane permeability, isolated liver mitochondria were incubated with the test compounds. Isolated mitochondrial fractions have been used as a biological model by pharmaceutical companies as a sensitive and reliable biosensor for drug-induced toxicity (Pereira et al, 2009).

4.2.1.2. Results

4.2.1.2.1. Effects of Phenolic Compounds on Cell Proliferation

In order to choose the concentrations of the parent and derivative compounds (Fig.7) to be used in the different experiments, preliminary assays with a wide range of concentrations have been performed and demonstrated that concentrations of the test compounds between 25 μM and 75 μM inhibit the proliferation of the human cancer cell lines investigated. Therefore, for further experiments, phenolic acids and their derivatives were used at concentrations between 25 and 75 μM, and were incubated for 1, 3 and 7 days with a panel of human breast cancer cells (MCF-7, MDA-MB-231 and HS578T), and with non-neoplastic cells (BJ).

From the proliferation curves obtained (Figs. 19 and 20), one evident finding is that the parent compounds, caffeic (CA) and ferulic acid (FA) did not inhibit the proliferation of any of the four cell lines used. In fact, stimulation of cell proliferation was observed in some cases, one particular example being the effect of 25 and 50 mM caffeic acid, which caused a 1.5-fold increased in HS578T cell proliferation after 1 day of treatment (Fig. 19).

Among the caffeic acid derivatives, hexyl caffeate (HC) and caffeoylhexylamide (HCA) showed a general inhibition of proliferation of all cell lines tested (Fig. 19). The

most striking effect was seen with HCA, which, after 7 days of incubation caused around 80-90% inhibition of proliferation of MCF-7, BJ and HS578T cells. Interestingly, HC showed a stronger effect on BJ fibroblasts (with around 50% inhibition of proliferation for 7 days of incubation) and had no effect on HS578T breast cancer cells.

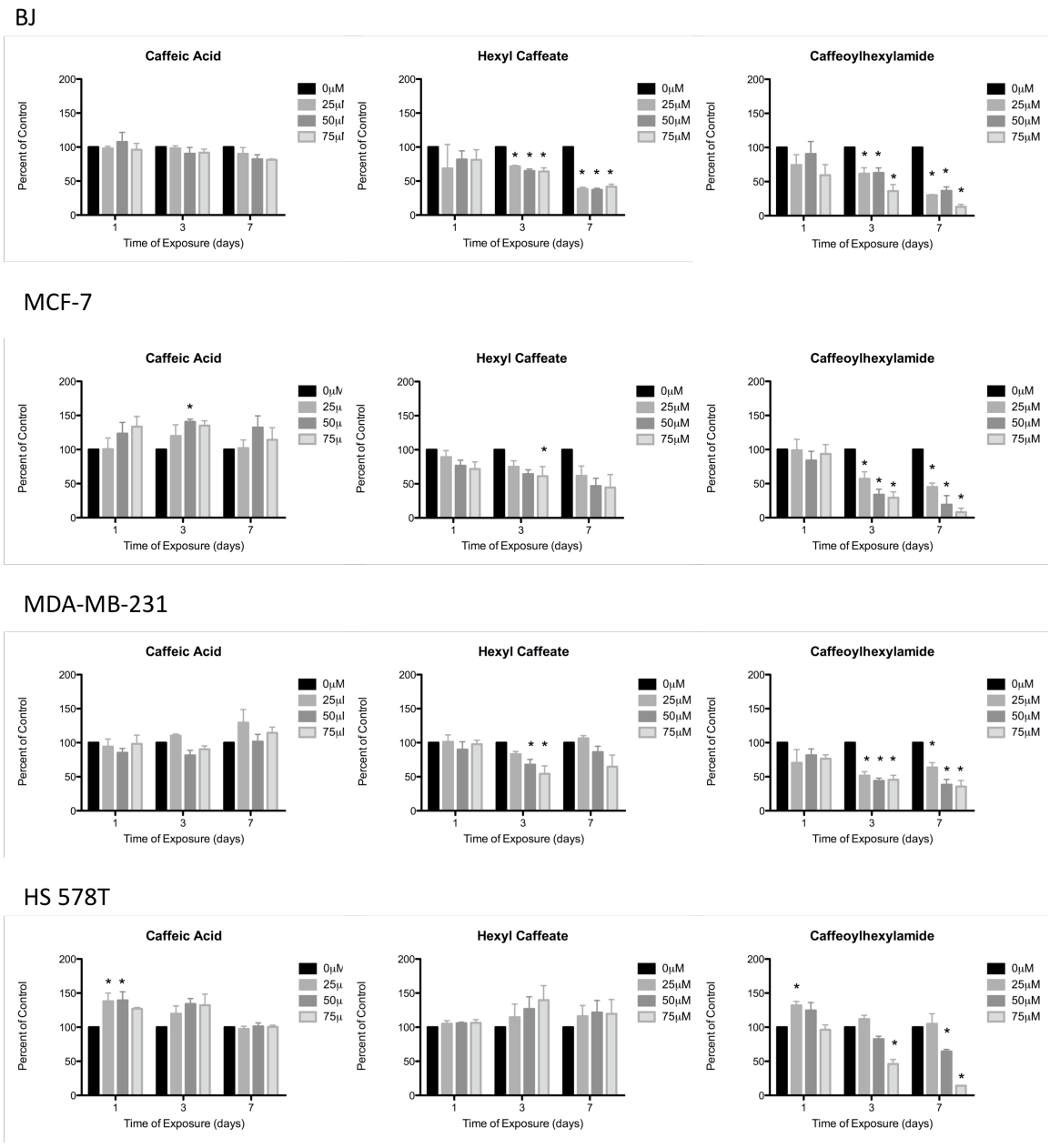

Fig.19 - Antiproliferative effect of caffeic acid derivatives. Cells were incubated with a range of concentrations up to 75 μM during 1, 3 and 7 days. Cell proliferation was accessed by sulforhodamine B (SRB) colorimetric assay as described under Material and Methods and plotted against time of exposure and concentration of caffeic acid and derivatives. The control value for each time point was determined as 100% to account for the differential proliferation of the cell lines in study. Data presented as means ± S.E.M. of four different experiments. Samples identified by asterisks (*) denote a significant difference from controls ($p < 0.05$).

Ferulic acid derivatives hexyl ferulate (HF) and feruloylhexylamide (HFA) showed dissimilar effects according to the cell line tested (Fig. 20). MCF-7 cells were particularly susceptible to both compounds, especially for longer incubation periods, which HS578T appearing to be largely insensitive, with the exception with a 25% inhibition of proliferation observed when HFA was incubated for 3 days (Fig. 20).

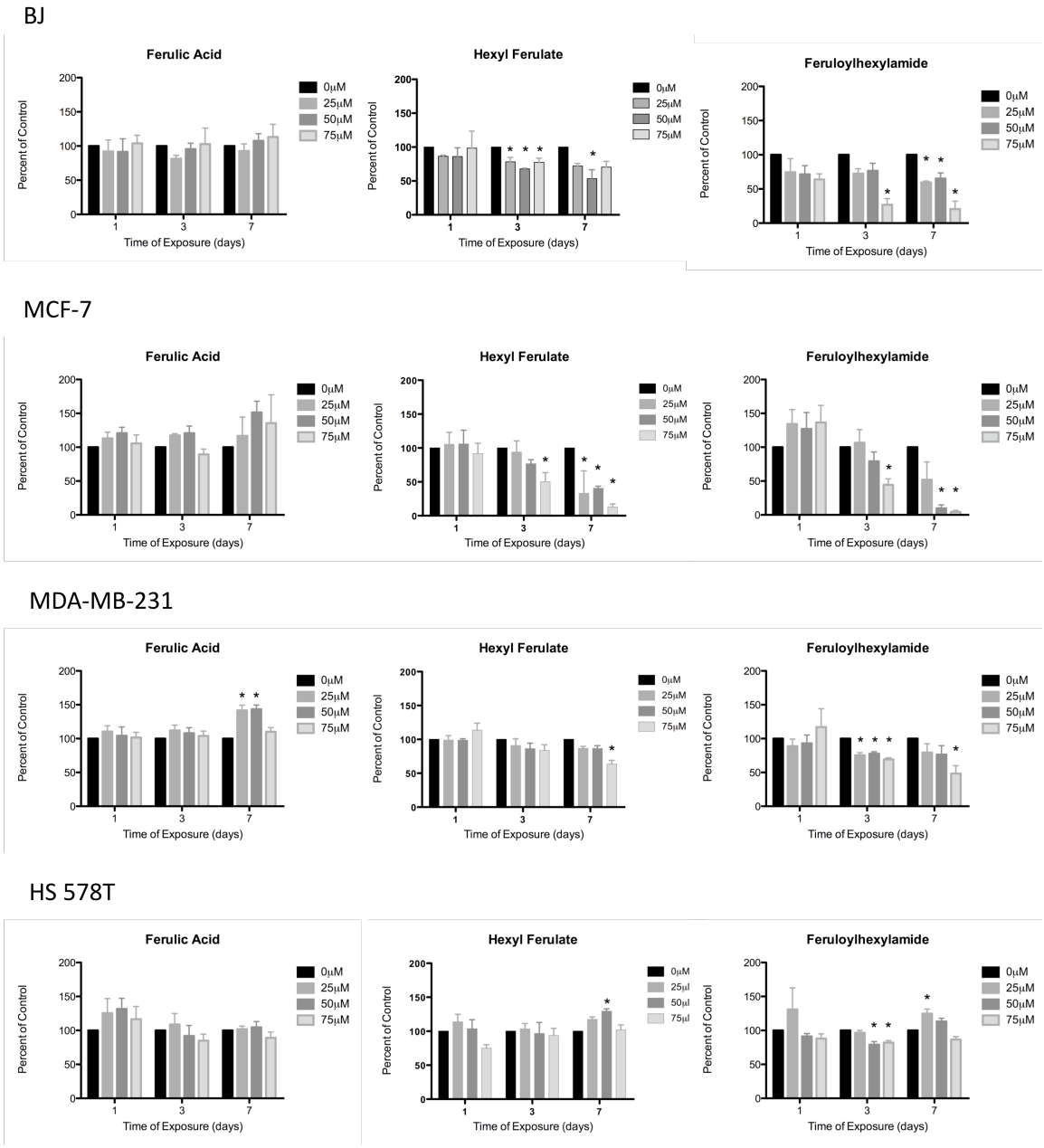

Fig.20 - Effects of ferulic acid and derivatives on cell proliferation (see Material and Methods and Fig. 2 legend for technical details). The control value for each time point was determined as 100% to account for the differential proliferation of the cell lines in study. Data presented as means ± S.E.M. of four different experiments.(*) Significant difference from controls ($p < 0.05$).

4.2.1.2.2. Effects of Phenolic Compounds on Cell Cycle and Apoptosis

Although very indicative, inhibition of cell proliferation as measured by the sulforhodamine B method does not distinguish between cell death and cell cycle inhibition. Hence, in order to gain deeper insights into the mechanisms by which the test compounds decrease cell proliferation (Figs. 19 and 20), cell cycle and apoptosis were analyzed. To this purpose, a single concentration of the test compounds was chosen. The different human tumor and non-tumor cell lines were incubated with 75 μM of the test compounds for 2 and 4 days, and their cell cycle status analyzed by flow cytometry. Two and four days of treatment time were chosen for the experiments in order to have both a short and a long-time exposure, while avoiding losing a large number of cells due to extensive cell death.

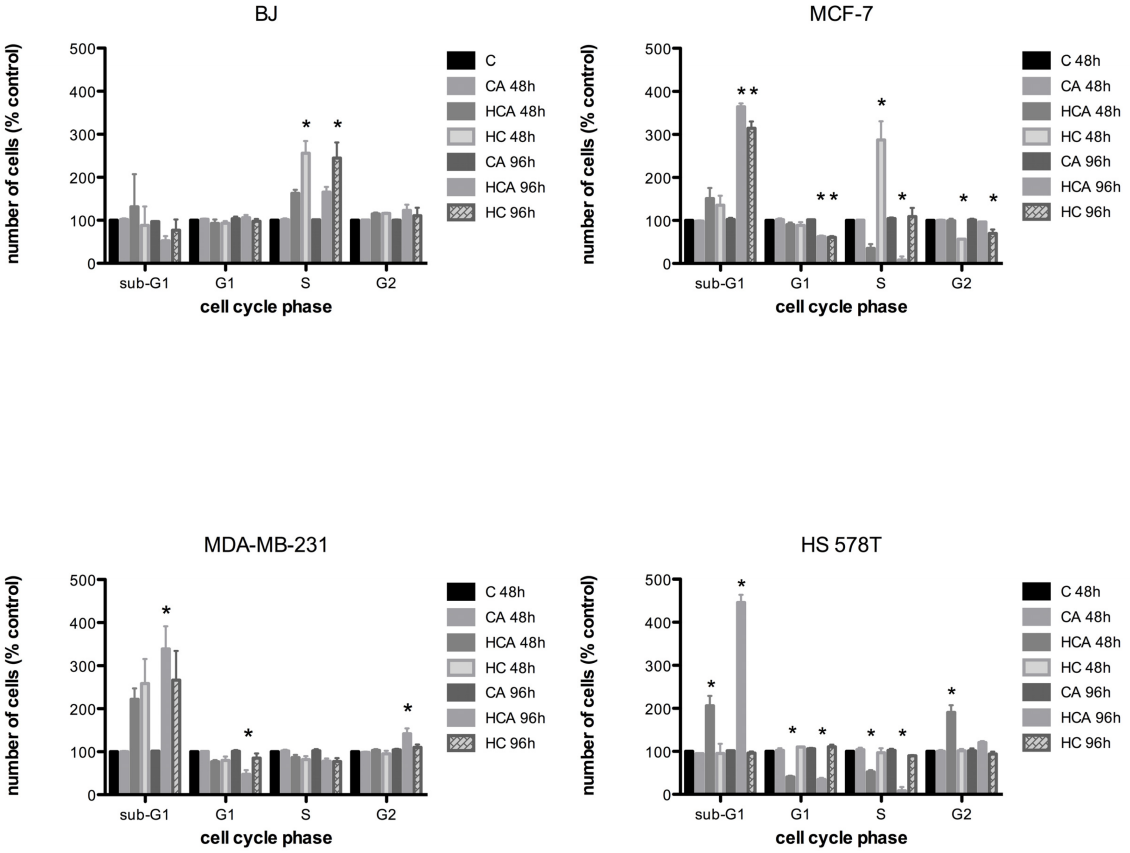

Fig.21 - Cell cycle analysis of BJ, MCF-7, MDA-MB-231 and HS578T cells, treated with 75μM of caffeic acid and derivatives for 48 and 96 hours. Cell cycle was analyzed by flow cytometry. The values shown are the averages of four independent experiments; bars indicate the standard error of the mean S.E.M. (*) Significant difference from controls ($p < 0.05$).

In agreement with cell proliferation assays (Figs. 19 and 20), the parent compounds CA and FA did not have any impact on the cell cycle of any of the cell lines studied (Figs. 21 and 22). The increased cell proliferation observed by the SRB technique was not confirmed in some cases by altered cell cycle. The two CA derivatives, HC and HCA, induced an increase in the percentage of cells in S-phase for the BJ cell line for the longest incubation period, although no apoptotic DNA (sub-G1) was measured. In MCF-7 cells, 48 hours of treatment with HC resulted in S-phase cell cycle arrest, while 96 hours of incubation resulted in cell death. In this same cell line, another very significant result was observed for 96 hours of incubation, when HCA caused an increase in sub-G1 peak, suggesting cell death by apoptosis, and a marked decreased in cells in S phase (Fig. 21). The decreased proliferation caused by HC and HCA in MDA-MB-231 cells (Fig. 21) was translated into an 2 to 3-fold increase in apoptotic sub-G1 peaks for both compounds (48 and 96h), although statistical significance was only observed for 96h incubation with HCA. A small, but significant decrease in cells in G1 phase and a increase number of cells in G2 cells caused by HCA for 96h was also observed (Fig. 21). Finally, HCA showed mixed effects on HS578T cells, with a significant increase in the number of cells in sub-G1 for 48h and 96h, a decreased number of cells in G1 and S phases for both times studied and increased number of cells in G2 phase for 48 hours (Fig. 21). Confirming the lack of effects on cell proliferation (Fig. 19), HC had no effects on the HS578T cell line (Fig. 21).

Ferulic acid derivatives (HF and HFA) were less effective than caffeic acid derivatives concerning cell cycle effects. BJ fibroblast cell cycle was not affected by any of the compounds studied, whereas HS578T suffered a minor, but significant, decrease in the number of cells in G2 phase when treated with HF for 96h (Fig. 22).

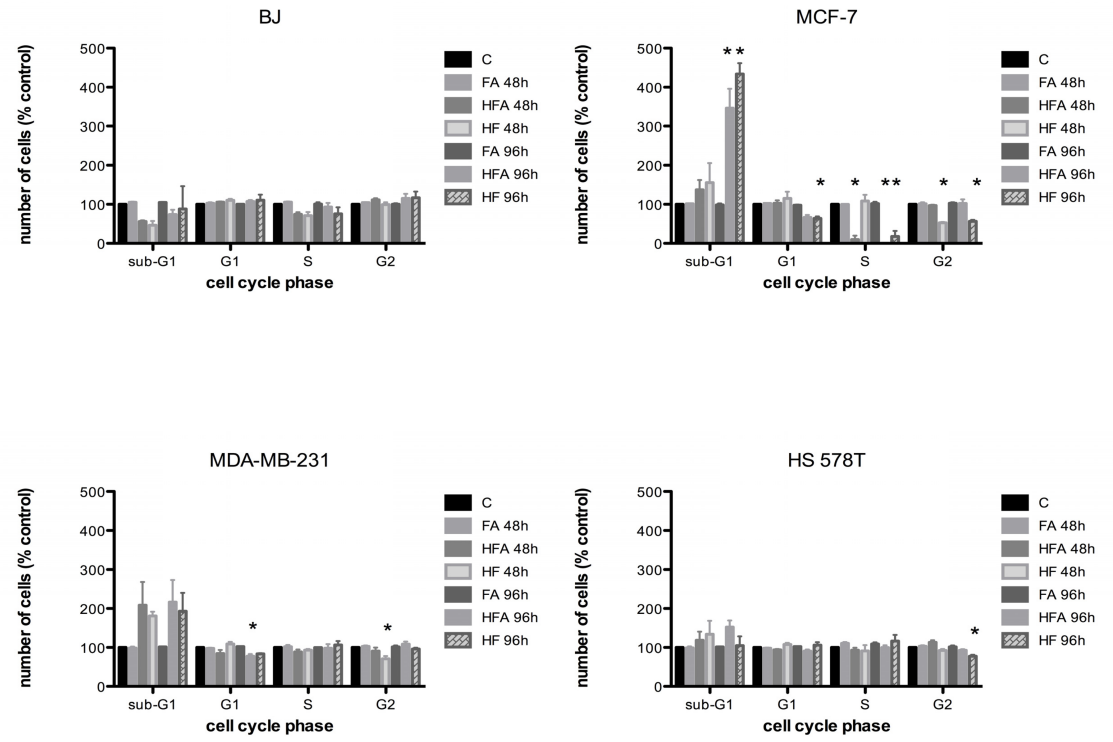

Fig.22 - Cell cycle analysis of BJ, MCF-7, MDA-MB-231 and HS578T cells, treated with 75µM ferulic acid and derivatives for 48 and 96 hours. Cell cycle was analyzed by flow cytometry. The values shown are the averages of four independent experiments; bars indicate the standard error of the mean S.E.M. (*) Significant difference from controls ($p < 0.05$).

Effects were somehow more visible for the MDA-MB-231 cell line, where a non-statistically significant increase in cells in sub-G1 phase were observed for both compounds during 48 and 96h, an approximately 10% decrease in cells in G1 phase (HFA, 96h) and around 20% decrease in cells in G2 phase (HF, 48h), were observed (Fig.22). Finally, most of the effects from ferulic acid derivatives were observed on MCF-7 cells. In this case, a very significant increase in apoptotic sub-G1 was observed for both compounds for 96 hours of incubation time. A large decrease in the number of cells in S phase was also observed for 48h (HFA) and 96h (HFA and HF). In fact, no cells in S phase were detected after 96h incubation with HFA (Fig.22).

By using Hoechst 33342 to label cell nuclei, apoptotic chromatin condensation can be detected. We performed this protocol after 48 hours of incubation and counted apoptotic-like nuclei. One major limitation of this method is that only adherent cells are counted, which strongly minimizes the extent of apoptosis. Nevertheless, it was possible to observe that HF was the most potent compound inducing chromatin apoptotic alterations in MCF-7 (25.1±3.7% apoptotic cells vs. 0±0% for control) and MDA-MB-231

(18.6±4.9% apoptotic cells vs. 0±0% for control) cells. For this same time point, HCA caused also an increase in the percentage of apoptotic nuclei in MDA-MB-231 cells (25.1±3.7% apoptotic cells vs. 0±0% for control).

Interestingly, by investigating by vital microscopy the effects of the two parent compounds and the two of the more active derivatives (HCA and HF, 75 mM), the decrease of MCF-7 proliferation is accompanied by altered cell shape, namely rounding up of cells, membrane blebbing and loss of mitochondrial membrane potential (indicated by white arrows in Fig. 23), which are typically from an apoptotic phenotype. From Fig. 23, it is seen that HF causes the highest degree of cell alterations, including loss of mitochondrial TMRM accumulation, although, in this regard, HCA is shown to induce more visible effects on the breast cancer cell MCF-7 than on the BJ line. The lower panel of Fig. 23 shows in more detail alterations in mitochondrial membrane potential caused by 75 mM HCA in MDA-MB-231 cells, as compared with a small, if any, effect of 75 mM HF in this cell line after a 48h incubation. Mitochondrial depolarization is seen in TMRM labeled cells treated with HCA.

BJ

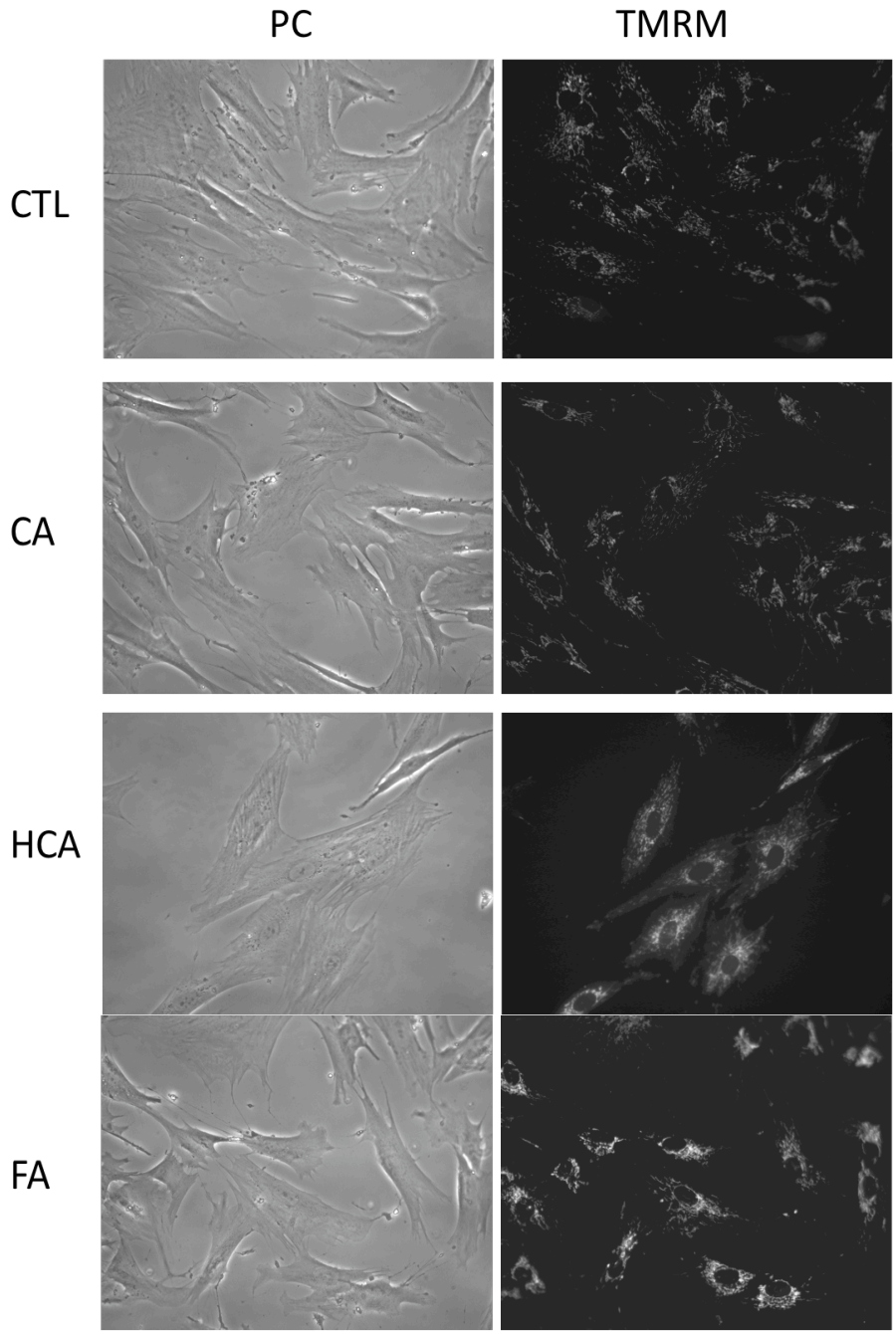

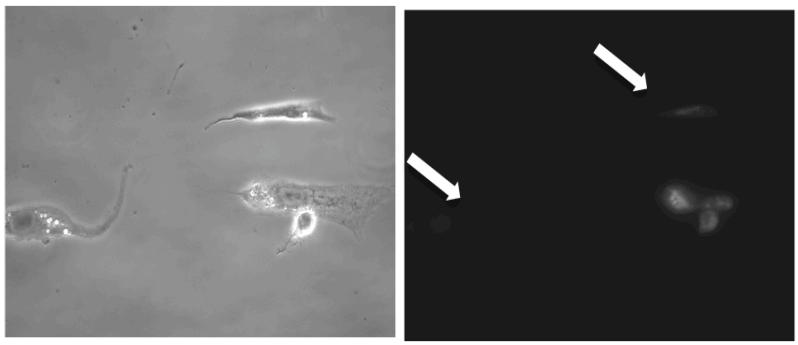

MCF-7

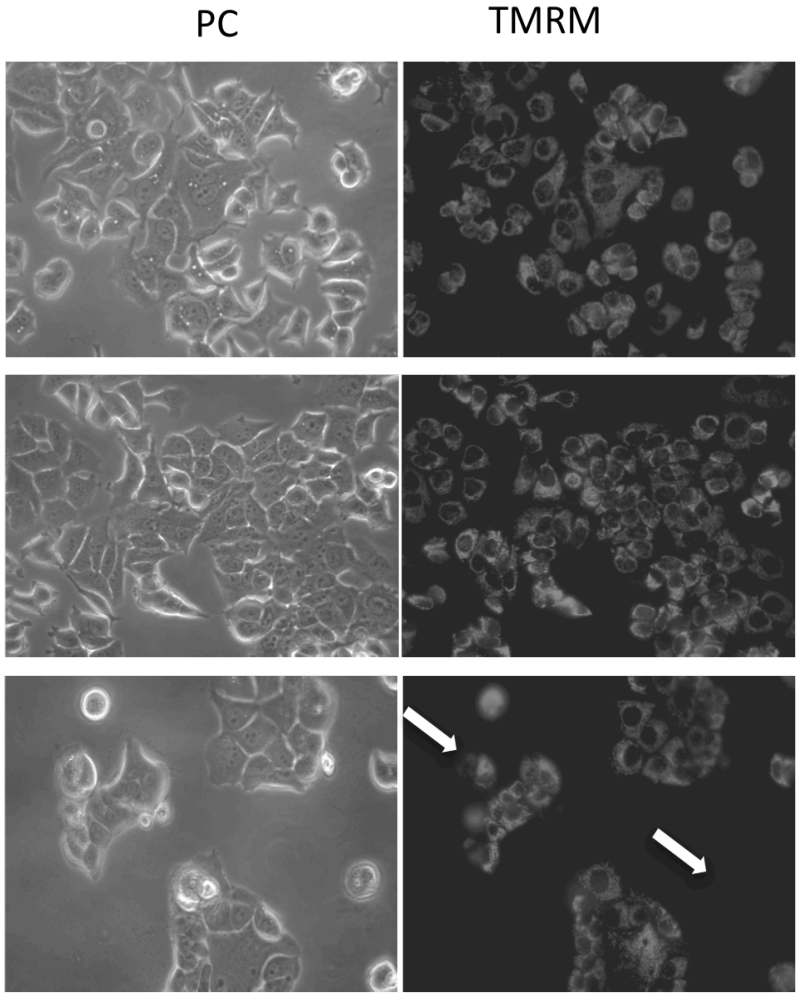

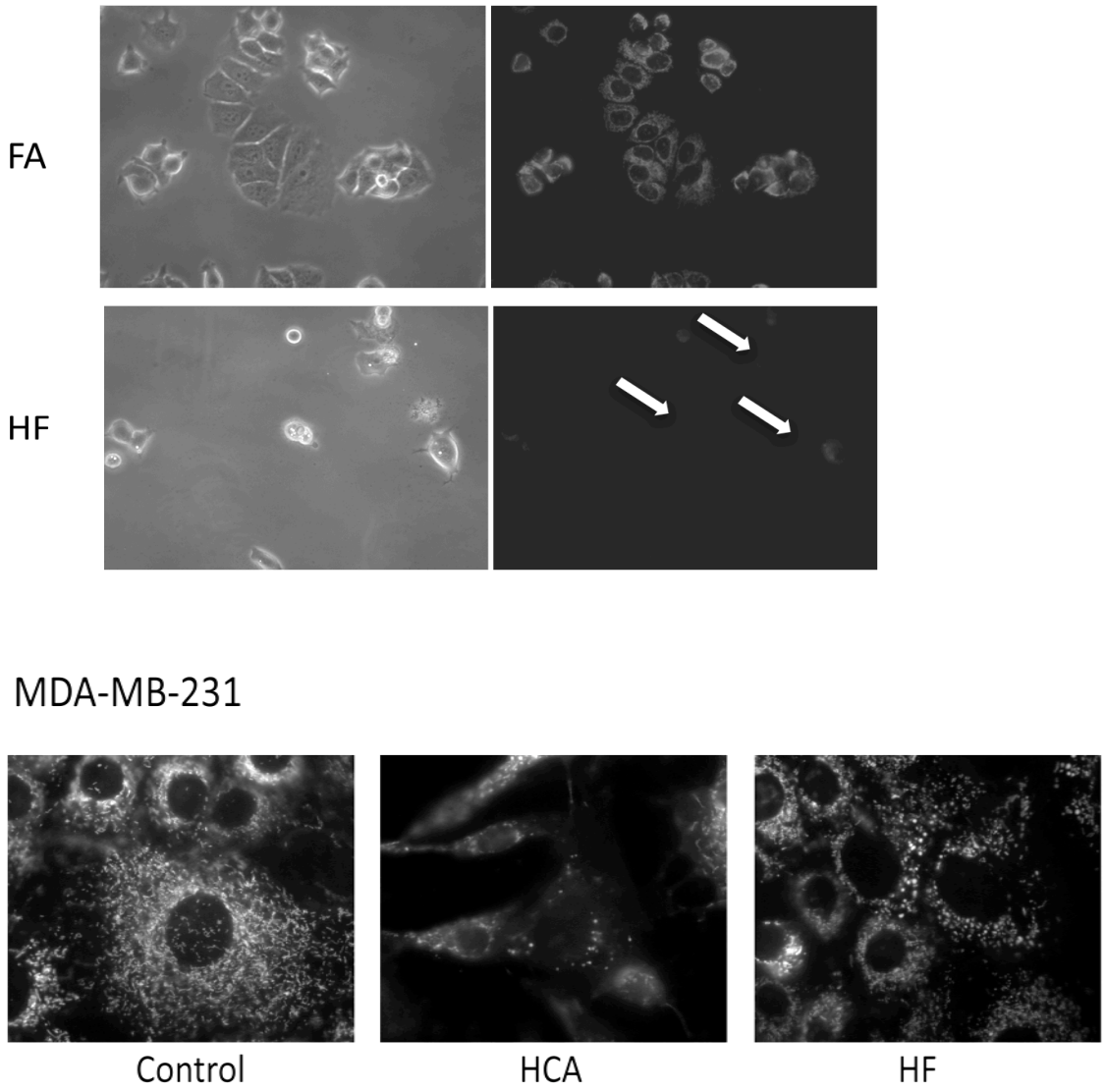

Fig.23 - Epifluorescence micrographs showing the effects of caffeic and ferulic acids and the derivatives HCA and HF on cell morphology and mitochondrial polarization in BJ and MCF-7 cell lines (upper set of images) and MDA-MB-231 (lower set of images). Cells were treated with ethanol vehicle only (0.01 % v/v, control) or 75μM of the test compounds for 48 hours. Cells were labeled with TMRM, which is accumulated by polarized mitochondria. Note as loss of mitochondrial polarization is first characterized by increased cytosolic TMRM fluorescence, followed by complete loss of cellular labeling, indicated in the upper set of images by white arrows. Mitochondrial depolarization is also visible in the lower images, when MDA-MB-231 cells were incubated with 75μM HCA but not with 75μM HF. The images are representative of three independent preparations.

After the initial set of experiments, the MCF-7 cell line was chosen for further experiments in order to clarify the activation of signaling pathways involved in

apoptosis and cell cycle regulation. Overall, this cell line was the most affected in terms of inhibition of proliferation and cell cycle. MCF-7 cell death caused by 75 μM HCA involves caspase 8 and 9 activation, as observed by Western Blotting. Cleaved, active fragments were detected for 96h but not for 48h of HCA treatment for both caspases (Fig. 24), which suggests involvement of the intrinsic and extrinsic apoptotic pathways. Cell death was also confirmed by a decrease in the band corresponding to full length poly(ADP-ribose) polymerase (PARP) for 96 hours of treatment. Although HCA appears to increase p53 protein in total extracts after 96h of treatment, no increase in the band corresponding to p21 was detected. The pro-apoptotic protein Bax and the anti-apoptotic protein Bcl-2 appeared not to be affected by HCA treatment for 48 or 96h (Fig. 24). The results were somewhat different when 75 μM HF was incubated with MCF-7 cells. No caspase 8 active fragment was detected for 48 and 96h, although an active caspase 9 fragment appears to be present for 48h (but not 96h) of treatment, simultaneously with a visible increase in p53 and Bax protein bands.

Regarding the two parent compounds (CA and FA), the most noticeable change was an apparent increase in p53 for 48h and 96h, although no alterations in other proteins were noted.

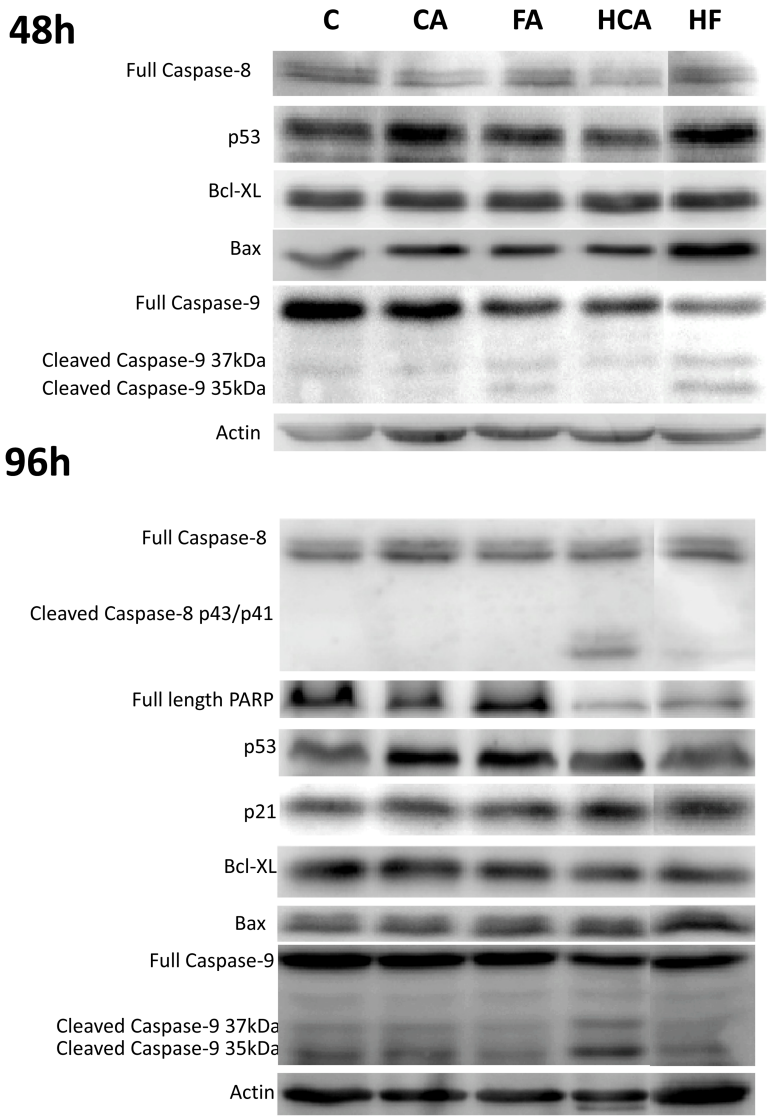

Fig.24 - Detection by Western blotting of proteins relevant for alterations in cell death and cell cycle in total fractions from MCF-7 cells. Protein loading was the same in each lane, confirmed by actin labeling. Cells were incubated with the test compounds for 48 and 96 hours. The results are representative of 3-4 separate experiments.

4.2.1.2.3. Effect of the phenolic compounds on isolated mitochondrial fractions

The final step of the present study was investigating direct mitochondrial effects of the test compounds by using isolated liver mitochondrial fractions as a biological model. As end-points for mitochondrial toxicity, mitochondrial respiration (state 3, state 4 and uncoupled) and $\Delta\Psi$ (maximum-attained $\Delta\Psi$, ADP-induced depolarization and phosphorylative lag phase) parameters were measured.

Regarding mitochondrial respiration, the effects of all test compounds on mitochondrial bioenergetics were made by using complex I (glutamate-malate) and complex II (succinate) substrates. When the former were used, significant alterations of mitochondrial respiration were observed with the parent compound CA (50 mM), which slightly decreased state 3 respiration (90.2 ± 2.1% of control value, $p<0.05$), with HF, which increased state 3 respiration (to 113.3 ± 3.5% of control, $p<0.05$) and with HFA (75 mM), which not only increased FCCP-uncoupled respiration (to 154.5 ± 14.1% of control, $p<0.05$) but also decreased the RCR (69.2 ± 5.4% of control values, $p<0.05$). When succinate was used as substrate in the presence of rotenone, a few alterations were observed. HF (75 mM) decreased the RCR (to 74.8 ± 6.1% of the control value, $p<0.05$), which was mostly caused by an increase on state 4 respiration (146.2 ± 16.3% of control values, $p<0.05$).

Regarding the generation of the transmembrane electric potential ($\Delta\Psi$), the effects of the different compounds tested were minimal. Only one alteration was measured, which was a decreased ADP-induced depolarization (down to 82.9 ± 4.8% of control values, $p<0.05$) caused by HCA.

Next, the phenolic compounds were investigated according to their ability to induce the MPT. MPT pore opening has been closely related with mitochondrial toxicity of different xenobiotics and with induction of cell death (Halestrap A, 2009). Calcium-induced mitochondrial swelling is one hallmark of MPT induction and can be followed spectrophotometrically. Figure 8 (right panel) shows a representative recording of MPT induction after calcium addition and the effect of pre-incubation with the different test compounds. In this regard, the results were somehow unexpected. For example, the parent compound FA induced the MPT as demonstrated by increased calcium-dependent mitochondrial swelling amplitude; this effect was abolished in the derivatives, although HFA caused a non-statistically significant increase in calcium-induced swelling (Fig. 25, C and D). As for caffeic acid derivatives, only HC presented in vitro MPT-inducing properties for the highest concentration tested (Fig. 25A and B). A negative control was made with Cyclosporin-A (CsA), the specific MPT inhibitor *(*Broekemeier et al, 1989), pre-incubated with mitochondria and the highest concentrations of the compounds to be tested. Swelling amplitude was decreased with CsA (Fig. 25).

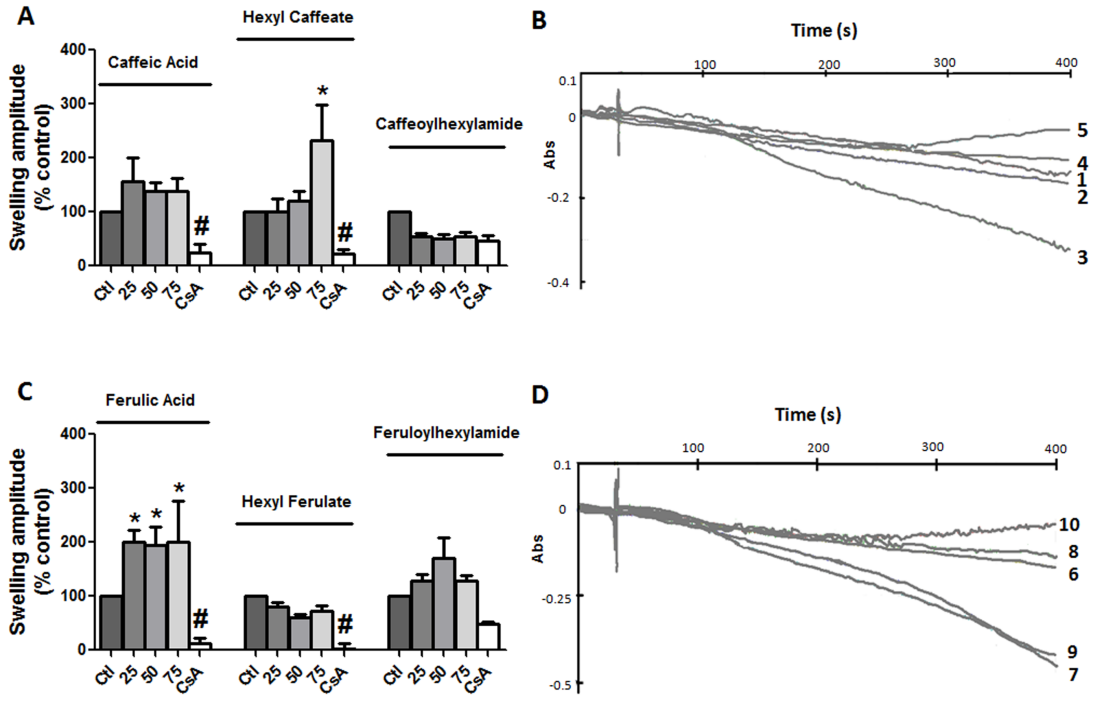

Fig.25 - Effects of different concentrations of the test compounds on calcium-induced MPT pore, as followed by measuring variations in mitochondrial volume. Results are shown for caffeic acid and derivatives (A) and ferulic acid and derivatives (C). Mitochondrial swelling amplitude was calculated as the difference between the base line absorbance and the absorbance after 400 seconds. Data are means ± S.E.M. of at least five different experiments. Typical recording of the effect of caffeic acid and derivatives (B) and ferulic acid and derivatives (D) on mitochondrial swelling. Mitochondrial (1.5 mg) were energized by succinate. After a basal line was established, 20μM calcium was added to induce the MPT pore. Mitochondria were incubated with 75μM of phenolic acids. In (B): Line (1) control, (2) caffeic acid, (3) hexyl caffeate, (4) caffeoylhexylamide, (5) cyclosporin A. In (D): Line (6) control, (7) ferulic acid, (8) hexyl ferulate; (9) Feruloylhexylamide; (10) Cyclosporin A. Cyclosporin A was incubated before the addition of calcium and was able to prevent mitochondrial swelling. The recordings showed here are representative of at least five independent mitochondrial preparations.

4.2.1.3. Discussion

Phenolic acids have been recognized not only for their properties on the prevention or delay of *in vitro* and *in vivo* deleterious oxidation processes, due to intrinsic free radical scavenging and antioxidant activity, but especially for their cytotoxic effects towards neoplastic cells. Interestingly, it is also known that low-molecular-weight phenolic acids can produce both cytoprotective and cytotoxic effects

in different settings (Fedotcheva et al, 2008), including cytotoxicity towards breast cancer in *in vitro* and *in vivo* experiments (Jung et al, 2010). However, details are still scarce regarding their mechanisms of action.

The present work was aimed at studying the cytotoxicity of a series of caffeic and ferulic acid ester and amides lipophilic derivatives (Roleira et al, 2010) towards human breast cancer cells, as well as their direct effects on isolated hepatic mitochondrial fractions. The objective was to identify if the molecular alterations aimed at increasing the lipophilicity of the test compounds would render them more active towards breast cancer cells, and also by increasing their reactivity towards mitochondria.

Hexylcinnamic amides were synthesized in moderate/high yields by a one-pot condensation reaction that occurs in equimolar amounts between the corresponding cinnamic acids and hexylamine. The coupling reagent selected for carboxylic acid activation was (benzotriazol-1-yloxy) tris(dimethylamino)phosphonium hexafluorophosphate (BOP) (Rajan et al, 2001). As the classic acid-catalyzed Fisher esterification is not appropriate when using long chain alkyl alcohols, the hexylcinnamic esters were obtained by base-catalyzed alkylation from the corresponding cinnamic acids with in situ generation of the carboxylate anions and subsequent reaction, at room temperature, with hexylbromide (Son et al, 2001; Nomura et al, 2002). The hydrophilic parent compounds caffeic (CA) and ferulic (FA) acids are thus modified by adding an alkyl chain through an ester or an amide bond (Fig. 7), originating hexyl caffeate (HC), hexyl ferulate (HF), caffeoylhexylamide (HCA) and feruloylhexylamide (HFA), respectively. The synthesized compounds were purified and then identified by both NMR and EI-MS, this data being in accordance with previous reports (Roleira et al, 2010). Raman spectra were also obtained for the solid samples of the synthesized compounds.

As expected, the structural modification performed in the phenolic systems led to an increase in lipophilicity, which is expected to favor the intracellular accumulation of the compounds. In fact, CA (logD 0.16) and FA (logD 0.42) have relative low lipophilicity compared to the new compounds, where HC (logP 3.91), HCA (logP 3.61), HF (logP 4.05) and HFA (logP 3.58) (Roleira et al, 2010).

Despite the facts that the parent compounds revealed no toxicity towards the cell lines studied, the derivatives were found to exhibit distinct effects on cell proliferation

depending on the cell line studied. The experiments performed in non-cancerous cells (the BJ cell line) indicate that some of these new compounds, particularly the caffeate derivatives, can display some cell growth inhibition towards normal cells, affecting both cell density and viability. However, these effects were mostly based on cell cycle arrest rather than cell death (Figs. 19 and 21), which is demonstrative of some sparing effect on non-tumor cells. Cell death caused by the phenolic derivatives was confirmed by mitochondrial depolarization (Fig. 23), sub-G1 peaks (Figs. 19 and 20) and chromatin condensation. Interestingly, it can be seen from Figs. 19 and 20 that amide derivatives of both caffeic and ferulic acids are more active towards inhibition of cancer cell proliferation.

In the present study, three different breast cancer cell lines were used, divided into estrogen receptor-positive breast cancer (MCF-7) and estrogen receptor-negative breast cancer cells (MDA-MB-231 and HS578T). MCF-7 cells showed to be the more susceptible to the two ferulic acid derivatives (Fig. 20). Knowing that some drugs can repress estrogen receptor alpha (ERα) and cyclin D1-dependent transcription, leading to G1 cell cycle arrest *(*Alao et al, 2004), it can be suggested that the test compounds can interact with estrogen receptors or with downstream signaling pathways, contributing to the increased susceptibility of MCF-7 cells. Other biophysical properties can also be responsible for differential cell response to chemotherapy, including alterations in the composition of cell membrane lipids, which can decrease intracellular drug transport via diffusion *(*Peetla et al, 2010*)*. Moreover, multidrug resistance may contribute to possible different drug toxicity, if the proteins contributing to such resistance are not equally present in the cell lines tested *(*Doyle and Ross, 2003*)*.

By focusing on the mechanisms of apoptotic signaling triggered by the test compounds on MCF-7 cells, data from cell cycle analysis suggests that the derivatives in study cause an initial block of S phase. It is known that cell cycle regulators, such as p53, play an important role in the process of apoptosis, regulating expression of Bcl-2 family proteins that modulate the mitochondrial pathway of apoptosis *(*Vasev and Moll, 2009; Sardão et al, 2009*)*. The apparent increase in p53 resulting from incubation with HF (48h, Fig. 24) can impact the progression of the cell cycle. Nevertheless, an apparent increase in p53 in MCF-7 cells treated with CA (48h and 96h) and FA (96h) was also observed, although no effects were observed in terms of cell cycle or apoptosis, which is line with

an absence of effects on Bax or p21 (Fig. 24). The results from Fig. 24 suggest that HCA is acting in both the intrinsic and extrinsic pathways for apoptosis, although the mechanism is still unknown. The results are not surprising since it has been described that phenolic acids can interact with cell surface receptors such as tumor necrosis factor related apoptosis inducing ligand (TRAIL), promoting caspase-8-dependent cell death *(*Szliszka et al, 2009*)*. By its turn, the data appears to suggest that HF mostly acts through the mitochondrial pathway involving p53 and Bax (Fig. 24), and mediated by mitochondrial depolarization (Fig. 23) with consequent activation of caspase 9, which is more visible for 48h, and resulting in increased cell death (Fig. 20 and 22).

Since mitochondria are involved at the crossroads of carcinogenesis, cancer chemotherapy and tumor survival, as well as drug-induced toxicity, we investigated whether the parent compounds and their derivatives could exert direct effect on isolated rat hepatic mitochondria. Although normal liver and cancer cell mitochondria present certain structural and functional differences *(*Mayevsky A, 2009; Gogvadze et al, 2010b*)*, we believe that sufficient similarities exist to justify using isolated liver mitochondria as models to gain insights into the interactions of xenobiotic compounds with mitochondria. Also, isolated mitochondrial fractions present the advantage of a much higher isolation yield so that more aspects of mitochondrial function and compound-induced toxicity can be studied with one single isolation procedure. Studies on isolated mitochondrial fractions from non-tumor tissues also can supply clues on the toxicity of the test compounds to non-target organs. Some direct effects of the parent compounds and lipophilic derivatives were observed on mitochondrial bioenergetics but the most surprising result was an expected induction of the MPT by FA, which was never before reported in the literature. Since no toxic effects of FA on intact cells were observed, this may indicate that FA does to interact with mitochondria in intact cells, at least in the concentrations that are able to induce the MPT. The mechanisms by which FA caused MPT induction are unknown at the moment and deserve further attention. Also, with the exception of HC, which caused MPT induction for the highest concentration tested (75 mM), the new lipophilic derivatives were shown to be less toxic to isolated mitochondrial fractions regarding MPT induction (Fig. 25). Apparently, there was not a direct relationship between the toxicity on isolated hepatic mitochondrial fractions and the effects on intact cells, which may mean that this organelle is not part of the main

mechanism of cytotoxicity of the new derivatives. We have previously demonstrated that the cell toxicity of the phytochemical berberine presented a good degree of equivalency to the effects observed in isolated hepatic mitochondria, demonstrating in this case a classic example of a compound which primary mechanism of toxicity relies on mitochondria (Pereira et al, 2007). Indirectly, the data on isolated mitochondrial fractions also suggest the relatively low toxicity of the new derivatives for concentrations lower than 50 mM, which can be a positive sign for further human safety evaluation of these novel molecules (Pereira et al, 2009, Sardão et al, 2008).

Although our objective of synthesizing lipophilic derivatives with higher ability to interact with cell systems was achieved, further research will be required to define more specifically the mechanisms of action and to propose the use of these novel compounds on cancer prevention and treatment. One particular aspect is the fact that the compounds exerted the majority of their effects on cancer cells at concentrations higher than 25 mM and for incubations higher or equal to 3 days. Although this appears a high concentration which would be difficult to maintain in the serum for that amount of time, there are clues that may indicate otherwise. For example, the increased lipophilicity of the derivatives here tested may increase their higher persistence in a lipid environment. Although data is not still available on the bioavailability of the derivatives here tested, more has been published on the parent compounds themselves, since they are present in the human diet. One study suggested that the concentration of caffeic acid in the blood of humans, with normal intake of food and average coffee intake is around 2.4 μg/mL, or 13 mM (Huang et al, 2009). Individuals that drink several cups of coffee per day, may ingest as much as 500-800 mg hydroxycinnamic acids per day (Manach et al, 2004). Wang et al. measured caffeic acid plasma concentrations after an I.V.bolus of 4.5 mg/kg to Sprague-Dawley rats. The peak of plasma concentration was around 22 mM, although it rapidly decayed within 90 minutes (Wang et al, 2006). In order to maintain higher concentrations in the plasma during longer times, one alternative would be liposomal encapsulation, although a series of technical issues still need to be solved (Coimbra et al, 2011). A further approach is that the test compounds may be used jointly with conventional therapies, although the outcome may not always be an increased tumor cell killing.

In conclusion, we have investigated the cytotoxicity of novel lipophilic caffeic

and ferulic acid derivatives in human breast cancer cells and in a non-tumor cell line. The inclusion of an alkyl chain through an ester or an amide bond on both caffeic and ferulic acid increase their cytotoxicity towards the cell lines studied, especially against the estrogen-positive MCF-7 cell line. The data suggests possible structural modifications in phenolic acids usually present in the human diet, in order to increase their interaction with tumor cells and gain easier access to intracellular targets. We also conclude that from the data obtained, direct toxicity at the mitochondrial level may not be the mechanism of action for the new derivative compounds.

4.2.2. Lupane triterpenoids derivatives as potential new chemotherapeutics

4.2.2.1. Background and Objectives

Plants generally produce natural products as a defense against flora pathogens, thus such products have also important applications for humans. In the past, Native Americans used birch bark in folk medicine, and over the years, some birch bark constituents, triterpenoids, showed to have low toxicity and therefore were used in drug, cosmetics, dietary supplements, biocides, etc. (Krasutsky, P., 2006). Nowadays, scientific research has revealed remarkable biological and medical properties of these triterpenes and their derivatives (Li et al, 2010). Among *Betula papyrifera* extracts, betulin and betulinic acid are the most abundant triterpenoids present, in amounts of 72.4% and 5.4% respectively (Krasutsky, P., 2006). In the last decade, these compounds have been under intensive research due to discovery of their anti-cancer and anti-HIV properties (Huang and Chen, 2002). Further on, their anti-bacterial (Alakurtti et al., 2006) and anti-viral (Pavlova et al., 2003) activities were discovered to be extremely relevant. Earlier, Yasukawa *et al.* (1991) showed that betulinic acid was a very potent chemical, inhibiting inflammation and presenting tumor suppression activity at very low concentration (5μM). Further on, Galgon et al. (2000) performed experiments showing that this pentacyclic triterpenoid induced apoptosis in melanoma cells, later showing this activity to be specific for tumors derived from neuroectoderm (Mullauer et al., 2009). We know today that betulinic acid has anti-cancer activity in many other malignancies, namely leukemia, prostate, ovarian, breast, lung, and colon cancer (Fulda S, 2009). One of the most important finding is that betulinic acid acts selectively towards tumor cells, not affecting normal cells (Fulda et al, 1998).

Betulinic acid triggers apoptosis in cancer cells by affecting mitochondria membrane permeabilization (Fulda and Kroemer, 2009), which is a promising approach since cancer cells normally have methods to evade from apoptosis, thus becoming resistant to traditional therapies (Armstrong, J., 2007). Even if betulinic acid is *per se* a revelant and active anti-cancer agent, research on the structure-activity of betulinic acid derivatives is underway, with the ultimate goal to increase the solubility of these compounds in water, reduce possible harmful side effects and increase the efficacy in

controlling tumor growth (Krasutsky, P., 2006).

Recently, a number of semi-synthetic derivatives of lupane triterpenoids have been synthesized at the Natural Resources Research Institute of the University of Minnesota, USA, having as base-structure the compounds betulin and betulinic acid. Holy et al. (2010) studied the activity of the new compounds in cancer cells, and concluded that these dimethylaminopyridine (DMAP) derivatives could suppress cell growth and disrupt mitochondria dynamics, suggesting that can act as mitocans. As a follow-up for the work of Holy et al. (2010), we performed several experiments to better identify the molecular mechanisms of several new DMAP derivatives (Fig.8), including their effect on breast cancer cells in terms of cell proliferation, cell cycle and cell death, as well as their toxicity towards isolated mitochondrial fractions. The objective of this section is to identify mitochondria in breast cancer cells as a target for these novel DMAP derivatives, showing that these novel compounds are good mitocan candidates, with low toxicity in normal cells and therefore, with the possibility to be used in cancer therapy.

4.2.2.2.Results

4.2.2.2.1. Cell proliferation is disturbed by lupane triterpenoids action

To evaluate the effect of the new semi-synthetic derivatives of lupane triterpenoids (see Material & Methods, Fig.8), on cell proliferation, a dose-response assay using sulforhodamine B (SRB) method was carried. Monolayer cultures of MDA-MB-231, HS578T and MCF-7 human breast cancer cell lines and non-tumor human fibroblast BJ cell line, were incubated in regular glucose medium with increasing concentrations of the compounds (0.125 - 2μg/ml) for 1, 3 and 5 days. On the non-tumor cell line (Fig.26), a significant inhibition of cell growth was observed for most compounds at the third and fifth days, especially for concentrations above 0.25μg/ml, with the exception of OK34 and OK37 compounds.

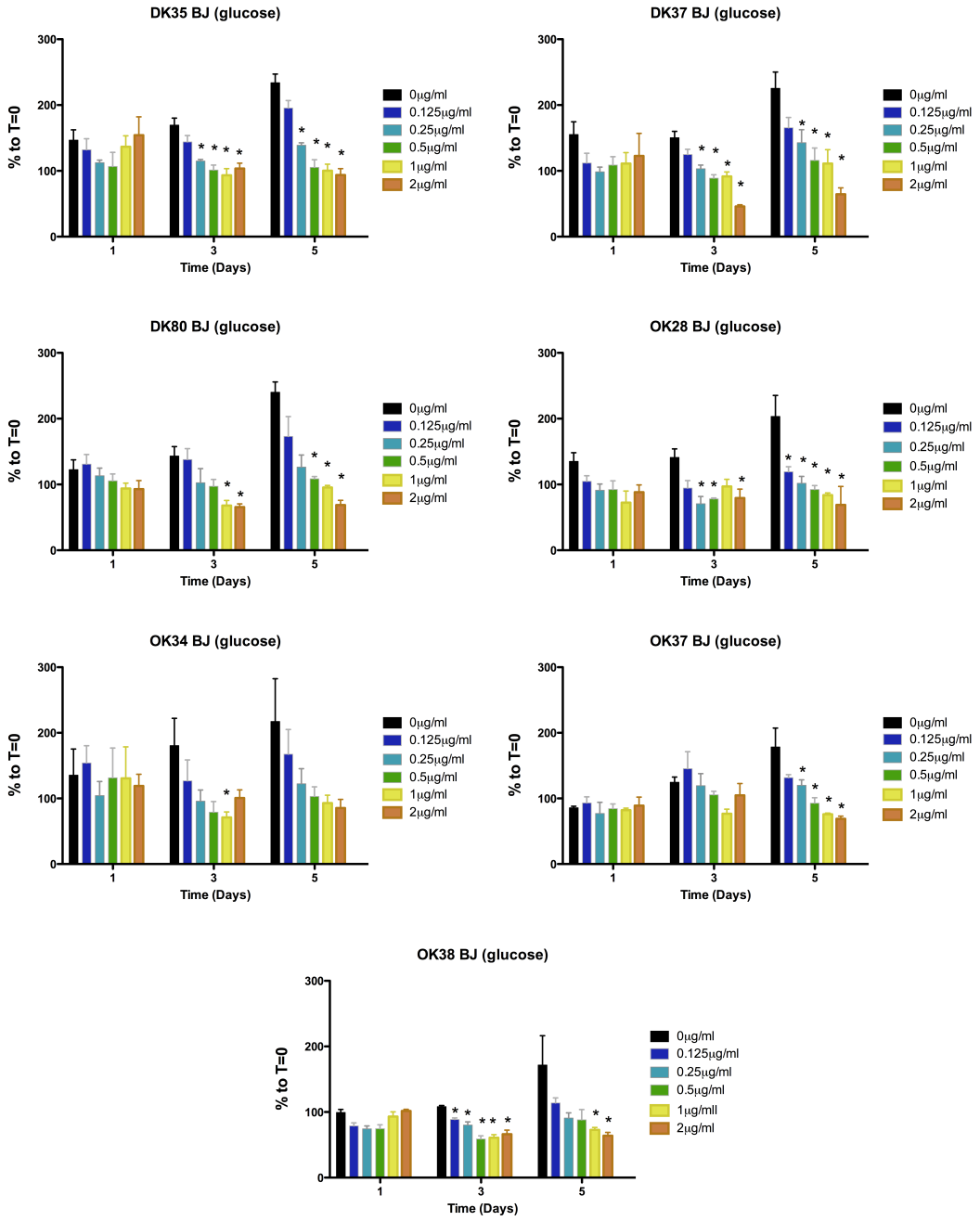

Fig.26 - Lupanes triterpenoid and non-tumor BJ cell proliferation. Triterpenoids interfere with cell proliferation of the BJ fibroblast cell line. $1x10^4$ cells/ml of breast cancer cells and $2x10^4$ cells/ml of normal fibroblasts were seeded in 48-well plates. Cells were grown in glucose medium and exposed during 1, 3 and 5 days to a range of triterpenoids concentrations, from 0.125 to 2µg/ml. The triterpenoids tested were DK35, DK37, DK80, OK28, OK34, OK37 and OK38, whose structures are represented in chapter 3, Material and Methods (Fig.2), with more information is available in Holy et al. (2010) (REF number). Cell proliferation was accessed by the sulforhodamine B method (SRB) and the results are expressed as a percentage of the control, which represents the density of cells right before drug (or vehicle) treatment (T=0). All

experiments were performed in quadruplicate and represent means +/- SEM, * p<0.05 vs. control.

However, these same compounds did not have a significant impact on MDA-MB-231 cell proliferation (Fig.27), with only DK80 (for concentrations as higher as 1µg/ml at the third and fifth days) and OK37 (for concentrations 0,25µg/ml at the fifth day) showing inhibitory effects on cell proliferation.

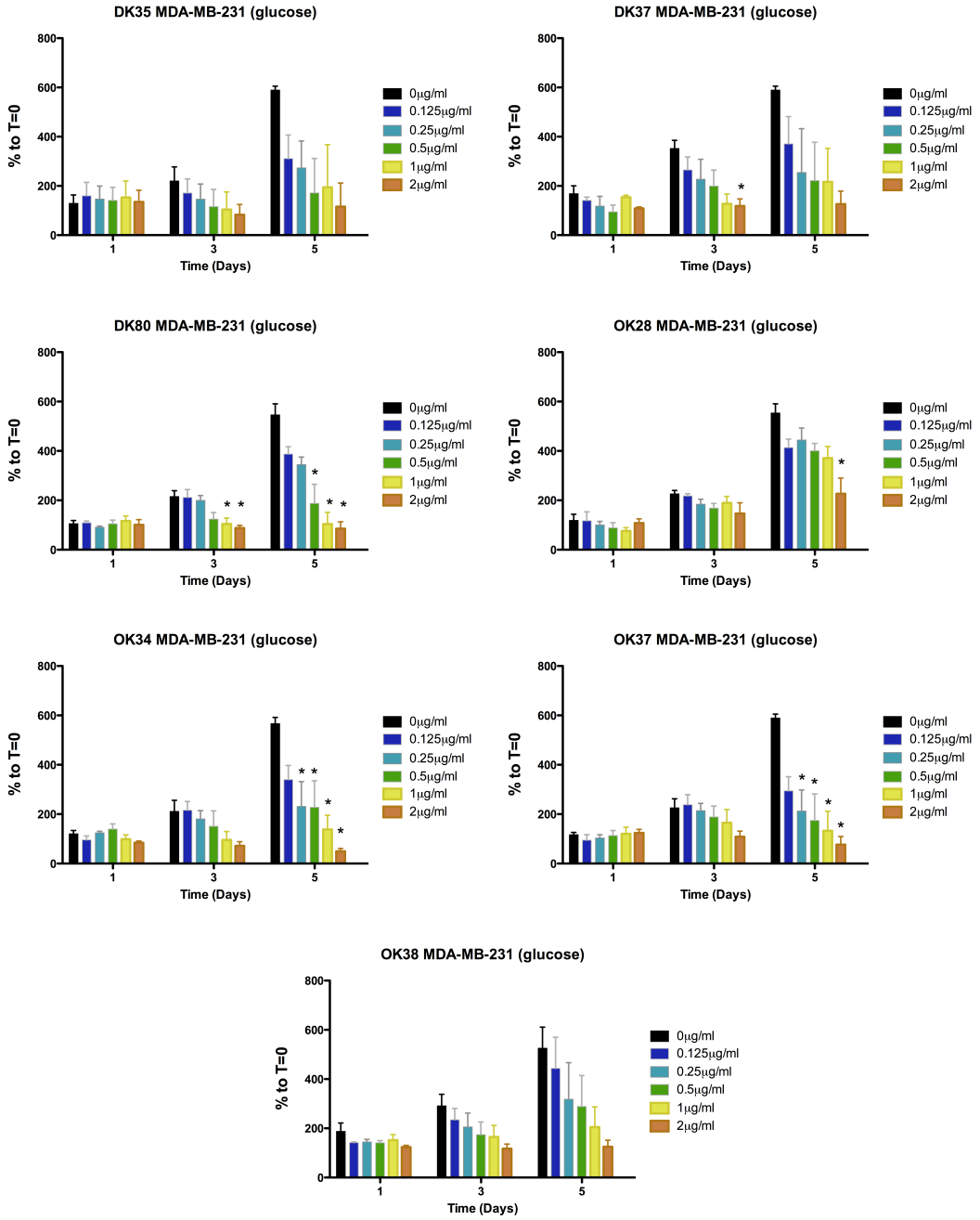

Fig.27 - Inhibition of MDA-MB-231 cell proliferation by the test compounds cells. MDA-MB-231 cells were the least affected with the treatment. The human breast cancer MDA-MB-231 cell line was incubated with the same triterpenoids compounds and under the same conditions

mentioned in Fig.26. The experiments were performed in quadruplicate and represent means +/- SEM, * p<0.05 vs. control.

All the compounds tested disturbed greatly the proliferation of MCF-7 and HS578T cells (Fig.28 and Fig.29, respectively). The triterpenoids DK35, OK28, OK34, OK37 and OK38 significantly inhibited MCF-7 cell proliferation at the fifth day, while DK37 and DK80 showed inhibitory signs after the third day of exposure. HS578T cell proliferation was inhibited starting from the third day of treatment by DK80, OK34, OK37 and OK38, while DK35, DK37 and OK28 exerted significant inhibition of cell proliferation at the fifth day. Interestingly, OK34 and OK37 had a lower effect on both normal BJ and tumor MCF-7 cell lines, however both compounds affected the resistant breast cell lines MDA-MB-231 and HS578T. In fact, OK34 and OK37 seem to have very similar effect in all types of cells. In the same manner, both DK35 and DK37 also seem to have similar effects in the cell lines studied, although DK37 seems to present a stronger effect.

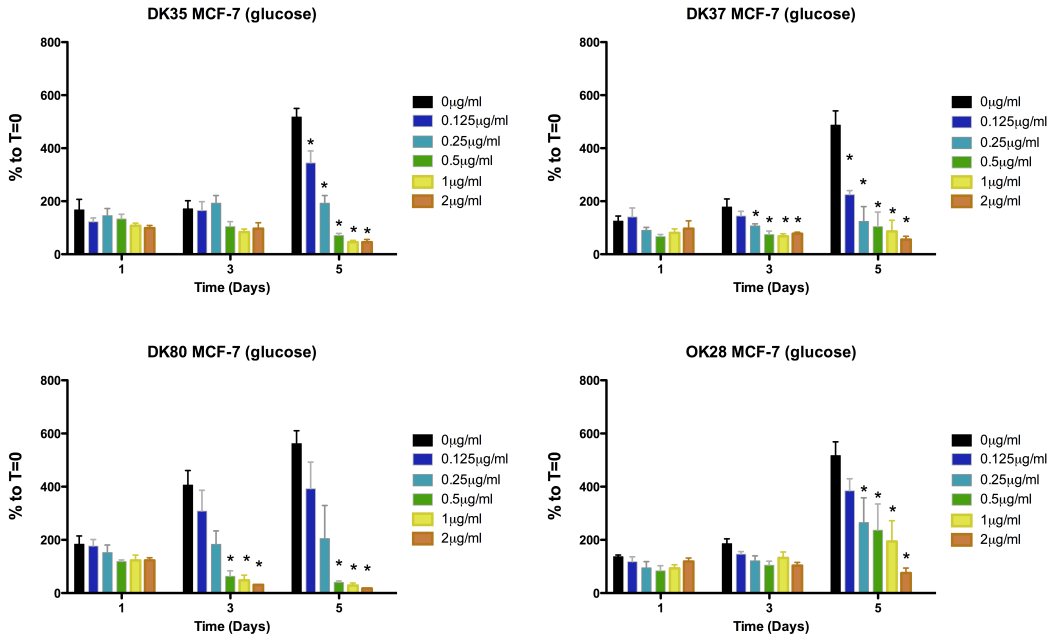

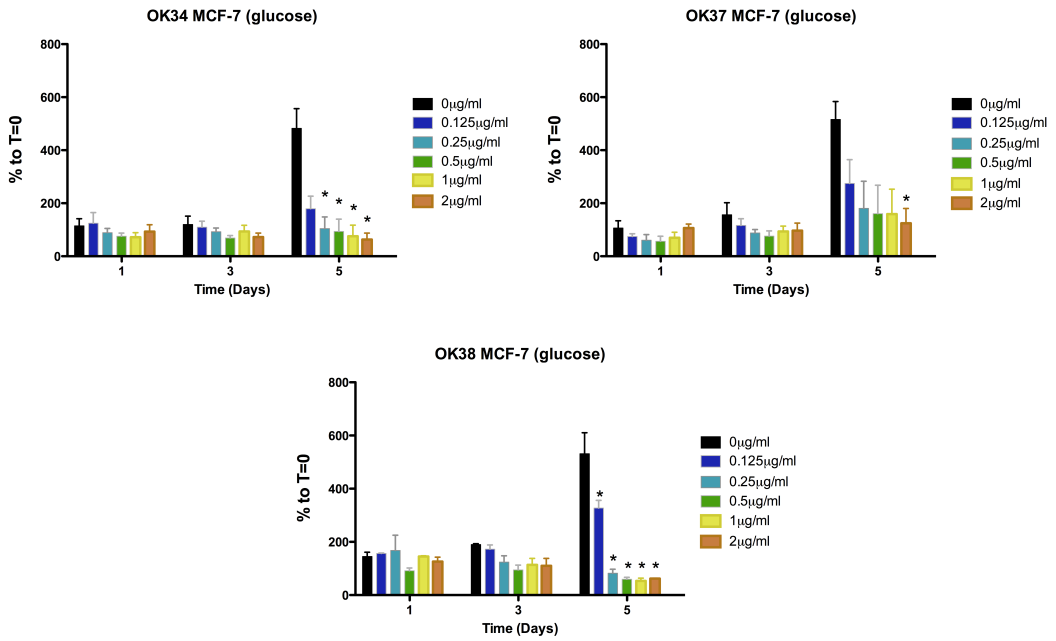

Fig.28 - Inhibition of MCF-7 proliferation by the test triterpenoids. MCF-7 cell proliferation was inhibited by the test triterpenoids.. The human breast cancer MCF-7 cell line was incubated to the same triterpenoids compounds and in the same conditions mentioned in Fig.26. The experiments were performed in quadruplicate and represent means +/- SEM, * $p<0.05$ vs. control.

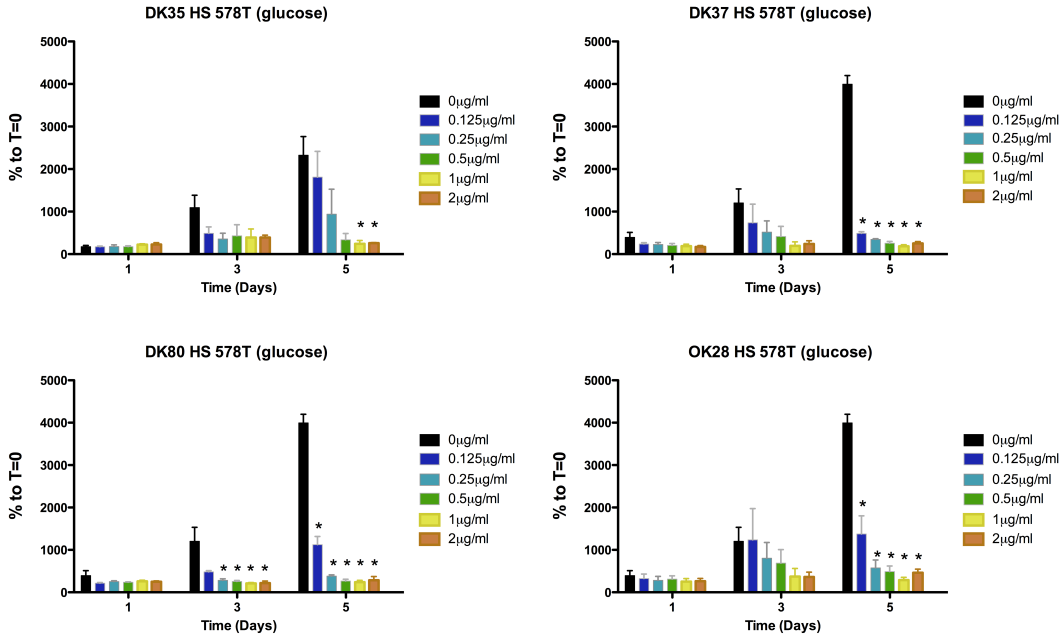

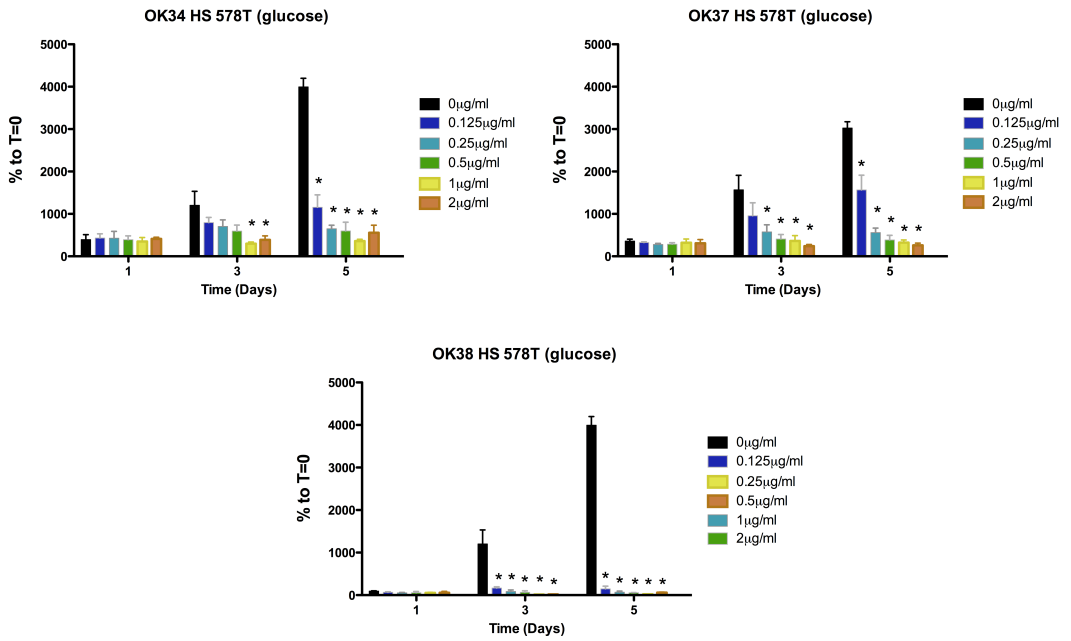

Fig.29 - Inhibition of HS578T proliferation by the test triterpenoids . HS578T cells proliferation was significantly inhibited. The human breast cancer HS578T cell line was exposed to the same triterpenoids compounds and in the same conditions mentioned in Fig.26. The experiments were performed in quadruplicate and represent means +/- SEM, * p<0.05 vs. control.

Since HS578T and MCF-7 cells were the most susceptible cell lines to the test compounds, and since HS578T cells are more aggressive due to their invasive capacity, we have chosen the latter cell line for the following experiments. For the next step of the work, we have tested the recovery of cancer cells after treatment with the triterpenoids. The experimental procedure consisted in exposing HS578T breast cancer cells to the test compounds for 6 hours and then removing the media containing the compounds by washing the wells two times with PBS and two other times with fresh medium (Fig.30). In general, cells do not recover at the end of the fifth day when previously exposed to the highest concentrations, 0.5µg/ml, 1µg/ml and 2µg/ml for OK34 and OK37 and 1µg/ml and 2µg/m for DK35, DK37, DK80 and OK28. The exception was OK38. With this compound, cancer cells did not recover. This experiment is important to verify how efficient and persistent is a certain anti-cancer drug. In clinical terms, it is important that tumor re-grow does not occur during treatment pauses. Not having cell proliferation recovery after drug washing is a positive sign.

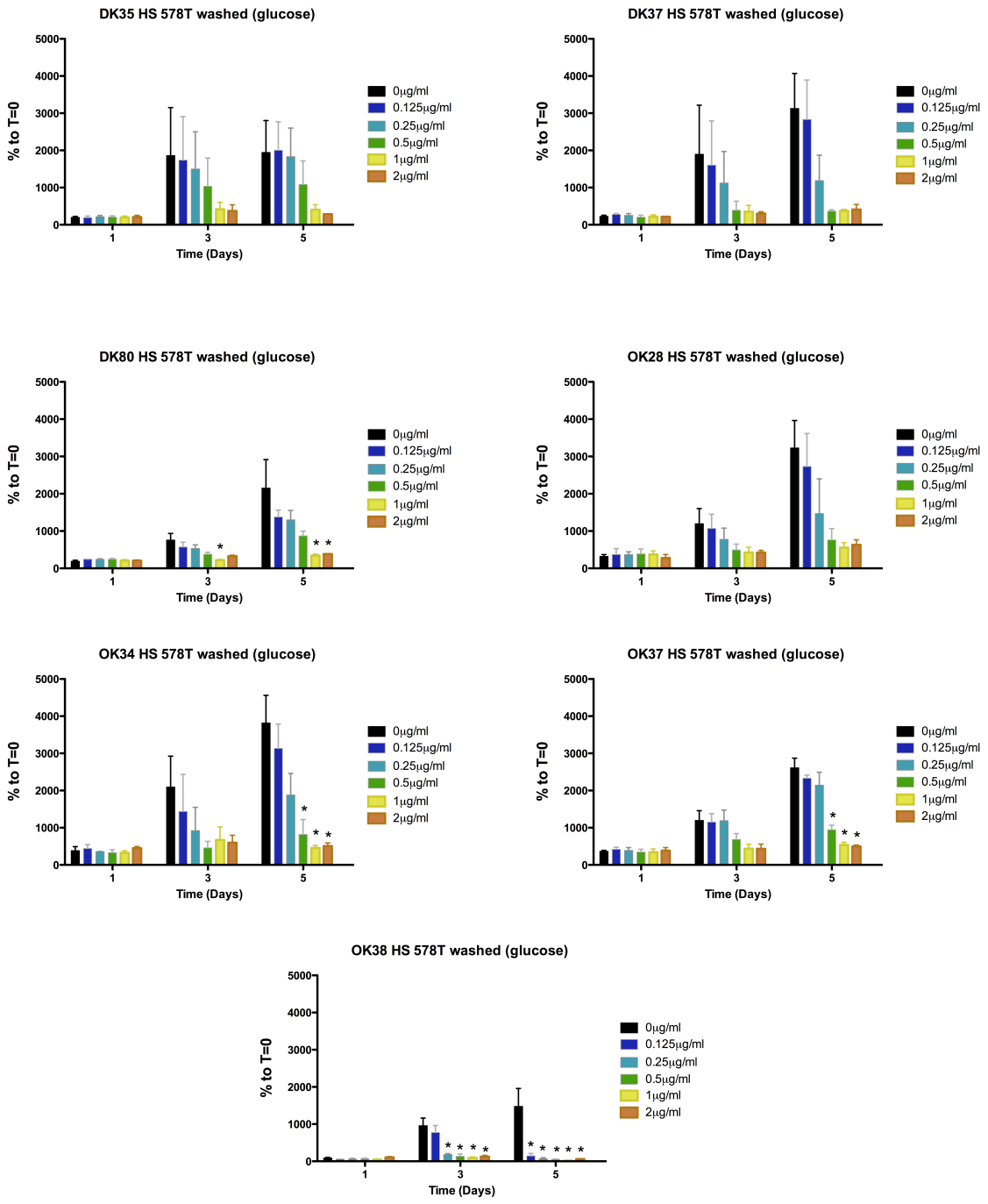

Fig.30 - Recovery of HS578T breast cancer cells after treatment with triterpenoids. HS578T cells were exposed to the different triterpenoids at concentrations from 0.125 to 2µg/ml during 6hours. Cells were then washed and new glucose medium was added. Cell proliferation was accessed by sulforhodamine B (SRB) and the results are expressed as a percentage of the control (non-treated) cells, taken as 100%, to equalize for different growth rates between cell lines and time of drug addition (T=0). All experiments were performed in quadruplicate and represent means +/- SEM, * $p<0.05$ vs. control.

The sulforhodamine B method does not inform us whether a drug treatment causes cells to die or to arrest their cell cycle. Thus, in order to better evaluate the effects of the test compounds, cell cycle status was analyzed by flow cytometry (Fig.31). Here, we used a single concentration (0.5µg/ml), which corresponds to the ID_{50} (50% growth inhibiting dose) observedin the cell line HS578T cells for 24 and 48 hours. All the triterpenoids showed a similar pattern of cell cycle arrest, with an increase of % of cells in G0/G1 phase and a decrease of the % of cells in S phase. For OK28, a decrease in the % of cells in G2/M phase was also observed.

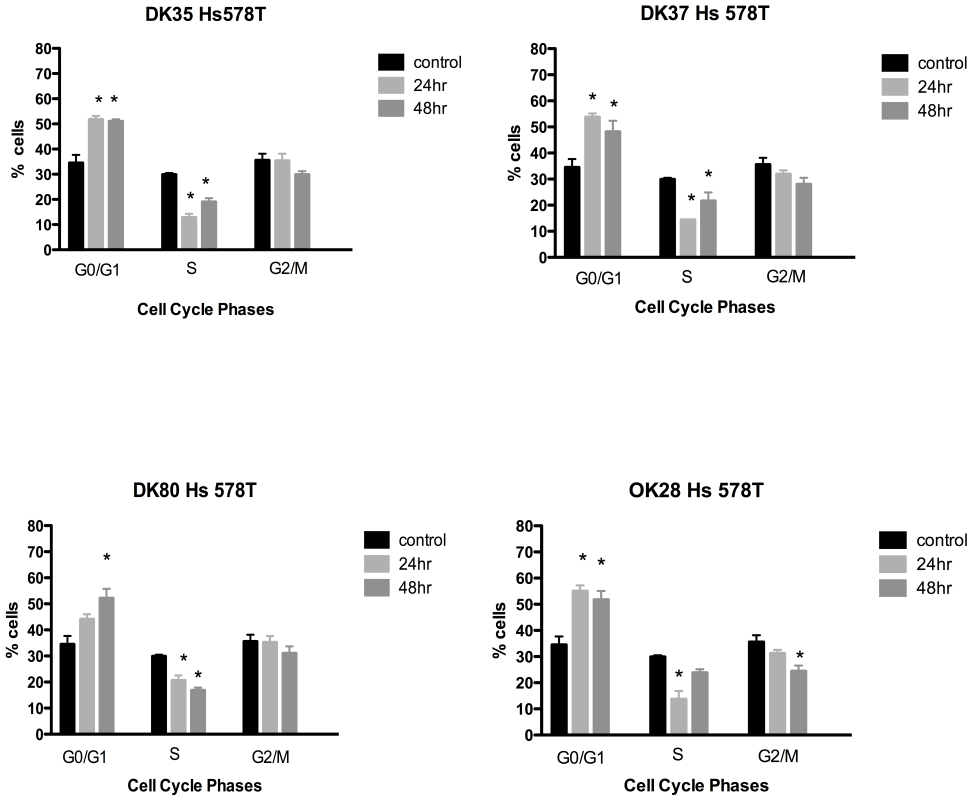

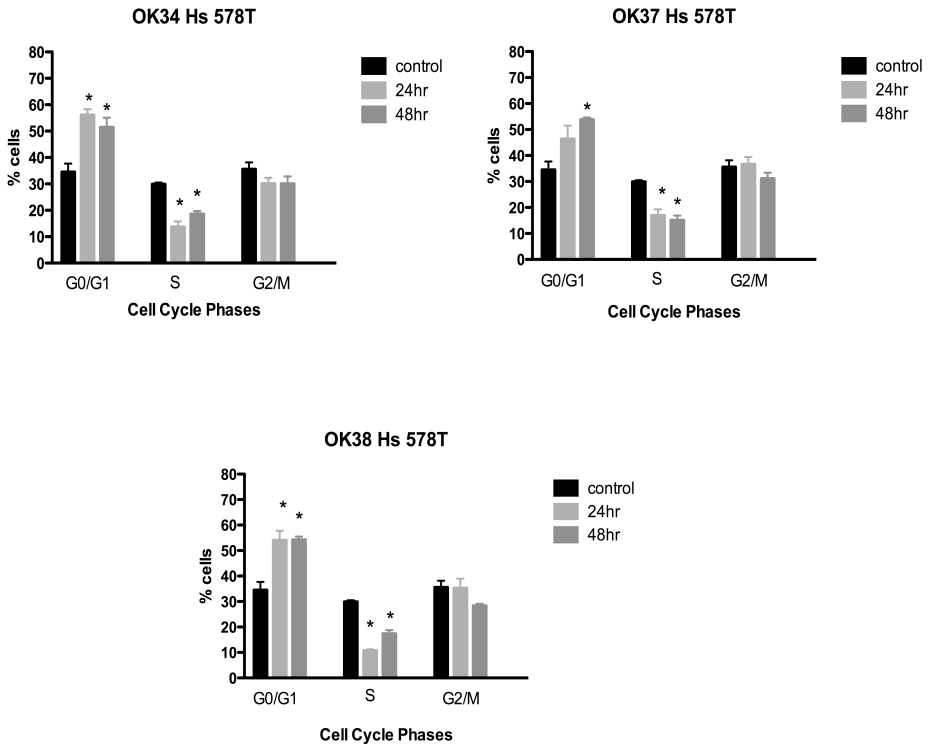

Fig.31 - Triterpenoids arrest HS578T cell cycle progression. Triterpenoids compounds (DK35, DK37, DK80, OK28, OK34, OK37 and OK38) affected HS578T cell cycle, after 24 and 48 hours of exposure. Flow cytometry assays show that all the compounds lead to an increase of cell number in G1/G0 phase, while cells in S-phase decreases. Data are means +/- SEM of 4 separate experiments, * $p<0.05$ vs. control.

Another strategy to control tumor growth is by combining two or more drugs, in order to disturb cancer cells at low doses, and therefore enhance their elimination, while reducing side-effects on non-tumor cells (Filomeni et al, 2011). Thus, we performed an experiment where we combined clinical used chemicals (which are commercially accessible), including Paclitaxel (Taxol), Doxorubicin (Dox) and Cisplatin (Cispla) together with the test triterpenoid compounds in HS578T cells during 3 days (Fig.32). The objective was to use a compound concentration that would inhibit 25% of cell proliferation and observe possible addition or synergistic effect of the clinically used compounds. The results showed that, with the exception of Taxol, no synergistic effects were observed in any case studied. The test compounds together with Taxol did show to have a significant reduction of cell proliferation, especially when DK37, DK80 and OK28 were used.

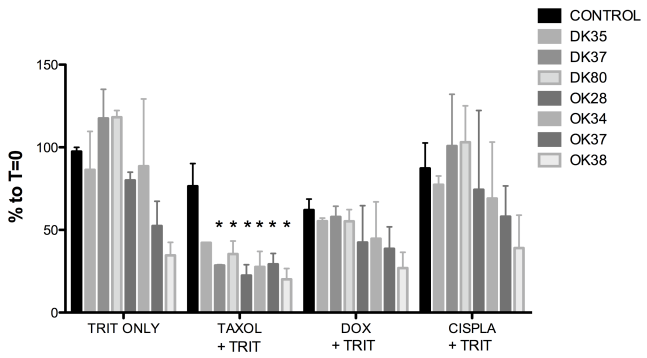

Fig.32 - Synergistic effects of test triterpenoids and clinically used anti-cancer drugs on HS578T breast cancer cells. HS578T cells were exposed during three days to triterpenoids compounds (DK35, DK37, DK80, OK28, OK34, OK37 and OK38) in conjugation with commercial agents Taxol, Doxorubicin and Cisplatin. No synergistic effect is observed, except for the combination with Taxol. Cell proliferation was analyzed by the sulforhodamine B assay. The results are means +/- SEM of 3 separate experiments, * $p<0.05$ vs. control.

From the above results, a sub-set of compounds that include DK37, DK80, OK34 and OK38 were selected for the following experiments, since they were shown to be more active against breast cancer cells.

4.2.2.2.2. Mitochondrial structure and function are altered by lupane triterpenoids

To detect changes in mitochondrial membrane polarization tetramethylrhodamine methylester (TMRM) was used in this study as a fluorescent polarization-dependent probe. For imaging mitochondrial alterations, we used normal BJ fibroblasts, HS578T breast cancer cells and introduced a new cell line the non-tumor breast cell line HS578Bst, which is the non-tumor equivalent to HS578T cells. Cells were labeled with TMRM and mitochondrial morphology and polarization were observed by fluorescence micrscopy. As observed and described in a previous section (chapter 4.1), non-tumor cells appear to have a more elongated and diffuse mitochondrial network, while cancer cells show to have condensed mitochondrial masses localized in a peri-nuclear region. Moreover, confirming what we reported before, the intensity of TMRM mitochondrial fluorescence was higher for cancer cell lines than for the normal cell line. For this experiment, the test compounds DK37, DK80, OK34 and OK38 were used and cells were exposed to different concentrations, starting from 0.125µg/ml to 2µg/ml for 6

hours in a set of preliminary experiments (data not shown).

Agents that interfere with mitochondria can lead to a ΔΨm drop and loss of TMRM accumulation, which in visual terms means that the mitochondrial network fluorescence would no longer be visible. Fig.33 shows images that correspond to the effect of the compounds mentioned above at a concentration of 0.25μg/ml, for 6 hours of treatment. Overall, for the concentration of triterpenoids used, it appears to affect mitochondria network of both tumor and non-tumor breast cells, but does not show any effect on the other normal cell line used, BJ fibroblasts. The test compounds ultimately lead to a rounding up of mitochondria and loss of TMRM fluorescence intensity. Roughly based on the strength of the compound, the strongest seems to be OK38, to which all the three cell lines tested are affected. DK37 seem to have a higher effect on HS578Bst cells, while OK34 seems to affect more HS578T cells, where mitochondrial fluorescence appear brighter than untreated cells, suggesting a possible hyperpolarization of mitochondria membrane. DK80 appear to affect both breast cell lines equally. Quantification of TMRM fluorescence by flow cytometry needs to be performed in order to quantify the variation in flurescence signal.

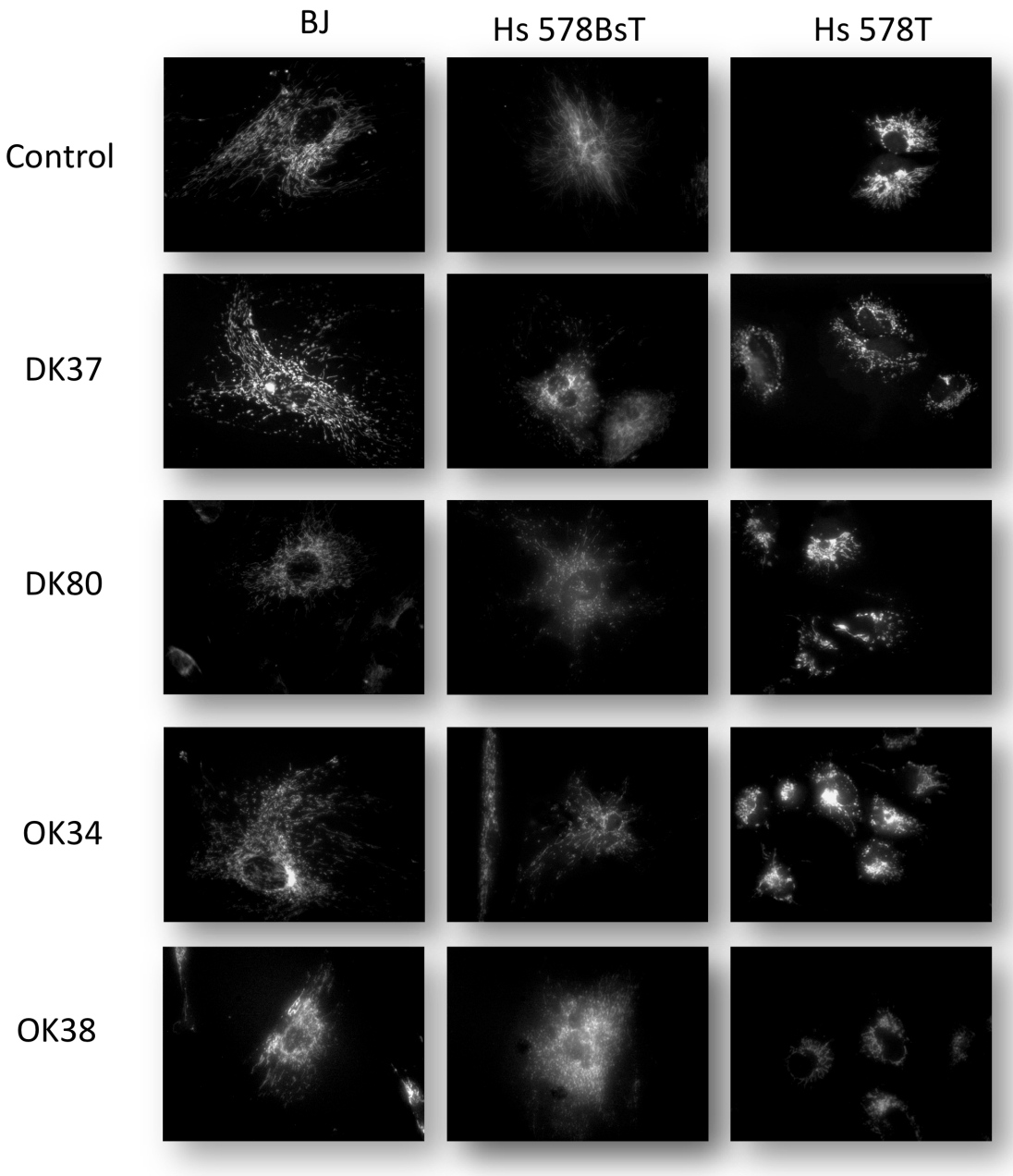

Fig.33 - Triterpenoids disturb mitochondrial polarization and morphology. Non-tumor BJ fibroblasts and breast HS578Bst, and the breast cancer cell line HS578T were treated with vehicle or 0.25µg/ml of DK37, DK80, OK34 and OK38 for 6 hours. Cells were labeled with TMRM and imaged by confocal microscopy in order to observe alterations in mitochondrial polarization. The images are representative of four independent preparations.

4.2.2.2.3. Direct effects of triterpenoids on mitochondrial oxidative phosphorylation – galactose media experiments

In chapter 4.1. we have tested some mitochondrial poisons when cells were grown in a glucose-free/ galactose-glutamine medium and in that particular experiment, we verified that for the concentrations used, MCF-7 cells were the most susceptible to treatments. Here, we exposed the same cell lines, MDA-MB-231, MCF-7 and HS578T breast cancer cells growing in the same conditions (galactose-glutamine medium), to the test triterpenoids. Once more a dose-response sulforhodamine B (SRB) assay was used and we verified that the compounds significantly inhibit the cell proliferation of MDA-MB-231 and MCF-7 for all concentrations at the third and fifth days of treatment (Fig.34 and 35, respectively).

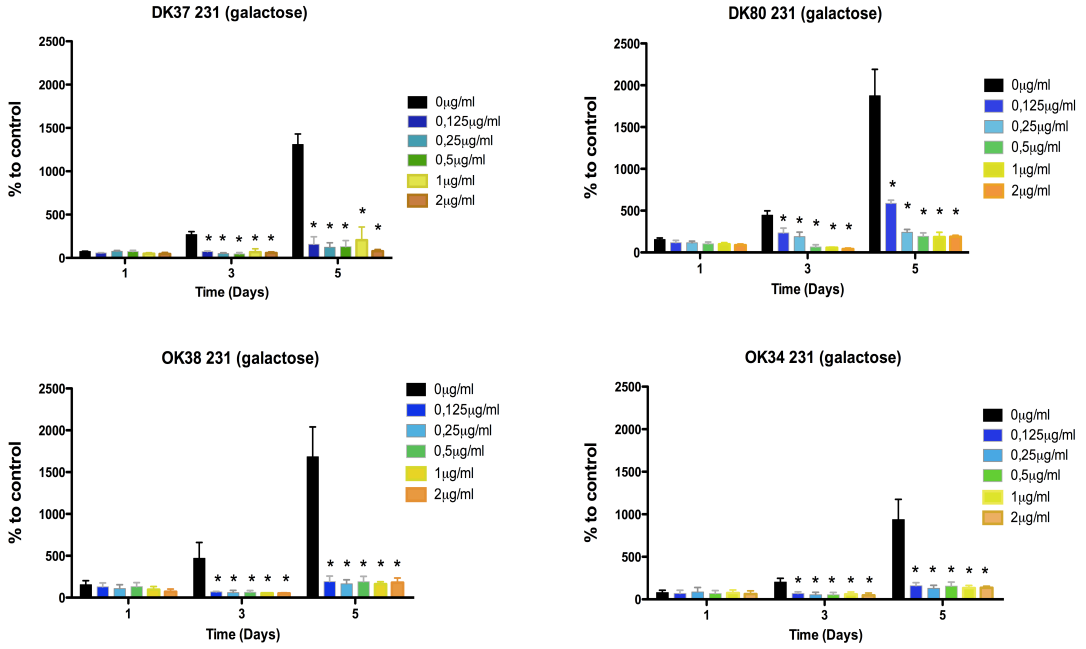

Fig.34 - Effects of triterpenoids on MDA-MB-231 cell line proliferation in glucose-free, galactose/glutamine media. Human breast cancer MDA-MB-231 cell line grown in galactose/glutamine medium, were exposed to different concentrations of triterpenoids, namely DK37, DK80, OK34 and OK38 for 1, 3 and 5 days. Comparatively to cells grown in glucose (see Fig.1), these cells showeda higher inhibition of cell proliferation. Cell proliferation was accessed by sulforhodamine B (SRB) and the results are expressed as a percentage of the control , which represents the density of cells right before drug (or vehicle) treatment (T=0) . Data are means +/- SEM of 4 separate experiments, * $p<0.05$ vs. control.

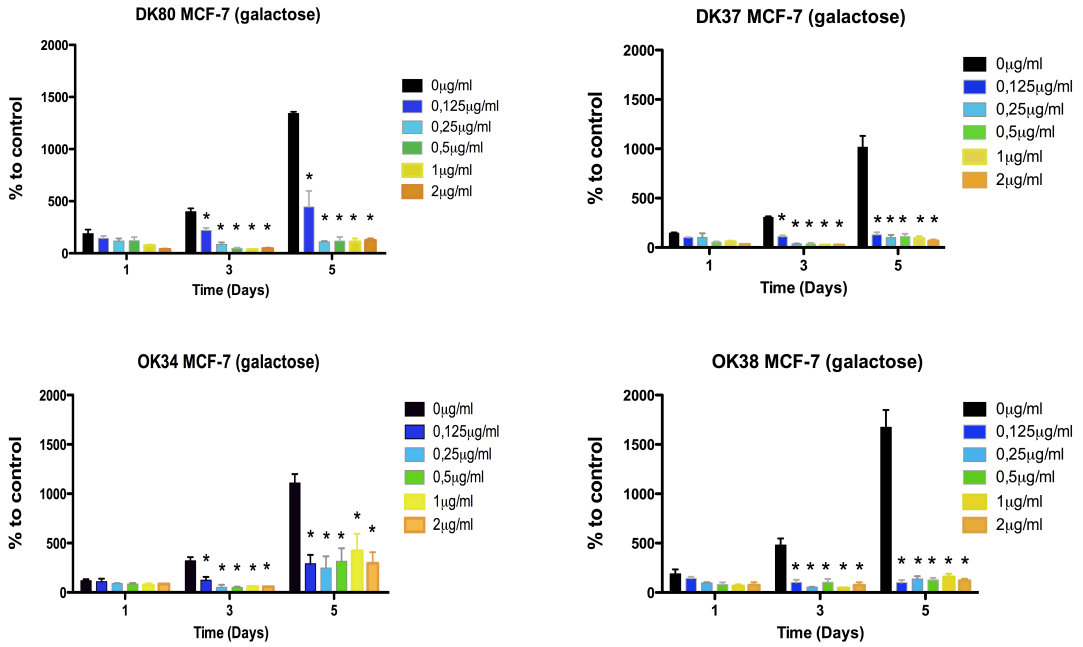

Fig.35 - Effects of triterpenoids on MCF-7 cell line proliferation in glucose-free, galactose/glutamine media. Human breast cancer MCF-7 cell line grown in galactose/glutamine media, were incubated with different concentrations of triterpenoids DK37, DK80, OK34 and OK38 for 1, 3 and 5 days. The conditions were the same described in Fig.34. Data are means +/- SEM of 4 separate experiments, * $p<0.05$ vs. control.

Surprisingly, the cell line that showed to be susceptible to the compounds in normal glucose condition, HS578T, was less affected than the other cell lines in these new conditions (Fig.36). Only DK37 seems to affect the HS578T cell line on the third and fifth days of proliferation, while OK34 did show effects on the third day, but not on the fifth day of incubation. Contrarily, an inhibition of cell proliferation with OK38 was preferentially observed on the fifth day. No significant effect is verified for DK80 in HS578T cells.

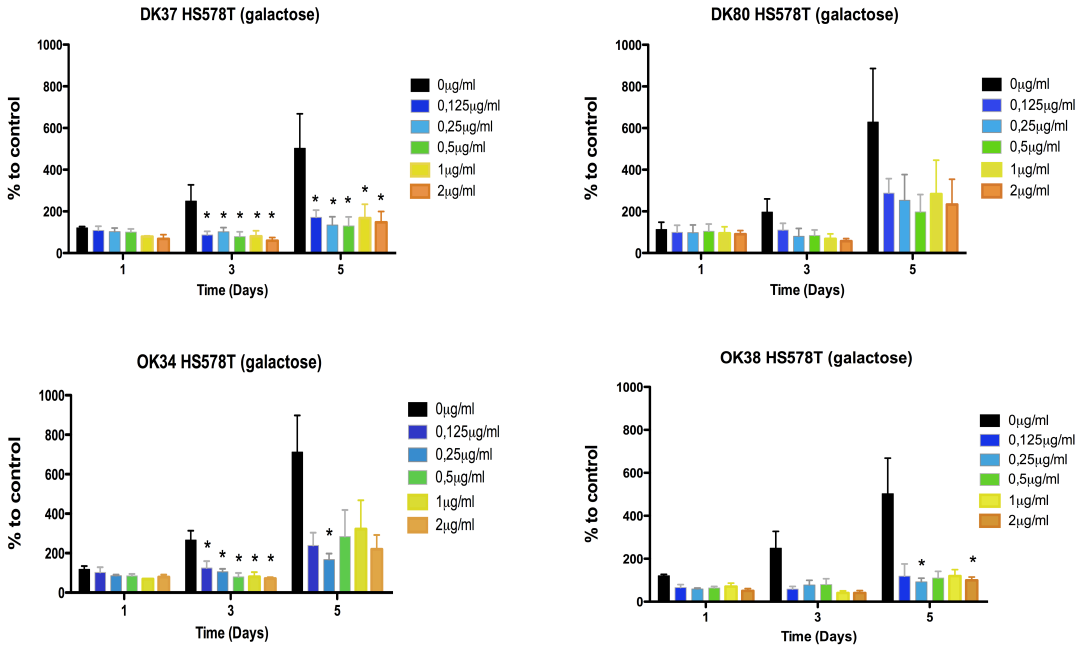

Fig.36 - Effects of triterpenoids on HS578T cell line proliferation in glucose-free, galactose/glutamine media. Human breast cancer HS578T cellsgrown in galactose/glutamine were incubated with different concentrations of triterpenoids DK37, DK80, OK34 and OK38 for 1, 3 and 5 days. The conditions were the same described in Fig.34. Data are means +/- SEM of 4 separate experiments, * $p<0.05$ vs. control.

4.2.2.2.4. Triterpenoids derivatives influence cell differentiation state

Mani et al. (2008) suggested that tumors contain a sub-population of cancer stem-like cells, which is responsible for cancer resistance, re-population and aggressiveness. *In vitro,* different breast cancer cells sub-populations can be identified by cell surface markers such as CD44 and CD24, where $CD44^{high}/CD24^{low}$ is a marker for cancer stem-like cells and $CD44^{low}/CD24^{high}$ represents more differentiated cells. The objective of this experimental approach was to identify the different sub-populations of the cell lines in study with the goal to verify which sub-population are being more affected by the triterpenoids at a concentration of 0.5µg/ml for 24hours. Moreover, the same experiment was performed with cells grown in both glucose and galactose/glutamine medium. Fig.37A shows a representative graph of FACS analysis of MCF-7, MDA-MB-231 and HS578T cells when exposed to the triterpenoid DK37 for 24 hours. The cell surface marker CD44 antibody was labeled with with APC flourophore and CD24 with

FITC flourophore. Fig.37B shows the quantitative analysis of the study for the four compounds tested. MCF-7 cells, which are shown to be preferentially differentiated cells, start losing both cell surface markers when treated with the test compounds, especially DK37 and DK80 in glucose media. DK80 also seems to induce the loss of the same surface markers, leading to a $CD44^{low}/CD24^{low}$ phenotype. Interestingly, in galactose/glutamine media, where cells are even more differentiated, treatment with the test compounds lead to a change from $CD44^{low}/CD24^{high}$ phenotype to a higher percentage of cells showing both surface markers, in a similar manner to what occurred in glucose, suggesting cells are becoming more undifferentiated. Interestingly, when grown in glucose media, MDA-MB-231 cells, become overall more differentiated in the presence of the test compounds, as seen by the expression of both cell surface markers, while in galactose and in the presence of the same compounds, the MDA-MB-231 cell line tended to be more undifferentiated. In the HS578T cell line, the compounds did not affect any of the sub-populations in any of the tested conditions already described.

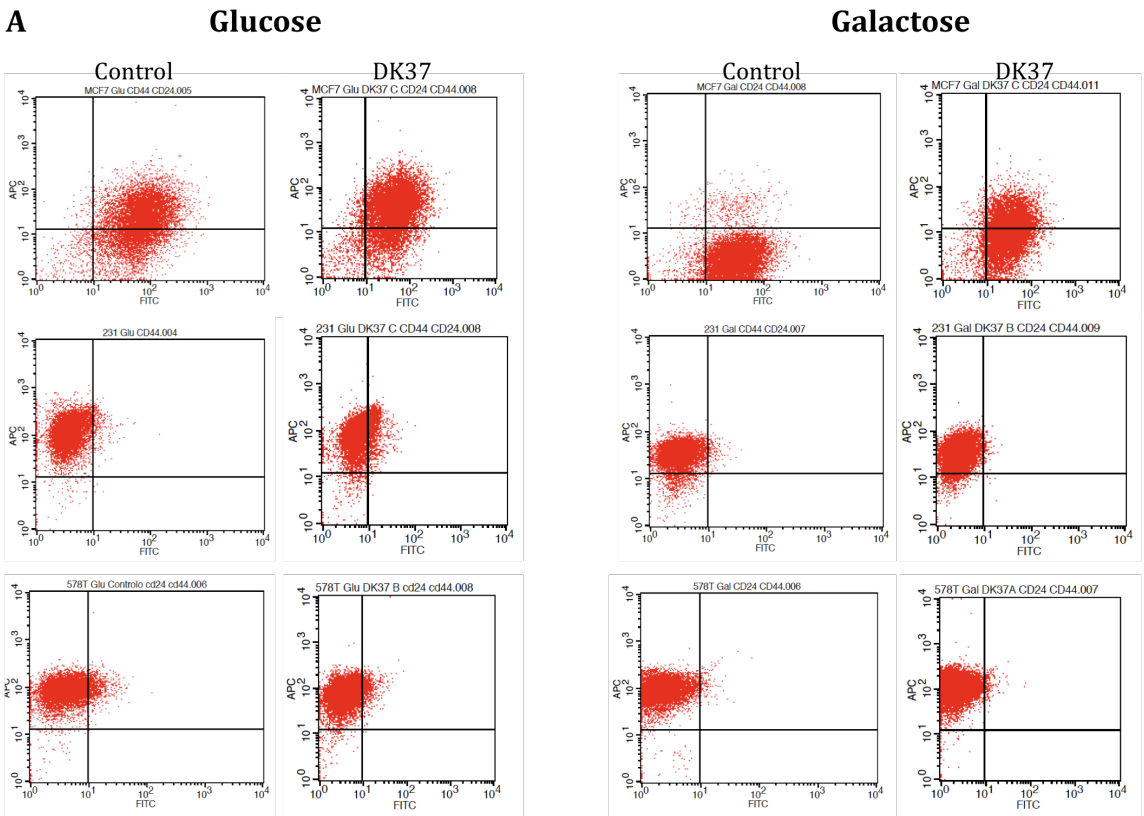

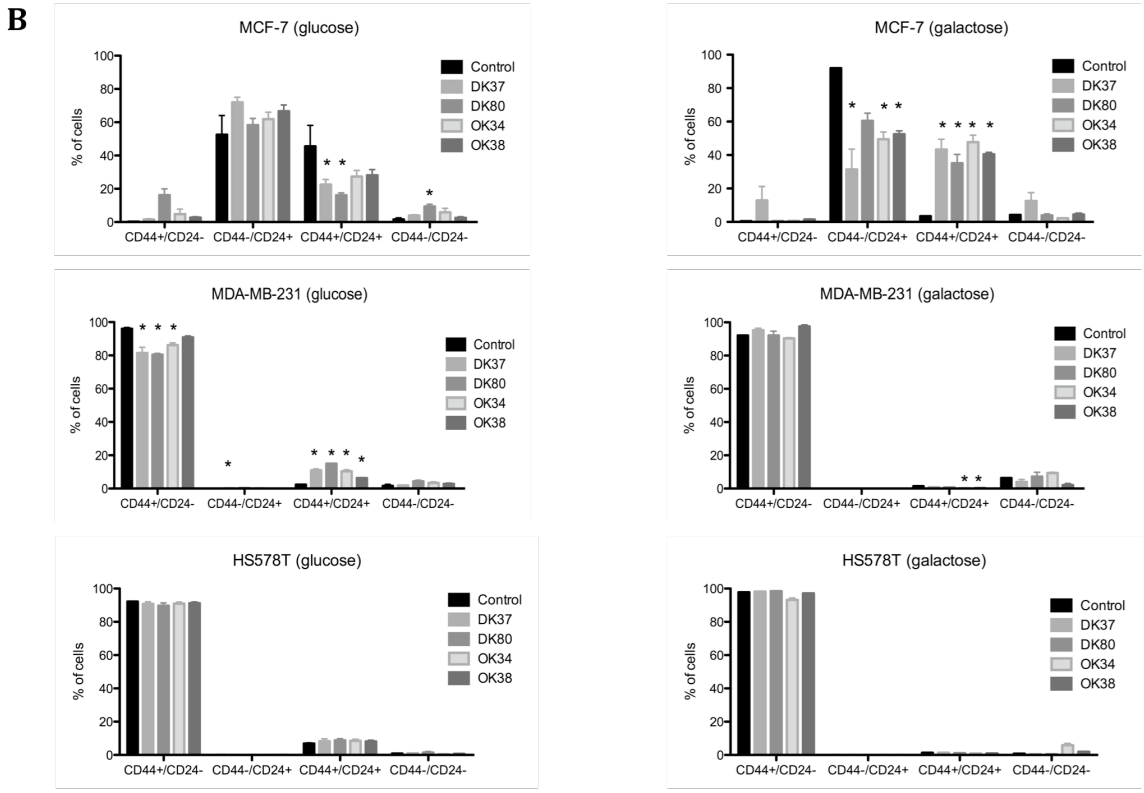

Fig.37 - Triterpenoids effects on breast cancer cells subpopulations. (A) Representative FACS analysis of CD44/CD24 cell surface markers of breast cancer cell lines cultured in glucose and galactose/glutamine media, when exposed to DK37 **(B)** Percentage of $CD44^{high}/CD24^{low}$ stem-like cells and $CD44^{low}/CD24^{high}$ differentiated cells cultured in glucose and galactose/glutamine media when incubated with 0.5μg/ml of triterpenoids (DK37, DK80, OK34 and OK38) for 24 hours. The results are representative of four separate experiments, with (*) as significant difference between conditions (media composition) ($p < 0.05$).

4.2.2.2.5. Transcription profiles of HS 578T cells after OK34 treatment

To obtain a full spectra of all alterations suffered by breast cancer cells in culture treated with this class of compounds, we used OK34 and treated HS 578T with this compound (0.5μg/ml for 48hours) and performed a comparative global gene expression analysis. OK34 was selected since it was the most promising compound in terms of higher effects on tumor cells, although maintaining a lower toxicity on non-tumor cells. We used the Affymetrix gene array analysis to test whether genes were down-regulated or up-regulated upon treatment with OK34. After correction for multiple testing GCRMA, Log2 transformation, quantile normalization and a median polish, 2271 probe

sets showed to be significant by the p-value cutoff of 0.05. The most significant genes which transcription was up-regulated were collagen-type XV-alpha 1 (COL15A1), brain expressed X-linked 2 (BEX2), prostaglandin-endoperoxide synthase 2 (PTGS2) and metallothionein 1M (MT1M), while the genes which transcription was down-regulated were interleukin 7 receptor (IL7R), cadherin 6, type 2, K-cadherin - fetal kidney (CDH6), chemokine C-C motif ligand 2 (CCL2) and platelet-derived growth factor receptor-like (PDGFRL) (Table 1).

Table1. Gene expression of HS578T cells after triterpenoid OK34 treatment. Breast cancer cells HS578T were exposed for 48hours to 0.5µg/ml of OK34. The Affymetrix HG133 chip used has over 47000 transcripts, with complete coverage of the human genome plus an additional 6500 genes. Two ways hierarchical clustering of OK-Control significant probe sets, resulted in 2271 probe sets that were reduced to 210 genes. The 1.5 fold difference between OK34 and Control and JMP Genomics was used to get the significant set with a cutoff of FDR 0.05. Here the eight genes whose expression was most altered are represented, where the first four represent up-regulated expression, and the second set of four represent the four genes whose gene expression was down-regulated. Data correspond to three separate experiments. (1) (Amenta et al., 2000); (2) (Naderi et al, 2007); (3) (Pantaleo et al, 2008) ;(4) (Nyalendo et al, 2009); (5) (Pellegrini et al, 2010); (6) (Sellar et al, 2001); (7) (Arnold et al, 2005); (8) (Seitz et al, 2006)

Gene	Exp. Value	Involvement in Cancer
COL15A1- collagen-type XV-alpha 1	5.649	Invasive process (1)
BEX2 - brain expressed X-linked 2	4.764	Inhibition of apoptosis (2)
PTGS2 - prostaglandin-endoperoxide synthase 2	4.370	Inhibition of apoptosis and promotes angiogenesis (3)
MT1M – metallothionein 1M	3.997	Tumor progression (4)
IL7R - interleukin 7 receptor	3.269	Anti-tumor activity (5)
CDH6 - cadherin 6, type 2, K-cadherin – fetal kidney	2.778	Metastasis and invasion (6)
CCL2 - chemokine C-C motif ligand 2	2.634	Tumor progression (7)
PDGFRL - platelet-derived growth factor receptor-like	2.626	Putative breast cancer tumor suppressor gene (8)

The mentioned genes are intrinsically associated and are involved in invasion, metastasis and apoptosis inhibition. However, CDH6 and CCL2 downregulation seem to have a reversal effect, promoting tumor regression. Moreover, intriguing information on the interconnectivity of the significant genes was obtained through network analysis, where an upregulation of many genes involved in the Akt pathway was observed. Akt pathway was shown to regulate cell proliferation and survival and is activated early in breast cancer (Bose et al, 2006). Despite this, there are other genes, such as transmembrane 4 L six family member 1 (TM4SF1-encoded protein is a cell surface

antigen and is highly expressed in different carcinomas) which is down-regulated. qRT-PCR and Western Blotting will be used to confirm the alterations detected in the Affymterix chip.

One disadvantage was that the Affymetrix chip used did not contain mitochondrial-encoded genes. Therefore, we performed a set of qRT-PCR experiments in order to evaluate differences in mitochondrial genes, including ND1, ND5, ND6, CytB, COX I and COX III, upon triterpenoid exposure. HS578T cells were treated with 0.5μg/ml of OK34 compound for 48 hours (Fig. 38), the same exact conditions used for the Affymetrix experiment. The results show that all the transcripts were reduced, but significant differences were only observed for the COX III transcript.

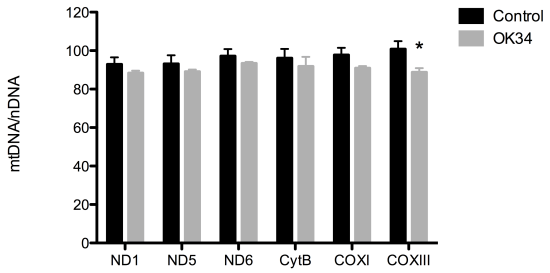

Fig.38 - mtDNA complementary gene expression of HS578T cells after OK34 treatment. Mitochondrial encoded transcripts are decreased comparatively to control, however significance was only achieved for COX-3. HS578T cells were grown in glucose, treated with vehicle or 0.5μg/ml of OK34 for 48hours. Since the Affymetrix Human Genome U133 Plus 2.0 Chip did not containe mtDNA genes, a qRT-PCR assay to analyze ND1, ND5, ND6, COX1, COX-3 and CytB mRNA expression was performed to complement the chip information. Data are means +/- SEM of 3 separate experiments, * $p<0.05$ vs. control.

Further evidence for direct mitochondrial effects was obtained by testing the effects of DK37, one of the triterpenoids used in this study on mitochondrial fractions isolated from the livers of Wistar-Han rats. By using mitochondrial fractions, other cellular effects of the triterpenoids can be excluded. Several end-points for mitochondrial function were evaluated including respiration, generation of the transmembrane electric potential and induction of the MPT pore. Assays were conducted by energizing mitochondria via complex I (glutamate-malate) and complex II (succinate in the presence of rotenone).

Respiration data (Figs. 39 and 40) indicates that DK37 had no effect whatsoever

on that parameter. State 3 and 4 were not altered, at least for concentrations up to 1.33 μg/mg, the same occurring with state 4 respiration in the presence of the Fo-F1 synthase inhibitor oligomycin and uncoupled respiration (in the presence of the protonophore FCCP). The respiratory control ratio (RCR) and the ADP/O ratio were also not altered. Both values were indicative of well-coupled mitochondrial preparations.

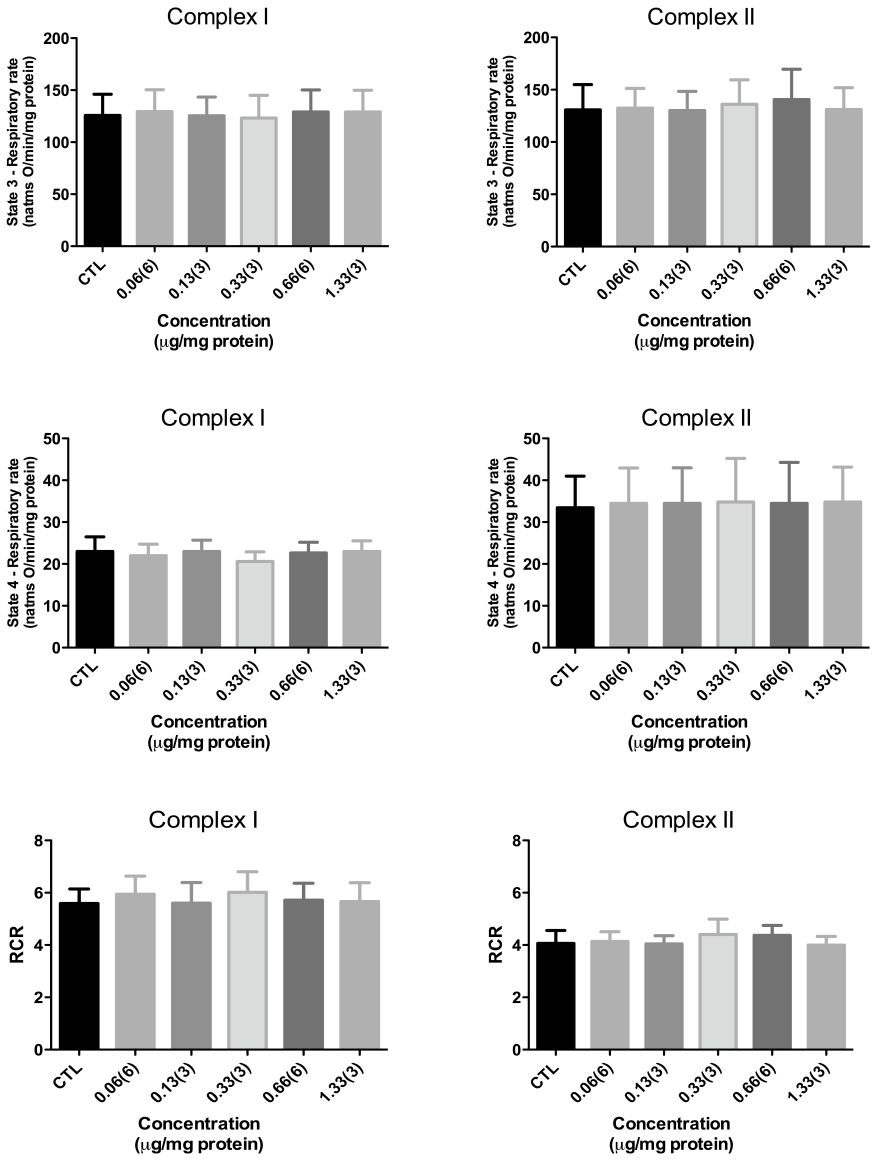

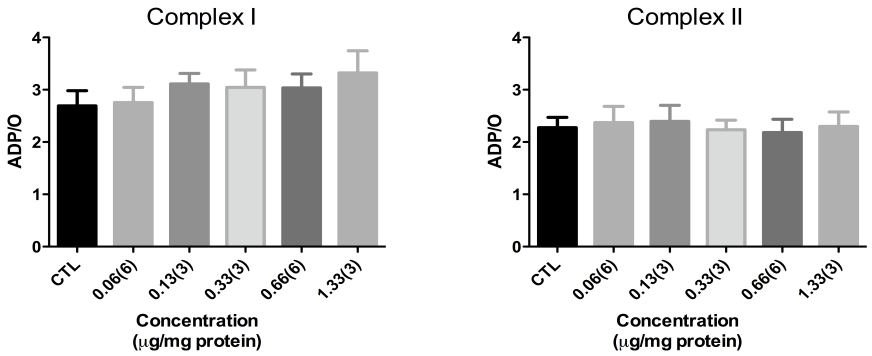

Fig.39 - Effects of DK37 on isolated mitochondrial respiration. State 3 was measured after addition of 125nmol of ADP and state 4 after complete ADP phosphorylation.Mitochondrial respiration was initiated by 5mM of glutamate/malate for complex I energization and 5mM succinate plus rotenone for complex II energization. The RCR was calculated as the ratio between respiration state 3 and state 4. The ADP/O was calculated as the number of nmol ADP phosphorylated by nano-atoms of oxygen consumed during ADP phosphorylation. The results are expressed in absolute values. Data are means ± S.E.M. of 5-6 different preparations.

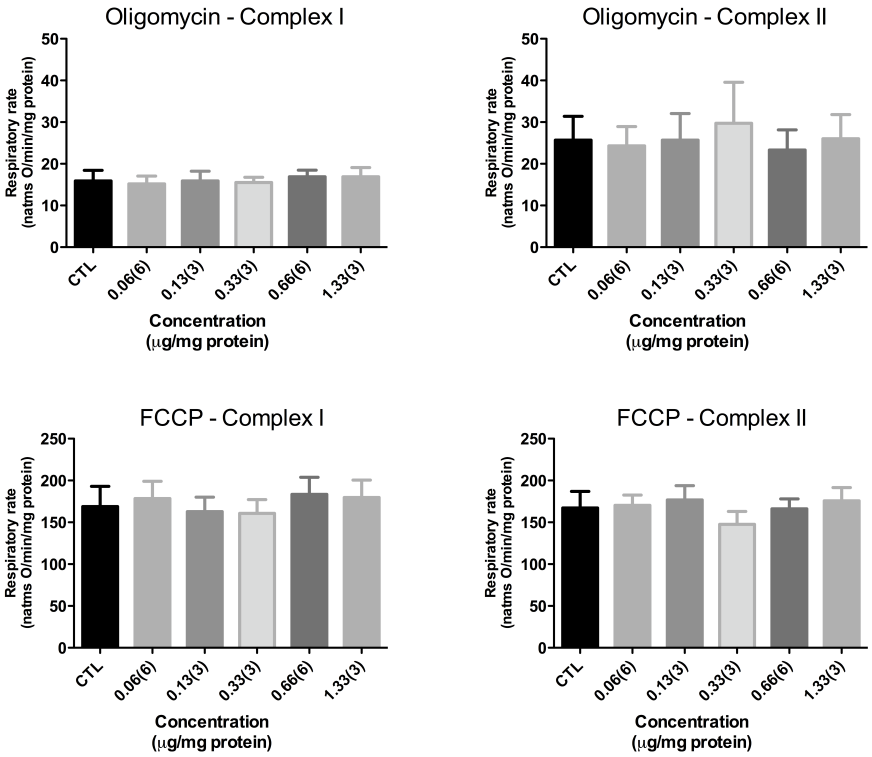

Fig.40 - Effects of DK37 on mitochondrial respiration (II). Oligomycin (1μg) and FCCP (1μM) were added to the system in order to inhibit passive proton flux through the ATP synthase during state 4 respiration and to uncouple respiration, respectively. The results are expressed in absolute values. Data are means ± S.E.M. of 5-6 different preparations.

The absence of effects regarding mitochondrial respiration was well correlated with no effects in the developed transmembrane electric potential, as measured with a TPP^+ electrode (Fig. 41), the exception being a reduction in the depolarizing effect of ADP (middle panel), which was more visible when complex I substrates were used.

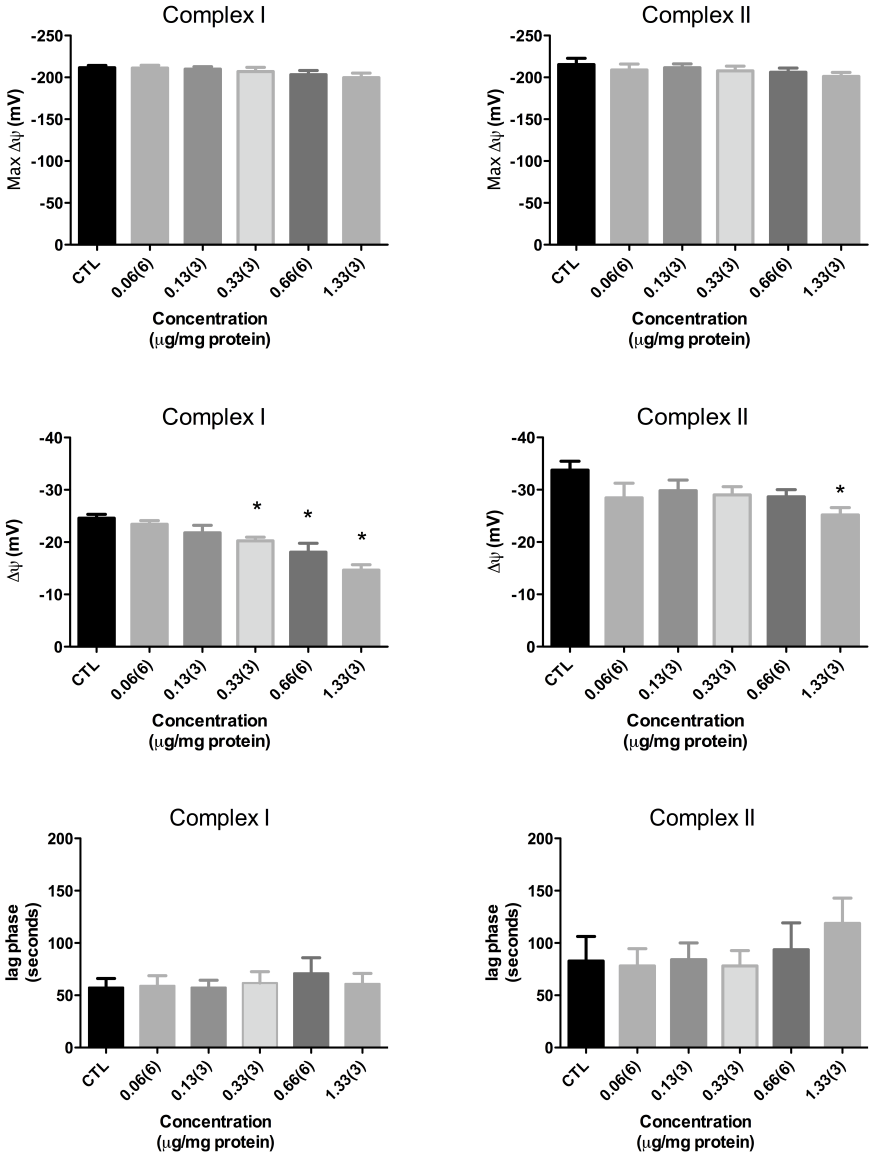

Fig.41 - Effects of DK37 on the transmmebrane electric potential fluctuations. Max Δψ developed (upper panel), ADP-induced depolarization (middle panel) and phosphorylative lag phase (lower panel) was measured by using a TPP+-selective under the conditions in Fig.40 and calculated as described in the Materials and Methods section (*) Significant difference compared to control ($p< 0.05$).

Finally, the most significant effect was that DK37 was able to induce the MPT pore in vitro. When the test compound was pre-incubated with mitochondria and the MPT pore was induced with calcium, the amplitude of mitochondrial swelling increased in a dose-dependent manner (Fig. 42). For the highest concentration of DK37 tested (1.33 μg/mg), swelling amplitude was five times higher than in the control (calcium-only). This MPT pore-inducing effect occurred without alterations in respiration or membrane potential and was inhibited by cyclosporin-A, the specific MPT pore inhibitor (Broekemeier et al, 1989).

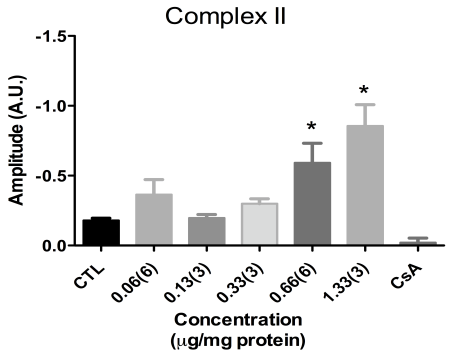

Fig.42 - Effects of DK37 on MPT pore opening. Mitochondrial swelling was evaluated by measuring light dispersion variations measured at 540nm, as described in the Materials and Methods section. Swelling amplitude was calculated as the difference between basal line absorbance and absorbance registered 600s after calcium (20μM) addition. Mitochondria were energized with succinate in the presence of rotenone. Data are means ± S.E.M. of 5-6 different preparations. (*) Significant difference compared to control ($p < 0.05$).

4.2.2.3.Discussion

A successful strategy of killing cancer cells is based on the activation of apoptotic pathways, which can be silenced or modified in tumors. In this context, mitochondria are a promising target to increase the tumor susceptibility to chemotherapy-mediated death (Gogvadze et al, 2010). One characteristic of some cancer cells is an altered mitochondrial membrane potential when compared with normal cells (ΔΨm) (Kim et al, 2011). Some groups have shown that some carcinoma cells have significantly higher ΔΨm than normal cells (Wang et al, 2007). New cationic derivatives of lupane triterpenoidswere already pointed out as possible mitocans against human melanoma (Holy et al., 2010). Thus, the same family of compounds is now tested in the present

work in breast cancer cells with the objective to investigate in further detail mitochondrial and overall cell effects, confirming their ability as mitocans. MCF-7, HS578T and MDA-MB-231 human breast cancer cells were the cell models used to test the new compounds, while HS578Bst breast and BJ fibroblast cell lines were used as non-tumor controls.

The data shows that that MCF-7 (Fig.28) and HS578T (Fig.29) cells are the most susceptible lines to the triterpenoid derivatives, since a a great inhibition of cell proliferation was observed. The compounds OK34 and OK37 show to have the lower impact on the non-tumor BJ cell line (Fig.26), which may signify a lower toxicity for non-tumor targets. Interestingly, OK34 and OK37 did affect the usually resistant breast cell line MDA-MB-231 (Fig.27). In fact, it was observed that both compounds have similar effect on all cells tested, which is hardly surprising since their chemical structure is very similar, with only a different counterion (Cl or Br, respectively), suggesting that this alteration does not interfere with cell proliferation, as previously described (Holy et al, 2010). Moreover, both DK35 and DK37 also seem to have similar effects, although DK37 seems to have stronger effects overall. It might be due to a possible higher accumulation in cells since this compound has an extra nitrogen in the chemical structure, which may suffer protonation/deprotonation cycles. Furthermore, we simulated a pause in chemotherapy treatment, by adding the drug for a certain period of time and then washing it and observing cancer cells recovery (Fig.30). For this experiment, HS578T breast cancer cells were used. It was observed that for all the compounds at their highest concentrations (0.5μg/ml; 1μg/ml and 2μg/ml), cells could not recover at the end of the five days. Moreover, cells could not recover from any OK38 concentration, confirming the potency and irreversibly of the effects caused by this compound. Among all the compounds tested, OK38 had the greatest inhibitory effect on cell proliferation. The data on cell proliferation suggest that cell cycle arrest or cell death may be occurring. Thus, to further explore this issue, cell cycle analysis was performed. All the triterpenoids derivatives tested demonstrated a similar cell cycle arrest pattern, where an increase of cells in G0/G1 phase was observed (Fig.31). This kind of cell cycle block is normally associated with DNA damage, although other mechanisms can also cause such arrest. For instance, it was demonstrated that a down-regulation of cyclins D can contribute to G1 block, resulting from a decrease in ATP levels after exposure to mitochondrial

poisons (Gemin et al, 2005). Not discarding a possible direct DNA damage and other possible factors, we suggest that the triterpenoids derivatives are affecting mitochondria, interfering with ATP production, leading to a G1 cell cycle arrest. Similar effect is observed with Berberine (section 4.3.1). In fact, Holy et al. (2010) proposed that the triterpenoids used exert primarily mitochondrial effect followed by an inhibition of cell proliferation. In order to confirm cell death, further assays will be performed later.

In order to verify a possible combination of the test compounds with clinical compounds currently use in chemotherapy, synergy assays were performed with Doxorubicin (Dox), Paclitaxel (Taxol) and Cisplatin (Cispla). The results showed that the triterpenoids may have a synergistic effect with Taxol (Fig.32). Taxol is a well-known anti-tumor agent, which suppresses microtubules dynamics (Ganguly et al, 2011). However, some types of tumors are Taxol resistant or acquire resistance during treatment, which can be associated to mitochondrial biogenesis induced by Taxol (Orr et al, 2003). Since we think that the test triterpenoids are affecting mitochondria integrity, the present results show a strategy to overcome Taxol resistance issue, although new tests should be done to uncover the mechanism of action of the synergy between Taxol and the test compounds hereby used.

Vital microscopy analysis was performed with the intent to verify the mitochondrial interaction of the test compounds (Fig.33). It was observed that at a concentration of 0.25μg/ml for 6 hours, OK38 disrupted the mitochondrial network of tumor (HS578T) and non-tumor cell lines (HS578BsT and BJ), while the other triterpenoids DK37, DK80 and OK34 seems to interfere with both non-tumor and tumor breast cell lines. As was previously discussed, high accumulation of cations in mitochondria can lead to mitochondrial depolarization through several mechanisms, disrupting mitochondrial function and structure, and promoting cell death in extreme events (Murphy, M., 1997).

To further investigate the possible primary role of mitochondria in the mechanism of toxicity of the novel triterpenoid compounds, the cancer cell lines MCF-7, MDA-MB-231 and HS578T were grown in galactose/glutamine media in order to force cells to exclusively use OXPHOS for ATP production (Marroquin et al, 2007). With this strategy, direct actions of the triterpenoids in mitochondria can be observed. Under these conditions, cancer cells use glutaminolysis and the Krebs cycle as primary sources

of electrons for the respiratory chain (Dang C., 2010). All compounds were shown to dramatically inhibit the cell proliferation of MCF-7 and MDA-MB-231 cancer cells for all concentrations tested. Interestingly, HS578T show to be the least affected under these growth conditions, despite the fact that this cell line was greatly affected when growing in normal glucose media. In fact, we mentioned in section 4.1 that HS578T cells respond differently to mitochondrial poisons, when compared to other cancer cell lines. It seems that these cells have a still largely unknown mechanism to overcome the action of mitochondrial poisons. We proposed that HS578T cells may have higher levels of antioxidants, to control mitochondrial ROS generation promoted by the poisons. In fact, some tumors up-regulate their radical scavenging systems to adapt to intrinsic oxidative stress, which, for instance, can confer drug resistance (Trachootham et al, 2009). Clearly more work has to be performed in this subject and explore different possibilities, including up-regulation of antioxidant systems or that this cell line is particularly susceptible to disturbances of the glycolytic pathway, which would not be working when cells are grown in galactose/glutamine media.

Interestingly, direct evidence of mitochondrial effects of one of the triterpenoids studied, DK37, was obtained by using isolated rat liver mitochondria. Isolated mitochondrial fractions are considered a prime biosensor to test compound toxicity (Pereira et al, 2009) and to predict drug safety in the pharmaceutical industry (Dykens and Will, 2007). The results obtained are somewhat interesting. Despite the absence of effects on mitochondrial respiration and generation of the maximal transmembrane potential (Figs. 39-41), DK37 caused a dose-dependent cyclosporin-A-sensitive induction of the MPT pore (Fig. 42). This may imply that DK37 may have a direct effect on any pore component or be caused by oxidative stress, since no other effects were noticed. The exception was a decrease induced by DK37 on the depolarization caused by ADP. Although it is still too early to draw any conclusions, one possible target candidate for DK37 would be a component of the phosphorylative system, such as the ANT or the phosphate sinporter, this despite the fact that the ADP/O, which is a measure of phosphorylative efficiency, was not affected by DK37. Interestingly, both the ANT and the phosphate sinporter were proposed to be part of the pore structure, or at least to regulate pore formation and opening (Halestrap A., 2009). The MPT has been correlated with a series of deleterious effects to the cell, including mitochondrial depolarization,

ATP depletion and cell death, which most of times occurs by necrosis (Rasola and Bernardi, 2011), (Kinnally et al, 2011). In fact, MPT pore induction, regardless of the exact mechanism, may well be one of the mechanisms by which the triterpenoids here studied cause mitochondrial dysfunction and cell death.

Many drugs tested to control tumor growth, fail due to a clinical relapse of the tumor, which.occurs since the self-renewing tumor stem cells are left untouched by the drugs, allowing tumor re-grown. It is also known that differentiated cell lines can become undifferentiated, but at a low rate. It is though important to look for agents that would target both cancer stem-like cells and differentiated cancer cells within tumors (Gupta et al, 2009).

Therefore, cell surface markers were use to identify which of subpopulations of cancer cells (i.e., cancer stem-like cells and differentiated cells), were being more affected by the treatments (Fig.37). For the concentration and time exposure used, no differences were detected for HS578T cells. However, it seems that MCF-7 and MDA-MB-231 cell lines present alterations upon treatment. After treatment, MDA-MB-231 cells appear to have a lower content in cancer-stem cells ($CD44^{high}/CD24^{low}$) and an increased number of cells expressing both cell surface markers. Whether this results from selective elimination of cancer stem cells or progressive differentiation, it remains to be investigated.

The results for MCF-7 cells are more difficult to explain. In glucose medium and in the presence of triterpenoids, MCF-7 cells tend to be mostly undifferentiated, with an increase in cells expressing $CD44^{high}/CD24^{low}$. In galactose/glutamine media, when no treatment was applied, cells expressed essentially $CD44^{low}/CD24^{high}$, while in the present of triterpenoids the number of cells expressing both cell surface markers increased. It is known that well differentiated cancer cells are blocked from further differentiation and aggressiveness (Iwasaki and Suda, 2009). However, the same cancer cells may activate cell survival mechanisms that lead to undifferentiated phenotype, to resist stress induction. It is also possible that the interaction of the test compounds with mitochondria may result in unbalanced production of ROS and ATP decline, which may alter differentiation signaling pathways.

After treatment of HS578T cells with 0.5 μg/ml OK34 for 48 hours, a microarray was performed to explore transcriptional alterations. From the microarray performed, it

was verified that the majority of the most altered gene expression was associated with metastasis and invasion, and at the same time with activated Akt pathway. Under these same treatment conditions, an inhibition of cell proliferation and loss of mitochondrial potential was observed. The microarray results suggest that cancer cells are undergoing adaptation mechanisms to evade cellular stress caused by the triterpenoids derivative tested OK34. Although the genes that are associated with metastasis and invasion are being more expressed after treatment, we believe that for higher concentrations or longer times of exposure, cell death mechanisms will be activated. Therefore, further work will be done in order to analyze proteins that are associated with cell death. Moreover, genes involved in the Akt pathway were also shown to be more active. The Akt pathway is intrinsically associated with cell proliferation and survival, and is found to be deregulated in many cancers (Bose et al, 2006). Akt is activated downstream of PI3K and has multiple targets, including the activation of glycolytic enzymes (Jones and Thompson, 2009). Moreover, Miyamoto and coworkers (2008) suggested that the activation of the Akt pathway can protect against cytochrome c release and apoptosis, due to hexokinase II association to mitochondria, under enhanced oxidative stress. The data from the microarray must still be confirmed by different methods before getting to a final conclusion but it helps us explaining how breast cancer cells respond in terms of gene expression when treated with this class of compounds. Naito et al. (2008) proposed that a decrease in mtDNA copy number caused by ROS generation, hypoxia and chemotherapeutic agents, can result into a invasive phenotype. Thus, mitochondrial encoded transcripts were measured by qRT-PCR and a decrease in all the transcripts was observed, although only COX III yielded statistical significance. We showed in section 4.1 that HS578T cells have already a lower levels of the same COX III subunit, comparatively to the other cell lines. Lower levels of COX III are associated with undifferentiated cells and with progression of malignancy (Heerdt et al, 1990). Likewise, higher expression of COX III was previously associated with differentiated cells (Modica-Napolitano et al, 2007). Moreover, HIF-1 can modulate mitochondrial function in tumors, by regulating cytochrome c oxidase (COX), with COX I show to be downregulated, and perhaps COX III as well (Gogvadze et al, 2010b). More, the reduction of COX subunits can be due to ROS generation, which is justified by the proximity to ROS-production sources (Cannino et al, 2008).

In sum, we have tested a group of Dimethylaminopyrimidine derivatives of lupane triterpenoids in breast cancer cell lines with intention to complement and confirm their activity at mitochondrial level. For the concentration of 0.5μg/ml, it is observed an inhibition cell proliferation and induction of MPT pore and loss of membrane potential. Akt pathway is activated to protect mitochondria from potential oxidative stress and cell death. Moreover, the loss of mtDNA lead cells to invasive phenotype. However for higher concentrations it might lead cells to die. The new triterpenoids derivatives are also promising in combination with other chemotherapeutics, as showed with Taxol.

Although some work must still be finished, a preliminary assessment is that the tested triterpenoids can be considered as mitocans, due to their disruptive action of mitochondria physiology and integrity of breast cancer cells.

4.2.3. Berberine and sanguinarine as promising mitocans

Over the past several years clinical trials used plant-based agents for the prevention and management of several diseases. Intense research has focused on drugs targeting new cell mechanisms. Alkaloids, nitrogen containing bases widely distributed in several botanical families, have been intensively studied in the last decades as promising natural drugs. These natural chemicals have an important role in medicinal chemistry, being recognized for their chemopreventive properties. The compounds are also used in human dietary around the world for centuries (Maiti and Kumar, 2006). Among natural alkaloids, Protoberberine and benzophenanthrine are the most important groups, which are represented by berberine and sanguinarine, respectively, because of their broad range of biological harmless properties (Fedorak and Field, 1987; Bareto et al, 2003). A matter of significant current interest is that these compounds are in prospective development and use as effective pharmaceutical agents (Maiti and Kumar, 2006). Physical-chemical properties, which can affect cellular permeability and intracellular distribution will determine the interactions between alkaloids compounds and intracellular targets (Malikova et al, 2006).

4.2.3.1. Berberine

4.2.3.1.1. Background and Objectives

Berberine is an isoquinoline alkaloid present in a number of plant species that have long histories of use in ayurvedic, unani, Chinese, and Native American traditional medicine practices (Vogel V, 1990; Mantena et al, 2006). Berberine has been associated with a wide variety of biological effects, including anti-microbial, antiinflammatory, anti-diarrheal, anti-nociceptive and antipyretic activities. It has been reported to lower cholesterol, control blood sugar levels, and function as an anti-oxidant.

Recently, it has garnered considerable attention as a possible chemotherapeutic drug for cellular proliferative diseases such as psoriasis and cancer (reviewed in Maiti and Kumar, 2006; Grycova et al, 2007). A popular source of berberine and other isoquinoline alkaloids is the plant *Hydrastis canadensis*, or goldenseal. Goldenseal has been reported to be one of the five top-selling herbal products in the US, and, along with ginseng, is one of the most over-harvested plants in the US (Dworkin N., 1999). Consequently, there are a number of compelling reasons to study the actions, including possible harmful side effects, of berberine and related alkaloids.

A growing number of studies are focusing on the ability of berberine to function as an anti-cancer drug through its ability to induce apoptosis in a number of different malignant cell lines. Berberine has been reported to induce apoptosis through a mitochondrial pathway that includes upregulation of p53, alterations in Bcl-2/Bax ratios, a decrease in mitochondrial membrane potential, release of cytochrome *c*, and activation of caspases (Hwang et al, 2006; Inoue et al, 2005; Jantova et al, 2007). This is of particular interest in light of studies demonstrating a mitochondrial localization of berberine, raising the possibility that apoptosis results from mitochondrial damage induced by berberine. Alternatively, berberine also binds DNA and RNA (reviewed in Ref. Maiti and Kumar, 2006), and apoptosis may be triggered downstream of a DNA damage response. To investigate these questions in more detail, we treated K1735-M2 melanoma cells with different concentrations of berberine for various lengths of time and correlated berberine localization patterns with effects on cell proliferation, cell cycle progression, and cell death. The results of these studies indicate that the primary effect

of berberine in these cells is cytostatic rather than cytotoxic, and that the inhibition of cell proliferation reflects a multiphase response to berberine that is associated with concentration-dependent differences in localization patterns.

4.2.3.1.2. Results

4.2.3.1.2.1. Effect of berberine on cell proliferation

The effects of a range of concentrations of berberine (5–100 μM) on cell proliferation was measured for up to 6 days (Fig. 43). Sulforhodamine B assays demonstrate that a single application of berberine leads to a significant and dose-dependent inhibition of M2 proliferation over a number of days at concentrations as low as 5 μM (Fig. 43a). About 50μM berberine was strongly cytostatic, and 100 μM completely inhibited cell proliferation (Fig. 43b).

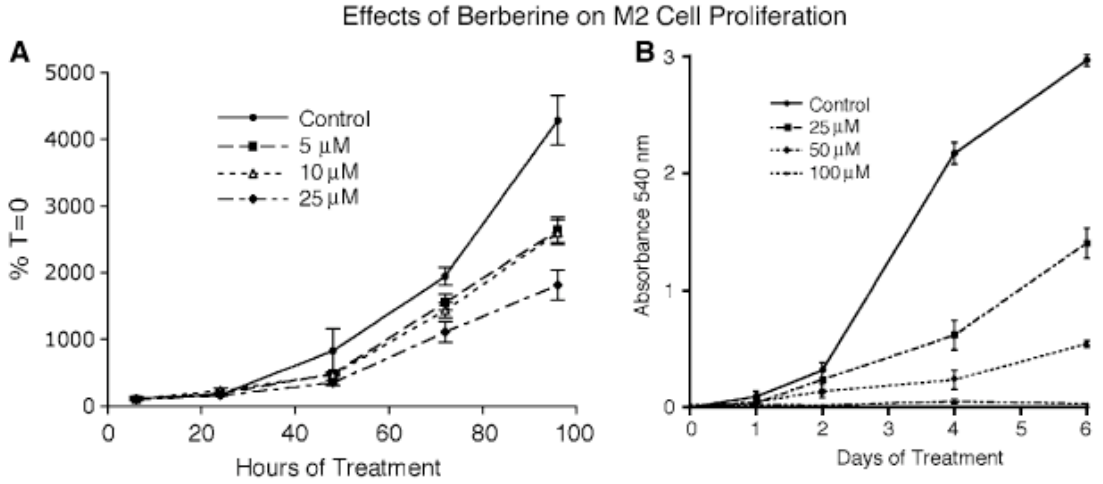

Fig.43 - Sulforhodamine B (SRB) proliferation assays of M2 cells exposed to berberine. A Cells were seeded at a concentration of $1x10^4$ cells/ml in 24-well plates, and allowed to recover for 1 day prior to drug addition. Cells were treated with 5, 10 or 25 μM berberine, or vehicle (DMSO) only (control). Proliferation was measured at 6, 24, 48, 72 and 96 h after the addition of berberine. Note the dose-dependent inhibition of cell proliferation. **B** SRB assay showing the effects of up to 100 μM berberine on cell proliferation. Proliferation was measured 1, 2, 4 and 6 days after the addition of 25, 50 or 100 μM berberine, or vehicle (DMSO) only (control). The reduction in the slope of the control between days 4 and 6 is due to the fact that the sample wells were becoming confluent with cells, thus slowing their proliferative rate. Twenty-five micromole berberine slows proliferation, 50 μM strongly inhibits it, and no increase in cell numbers occur in cultures treated with 100μM berberine. Both graphs reflect data from three independent experiments; *bars* indicate standard error of the mean. For a, significant differences between the control and 25 μM groups are present ($p < 0.05$); the 5 and 10 μM groups are not different from each other, but their values lie between the control and the 25 μM groups ($p < 0.05$).

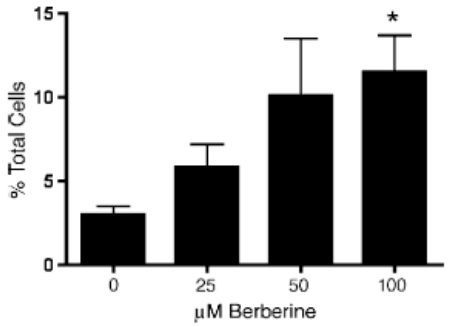

Fig.44 - Graph showing only modest increases in cell death in M2 cultures treated with up to 100µM berberine for 48 h. Shown is the percentage of cells with compromised plasma membranes, as detected with ethidium homodimer staining and Flow cytometry. The values reflect the averages of three independent experiments; the *bars* indicate the standard error of the mean. Only the 100µM cultures displayed a significant increase in the amount of cell death at this time point (*asterisks*; $p < 0.05$).

Microscopic examination of these cultures revealed few dead cells floating in the media at concentrations of berberine up to 50 µM, and modest numbers of dead cells in the 100 µM cultures. Quantitation of cell death by two different measures (loss of plasma membrane integrity, Fig.44, and appearance of cells with a sub-G1 DNA content, Fig. 47)supports these observations; up to 50µM berberine triggers very little M2 cell death, and only a low level of cell death is apparent after exposure to 100 µM berberine for 48 h (Figs. 44, 47). These results demonstrate that berberine has signiWcant cytostatic eVects, but is cytotoxic to these cells only at very high concentrations.

4.2.3.1.2.2. Uptake and compartmentalization of berberine

Because berberine is a fluorescent compound that can be detected by both epifluorescence microscopy and flow cytometry, we measured the uptake and distribution of berberine in living M2 cells using these methods. Measurements of total cellular fluorescence by flow cytometry showed that 100µM berberine took between 1 and 2 h to accumulate to a maximum level within cells, and this level was quite stable for at least 6 h (Fig. 45a). The half-maximal value was achieved within 30 min, which correlates well with the appearance of mitochondrial berberine fluorescence by microscopy (see below). Comparison of the fluorescence levels of different concentrations of berberine at a 2.5 h time point demonstrates that an essentially linear uptake of berberine occurs between 12.5 and 150 µM (the extent of the range tested; Fig.

45b). The effect of FCCP on the uptake of different concentrations of berberine was also examined. Addition of FCCP had little effect on the uptake of 50 μM or less berberine after 2 h, but significantly increased the berberine signal in cultures treated with 100 μM or more (Fig. 45c).

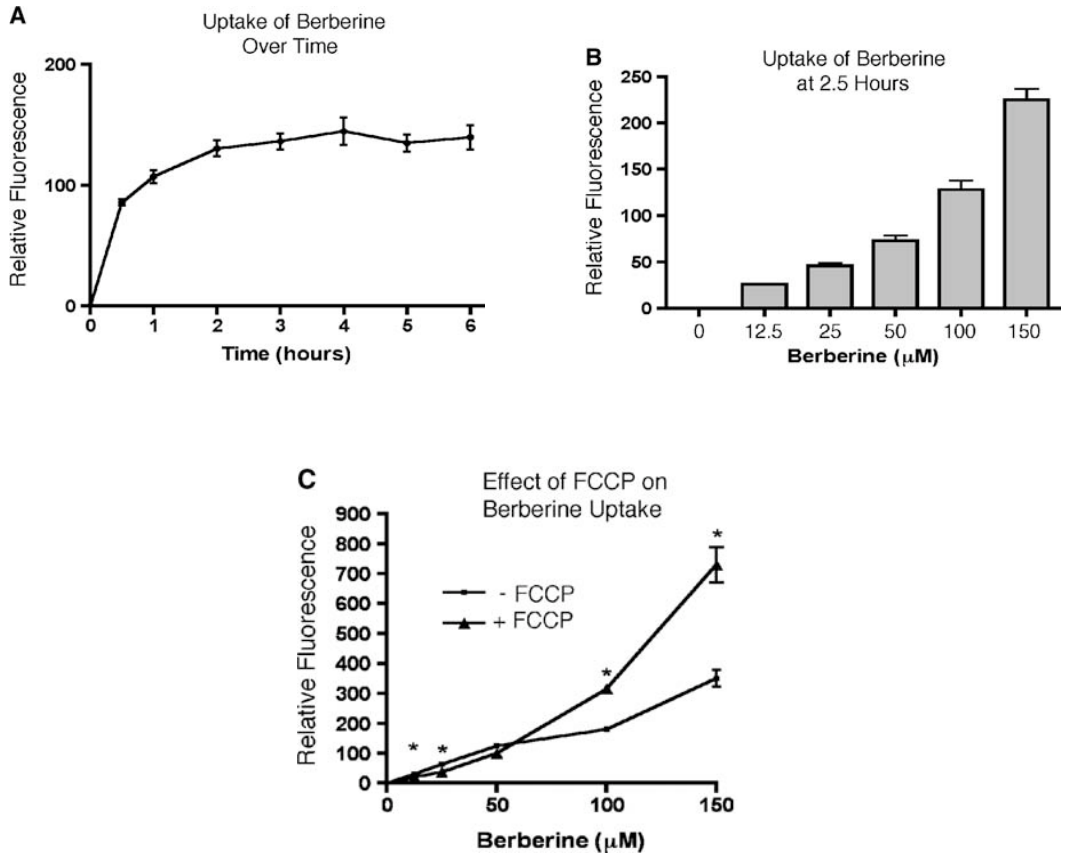

Fig.45 - Cellular uptake of berberine, measured by flow cytometry. A Uptake profile of cultures treated with 100 μM berberine. Half-maximal accumulation of berberine occurs in less than 30 min after addition, with maximal values being achieved about 2 h after addition. **B** Cellular fluorescence values of different concentrations of berberine, measured 2.5 h after addition. Note the essentially linear increase in fluorescence intensity with increasing berberine concentrations over the range tested. **C** Effect of the mitochondrial poison FCCP on berberine uptake by M2 cells. The addition of FCCP results in a significantly greater accumulation of higher concentrations berberine in these cells. The data points reflect the average of three independent experiments, and the *bars* represent the standard error of the mean (*asterisks*; $p < 0.05$).

Confocal microscopy demonstrates that the different concentrations of berberine exhibit different intracellular distribution patterns of fluorescent signals. Low concentrations of berberine (e.g., 12.5 μM or less) are not readily detectable within M2 cells at the gain settings used to avoid grossly oversaturating the signal emitted by higher concentrations of berberine. On the other hand, strong mitochondrial

fluorescence is apparent in cells treated with 25 or 50 μM berberine (Fig. 46). This fluorescence becomes noticeable by microscopy after about 20–30 min of incubation, which correlates well with the increase in signal detected by flow cytometry (Fig. 45a). The entire cytoplasm, as well as nuclei and nucleoli, becomes fluorescent in cells incubated in 100 μM or more berberine (Fig. 46).

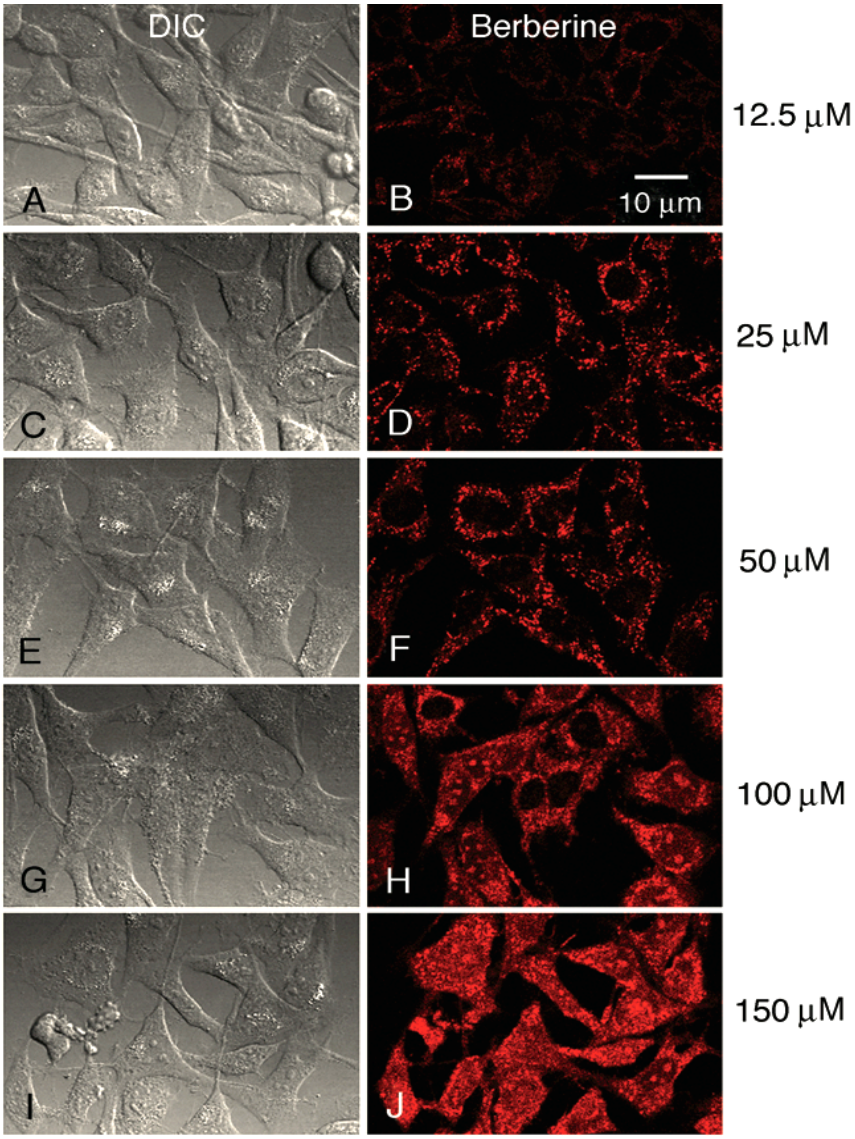

Fig.46 - Visualization of fluorescent berberine distribution in M2 cells by laser-scanning confocal microscopy. Cultures were photographed using the same instrument settings, 2 h after the addition of 12.5–150 μM berberine. **A, B** show the same fields of view of a culture treated with 12.5 μM berberine, by differential interference contrast (**A**, DIC) and fluorescence (**B**) optics. Berberine fluorescence is very low and can barely be detected (control cultures that received DMSO only as a vehicle control displayed a complete lack of fluorescence: not shown). **C, D** are the same field of view, showing cells treated with 25 μM berberine. Note the strong fluorescence of mitochondria, and the lack of appreciable cytoplasmic or nuclear labeling. **E, F** are the same field of view, showing cells treated with 50 μM berberine. The fluorescent signal remains

restricted to mitochondria. **G**, **H** are the same field of view, showing cells treated with 100 μM berberine. At this concentration, cytoplasm and nuclei (especially the nucleoli) are beginning to fluoresce. **I**, **J** are the same field of view, showing cells treated with 150 μM berberine. Note the progressive increase in cytoplasmic and nuclear fluorescence. All images the same magnification; scale bar in **b** represents 10 μm.

4.2.3.1.2.3. Effects of berberine on cell cycle

Different berberine concentrations and exposure times result in a number of distinct perturbations in cell cycle progression (Figs. 48, 49). Twenty-five micromole berberine leads to an increase in the percentage of cells in G1, which becomes more pronounced at days 2 and 3 after addition. In contrast, 100 μM berberine does not lead to a similar G1 increase, but rather results in a marked increase in the percentage of cells in G2/M. Fifty micromole berberine appears to be intermediate between these patterns in its effects. All concentrations of berberine tested (25, 50 and 100 μM) reduce the percentage of cells in S-phase, with a noticeable time-dependence effect for 25 μM.

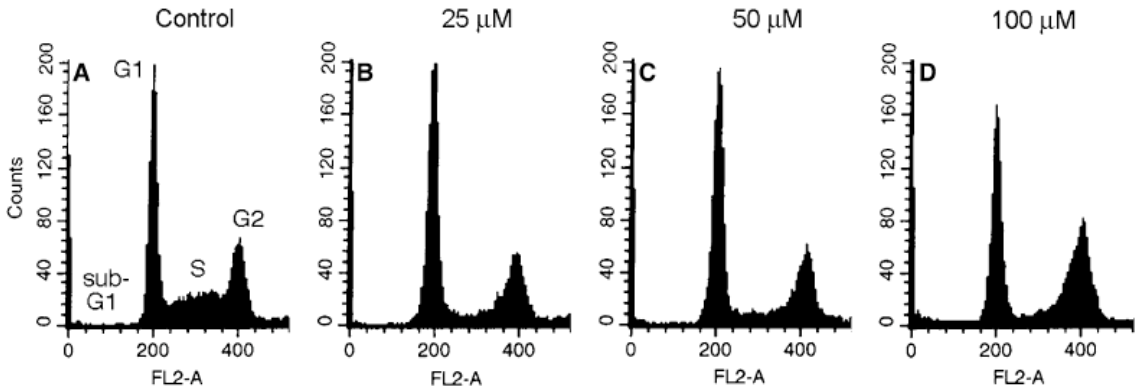

Fig.47 - Histograms of cell cycle distribution of K1735-M2 cells after treatment with vehicle only (control; A), or 25 (B), 50 (C) or 100 (D) μM berberine for 48 h. Shown is a representative example from four separate experiments that were averaged together to obtain the graphs shown in Fig. 48. Note the low numbers of cells in the sub-G1 area, indicating that apoptosis is not occurring to a large extent in these cultures. By this method, the percentage of cells with a sub-G1 content of DNA only rose from 0.49% in controls (**A**) to 5.5% in cultures treated with 100 μM berberine for 48 h (**D**; average of three independent experiments).

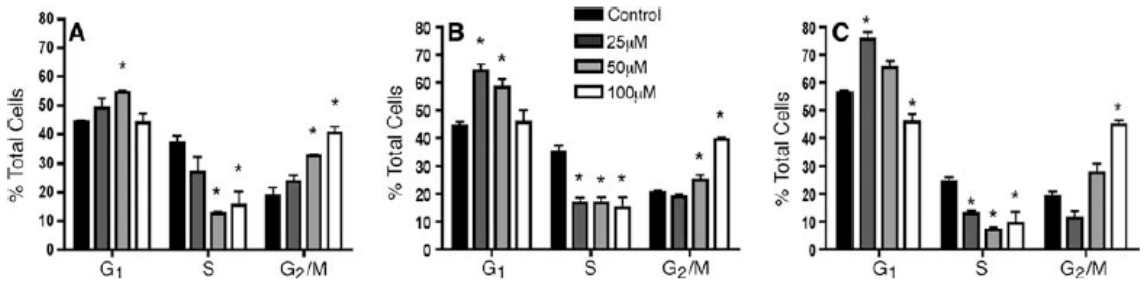

Fig.48 - Cell cycle analysis of cultures treated with 25, 50 and 100 μM berberine for 24 (A), 48 (B) or 72 (C) h. Twenty-five micromole berberine leads to an increase in the percentage of cells in G1 at all time points, and a decrease in numbers of cells in S-phase at 48 and 72 h. In contrast, 100 μM berberine leads to an increase in the percentage of cells in G2, as well as a reduction in the numbers of S-phase cells. The effects of 50 μM berberine appears to be intermediate between those of 25 and 100 μM. The values shown are the averages of three independent experiments; *bars* indicate the standard error of the mean. Samples identified by *asterisks* (*) denote a significant difference from controls ($p < 0.05$).

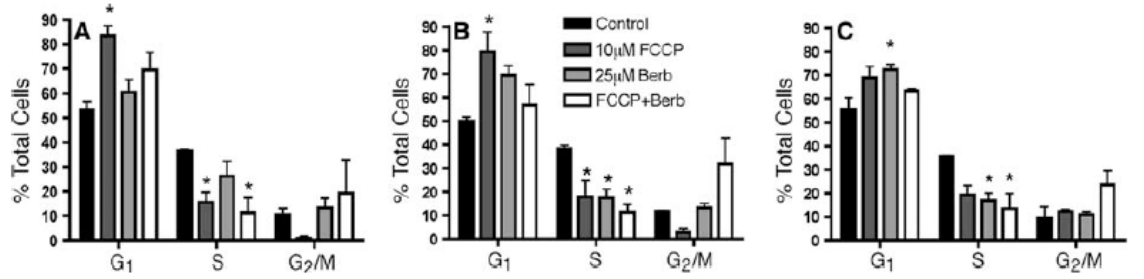

Fig.49 - Comparison of the effects of FCCP with those of berberine on cell cycle progression at 24 (A), 48 (B) and 72 (C) h of drug exposure. Similar to 25 μM berberine, 10 μM FCCP increases the number of cells in G1, and decreases the percentage of cells in S-phase. Interestingly, neither 25 μM berberine nor 10 μM FCCP by themselves caused a significant increase in the percentage of cells in G2/M, but a combination of both did. The values shown are the averages of three independent experiments; *bars* indicate the standard error of the mean. Samples identified by *asterisks* (*) denote a significant difference from controls ($p < 0.05$)

Because of the possibility that berberine may be interfering with normal mitochondrial function (due to its mitochondrial localization), the pattern of cell cycle disruption of a known mitochondrial poison, FCCP, was compared with that of berberine. Interestingly, 10 μM FCCP by itself bore many similarities to the effects of 12.5 and 25μM berberine (Fig. 50). Like these concentrations of berberine, FCCP caused an increase in G1, suppressed S-phase, and had little effect on the percentage of cells in G2/M. Co-treatment with 25 μM berberine and 10 μM FCCP dampened the increase in

G1, and increased the percentage of cells in G2/M. Therefore, the addition of FCCP to low concentrations of berberine resulted in cell cycle profiles that more resembled those of cells exposed to high concentrations of berberine alone.

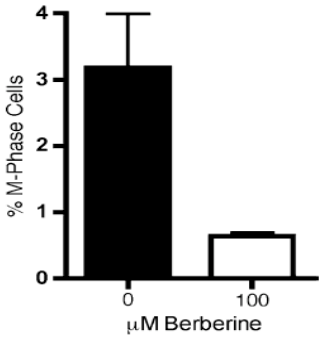

Fig.50 - Comparison of the number of cells in M-phase in control cultures (*black bar*) and cultures incubated in 100 μM berberine for 24 h. A significant reduction in the numbers of cells in M-phase occurs after treatment with this concentration of berberine ($p < 0.05$). The values are averages from three independent experiments; *bars* indicate standard error of the mean.

To distinguish whether the increase in the number of cells in G2/M following treatment with 100 μM berberine was due to a block in G2 or M, the number of M-phase cells (cells containing mitotic spindles and condensed chromatin) were counted after a 24 h exposure. The percentage of cells in M-phase was significantly decreased after treatment, indicating that high concentrations of berberine induce a G2 block prior to entry into M-phase (Fig. 51). To investigate the time-course of the reduction of cells in S-phase by berberine, M2 cells were treated with berberine, and then pulse-labeled with BrdU. Two hours after berberine addition, BrdU labeling was still observed in control, 25 and 50 μM berberine cultures, but the intensity of labeling appeared to be somewhat diminished in the 25, and especially 50 μM cultures (Fig. 52). In contrast, DNA synthesis was significantly reduced in cultures treated with 100 μM berberine, although some labeling was still present in these cells. 24 and 48 h after addition of berberine, BrdU labeling was still present in cultures treated with either 25 or 50 μM berberine, but the percentage of cells exhibiting a BrdU signal appears to be diminished. At 96 h of treatment, some cells are still labeled in the 25 μM berberine cultures, but BrdU uptake is essentially totally suppressed in the 50 μM cultures. DNA synthesis in the 100 μM cultures remained completely inhibited at all of these time points (Fig. 52).

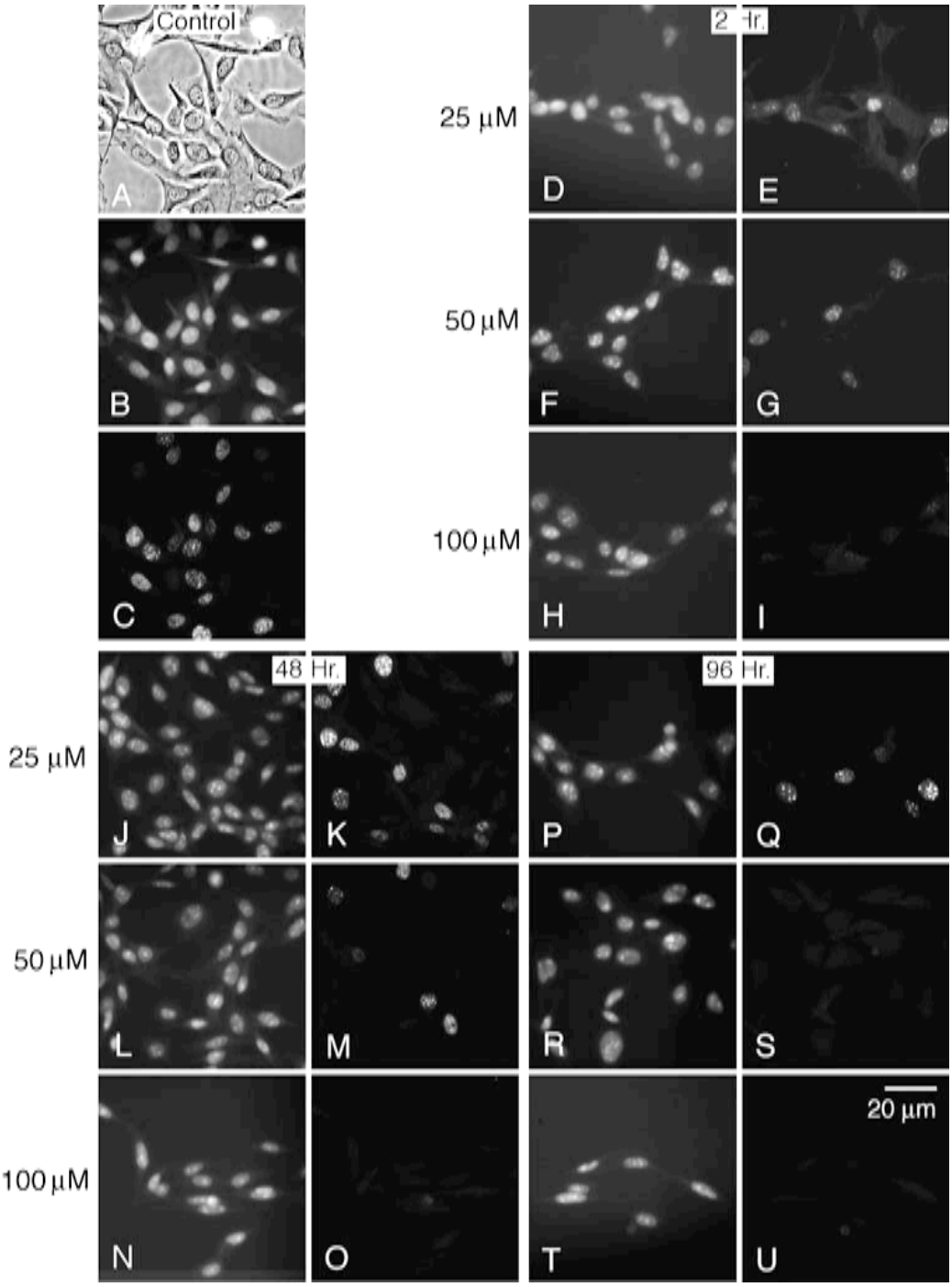

Fig.51 - BrdU incorporation in cells treated with different concentrations of berberine for different lengths of time. Hoechst staining identifies all nuclei in the Welds of view (**B**, **D**, **F**, **H**, **J**, **L**, **N**, **P**, **R** and **T**); BrdU fluorescence identifies those nuclei actively synthesizing DNA (**C**, **E**, **G**, **I**, **K**, **M, O**, **Q**, **S** and **U**). **A–C** Control culture, showing many nuclei actively synthesizing DNA (compare **c** with **B**). Also shown is the same field of view by phase contrast optics (**A**). **D–I** Cells treated with 25, 50 or 100 μM berberine for 2 h prior to BrdU labeling. Cells treated with 25 (**D**, **E**) and 50 μM (**F**, **G**) are still able to incorporate BrdU, while incorporation is completely inhibited in the 100 μM culture (**H**, **I**). **J–O** Cells treated with 25, 50 or 100 μM berberine for 48 h prior to BrdU

labeling. Cells treated with 25 and 50 μM berberine are still able to carry out DNA synthesis, but cells treated with 100 μM berberine remain unable to synthesize DNA. Note that fewer cells in the 25 and 50 μM berberine cultures exhibit BrdU labeling than are labeled in the control (no berberine) cultures (**A–C**). (**P–U**) Cells treated with 25, 50 or 100 μM berberine for 96 h prior to BrdU labeling. Although cells treated with 25 μM berberine are still able to synthesize DNA, BrdU labeling has been lost from the 50 μM berberine cultures. The 100 μM berberine culture remains unlabeled. All micrographs are the same magniWcation; *bar* in (**U**) represents 20 μm.

To determine whether mitochondrial accumulation of lower concentrations of berberine caused perturbations in mitochondrial structure or function, K1735-M2 and WM793 melanoma cells were incubated in 25 μM berberine for 6 h, and then labeled with TMRM, a polarization-dependent mitochondrial probe. Berberine treatment led to mitochondrial fragmentation in both of these melanoma cell lines (Fig. 52). In addition, a reduction in mitochondrial TMRM fluorescence intensity was noticeable, indicating that mitochondrial membrane potential is decrease in the presence of berberine.

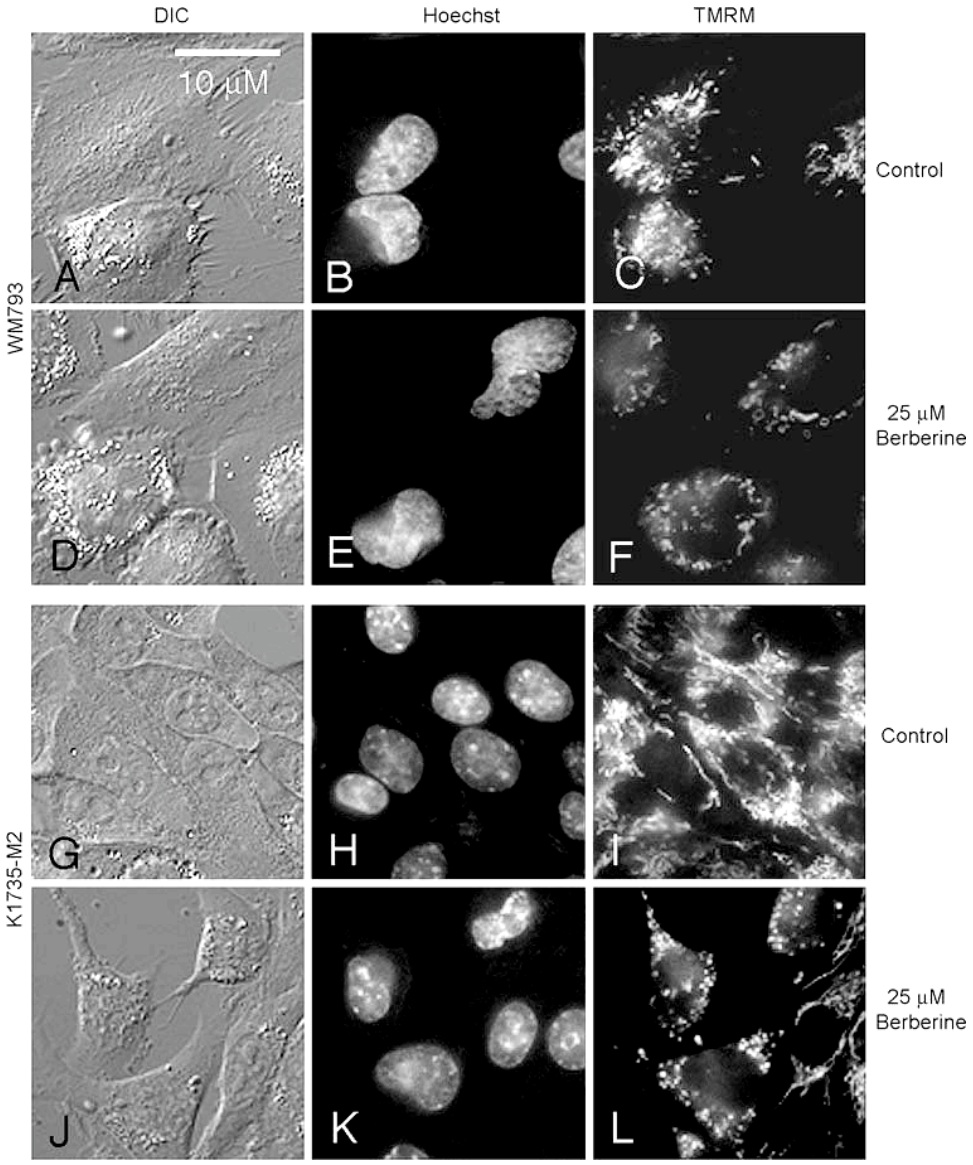

Fig.52 - Epifluorescence micrographs showing the effects of berberine on mitochondrial morphology and membrane polarization in two different melanoma cell lines. K1735-M2 mouse and WM793 human melanoma cells were treated with vehicle only (0.1% DMSO, control) or 25 μM berberine for 6 h prior to labeling nuclei with Hoechst, and mitochondria with the polarization-dependent probe TMRM. Note that berberine treatment causes mitochondrial fragmentation and a reduction in polarization (fluorescence intensity) in both melanoma cell lines. Other than these mitochondrial effects, the cells look morphologically very similar to the controls.

4.2.3.1.2.4. Berberine causes mitochondrial damage on k1735-M2 melanoma cells

To explore in detail mitochondrial alterations caused by berberine, we mostly focused in one berberine concentration (25 μM) because the objective was to cause notorious mitochondrial damage with concentrations not lacking relevance in *in vivo* systems. Cells incubated with berberine were fluorescently labeled with Hoechst 33342 and TMRM.

Because berberine and TMRM presents red fluorescence, a conflict between both signals could be a problem. However, TMRM has a higher fluorescence quantum yield, so the contribution of berberine fluorescence is non-significant. Figure 53, A and B, show that after 24 h of treatment, the filamentous mitochondrial network is dismantled, and mitochondria appear to be smaller and rounder in shape. Alterations in mitochondrial structure occur with intact cell viability, as observed by intracellular calcein-AM accumulation and TMRM fluorescence (Fig. 53C). Mitochondrial fragmentation did not increase the apparent number of mitochondrial bodies as observed by electron microscopy (EM) (Fig.53). In fact, by visualizing several fields from each treatment group, a lower number of mitochondrial bodies were observed after berberine treatment, although determination of mitochondrial mass by EM warrants several notes of caution. By comparing Fig. 53, A and B, it is also observable that loss of mitochondrial TMRM fluorescence accompanies fragmentation even for 6 h of exposure (Fig. 53, I and J). Berberine (50 μM) was used to investigate whether a dose-dependent effect could be found. In fact, the depolarization effect obtained with the higher concentration was not dissimilar from the result obtained with the lower concentration. Figure 53F shows control condensed mitochondria where cristae can be easily observed. In contrast, most mitochondrial bodies lost their typical shape, swelled, and appeared to loose their cristae after a 24-h incubation period with berberine, although different degrees of damage were observable (Fig. 53, D–H). The apparent decrease in mitochondrial numbers by electron microscopy was also supported by the finding that mtDNA copy number decreases when cells are treated with 25 μM berberine for 24 and 48 h (Fig. 53K). Surprisingly, when that maximum berberine concentration used in proliferation studies (100 μM) was used, no decrease in mtDNA copy number occurred.

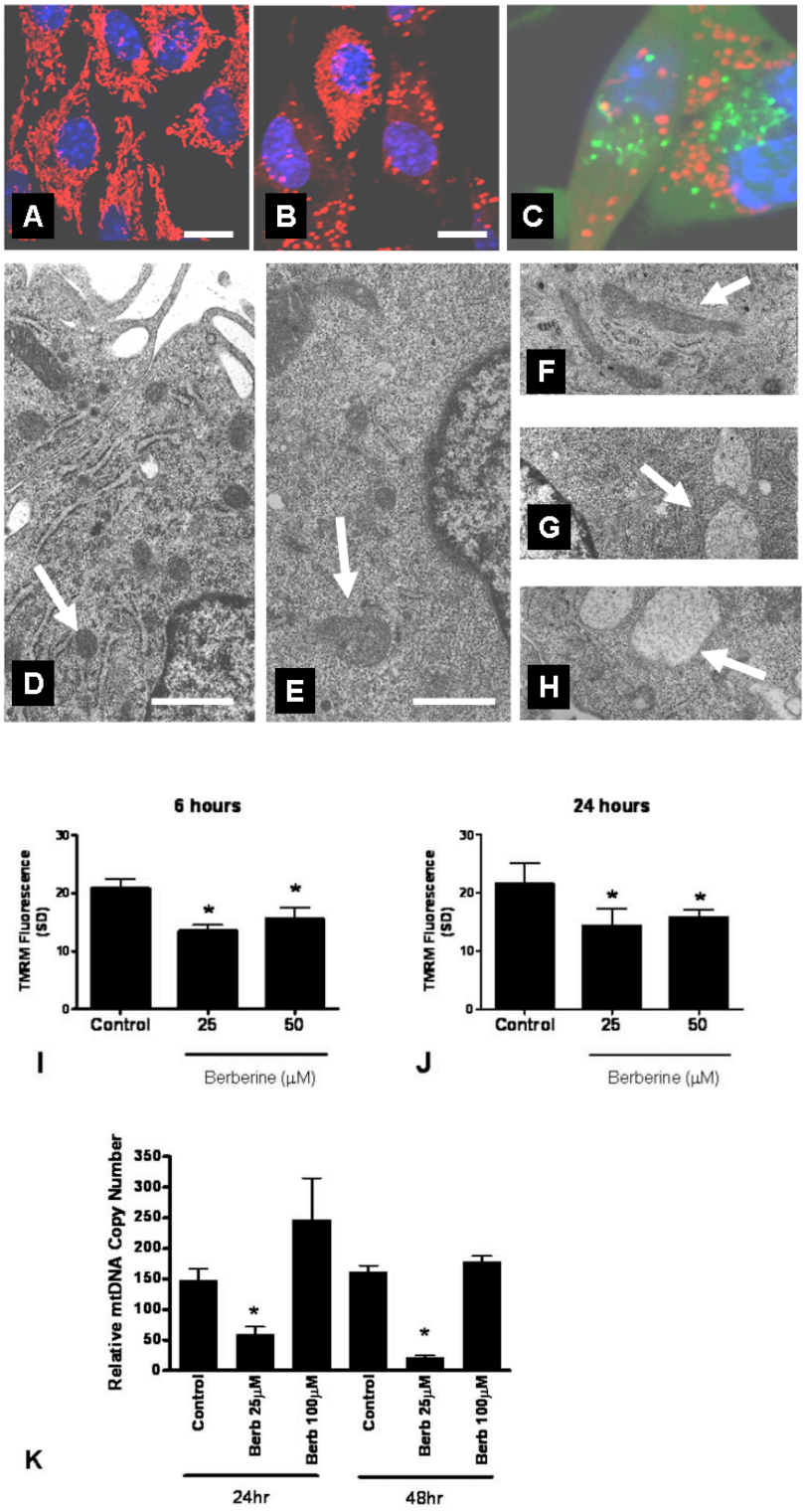

Fig.53 - Mitochondrial alterations induced by berberine. The effects of berberine on mitochondrial structure were evaluated by using confocal and electron microscopy. MtDNA copy numbers were evaluated by using real-time PCR. A and B, confocal microscopy of K1735-M2 cells treated with vehicle (A) and 25 μM berberine (B) during 24 h. White bar, 15 μm. Live cells were labeled with the fluorescent probes TMRM (mitochondria) and Hoechst 33342 (nuclei)

for 30 min before observation with a confocal microscope. C, detail of a cell treated with 25 μM berberine during 24 h, where fragmented and round mitochondria labeled with TMRM can be observed. Hoechst 33342 (nucleus) and calcein-AM (cytoplasm) were the two other probes used. Cytoplasmic calcein granules are also observable, although their origin has yet to be identified. D and E, electron microscopy (white bars, 5 μm) showing K1735-M2 cells treated with vehicle (D) and 25 μM berberine (E) during 24 h. White arrow, mitochondrial bodies. F to H, electron microscopy showing K1735-M2 cells treated with vehicle (F), 10 μM (G), and 25 μM berberine (H) during 24 h. White arrow, mitochondrial bodies. All three panels are the same magnification. I and J, evaluation of TMRM fluorescence in cells treated with vehicle and 25 and 50 μM berberine for 6 (I) and 24 (J) h. Quantification of cell fluorescence was made as described under *Materials and Methods*, $p < 0.05$ versus control. K, mtDNA copy number of cells treated with vehicle or 25 or 100 μM berberine. Relative mtDNA copy numbers were determined as described under *Materials and Methods*.

To test whether berberine increases oxidative stress, cells were incubated with the drug (25 μM) for 6 and 24 h. Forty-five minutes before the end of incubation period, cells were incubated with Hoechst 33342, TMRM, and CM-H_2DCFDA, a fluorescent probe for oxidative stress. Figure 54 shows that 6 h of exposure is not enough to cause a significant increase in intracellular oxidative stress as opposed to 24 h of drug exposure when an increase of probe fluorescence was observed in cells treated with 25 μM berberine. We also confirmed that the mitochondrial depolarization precedes the detection of oxidative stress.

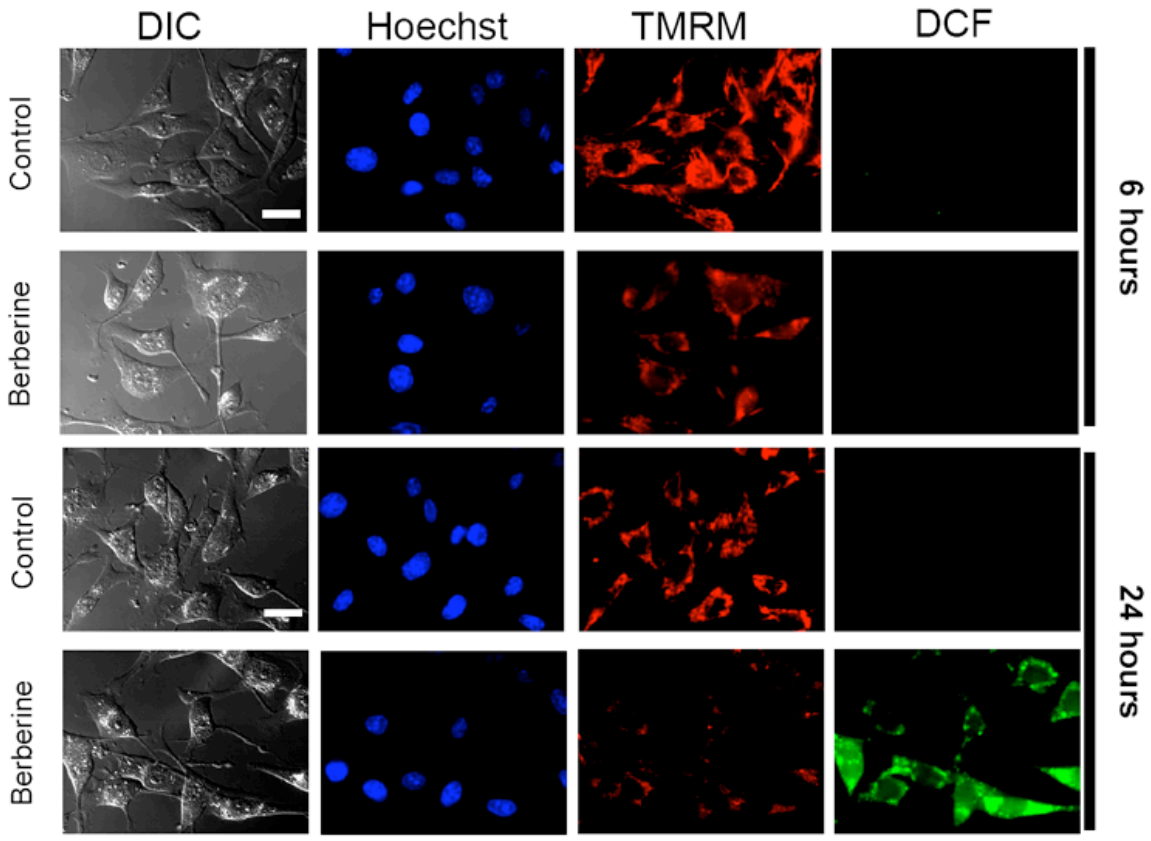

Fig.54 - Berberine induced mitochondrial depolarization and increased oxidative stress in K1735-M2 mouse melanoma cells. Cells were incubated with 25 "M berberine for 6 or 24 h. Forty-five minutes before the end of the incubation period, the fluorescent probes TMRM (red, mitochondria), Hoechst 33342 (blue, nuclei), and CM-H2DCFDA (green, oxidative stress) were incubated with cells and imaged with a Nikon Eclipse 3000 epifluorescence microscope.

4.2.3.1.3. Discussion

Berberine is a fluorescent compound, with absorbance peaks of 230, 267, 344 and 420 nm, and peak emission at 550 nm (Maiti and Kumar, 2006). Although it has been utilized as a fluorescent stain for mast cells (Berlin and Enerback, 1983; Dimlich et al, 1980), sperm and oocytes (Reyes et al, 2004), DNA and RNA (Curtis and Cowden, 1981), and mitochondria (Borodina and Zelenin, 1977), the kinetics of its uptake and distribution in living cells has not been extensively characterized. In this study, 25 and 50 μM berberine strongly labeled mitochondria, with little detectable cytoplasmic or nuclear fluorescence. However, both cytoplasm and nuclei became noticeably fluorescent at higher concentrations of berberine (100 and 150 μM). Previous studies demonstrated that berberine displays a striking increase in fluorescence in the

hydrophobic regions of polarized mitochondrial membranes, apparently due to an increase in quantum yield (Mikes and Dadak, 1983). Although more berberine binds to energized mitochondria than non-energized mitochondria, this difference has been reported to be relatively minor (Mikes and Dadak, 1983). Similarly, a dramatic increase in fluorescence quantum yield also occurs upon DNA binding (Gong et al, 1999). This behavior complicates the quantitative assessment of berberine localization within cells by fluorescence methods. However, the overall berberine signal in nuclei, which, like mitochondria, would also be expected to display increases in fluorescence quantum yield as berberine binds DNA, is very low in M2 cells treated with 25 and 50 μM berberine. Instead, both nucleus and cytoplasm become steadily more fluorescent as the concentration of berberine added to the cultures increases above 50 μM. Although detailed washout experiments have not been conducted, the cytoplasm and nucleus appear to have affinity for berberine, as the flow cytometry data was obtained from cells that had been washed out of berberine (resuspended in PBS) for approximately 15 min. This conclusion is supported by previous studies reporting staining of nuclei and cytoplasm by berberine (Slaninova et al, 2001; Yang et al, 1996). We interpret these results as indicating that most berberine preferentially accumulates in mitochondria at lower concentrations (<50 μM), but these binding sites become saturated at higher concentrations (>50 μM), and berberine subsequently accumulates in the cytoplasm and nucleus. If this is the case, then two sets of effects could be expected to occur in berberine-treated cells: cells exposed to lower concentrations of berberine would be predicted to display primarily mitochondrial effects, whereas cells exposed to higher concentrations of berberine could additionally exhibit a host of other alterations, including effects resulting from perturbations of DNA organization and function.

Interesting was to observe a decrease of mtDNA copy number for 25 but not for 100 μM. Berberine is known to intercalate into doublestranded DNA, forming adducts that can inhibit DNA replication (Kuo et al., 1995), which could explain the reduced mtDNA copy numbers in cells treated with low concentrations of berberine. It is possible that the lack of reduction in mtDNA copy number in cells treated with 100μM berberine reflects a compensatory mechanism that attempts to overcome the decreased mitochondrial ATP production by increased mtDNA copy number. Alternatively, it could be that the higher levels of oxidative stress induced by lower concentrations of

berberine result in mtDNA destruction that is either blocked by the antioxidant effects of higher concentrations of berberine or somehow inhibited by a "protective" effect of a larger quantity of intercalated berberine. It would be of interest to obtain and compare accurate measures of mitochondrial mass with mtDNA quantity in cells treated with different concentrations of berberine.

Mitochondria are well known to produce free radicals as a consequence of mitochondrial respiration (Sastre et al., 2000). Assays with dichlorofluorescein, a probe whose fluorescence increase in the presence of oxidants, show that berberine increases oxidative stress in K1735-M2 cells.

Moreover, flow cytometry data indicates that total cellular accumulation of berberine did not appear to be saturated at the highest concentration (150 μM) used in this study. On the other hand, time-course studies using 100 μM berberine indicate that uptake reached a maximum by about 2 h, with about 50% entering cells within 30 min. Addition of 10 μM FCCP significantly enhanced the accumulation of 100 and 150 μM berberine in M2 cells, raising the possibility that berberine is a substrate for drug efflux pumps, and that reduction of ATP levels by FCCP interferes with the export of higher concentrations of berberine. Berberine has been reported to inhibit P-gp activity in a number of transformed cell lines (Min et al, 2006), to mildly activate P-gp ATPase activity in brain (He and Liu, 2002), and to up-regulate the expression of P-gp in oral, gastric, and colon cancer cells (Lin et al, 1999). Inhibitors of MDR1 and MRP1, as well as reduction of ATP levels with sodium azide increased the cellular accumulation in human KB3-1 cells (Shitan et al, 2007).

Of course, for clinical relevance, uptake and metabolism of berberine in an in vivo situation must take into account route of delivery and pharmacokinetic considerations. Berberine has been shown to be rapidly absorbed by the small intestine in rats (Zuo et al, 2006), and less than 5% is eliminated from urine and bile after a bolus i.v. injection (Chen and Chang, 1995). Relatively more metabolites than berberine were recovered from urine of human volunteers after oral ingestion of berberine (Pan et al, 2002), suggesting that berberine metabolites may play important roles in vivo. Berberine is metabolized by the liver to berberrubine, thalifendine, demethyleneberberine, and jattrorhizine; interestingly, berberrubine and thalifendine inhibit topoisomerases II and I, respectively, and berberrubine has been shown to possess antitumor properties (Hoshi

et al, 1976; Makhey et al., 1995). Based on in vitro findings that 1, 5 and 10 μg/ml berberine were cytotoxic to B16 mouse melanoma cells, daily i.p. injections of 1, 5 and 10 mg/kg berberine were carried out in an in vivo melanoma transplant model; tumor weights were significantly reduced in the 5 and 10 mg/kg animals (Letasiova et al, 2005). These findings indicate that the lower concentrations of berberine used in this study are within the range of clinical relevance.

Subjectively, the strong mitochondrial berberine signal suggests that this compound could directly impact mitochondrial function. Previous studies in fact have shown that berberine inhibits NADH dehydrogenase and respiratory activity (Barreto et al, 2003). In addition, mitochondrial participation in berberine-induced apoptosis has been demonstrated in a number of studies (Jantova et al, 2006). Mitochondrially-relevant effects of berberine exposure include changes in Bcl-2/Bax ratios, reactive oxygen species production, and a reduction in mitochondrial membrane potential (Lin et al, 2006). In this report, we demonstrate that berberine induces mitochondrial fragmentation and diminishes polarization in K1735-M2 and WM793 melanoma cells. We have extended these studies using isolated liver mitochondria, and have found that berberine primarily affects complex I function, inhibiting respiration and increasing oxidative stress, besides interacting with the ANT (Pereira et al., 2008 and Pereira et al, 2009).

A number of studies have reported various effects of berberine on cell cycle progression in different types of cancer cell lines. G1 arrest has been reported for epidermal (Mantena et al, 2006b) and prostate (Mantena et al, 2006) carcinoma cells. However, berberine can arrest gastric carcinoma (Lin et al, 2006) and HL-60 leukemia cells in G2/M (Lin et al, 2006b). In contrast, berberine has been reported to have little effect on cell cycle traverse in U937 leukemia and B16 melanoma cell lines (Letasiova et al, 2006). Our results with K1735-M2 melanoma cells show that the exact nature of cell cycle perturbation depends on the concentration of berberine used, with lower concentrations resulting in G1 arrest, and higher concentrations leading to a G2 arrest. Consequently, the conflicting information in the literature may reflect in part the different concentrations of berberine used in different studies. In addition, different cells lines exhibit significantly different sensitivities to this alkaloid. For example, almost two orders of magnitude difference in IC50 values were reported in the same study for

leukemia and melanoma cell lines (Letasiova et al, 2006).

Expression of key cell cycle regulatory molecules appears to be altered in response to berberine exposure. Down regulation of cyclins D1, D2 and E, and CDKs 2, 4 and 6, together with increased expression of the CKIs p21 and p27 were suggested to be responsible for the G1 arrest observed in berberine-treated prostate carcinoma cells (Mantena et al, 2006).

In the studies showing G2/M arrest in promyelocytic leukemia and gastric carcinoma cells, it was found that the expression of cyclin B and CDK1 were decreased, while the levels of Wee1 were increased. The authors concluded that the G2/M arrest was caused by these effects of berberine on these molecules (Lin et al, 2006b). Early studies showed that low glucose levels can lead to a G1 arrest (Holley and Kiernan, 1974), as can interfering with mitochondrial function (VanDenBogert et al, 1986). A mechanistic link between ATP depletion and cell cycle arrest has recently been obtained by the demonstration that glucose limitation can activate the energy sensor AMPK, as well as p53 (Jones et al, 2005). In *Drosophila* embryos, a 60% reduction in ATP levels resulting from a mutation in a mitochondrial electron transport chain protein allows cells to survive, grow, and differentiate, but blocks cell division via activation of AMPK. AMPK activation activates p53, reduces levels of cyclin E, and results in a G1 arrest (Mandal et al, 2006). In addition, reducing ATP levels with mitochondrial poisons also may result in a down-regulation of D-type cyclins, further contributing to a G1 arrest (Gemin et al, 2005). We propose that the increase in the percentage of M2 cells in G1 following lower doses (25 and 50μM) of berberine reflect the effects of mitochondrially-concentrated berberine on respiratory function, resulting in lower ATP levels and activation of a G1 ATP checkpoint. This proposal is supported by the finding that ATP levels are reduced in cells treated with berberine (Pereira et al. submitted). Berberine has been reported to inhibit DNA synthesis (Letasiova et al, 2006b) and induce S-phase cell cycle arrest (Lin et al, 2006b). We found that in M2 melanoma cells, short-term exposure to berberine had little direct effect on DNA synthesis except at very high doses. The ability of high concentrations (100 μM) of berberine to arrest DNA synthesis was maintained for extended periods of time, namely, up to 4 days of treatment, the longest time point examined in this study. Because berberine is a DNA-binding compound, we presume that the rapid inhibition of DNA synthesis by high concentrations of berberine

reflects altered replication across berberine-bound DNA, or inhibition of the replication complex itself. In contrast, lower concentrations of berberine (25 and 50 μM) do not immediately block DNA synthesis, but instead exhibit a delayed effect on BrdU uptake. BrdU-labeled cells could be found at all time points in cultures treated with 25 μM berberine, but the number of labeled cells appeared to be diminished with extended drug exposure times (24 h and longer). Notably, BrdU uptake could be completely suppressed in cultures incubated in 50 μM berberine, but this effect took between 48 and 96 h to occur. These observations, together with the flow cytometry data, suggest that lower doses of berberine (<100μM) allow cells to progress through S-phase, but subsequent entry into S is inhibited due to cell cycle arrest. At low concentrations of berberine, this arrest may reflect mitochondrial perturbation and initiation of the G1 "ATP checkpoint" described above. Higher concentrations of berberine resulted in a G2/M arrest, which is suggestive of a DNA damage/p53 activation response (Bunz et al, 1998;Taylo and Stark, 2001). Although we did not directly assay DNA damage in this study, previous workers have presented evidence for berberine-induced DNA damage and p53 activation (Letasiova et al, 2006b). Our results demonstrate that different concentrations of berberine lead to distinct cellular responses that are correlated with specific cellular localization patterns. Interestingly, an earlier study also correlated differences in berberine concentration and distribution with the responses of Balb/c 3T3 cells. In that study, 100 μM berberine was mostly located in the cytoplasm and induced a G2/M arrest (similar to our results), while 200 μM was concentrated in the nucleus and triggered apoptosis (Yang et al, 1996). Together, these data suggest that the following multiphase model of action can be proposed: low concentrations of berberine are selectively accumulated by mitochondria, resulting in altered mitochondrial function, a reduction in ATP synthesis, activation of a G1 energy checkpoint, and consequently a slowing or arrest of cell proliferation. Higher concentrations of berberine saturate the mitochondrial binding capacity and subsequently accumulate in the cytoplasm and nucleus, and directly interfere with DNA synthesis. The nuclear effects of high concentrations of berberine may activate p53 and Wee1, and inhibit cyclin B, leading to a G2 block prior to entry into M-phase. Very high concentrations may result in cell cycle perturbation and/or DNA damage suficient to trigger apoptosis. It therefore appears that berberine would function more as a mitochondriotropic and cytostatic agent than a

nuclear-damaging and cytotoxic agent at clinically relevant concentrations. It is possible that these multiphase effects resulting from dose-dependent patterns of intracellular berberine localization can be exploited in the future to treat cell proliferative diseases where arrest of cell growth instead of induction of cell death is an acceptable treatment outcome, as well as in the ongoing search for natural products that synergize with current standard-of-care chemotherapeutics.

4.2.3.2. Sanguinarine

4.2.3.2.1. Background and Objectives

Sanguinarine (SANG, 13-methyl benzodioxolo [5,6-c]-1,3-dioxolo[4,5-i] phenanthridinium), (Dyke et al, 1968; Mackraj et al, 2008) is an alkaloid derived from the root of *Sanguinaria Canadensis* and other plants from the Papaveraceae family. SANG is a benzophenanthridine structural homologue of chelerythrine (Pi et al, 2008). SANG is known to exert a wide range of biological properties including antimicrobial (Baker, K., 1993), antifungal (Balanyk, 1990), anti-inflammatory (Allen, C., 1999) and antineoplastic activity; it has been shown to inhibit a variety of human tumor cell types at micromolar concentrations, without affecting normal cells (Anderson et al, 2005; Godowski, K, 1989). It also inhibits several enzymes such as lipoxygenase (Giuliana et al, 1997), cholinesterase (Dvorak et al, 2006), sodium/potassium and calcium ATPases in skeletal muscle (Kaminskyy et al, 2008; Malikova et al, 2006), and alters tubulin assembly (Kemeny-Beke, 2006).

Some examples exist regarding the anti-proliferative activity of SANG. For example, it has been described that SANG causes death of human colon cancer cells (Vavreckova et al, 1996) and blocks the nucleocytoplasmic trafficking of cyclin D1 and topoisomerase II (220) in breast cancer MCF-7 cells. In another example, SANG was demonstrated to induce the expression of pro-death Bcl-2 proteins including Bax or Bak in immortalized human HaCaT keratinocytes (Kuznetsova et al, 2002).

The role of mitochondria in drug-induced cell death is well documented (Faddeeva and Beliaeva, 1988; Seifen et al, 1979) and several anti-cancer agents are known to cause cell death through interacting with the organelle (Lopus and Panda, 2006). Relatively little is known regarding the effects of SANG on isolated mitochondria. Barreto et al. (Matkar et al, 2008) identified complex II as a mitochondrial target for SANG, although only oxygen consumption was used as an experimental end-point. Other reports indicate that SANG causes oxidative stress, mitochondrial depolarization and cytochrome c release (Holy et al, 2006; Adhami et al, 2003; Jeong and Seol, 2008).

Phytochemicals with anti-proliferative activity are promising agents against resistant tumours, including melanoma. Advanced melanoma can be highly aggressive,

metastatic, and resistant to conventional chemotherapy (Ivanov et al, 2003; Helmbach et al, 2001). Hence, there is an urgent need to find novel chemotherapeutics with selective and powerful effects on melanoma.

The objective of the present work is to investigate the effect of low micromolar concentrations of SANG on a mouse metastatic melanoma cell line and determine the role of mitochondria on SANG-induced cytotoxicity. Mouse K1735-M2 cells are a very aggressive and invasive form of metastatic melanoma (Repesh et al, 1993; Pereira et al, 2007), which has been used to investigate the potential anti-tumour effect of berberine, another alkaloid with potential to be used as an effective chemotherapeutic on melanoma (Pereira et al, 2007; Serafim et al, 2008). Data on intact cells were correlated with effects on isolated hepatic mitochondria, and we examined the possibility that SANG may have an inductive effect on the mitochondrial permeability transition pore (MPT pore), a deleterious condition for cells (Rasola and Bernardi, 2007; Kroemer et al, 2007).

4.2.3.2.2. Results

4.2.3.2.2.1. Effect of sanguinarine in K1735-M2 cell line proliferation

In order to investigate the effects of SANG on cell proliferation and cell death, K1735-M2 rat cells were incubated in the absence and presence of increasing concentrations of the drug (2, 4 and 8**μ**M) for 12, 24, 36 and 48 hours. In Fig. 55, panel A, the survival curve shows that SANG has a dose/time-dependent effect inhibiting K1735-M2 cell proliferation. The inhibitory effect on cell proliferation is more visible after 12 h of incubation with SANG. After 48 hours of incubation, 8 **μ**M SANG has a profound effect on cell proliferation, most likely because of induction of cell death as the corresponding line is below control levels. Panel B is the same experiment but with the extra addition of the mitochondrial uncoupler FCCP. Data shows that FCCP synergistically increases the effect of 4 **μ**M SANG. Also interesting is the fact that FCPP, per se, was not able to decrease cell mass during the full time frame of the experiments. A third trial was performed to confirm cell death induced by SANG. When measuring cell death by flow cytometry, a significant difference was observed for the highest concentration tested (8**μ**M), which caused more than 20% of cell death.

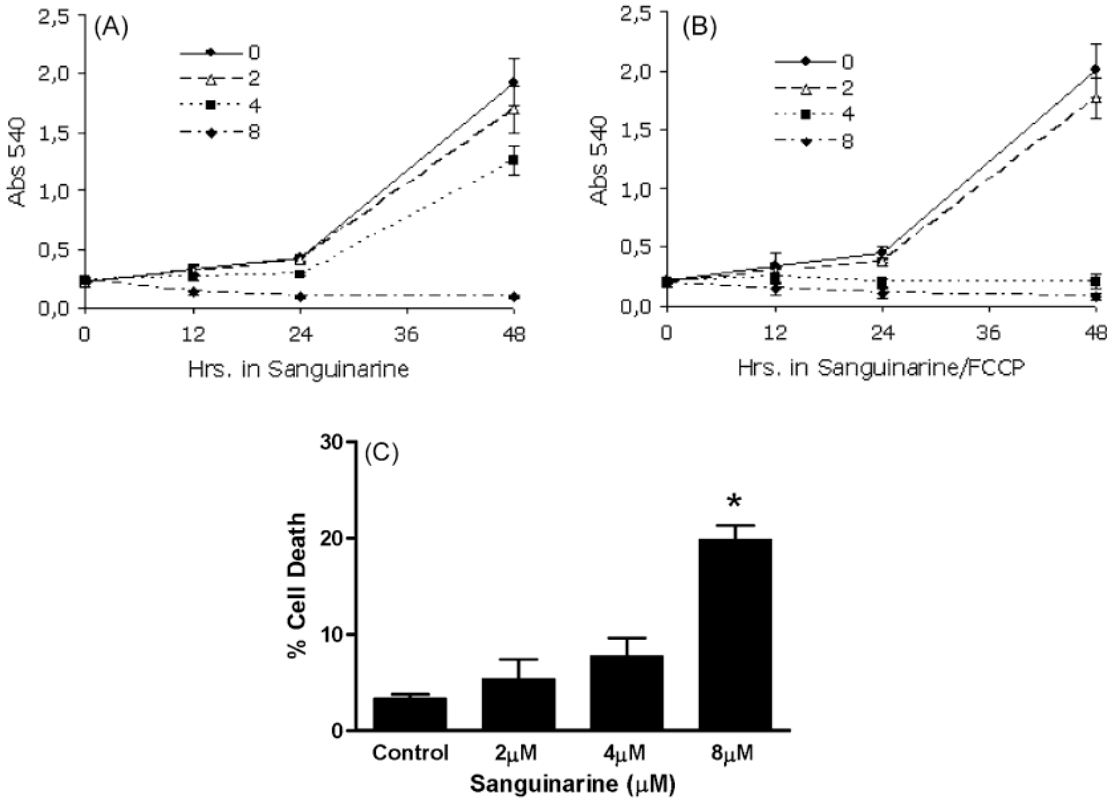

Fig.55 - Inhibition of cell proliferation and induction of cell death by SANG. (A) Inhibition of cell proliferation by SANG as measured by using the sulforhodamine B assay. Data in the ordinate represent the absorbance of the dye, which is proportional to the amount of cells. Data are means W S.E.M. of three independent experiments. (B) As in (A), except that cells were previously incubated with 10 mM FCCP for 30 min before adding SANG. The two molecules were present throughout the entire time frame. Data are means W S.E.M. of three independent experiments. (C) Determination of cell death after incubating cells with SANG for 24 h. Ethidium homodimer and calcein-AM were used as a tool to measure cell death by flow cytometry. Ethidium homodimer-positive, calcein-negative cells were considered necrotic. *p < 0.05 vs. control. Data are means W S.E.M. of three independent experiments.

4.2.3.2.2.2. Sanguinarine preferably accumulates in K1735-M2 cells nuclei

In order to assess the intracellular site for SANG accumulation, K1735-M2 cells were incubated with 4***μ***M SANG for 3 hours. Intracellular accumulation of the drug was identified by epifluorescence microscopy as SANG exhibits self-fluorescence (Holy et al, 2006). TMRM, a cationic fluorescent probe that accumulates in mitochondria was used to assess the co-localization of the alkaloid and TMRM. The set of images of Fig. 56, upper panel, clearly shows that SANG (green fluorescence) is accumulated by the cell nuclei at a greater level than by mitochondria, this despite the molecule having a positive charge (Fig.9). In the absence of TMRM, SANG was also not significantly detected in

extranuclear spaces. Next, SANG intracellular accumulation was quantified by flow cytometry; the upper panel of Fig.56 reveals that the relative fluorescence increases directly with the increasing SANG concentrations even for concentrations much higher than the ones used in most experiments.

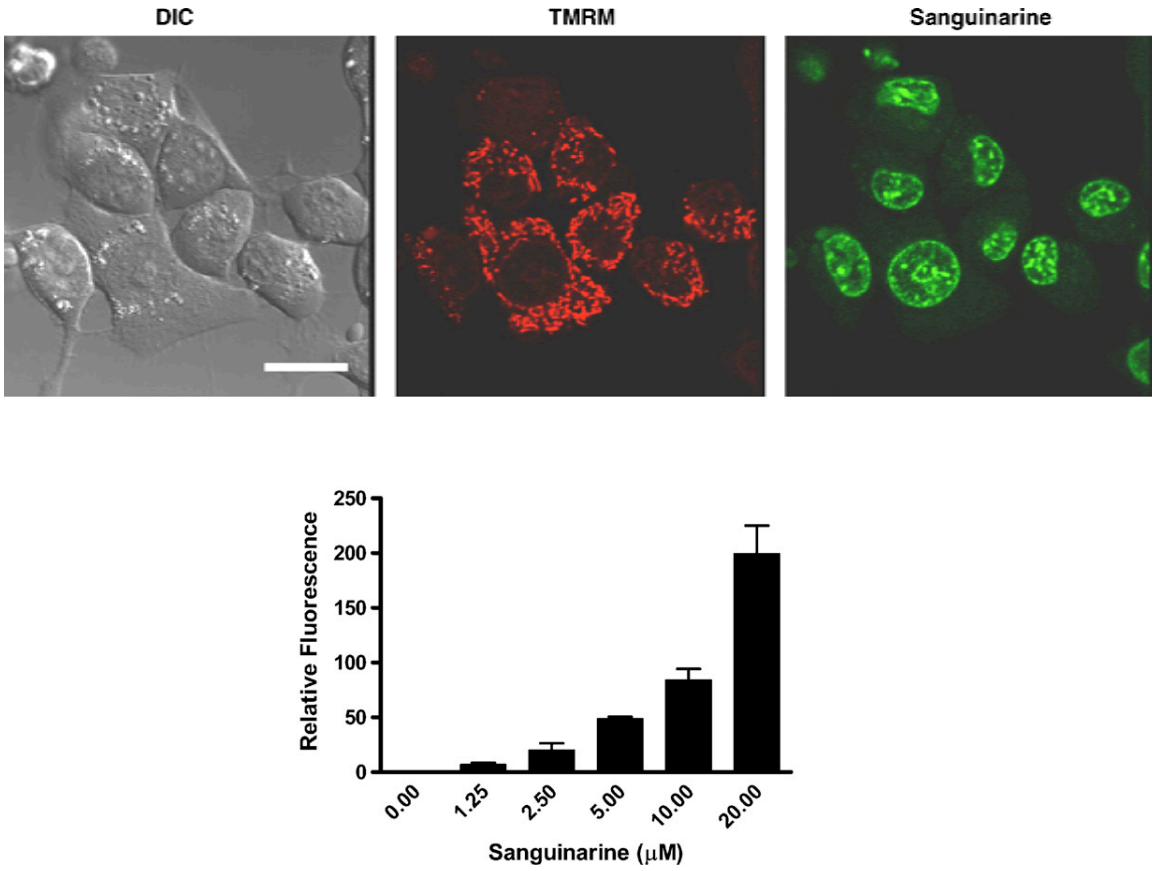

Fig.56 - Nuclear accumulation of SANG. Upper panel, epifluorescence microscopy of K1735-M2 cells treated with 4 mM SANG for 3 h. Cells were also co-incubated with 100 nM TMRM (red) which accumulates in polarized mitochondria. An image obtained by differential interference contrast is also shown. White bar represents 15mm. Lower panel, SANG accumulation as quantified by flow cytometry. Cells were exposed for 150 min with 1.25, 2.5, 5, 10 and 20 mM SANG. Data are means W S.E.M. of three independent experiments.

4.2.3.2.2.3. Sanguinarine induces morphologic changes and mitochondrial depolarization in K1735-M2 cells

Cells pre-treated with SANG were incubated with TMRM (mitochondria), Hoechst 33342 (nuclei) and calcein-AM (cell viability) for 30 minutes at 37°C. Figure 57 shows several images obtained by epifluorescence. Panels A-D shows a control group, with cells showing 70-80% confluence (A), a vast majority of cells maintaining viability

(B), normal nuclear morphology (C) and normal mitochondrial polarization (D). By treating cells with 8 mM SANG for 24 hours, most cells round up and detach (E), although most still maintain membrane integrity (F) and present abnormal nuclei, with clear signs of condensed chromatin (G). Also, the majority of cells exhibit mitochondrial depolarization (H). A higher magnification of cells treated with 4 mM SANG for 24 hours shows that two distinct populations of cells co-exist. Although by phase-contrast, cells have mostly a normal appearance (K), some are completely depolarized (L), not showing any TMRM labelling whatsoever. In contrast, control cells (I, J) display a normal appearance and TMRM mitochondrial labelling. Because of these mitochondrial effects, some selected concentrations of SANG were also used to investigate if mtDNA copy number is altered with treatment for 24 hours. In fact, no significant alterations in mtDNA were detected (M) for any of the concentrations studied.

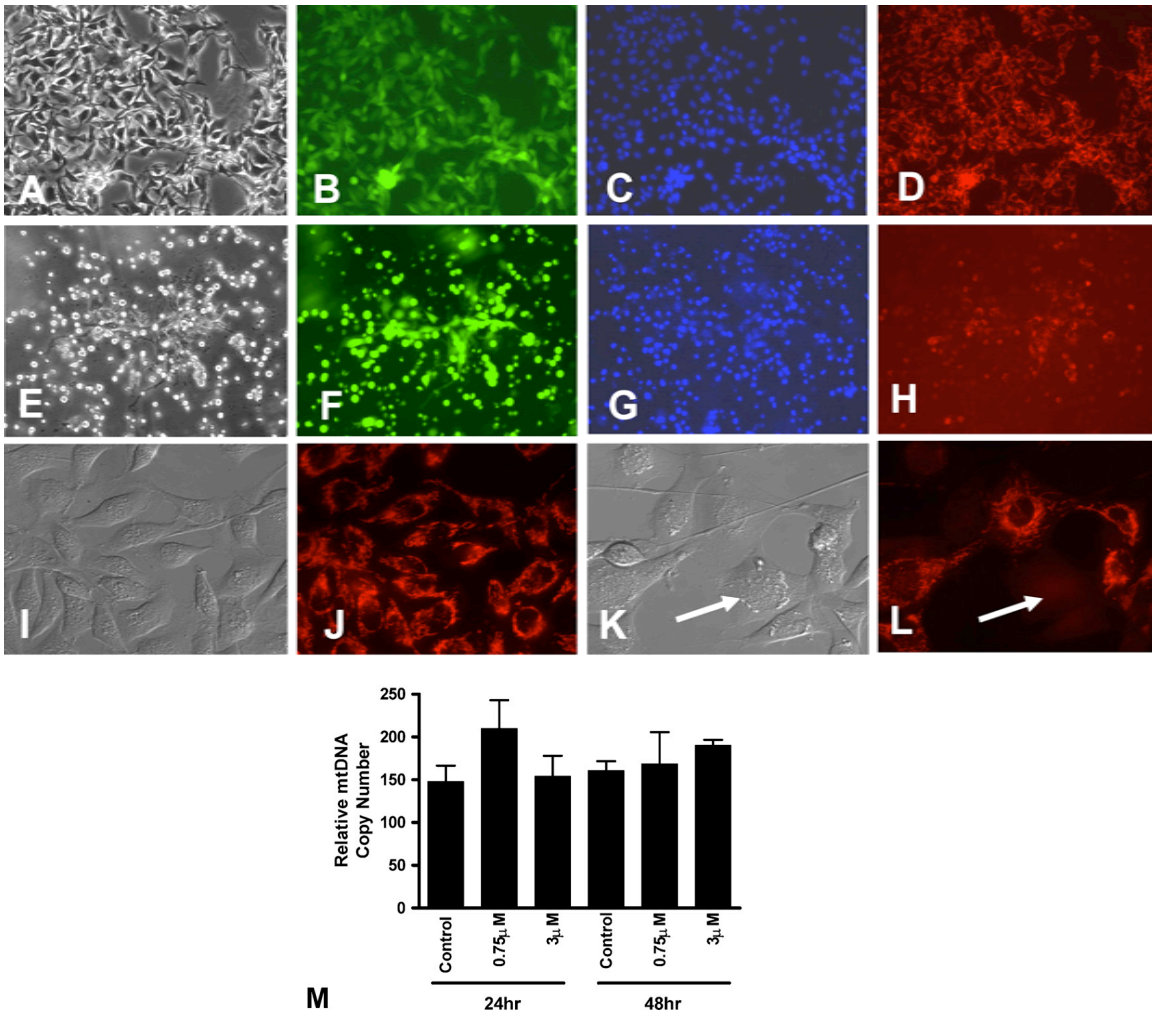

Fig.57 - Vital imaging of K1735-M2 cells treated with SANG. Cells were incubated with TMRM (100 nM), Hoechst 33342 (1 mg) and calcein-AM (300 nM) for 30 min at 37 8C. Panels A–D: Control cells treated for 24 h with the vehicle DMSO ((A) phase contrast, (B) calcein-AM, (C) Hoechst, (D) TMRM). Panels E–H: Cells treated with 8 mM SANG for 24 h ((A) phase contrast, (B) calcein-AM, (C) Hoechst, (D) TMRM). Panels I and J: Control cells treated for 24 h with the vehicle ((I) 600T DIC, (J) TMRM). Panels K and L: Cells treated with 4 mM SAN for 24 h. Notice the cell with the white arrow which although showing normal morphology, has no mitochondrial TMRM accumulation. Panel M: Quantification of mitochondrial DNA copy number by RTPCR as described in Section 2.

4.2.3.2.2.4. Sanguinarine-induced mitochondrial depolarization is not associated with oxidative stress

In order to evaluate whether cells with depolarized mitochondria have increased oxidative stress, co-labelling of 4 mM SANG-treated cells with TMRM and the redoxsensitive probe CM-H2DCFDA was performed after 6 and 24 hours of treatment (Fig. 58).

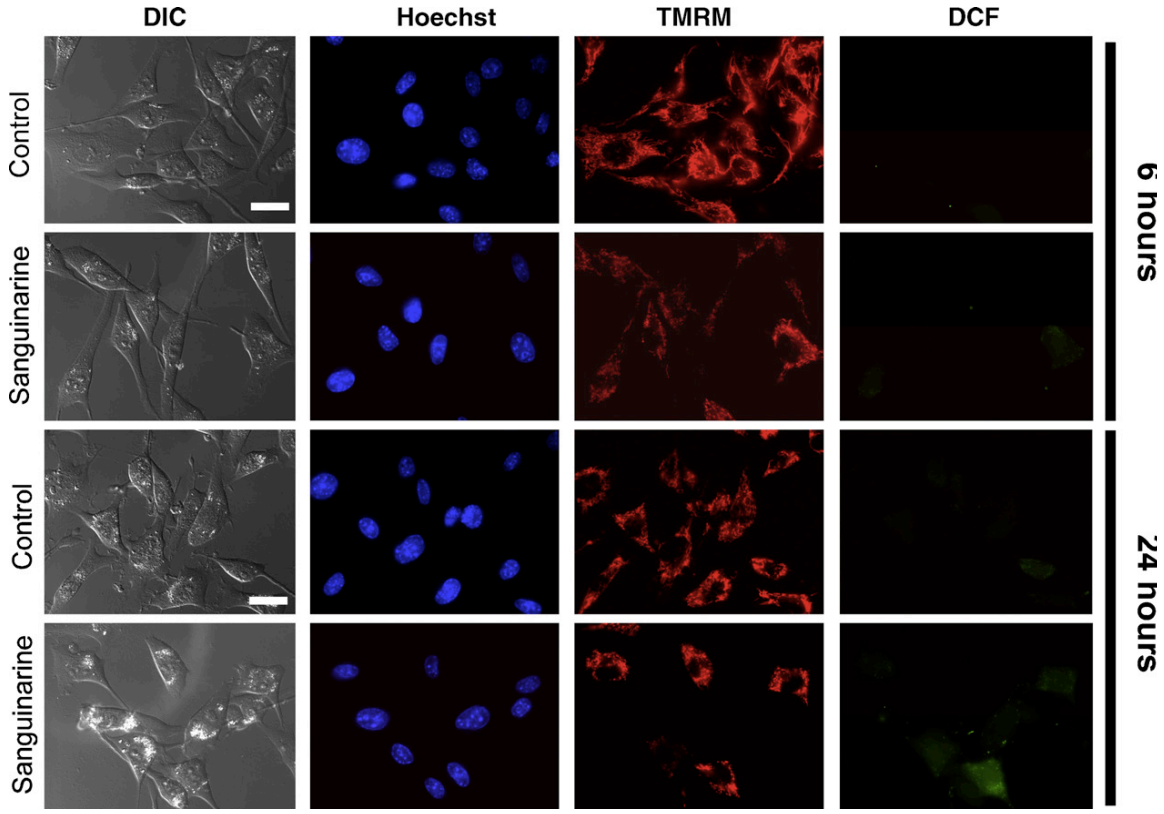

Fig.58 – SANG causes mitochondrial depolarization but does not generate free radicals when incubated with K1735-M2 cells. Cells were incubated with 4 mM SANG for 6 or 24 h. 45 min before the end of the incubation period, the fluorescent probes TMRM (red, mitochondria), Hoechst (blue, nuclei) and CM-H2DCFDA (green, oxidative stress) were added to the cell suspension and cells were imaged with a Nikon Eclipse 3000 epifluorescence microscope. Notice that a sub-set of cells still have polarized mitochondria after 24 h of incubation (last row, TMRM column), although no intracellular oxidative stress is evident.

As described above, SANG shows a clear time-dependent effect on mitochondria, with a general mild depolarization observed after 6 hours and an "all-or-nothing" effect for 24 hours. In the two time-points studied, no increase in cell fluorescence due to oxidative stress was observed, showing no direct correlation between mitochondrial depolarization and oxidative stress. The same protocol confirmed that berberine, an alkaloid similar to SANG caused an increase in cell oxidative stress (Pereira et al, 2007).

4.2.3.2.2.5. Sanguinarine does not cause significant effects on the K1735-M2 cycle

It has been described that SANG arrests the cell cycle of several cancer cell lines (Malikova et al, 2006; Lee et al, 2008) but no information was available regarding melanoma, with the exception of a single study (Kemeny-Beke et al, 2006). Fig. 59 describes the data obtained by evaluating cell cycle alterations induced by SANG on K1735-M2 cells. The most noticeable result is an increase in the sub-G1 peak in a dose and time-dependent manner. Although for 24 h of incubation time no significant differences are found, an increase in sub- G1 peaks occurs for 48 and 72 h. As consequence, the number of cells in G1, S or G2 phases of the cell cycle decrease accordingly, which is more severe for the highest SANG concentration used and for higher exposure times. Of particular interest is the decrease of cells in S phase observed for 24 h for all SANG concentrations tested and the decrease in the number of cells in G1 phase observed for 72 h.

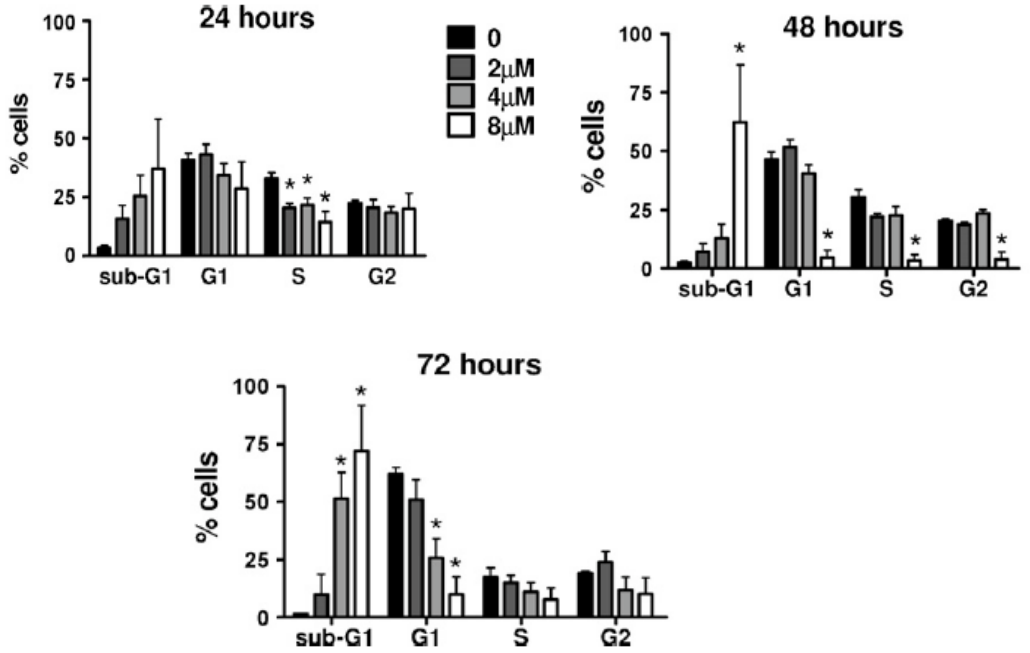

Fig.59 – Effect of SANG on K1735-M2 cell cycle and sub-G1 phases. Nuclear binding of propidium iodide was used to determine cell cycle phase. Cells were incubated with SANG for 24, 48 and 72 h, as described in Section 2. Results are represented as % total cells. Data are means W S.E.M. of three independent experiments. *p < 0.05 vs. control for the same time point.

4.2.3.2.2.6. Sanguinarine activates caspase 3 and 9

By using a colorimetric method, an increase in caspase-like activity was investigated in extracts from cells treated with SANG for 6 and 24 hours. The data in Figure 60 shows that for 6 hours of treatment, 4 μM SANG causes an increase for caspase 3 and 9-like activity. Treatment of cells with 8 μM resulted into a large increase of caspase 3-like activity, although a clear loss of cell mass was determined. For 24 hours incubation, no significant alteration of caspase 9 activity was observed for the concentrations tested while 4 μM SANG resulted into an increase of caspase 3-like activity.

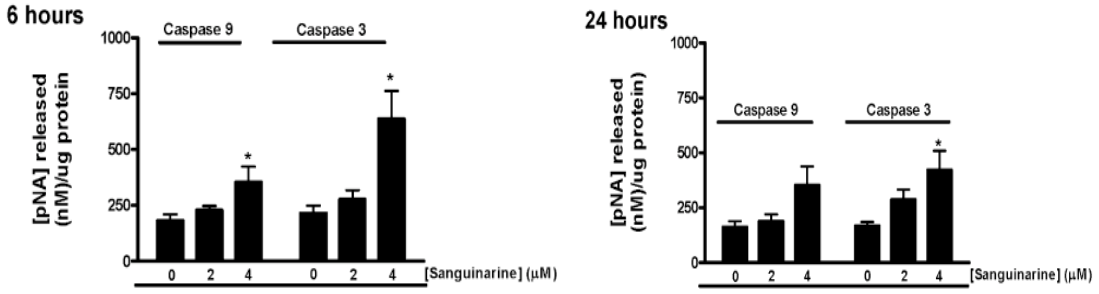

Fig.60 – Caspase 3 and 9-like activity in K1735-M2 cells treated with SANG. Cells were treated as described in Section 2 with SANG for 6 and 24 h. For higher SANG concentrations, it was not possible to obtain enough protein to conduct all experiments. Data are means W S.E.M. of five independent experiments. *p < 0.05 vs. control for the same time point.

4.2.3.2.2.7. Role of Bax and p53 on Sanguinarine-induced Cytotoxicity

For the data obtained regarding SANG-induced mitochondrial depolarization, one possible explanation would be that SANG causes DNA damage, which is followed by p53 activation and increased Bax expression. By its turn, Bax is recognized to induce mitochondrial dysfunction upon apoptotic stimuli (James et al, 2007). By performing Western Blotting on total cell extracts, an increase in the protein p53 was indeed found (Fig. 61A). The density of the band increased in a dose-dependent manner but had no correspondence in an increase in Bax or APAF-1 concentration in the same samples. When analyzing mitochondrial fractions obtained from the same cells, the same trend of results was found, meaning that increased mitochondrial p53 but not Bax translocation occurs (Fig. 61B). The lack of Bax up-regulation in the mechanism of SANG-induced cytotoxicity was confirmed by performing sulforhodamine B assays with two

compounds that are supposed to inhibit the mitochondrial role of Bax on the induction of cell death. The two compounds used were Bax-inhibiting peptide V5 and Bax-channel blocker (Yoshida et al, 2004; Bombrun et al, 2003).

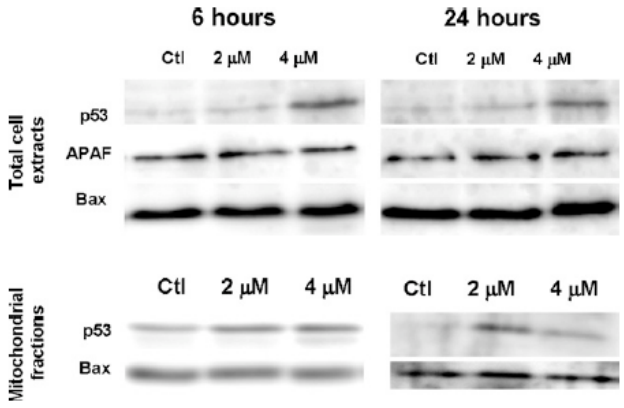

Fig.61 – Detection by Western blotting of p53, Bax, APAF-1 in total fractions and p53 and Bax in mitochondrial extracts from K1735-M2 cells. Equal protein loading in each lane was confirmed by Ponceau labelling. Cells were incubated with 2 and 4 mM SANG for 6 and 24 h and total extracts and mitochondrial fractions were collected as described. The results are representative of 3–5 separate experiments.

4.2.3.2.2.8. Does DNA Damage Correlate With Mitochondrial Depolarization Induced by Sanguinarine?

To test whether SANG resulted in nuclear DNA damage, SANG and control cells were labelled with an antibody to phosphorylated histone H2AX (H2AXγ), which is a recognized marker for DNA damage (Kao et al, 2006). An increase in nuclear fluorescence in the SANG-treated group was readily observed by immunofluorescence (Fig. 62 upper panel and lower panel, left graph). Cells were double-labelled with MitoTracker Red and the level of nuclear fluorescence of H2AXγ was measured in cells with polarized vs. cells with depolarized mitochondria. As seen in Fig. 62, lower panel, right graph, cells with low mitochondrial polarization possessed higher levels of nuclear H2AXγ labelling, demonstrating a relation of both events. It is worth mentioning that vital imaging with TMRM resulted into an all-or-nothing effect while using MitoTracker Red with fixed cells always resulted in cells with low basal fluorescence vs. cells with high, mitochondrial-derived, fluorescence.

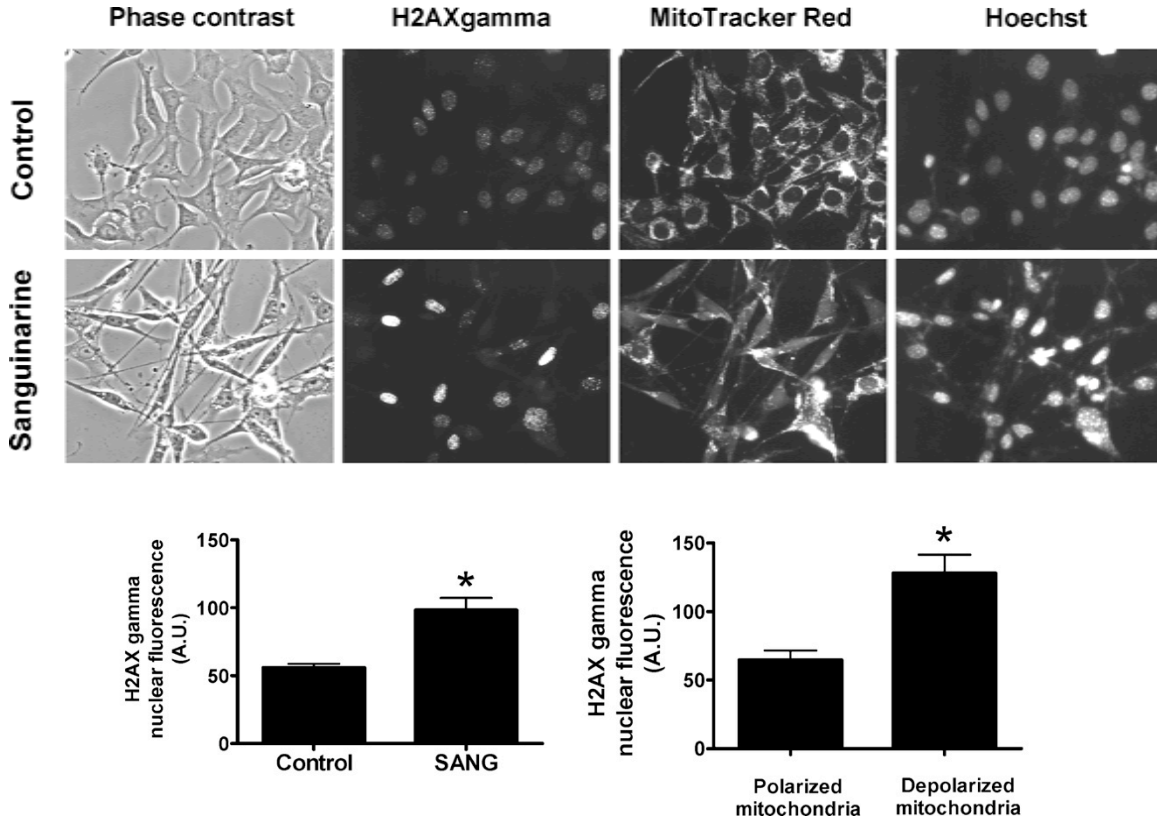

Fig.62 – Relationship between SANG-induced mitochondrial depolarization and H2AXγ. Upper panel, epifluorescence microscopy of control and SANG-treated (2 mM SANG for 16 h) K1735-M2 cells. The panels represent phase contrast, MitoTracker Red and nuclear H2AXγ and Hoechst labelling. Lower panel, left graph, quantification of nuclear H2AXγ fluorescence in control and SANG-treated cells. Lower panel, right graph, quantification of nuclear H2AXγ fluorescence in cells with polarized vs. cells with depolarized mitochondria. The latter group included cells without specific mitochondrial MitoTracker Red labelling. Data are means W S.E.M., of multiple independent experiments. *$p < 0.05$ vs. other experimental group.

4.2.3.2.3. Discussion

Several plant extracts containing sanguinarine (SANG) as their active compound have been used in traditional Chinese and North American traditional medicine for centuries due to their wide range of pharmacological effects (Mitscher et al, 1987). A search in the literature clearly indicates that traditional medicine is growing in interest due to the discovery of novel applications or to the knowledge of the mechanisms behind the known effects. One particular case is the alkaloid berberine that was recently discovered by us to be a mitochondrially-targeted alkaloid, inducing an arrest of proliferation in a murine melanoma cell line (Pereira et al, 2007; Serafim et al, 2008). For the present study, we investigated whether SANG, an alkaloid similar to berberine, could also be cytotoxic for the same melanoma cell line.

The K1735 cell line is a very invasive melanoma cell line and is considered a good model for metastatic melanoma (Repesh et al, 1993; Repesh et al, 1989).

In the present work, we demonstrate that SANG inhibits cell proliferation by causing cell death and an arrest of proliferation of K1375-M2 cells. Another published work demonstrated that SANG causes G1 arrest in vascular smooth muscle cells (Lee et al, 2008) and a disruption of nucleocytoplasmic trafficking of cyclin D1 in breast cancer MCF-7 cells (Holy et al, 2006). In the present research, some significant alterations in the cell cycle were observed for the concentrations tested, with an increase in the number of cells in G2 for 24 hours and a decrease in the number of cells in the number of cells in the G1 phase for 72 hours (Fig. 59).

The data obtained also indicates that SANG kills K1735-M2 cells by apoptosis, as measured by caspase activation. The results also confirms that SANG is highly effective in killing the invasive K1735-M2 cell line since it is effective below 10 mM.

Interestingly, when FCCP was pre-incubated with K1735-M2 cells, the cytotoxicity of SANG was increased for one of the concentrations tested. The result may indicate that for that precise concentration, SANG and FCCP may act in different targets. Another interesting hypothesis is that the decrease in the levels of ATP caused by FCCP, as described previously (Pereira et al, 2007), would increase the cytotoxicity of SANG by inhibiting the activity of the multi-resistance drug protein responsible for the efflux of chemotherapeutic agents (Shukla et al, 2008).

As previously described for MCF-7 cells (Holy et al, 2006), SANG is accumulated by the nuclei of K1735-M2 cells (Fig. 56). Using confocal microscopy and using SANG self-fluorescence, a larger nuclear to mitochondrial ratio of SANG accumulation was detected, this despite the similarity in structure with berberine, an alkaloid that is accumulated by polarized mitochondria (Pereira et al, 2007). One possible explanation for the differential accumulation may be that the positive moiety in SANG is less polar due to the existence of a methyl group linked with the nitrogen atom. By using flow cytometry, a direct relationship between drug concentration and cell fluorescence was obtained, indicating that SANG is accumulated by cells most likely by passive diffusion. No plateau in cell fluorescence was obtained even for concentrations of SANG that were much higher than the ones used in the present study. Although not measured in the present study, Holy et al. (2006) demonstrated that nuclear accumulation of SANG

decreases after a few hours, which may suggest localization to other intracellular targets as mitochondria, although further studies are needed to assess if SANG can exist in other extra-nuclear organelles in a non-fluorescent form.

SANG was found to cause the rounding up of cells and chromatin condensation, which are typical signs of apoptosis (Hall, P., 1999). Another interesting finding was that SANG causes a mixed effect on mitochondrial polarization (Fig. 57L). A complete lack of TMRM signalling was found inside some living cells, in contrast with other cells in the same field of view, which showed clear, although weaker than control, TMRM labelling. An association between mitochondrial depolarization and increased oxidative stress was not found for 6 and 24 hours (Fig. 58).

An attractive possibility is that mitochondrial depolarization could be associated with nuclear DNA damage, already identified in other tumour cell lines (Matkar et al, 2008; Ansari et al, 2005). DNA damage can lead to the activation of p53 (Meulmeester et al, 2008), which would lead to several biological effects among which the expression of pro-apoptotic proteins such as Bax and APAF-1 (Meulmeester et al, 2008). Both Bax and p53 can be translocated to mitochondria, with Bax forming channels in the outer mitochondrial membrane through where pro-apoptotic proteins enclosed in the inter-membrane space can be released. The role of p53 translocation to mitochondria is not as clear. Some researchers have proposed that the mitochondrial translocation of p53 can act to cause cell death or to protect the mitochondrial genome during several aggressions (Moll and Zaika, 2001). Because of this, one initial hypothesis would be that mitochondrial depolarization would be a consequence of Bax and/or p53 translocation to mitochondria.

Western blotting assays demonstrated that SANG induces an increase in p53 concentration in both total cell extracts and mitochondrial fractions, but no Bax upregulation was found in total cells extracts. Nevertheless, it would still be possible that selective accumulation of Bax in mitochondria would occur. However, Western blotting did not indicate that Bax translocation to mitochondria occurred. We also performed Western blotting against APAF, a downstream target of p53 and again, quantitative increases in either whole-cell or mitochondrial preparations were not observed. Although further work is necessary, it is possible that K1735-M2 do not respond to p53-mediated apoptotic stimuli due to mutations on the p53 binding site or

in the protein itself.

The true purpose of the present work was to identify the mechanisms of cell death induced by SANG. The results here shown demonstrate that SANG causes apoptosis for micramolar concentrations on an invasive metastatic melanoma cell line, which involves caspase 9 and 3 activation. The data indicates that in opposition to other tumour cell lines (Adhami et al, 2003; Nithipongvanitch et al, 2007), SANG does not increase Bax levels in K1735-M2 melanoma cells. A similar result was obtained in human CEM T-leukemia cells (Kaminskyy et al, 2008). The interesting result was that the absence of Bax over-expression occurred with an increase of p53 protein. Matkar et al. (2008) demonstrated that SANG-induced death in human colon cancer cells was p53-independent, although DNA damage was detected in K1735-M2 cells.

The results suggest that direct effects of the drug on the organelle after initial nuclear effects can account for mitochondrial dysfunction and lead cells to die upon caspase activation despite the fact that the p53-Bax pathway is not operating. The data presented suggest that SANG acts as a DNA damaging agent, showing also collateral damage to mitochondrial bioenergetics, in a fashion similar to doxorubicin, a powerful anticancer agent which acts both at the mitochondrial and nuclear level (Weerasinghe et al, 2001). SANG should be considered as a potential novel chemotherapeutic for the treatment of aggressive melanoma, with further tests required to identify potential advantages of combinations with other molecules.

V –Conclusion

5. Conclusion

Cancer is not a single disease, hence it cannot be beaten with a single therapy. Part of this is due to the genetic plasticity of tumor cell populations. Instead, different therapeutic approaches, genetic and/or epigenetic actions, as different fronts of battle, may reduce the death rates from various types of cancer.

In the present thesis, after briefly characterization of mitochondrial state in a panel of breast cancer cells, we have tested groups of molecules with potential activity to disrupt mitochondria of tumor cells. Our strategy passed through using different molecules such as phenolic acids (caffeic and ferulic acids derivatives), triterpenoids derivatives and benzophenanthrine alkaloids (berberine and sanguinarine).

From our findings, we concluded that caffeic and ferulic acids enhanced their activity towards breast cancer cells after increasing their lipophilicity, however, with no relevant direct effects on mitochondria. Interestingly was the unexpected and never before reported was that FA induces the mitochondrial permeability transition. Moreover, the new triterpenoids derivatives show to have a more potent action on mitochondrial structure and physiology, seen by the loss of membrane potential and induction of MPT pore. Consequently, these molecules, at lower dose, lead to a G0/G1 cell cycle arrest and consequent inhibition of cell proliferation. At higher concentrations, a decrease of cell number occurs, suggesting that breast cancer cells were dying (Fig.63)

On the other hand, berberine shows to have different mechanisms of action towards melanoma cell lines, where we emphasize the fact that berberine is preferentially accumulated in mitochondria at lower doses, such as 25μM, exerting a very relevant toxicity. Such preferential accumulation is conferred by the positive moiety, leading to a possible reduction of ATP and to a G0/G1 cell cycle arrest. At higher concentrations, 100μM, another pattern is observed, with berberine mostly located in cytoplasm and nucleus. At this concentration G2 cell cycle block is observed, due to a possible interference with DNA synthesis. Therefore, berberine shows to have a cytostatic effect towards melanoma cells and possibly by two distinct mechanisms, dependent on the concentration (Fig.63).

By it turn, sanguinarine is able to induce apoptosis of melanoma cells at much lower concentrations. Sanguinarine promotes apoptosis through p53, with activation of

caspase-3 and -9, although no increased Bax were detected. The mechanism of action of sanguinarine seems to initiate as nuclear DNA damage, followed by mitochondrial depolarization, which occurs downstream (Fig.63).

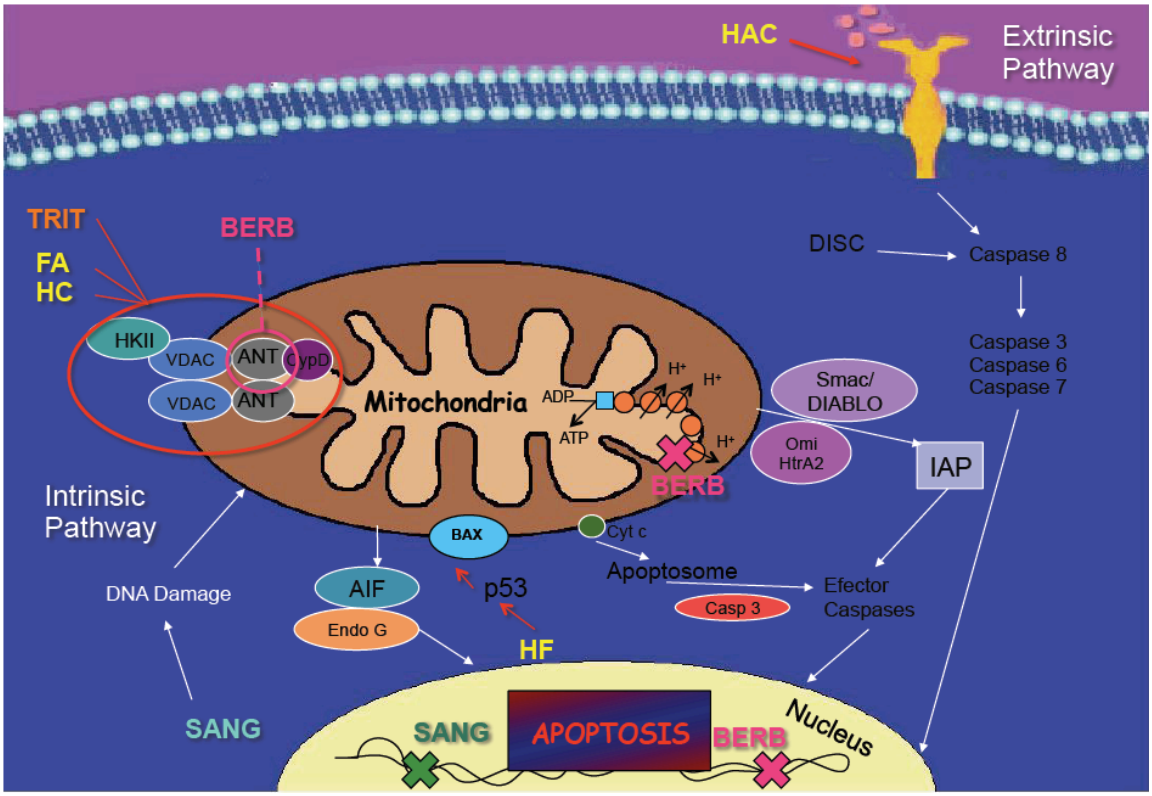

Fig.63 – Preferential intracellular targets of test compounds: Among phenolic compounds studied (yellow), ferulic acid (FA) as well as hexyl caffeate (HC) induced the MPT pore, the hexyl ferulate (HF) seems to induce apoptosis through p53-Bax axis, while caffeoylhexylamide (HCA) seems to induce extrinsic pathway. The triterpenoids (orange) also have a direct effect on MPT pore. Berberine (pink) has dual effect. For the lowest concentrations, accumulates in mitochondria and inhibits mitochondrial complex I, whereas for higher concentrations, nuclear accumulation is observed, which may result in DNA intercalation. Sanguinarine (green) targets primarily the nucleus, resulting in DNA damage and acting mitochondria downstream of the nuclear effect.

Overall, the studied molecules can be considered as potential models for the design of new potential drugs with defined mechanisms of action that target mitochondria in the tumor cells. Crossing these mechanisms of action of novel mitocans, with personalized information on the type of mitochondrial alterations existing in a certain type of tumor and how these alterations can be a target, will no doubt be a major breakthrough in oncology.

References

References

Acharya, B.R., Choudhury, D., et al., (2009). Vitamin K3 disrupts the microtubule networks by binding to tubulin: a novel mechanism of its antiproliferative activity. Biochemistry 48 (29), 6963–6974;

Adhami VM, Aziz MH, Mukhtar H, Ahmad N. (2003) Activation of prodeath Bcl-2 family proteins and mitochondrial apoptosis pathway by sanguinarine in immortalized human HaCaT keratinocytes. Clin Cancer Res; 9:3176-82;

Aggarwal and Shishodia. (2006) Molecular targets of dietary agents for prevention and therapy of cancer. Biochem Pharmacol vol. 71 (10) pp. 1397-421;

Alakurtti, S., Makela T., Koskimies S., Yli-Kauhaluoma J. (2006) Pharmacological properties of the ubiquitous natural product betulin. Eur J Pharm Sci vol. 29 (1) pp. 1-13;

Alao, J. P., Lam, E. W., Ali, S., Buluwela, L., Bordogna, W., Lockey, P., Varshochi, R., Stavropoulou, A. V., Coombes, R. C. and Vigushin, D. M. (2004) Histone deacetylase inhibitor trichostatin A represses estrogen receptor alpha-dependent transcription and promotes proteasomal degradation of cyclin D1 in human breast carcinoma cell lines. Clin. Cancer Res. 10, 8094-8104;

Al-Hajj, M., Wicha, M.S., Benito-Hernandez, A., Morrison, S.J., and Clarke, M.F. (2003). Prospective identification of tumorigenic breast cancer cells. Proc. Natl. Acad. Sci. USA 100, 3983–3988;

Alirol and Martinou. (2006) Mitochondria and cancer: is there a morphological connection?. Oncogene vol. 25 (34) pp. 4706-4716;

Allen CM. (1999) Viadent-related leukoplakia--the tip of the iceberg? Oral Surg Oral Med Oral Pathol Oral Radiol Endod;87:393-4;

Amenta PS, Briggs K, Xu K, Gamboa E (2000) Type XV collagen in human colonic adenocarcinomas has a different distribution than other basement membrane zone proteins. Hum Pathol. Mar;31(3):359-66;

Anderson KM, Stoner GD, Fields HW, Chacon GE, Dohar AL, Gregg BR, et al. (2005) Immunohistochemical assessment of Viadent-associated leukoplakia. Oral Oncol. 41:200-7.

Ansari KM, Dhawan A, Khanna SK, Das M. (2005) In vivo DNA damaging potential of sanguinarine alkaloid, isolated from argemone oil, using alkaline Comet assay in mice. Food Chem Toxicol;43:147-53;

Armstrong, J. (2007) Mitochondrial Medicine: Pharmacological targeting of mitochondria in disease. British Journal of Pharmacology vol. 151 (8) pp. 1154-1165;

Arnold, J., Huggard, P., Cummings, M., Ramm, G., and Chenevix-Trench, G. (2005) Reduced expression of chemokine (C-C motif) ligand-2 (CCL2) in ovarian adenocarcinoma. Br J Cancer vol. 92 (11) pp. 2024-2031;

Baker K. (1993) Mouthrinses in the prevention and treatment of periodontal disease. Curr Opin Periodontol:89-96;

Balanyk TE. (1990) Sanguinarine: comparisons of antiplaque/antigingivitis reports. Clin Prev Dent;12:18-25;

Barbara G. Heerdt, Heidi K. Halsey, Martin Lipkin, et al. (1990) Colonic Cancer Colonic Cell Differentiation, Transformation, and Risk for Oxidase in Human Expression of Mitochondrial Cytochrome c. Cancer Res. 50:1596-1600;

Barreto MC, Pinto RE, Arrabaca JD, Pavao ML (2003) Inhibition of mouse liver respiration by Chelidonium majus isoquinoline alkaloids. Toxicol Lett 146:37–47;

Belzacq, A., Hamel, C., Vieira, H., Cohen, I., et al. (2001) Adenine nucleotide translocator mediates the mitochondrial membrane permeabilization induced by lonidamine, arsenite and CD437. Oncogene. vol. 20 (52) pp. 7579-87;

Berlin G, Enerback L (1983) Fluorescent berberine binding as a marker of secretory activity in mast cells. Int Arch Allergy Appl Immunol 71:332–339;

Berridge, M, Herst, P., Tan, A. (2010) Metabolic flexibility and cell hierarchy in metastatic cancer. Mitochondrion. pp. 1-5;

Biasutto, L., Mattarei, A., Maotta, E., Bradaschia, A., et al. (2008) Development of mitochondriatargeted derivatives of resveratrol. Bioorg Med. Chem. Lett. 18, 5594–5597;

Biasutto, L., Dong, L., Zoratti, M., Neuzil, J. (2010) Mitochondrially targeted anti-cancer agents. Mitochondrion. vol. 10 (6) pp. 670-681;

Bombrun A, Gerber P, Casi G, Terradillos O, Antonsson B, Halazy S. (2003) 3,6-dibromocarbazole piperazine derivatives of 2-propanol as first inhibitors of cytochrome c release via Bax channel modulation. J Med Chem; 46:4365-8;

Borodina VM, Zelenin AV (1977) Fluorescence microscopy demonstration of mitochondria in tissue culture cells using berberine. Tsitologiia 19:1067–1068;

Bose, S., Chandran, S., Mirocha, J., Bose, N. (2006) The Akt pathway in human breast cancer: a tissue-array-based analysis. Mod Pathol vol. 19 (2) pp. 238-245;

Boutros and Almasan. (2009) Combining 2-deoxy-D-glucose with electron transport chain blockers: a double-edged sword. Cancer Biol Ther vol. 8 (13) pp. 1237-8;

Brandon et al. (2006) Mitochondrial mutations in cancer. Oncogene vol. 25 (34) pp. 4647-4662;

Bravo, L. (1998) Polyphenols: chemistry, dietary sources, metabolism, and nutritional significance. *Nutr. Rev. 56*, 317-333;

Broekemeier, K. M., Dempsey, M. E. and Pfeiffer, D. R. (1989) Cyclosporin A is a potent inhibitor of the inner membrane permeability transition in liver mitochondria. J. Biol. Chem. 264, 7826-7830;

Brooks C, Cho SG, Wang CY, Yang T, Dong Z. (2011) Fragmented mitochondria are sensitized to Bax insertion and activation during apoptosis. Am J Physiol Cell Physiol. 300:C447-C455;

Bunz F, Dutriaux A, Lengauer C, Waldman T, Zhou S, Brown JP, Sedivy FM, Kinzler KW, Vogelstein B (1998) Requirement for p53 and p21 to sustain G2 arrest after DNA damage. Science 282:1497–1501;

Cabibi, D., Martorana, A., Cappello, F., Barresi, E., Di Gangi, C., Rodolico, V. (2006) Carcinosarcoma of monoclonal origin arising in a dermoid cyst of ovary: a case report. BMC Cancer. vol. 6 (1) pp. 47;

Cadd, V., Hogg, P., Harris, a., Feller, S. (2006) Molecular profiling of signalling proteins for effects induced by the anti-cancer compound GSAO with 400 antibodies. BMC Cancer. vol. 6 (1) pp. 155;

Cannino, G., Ferruggia, E., Luparello, C., Rinaldi, A. (2008) Effects of cadmium chloride on some mitochondria-related activity and gene expression of human MDA-MB231 breast tumor cells. J Inorg Biochem vol. 102 (8) pp. 1668-76;

Canter, J. A., Kallianpur, A. R., Parl, F. F. & Millikan, R. C. (2005) Mitochondrial DNA G10398A polymorphism and invasive breast cancer in African-American women. Cancer Res. 65, 8028–8033;

Castedo M, Perfettini JL, Roumier T, Andreau K, Medema R, Kroemer G. (2004) Cell death by mitotic catastrophe: a molecular definition. Oncogene 23: 2825–2837;

Cereghetti and Scorrano. (2006) The many shapes of mitochondrial death. Oncogene vol. 25 (34) pp. 4717-4724;

Chance, B., Williams, G. R. and Hollunger, G. (1963) Inhibition of electron and energy transfer in mitochondria. III. Spectroscopic and respiratory effects of uncoupling agents. *J. Biol. Chem. 238*, 439-444;

Chen LB (1988). Mitochondrial membrane potential in living cells. Annu Rev Cell Biol 4: 155–181;

Chen CM, Chang HC (1995) Determination of berberine in plasma, urine and bile by high-performance liquid chromatography. J Chromatogr B 665:117–123;

Chen JQ, Yager JD. (2004) Estrogen's effects on mitochondrial gene expression: mechanisms and potential contributions to estrogen carcinogenesis. Ann N Y Acad Sci. 1028:258-72;

Chen, J., Cammarata, P., Baines, C., Yager, J. (2009) Regulation of mitochondrial respiratory chain biogenesis by estrogens/estrogen receptors and physiological, pathological and pharmacological implications. BBA - Molecular Cell Research vol. 1793 (10) pp. 1540-1570;

Chen, Z., Zhang, H., Lu, W., Huang, P. (2009) Role of mitochondria-associated hexokinase II in cancer cell death induced by 3-bromopyruvate. Biochimica et Biophysica Acta (BBA) - Bioenergetics vol. 1787 (5) pp. 553-560;

Chen, G., Wang, F., Trachootham, D., Huang, P. (2010) Preferential killing of cancer cells with mitochondrial dysfunction by natural compounds. MITOCH pp. 1-12;

Coimbra, M., Isacchi, B., van Bloois, L., Torano, J. S., Ket, A., Wu, X., Broere, F., Metselaar, J. M., Rijcken, C. J., Storm, G., Bilia, R. and Schiffelers, R. M. (2011) Improving solubility and chemical stability of natural compounds for medicinal use by incorporation into liposomes. *Int. J. Pharm*. [Epub ahead of print];

Cory, S., Huang, D., Adams, J. (2003) The Bcl-2 family: roles in cell survival and oncogenesis. Oncogene. vol. 22 (53) pp. 8590-8607;

Costantini, P., Jactot E., Decaudin D., Kroemer, G. (2000) Mitochondrion as a novel target of anticancer chemotherapy. J Natl Cancer Inst vol. 92 (13) pp. 1042-53;

Crozier, A., Jaganath, I. B. and Clifford, M. N. (2009) Dietary phenolics: chemistry, bioavailability and effects on health. *Nat. Prod. Rep. 26*, 1001-1043;

Cuezva, J., Krajewska, M., de Heredia, M., Krajewski, S, et al. (2002) The bioenergetic signature of cancer: a marker of tumor progression. Cancer Research. vol. 62 (22) pp. 6674-81;

Curini M, Epifano F, Genovese S, Marcotullio MC, Menghini L. (2006) 3-(4'-geranyloxy-3'-methoxyphenyl)-2-trans propenoic acid: a novel promising cancer chemopreventive agent. Anticancer Agents Med Chem; 6 : 571-577;

Curtis SK, Cowden RR (1981) Four fluorochromes for the demonstration and microfluoreometric estimation of RNA. Histochemistry 72:39–48;

Czuba, Z., Krol, W., Scheller, S. and Shani, J. (1992) Effect of cinnamic and acrylic acids' derivatives on luminol-enhanced chemiluminescence of neutrophils. *Z. Naturforsch. C 47*, 753-756.;

Dang, CV. (2010) Glutaminolysis: supplying carbon or nitrogen or both for cancer cells? Cell Cycle. 9(19):3884-6;

Debatin, K., Poncet, D., Kroemer, G. (2002) Chemotherapy: targeting the mitochondrial cell death pathway. Oncogene vol. 21 (57) pp. 8786-803;

Decaudin, D., Marzo, I., Brenner, C., Kroemer, G. (1998) Mitochondria in chemotherapy-induced apoptosis: A prospective novel target of cancer therapy (review). Int J Oncol; 12: 141–152;

Delmas D, Rebe C, Micheau O, Athias A, Gambert P, Grazide S et al. (2004). Redistribution of CD95, DR4 and DR5 in rafts accounts for the synergistic toxicity of resveratrol and death receptor ligands in colon carcinoma cells. Oncogene 23: 8979–8986;

Demaria, S., Pikarsky, E., Karin, M., Coussens, L., Chen, Y., et al. (2010) Cancer and Inflammation: Promise for Biologic Therapy. Journal of Immunotherapy. vol. 33 (4) pp. 335-351;

Deng YT, Huang HC, Lin JK. (2010) Rotenone induces apoptosis in MCF-7 human breast cancer cell-mediated ROS through JNK and p38 signaling. Mol Carcinog. 49(2):141-51;

Devasena T, Rajsekaran KN, Gunasekaran G, Viswanathan P, Menon VP. (2003) Anticarcinogenic effect of bis-1,7-(2-hydroxyphenyl)-hepta-1,6-diene-3,5-dione a curcumin analog on DMH-induced colon cancer model. Pharmacol Res. 47: 133-140;

Di Monte, D., Ross, D., et al., (1984). Alterations in intracellular thiol homeostasis during the

metabolism of menadione by isolated rat hepatocytes. Arch. Biochem. Biophys. 235 (2), 334–342;

Dias and Bailly. (2005) Drugs targeting mitochondrial functions to control tumor cell growth. Biochem Pharmacol. vol. 70 (1) pp. 1-12;

Diaz, F., Bayona-Bafaluy, et al (2002). Human mitochondrial DNA with large deletions repopulates organelles faster that full-length genomes under relaxed copy number control. Nucl. Acid. Res. 30(21): 4626-4633;

Diehn, M., Cho, R., Lobo, N., Kalisky, T., Dorie, M., Kulp, A., Qian, D., Lam, J., et al. (2008) Association of reactive oxygen species levels and radioresistance in cancer stem cells. Nature 458, 780-783;

Dietmar W. Siemann (2011) Tumor Microenvironment. Wiley-Blackwell, first edition. John Wiley & Sons, Ltd.

Dilda, P., Ramsay, E., Corti, A., Pompella, A., Hogg, P. (2008) Metabolism of the Tumor Angiogenesis Inhibitor 4-(N-(S-Glutathionylacetyl)amino)phenylarsonous Acid. Journal of Biological Chemistry. vol. 283 (51) pp. 35428-35434;

Dimlich RV, Meineke HA, Reilly FK, McCuskey RS (1980) The fluorescent staining of heparin in mast cells using berberine sulfate: compatibility with paraformaldehyde or *o*-phthalaldehyde induced fluorescence and metachromasia. Stain Technol 55:217– 223;

Don, A., Kisker, O., Dilda, P., Donoghue, N., Zhao, X., et al. (2003) A peptide trivalent arsenical inhibits tumor angiogenesis by perturbing mitochondrial function in angiogenic endothelial cells. Cancer Cell 3, 497–509;

Don and Hogg. (2004) Mitochondria as cancer drug targets. Trends Mol Med. vol. 10 (8) pp. 372-8;

Dong, L., Swettenham, E., Eliasson, J., Wang, X., Gold, M., Medunic, Y., et al. (2007) Vitamin E analogues inhibit angiogenesis by selective induction of apoptosis in proliferating endothelial cells: the role of oxidative stress. Cancer Res. 67, 11906–11913;

Dong, L.F., Freeman, R., Zobalova, R., Main-Hernandez, A., Stantic, M., Rohlena, J., et al. (2009) Suppression of tumor growth in vivo by themitocan 1001 alpha-tocopheryl succinate requires respiratory complex II. Clin. Cancer Res. 15 (5), 1002 1593–1600;

Doyle, L. A. and Ross, D. D. (2003) Multidrug resistance mediated by the breast cancer resistance protein BCRP (ABCG2). *Oncogene 22*, 7340-7358;

Dromparis, P., Sutendra, G., Michelakis, E. (2010) The role of mitochondria in pulmonary vascular remodeling. J Mol Med. vol. 88 (10) pp. 1003-1010;

Dudkina, N., Kouril, R., Peters, K., Braun, H., Boekema, E. (2010) Structure and function of mitochondrial supercomplexes. BBA – Bioenergetics. vol. 1797 (6-7) pp. 664-670;

Dunyaporn Trachootham, Jerome Alexandre & Peng Huang (2009). Targeting cancer cells by ROS-mediated mechanisms: a radical therapeutic approach? Nature Reviews Drug Discovery 8, 579-591;

Dvorak Z, Vrzal R, Maurel P, Ulrichova J. (2006) Differential effects of selected natural compounds with anti-inflammatory activity on the glucocorticoid receptor and NF-kappaB in HeLa cells. Chem Biol Interact; 159:117-28;

Dworkin, N. (1999) Where have all the Flowers gone?–herbal supplements threaten some herb species. Vegetarian Times Sept;

Dyke SF, Moon BJ, Sainsbury M. (1968) The synthesis of sanguinarine. Tetrahedron Lett; 36:3933-4;

Dykens and Will. (2007) The significance of mitochondrial toxicity testing in drug development. Drug Discov Today. vol. 12 (17-18) pp. 777-85;

Fearon, E. (1997) Human Cancer Syndromes: Clues to the Origin and Nature of Cancer . Science. Vol. 278 (5340) pp. 1043-1050;

Ellerby, H., Arap, W., Ellerby, L., Kain, R., Andrusiak, R., Rio, G., Krajewski, S., et al. (1999) Anti-cancer activity of targeted pro-apoptotic peptides. Nat. Med. 5, 1032–1038;

Elrod and Sun. (2008) Modulation of death receptors by cancer therapeutic agents. Cancer Biol Ther vol. 7 (2) pp. 163-73;

Faddeeva MD, Beliaeva TN. (1988) Inhibition of the activity of membrane-bound Ca2+- ATPase in the sarcoplasmic reticulum fragments of rabbit skeletal muscles by the alkaloid sanguinarine. Tsitologiia; 30:685-90;

Fadok, V., Bratton, D., Rose, D., Pearson, A., Ezekewitz, R., Henson, P. (2000) A receptor for phosphatidylserine-specific clearance of apoptotic cells. Nature 405, 85-90;

Fedorak, R. and Field, M. (1987). Antidiarrheal Therapy Prospects for New Agents. Digestive Diseases and Sciences, Vol. 32, No. 2. pp. 195-205;

Fedotcheva, N. I., Kazakov, R. E., Kondrashova, M. N. and Beloborodova, N. V. (2008) Toxic effects of microbial phenolic acids on the functions of mitochondria. *Toxicol. Lett. 180*, 182-188;

Feichtinger, R., Zimmermann, F., Mayr, J., Neueiter, D., Huser-Kronberger, C., et al. (2010) Low aerobic mitochondrial energy metabolism in poorly- or undifferentiated neuroblastoma. BMC Cancer vol. 10 pp. 149;

Ferreira, LM. (2010). Cancer metabolism: The Warburg effect today. Experimental and Molecular Pathology vol. 89 (3) pp. 372-380;

Filomeni, G., Cardaci, S., Da Costa Ferreira, A., Rotilio, G., Ciriolo, M. (2011) Metabolic oxidative stress elicited by the copper(II) complex [Cu(isaepy)2] triggers apoptosis in SH-SY5Y cells through the induction of AMP-activated protein kinase/p38MAPK/p53 signalling axis Evidence for a combined use with 3-bromopyruvate in neuroblastoma treatment. Biochem J [Epub];

Fiuza, S. M., Gomes, C., Teixeira, L. J., Girao da Cruz, M. T., Cordeiro, M. N., Milhazes, N., Borges, F. and Marques, M. P. (2004) Phenolic acid derivatives with potential anticancer properties--a structure-activity relationship study. Part 1: methyl, propyl and octyl esters of caffeic and gallic acids. *Bioorg. Med. Chem. 12*, 3581-3589;

Frank S, Gaume B, Bergmann-Leitner ES, Leitner WW, Robert EG, Catez F et al. (2001). The role of dynamin-related protein 1, a mediator of mitochondrial fission, in apoptosis. Dev Cell 1: 515–525;

Fresco, P., Borges, F., Diniz, C. and Marques, M. P. (2006) New insights on the anticancer properties of dietary polyphenols. *Med. Res. Rev. 26*, 747-766;

Fresco, P., Borges, F., Marques, M. P. and Diniz, C. (2010) The anticancer properties of dietary polyphenols and its relation with apoptosis. *Curr. Pharm. Des. 16*, 114-134;

Fukuda, R., Zhang, H., Kim, J.W, et al. (2007). HIF-1 regulates cytochrome oxidase subunits to optimize efficiency of respiration in hypoxic cells. Cell 129, 111–122;

Fulda and Debatin. (2005) Sensitization for Anticancer Drug–Induced Apoptosis by Betulinic Acid. NEO. vol. 7 (2) pp. 162-170;

Fulda and Debatin. (2006) Extrinsic versus intrinsic apoptosis pathways in anticancer chemotherapy. Oncogene. vol. 25 (34) pp. 4798-4811;

Fulda, S. (2009) Betulinic acid: A natural product with anticancer activity. Mol. Nutr. Food Res. vol. 53 (1) pp. 140-146;

Fulda and Kroemer. (2009) Targeting mitochondrial apoptosis by betulinic acid in human cancers. Drug Discov Today. vol. 14 (17-18) pp. 885-90;

Fulda, S., Gorman, A., Hori, O., Samali, A. (2010) Cellular Stress Responses: Cell Survival and Cell Death. International Journal of Cell Biology. vol. 2010 pp. 1-23;

Fulda, S., Galluzzi, L., Kroemer, G. (2010b) Targeting mitochondria for cancer therapy. Nature Publishing Group. vol. 9 (6) pp. 447-464;

Galluzzi, L., Maiuri, M., Vitale, I., Zischka, H., Castedo, M., Zivogel, L., Kroemer, G. (2007) Cell death modalities: classification and pathophysiological implications. Cell Death Differ vol. 14 (7) pp. 1237-1243;

Ganguly, A., Yang, H., Cabra, F. (2011) Class III β-Tubulin Counteracts the Ability of Paclitaxel to Inhibit Cell Migration. Oncotarget vol. 2 (5) pp. 368-77;

Gao, S. and Hu, M. (2010) Bioavailability challenges associated with development of anti-cancer phenolics. *Mini. Rev. Med. Chem. 10*, 550-567;

Gatenby and Gawlinski. (2003) The glycolytic phenotype in carcinogenesis and tumor invasion: insights through mathematical models. Cancer Research vol. 63 (14) pp. 3847-54;

Gatenby, R.A., Gillies, R.J., (2007). Glycolysis in cancer: a potential target for therapy. Int. J. Biochem. Cell Biol. 39, 1358–1366;

Gegg ME, Cooper JM, Chau KY, Rojo M, Schapira AH, Taanman JW. (2010) Mitofusin 1 and mitofusin 2 are ubiquitinated in a PINK1/parkin-dependent manner upon induction of mitophagy. Hum. Mol. Genet. 19(24): 4861-4870;

Gemin A, Sweet S, Preston TJ, Singh G (2005) Regulation of the cell cycle in response to inhibition

of mitochondrial generated energy. Biochem Biophys Res Commun 332:1122–1132;

Gerard GM D'Souza & Volkmar Weissig (2009). Subcellular targeting: a new frontier for drug-loaded pharmaceutical nanocarriers and the concept of the magic bullet. Expert Opin Drug Deliv.6(11):1135-48;

Germain M, Mathai JP, McBride HM, Shore GC. (2005). Endoplasmic reticulum BIK initiates DRP1-regulated remodelling of mitochondrial cristae during apoptosis. EMBO J 24: 1546–1556;

Giuliana G, Pizzo G, Milici ME, Musotto GC, Giangreco R. (1997) In vitro antifungal properties of mouthrinses containing antimicrobial agents. J Periodontol; 68:729-33;

Gledhill, J. R., Montgomery, M. G., Leslie, A. G. & Walker, J. E. (2007) Mechanism of inhibition of bovine F1-ATPase by resveratrol and related polyphenols. Proc. Natl Acad. Sci. USA 104, 13632–13637;

Gleiss, B., Gogvadze, V., Orrenius, S., Fadeel, B., (2002). Fas-triggered phosphatidylserine exposure is modulated by intracellular ATP. FEBS Lett. 519, 153–158;

Godowski KC. (1989) Antimicrobial action of sanguinarine. J Clin Dent;1:96-101.

Gogvadze, V., Norberg, E., Orrenius, S., Zhivotovsky, B. (2010) Involvement of Ca2+ and ROS in α-tocopheryl succinate-induced mitochondrial permeabilization. Int. J. Cancer vol. 127 (8) pp. 1823-1832;

Gogvadze, V., Zhivotovsky, B, Orrenius, S. (2010b) The Warburg effect and mitochondrial stability in cancer cells. Molecular Aspects of Medicine vol. 31 (1) pp. 60-74;

Gogvadze, V., Orrenius, S., Zhivotovsky, B. (2008) Mitochondria in cancer cells: what is so special about them? Trends Cell Biol vol. 18 (4) pp. 165-73;

Gong GQ, Zong ZX, Song YM (1999) Spectrofluorometric determination of DNA and RNA with berberine. Spectrochim Acta A Mol Biomol Spectrosc 55A:1903–1907;

Gornall, A. G., Bardawill, C. J. and David, M. M. (1949) Determination of serum proteins by means of the biuret reaction. *J. Biol. Chem. 177*, 751-766;

Gothel, S.F., Marahiel, M.A., (1999). Peptidyl-prolyl cis–trans isomerases, a superfamily of ubiquitous folding catalysts. Cell Mol. Life Sci. 55, 423–436;

Gozuacik and Kimchi. (2004) Autophagy as a cell death and tumor suppressor mechanism. Oncogene vol. 23 (16) pp. 2891-2906;

Green, D.R. and Kroemer, G. (2004). The pathophysiology of mitochondrial cell death. Science 2004; 305: 626-629;

Grycova L, Dostal J, Marek R (2007) Quaternary protoberberine alkaloids. Phytochemistry 68:150–175;

Guchelaar HJ et al. (1997) Apoptosis: Molecular mechanisms and implications for cancer chemotherapy. Pharm World Sci; 19: 119–125;

Gupta, P.B., Chaffer, C.L., and Weinberg, R.A. (2009). Cancer stem cells: mirage or reality? Nat. Med. 15, 1010–1012;

Hahm, E.R., Singh, S.V., (2007). Honokiol causes G0–G1 phase cell cycle arrest in human prostate cancer cells in association with suppression of retinoblastoma protein level/phosphorylation and inhibition of E2F1 transcriptional activity. Mol. Cancer Ther. 6 (10), 2686–2695;

Hajnóczky G, Csordás G, et al. (2006). Mitochodrial calcium signaling and cell death: approaches for assessing the role of mitochondrial Ca^{2+} uptake in apoptosis. Cell Calcium; 40: 553-560;

Halestrap, A. P. (2009) What is the mitochondrial permeability transition pore? *J Mol. Cell. Cardiol. 46*, 821-831;

Hall, P. (1999) Assessing apoptosis: a critical survey. Endocr Relat Cancer; 6:3-8;

Hanahan and Weinberg. (2000) The hallmarks of cancer. Cell. vol. 100 (1) pp. 57-70;

Hanahan and Weinberg. (2011) Hallmarks of Cancer: The Next Generation. Cell vol. 144 (5) pp. 646-674;

He L, Liu GQ (2002) Interaction of multidrug resistance reversal agents with *P*-glycoprotein ATPase activity on blood–brain barrier. Acta Pharmacol Sin 23:423–429;

Helmbach H, Rossmann E, Kern MA, Schadendorf D. (2001) Drug-resistance in human melanoma. Int J Cancer; 93:617-22;

Holley RW, Kiernan JA (1974) Control of the initiation of DNA synthesis in 3T3 cells: low-molecular weight nutrients. Proc Natl Acad Sci USA 71:2942–2945

Holt IJ, Harding AE, Morgan-Hughes JA. (1988) Deletions of muscle mitochondrial DNA in patients with mitochondrial myopathies. *Nature*; 331: 717–719;

Holy, J., Kolomitsyna, O., Krasutsky, D., Oliveira, P., Perkins, E., Krasustsky, P. (2010) Dimethylaminopyridine derivatives of lupane triterpenoids are potent disruptors of mitochondrial structure and function. Bioorganic & Medicinal Chemistry. vol. 18 (16) pp. 6080-6088;

Holy J, Lamont G, Perkins E. (2006) Disruption of nucleocytoplasmic trafficking of cyclin D1 and topoisomerase II by sanguinarine. BMC Cell Biol; 7:13.

Hoshi A, Ikekawa T, Ikeda Y, Shirakawa S, Iigo M (1976) Antitumor activity of berberrubine derivatives. Gann 67:321–325;

Huang L. and Chen C.Ho. (2002) Molecular Targets of Anti-HIV-1 Triterpenes. Volume 2, Number 1. pp. 33-36(4);

Huang, D. W., Shen, S. C. and Wu, J. S. (2009) Effects of caffeic acid and cinnamic acid on glucose uptake in insulin-resistant mouse hepatocytes. *J. Agric. Food Chem. 57*, 7687-7692;

Huang, W. Y., Cai, Y. Z. and Zhang, Y. (2010) Natural phenolic compounds from medicinal herbs and dietary plants: potential use for cancer prevention. *Nutr. Cancer 62*, 1-20;

Huang, P., Galloway, C., Yoon, Y. (2011) Control of Mitochondrial Morphology Through Differential Interactions of Mitochondrial Fusion and Fission Proteins. PLoS ONE vol. 6 (5) pp. e20655;

Huck-Hui Ng & & M. Azim Surani (2011) The transcriptional and signalling networks of pluripotency. *Nature Cell Biology* 13, 490–496;

Hughes, L., Malone, C., Chumsri, S., Burger, A., McDonnell, S. (2008) Characterisation of breast cancer cell lines and establishment of a novel isogenic subclone to study migration, invasion and tumourigenicity. Clin Exp Metastasis. vol. 25 (5) pp. 549-557;

Hwang J-M, Kuo H-C, Tseng T-H, Liu J-Y, Chu C-Y (2006) Berberine induces apoptosis through a mitochondria/caspases pathway in human hepatoma cells. Mol Toxicol 80:62–73;

Inoue K, Kulsum U, Chowdhury SA, Fujisawa S, Ishihara M, Yokoe I, Sakagami H (2005) Tumor-specific cytotoxicity and apoptosisinducing activity of berberines. Anticancer Res 25:4053–4059;

Ivanov VN, Bhoumik A, Ronai Z. (2003) Death receptors and melanoma resistance to apoptosis. Oncogene; 22:3152-61;

Iwasaki and Suda. Cancer stem cells and their niche. Cancer Science (2009) vol. 100 (7) pp. 1166-1172;

James D, Parone PA, Terradillos O, Lucken-Ardjomande S, Montessuit S, Martinou JC. (2007) Mechanisms of mitochondrial outer membrane permeabilization. Novartis Found Symp; 287:170-6; discussion 6-82;

Jang M, Cai L, Udeani GO, Slowing KV, Thomas CF, Beecher CW et al. (1997). Cancer chemopreventive activity of resveratrol, a natural product derived from grapes. Science 275: 218–220;

Jantova S, Cipak L, Letasiova S (2007) Berberine induces apoptosis through a mitochondrial/caspase pathway in human promonocytic U937 cells. Toxicol In Vitro 21:25–31;

Jantova S, Letasiova S, Brezova V, Cipak L, Labaj J (2006) Photochemical and phototoxic activity of berberine on murine Wbroblast NIH-3T3 and Ehrlich ascites carcinoma cells. J Photochem Photobiol B 85:163–176;

Jeong SY, Seol DW. (2008) The role of mitochondria in apoptosis. BMB Rep; 41:11-22;

Jia, L., Yu, W., Wang, P., Sanders, B. G. & Kline, K. (2008) *In vivo* and *in vitro* studies of anticancer actions of α-TEA for human prostate cancer cells. Prostate 68, 849–860;

Jin et al. (2008) Caffeic acid phenethyl ester induces mitochondria-mediated apoptosis in human myeloid leukemia U937 cells. Mol Cell Biochem. vol. 310 (1-2) pp. 43-48;

Jones and Thompson. (2009) Tumor suppressors and cell metabolism: a recipe for cancer growth. Genes & Development. vol. 23 (5) pp. 537-548;

Jones RG, Plas DR, Kubek S, Buzzai M, Mu J, Xu Y, Birnbaum MJ, Thompson CB (2005) AMP-activated protein kinase induces a p53-dependent metabolic checkpoint. Mol Cell 18:283–

293;

Jung, B. I., Kim, M. S., Kim, H. A., Kim, D., Yang, J., Her, S. and Song, Y. S. (2010) Caffeic acid phenethyl ester, a component of beehive propolis, is a novel selective estrogen receptor modulator. Phytother. Res. 24, 295-300;

K. Yasukawa, T. Matsumoto, M. Takeuchi and S. Nakagawa (1991). Sterol and triterpene derivatives from plants inhibit the effects of a tumor promoter, and sitosterol and betulinic acid inhibit tumor formation in mouse skin two-stage carcinogenesis Oncology, 48, 72;

Kaminskyy V, Lin KW, Filyak Y, Stoika R. (2008) Differential effect of sanguinarine, chelerythrine and chelidonine on DNA damage and cell viability in primary mouse spleen cells and mouse leukemic cells. Cell Biol Int; 32:271-7;

Kamo, N., Muratsugu, M., Hongoh, R. and Kobatake, Y. (1979) Membrane potential of mitochondria measured with an electrode sensitive to tetraphenyl phosphonium and relationship between proton electrochemical potential and phosphorylation potential in steady state. *J. Membr. Biol. 49*, 105-121;

Kang, B., Plescia, J., Dohi, T., Rosa, J., Doxsey, S., Altieri, D. (2007) Regulation of tumor cell mitochondrial homeostasis by an organelle-specific Hsp90 chaperone network. Cell. vol. 131 (2) pp. 257-70;

Kao J, Milano MT, Javaheri A, Garofalo MC, Chmura SJ, Weichselbaum RR, et al. (2006) gamma-H2AX as a therapeutic target for improving the efficacy of radiation therapy. Curr Cancer Drug Targets;6:197-205;

Karbowski M, Youle R. (2003) Dynamics of mitochondrial morphology in healthy cells and during apoptosis. Cell Death Diff; 10: 870-880;

Karunagaran D, Joseph J, Kumar TR. (2007) Cell growth regulation. Adv Exp Med Biol.; 595: 245-268;

Katsuhiro Kotake, Toshiaki Nonami, Tsuyoshi Kurokawa, et al. (1999) Human livers with cirrhosis and hepatocellular carcinoma have less mitochondrial DNA deletion than normal human livers. Life Sciences, Vol. 64, No. 19, pp. l785-1791;

Kelloff, G. J. (2000) Perspectives on cancer chemoprevention research and drug development. *Adv. Cancer Res. 78*, 199-334;

Kelso, G., Porteous, C., Coulter, C., Hughes, G., Portous, W., Ledgerwood, E., et al. (2001) Selective targeting of a redox-active ubiquinone to mitochondria within cells: antioxidant and antiapoptotic properties. J. Biol. Chem. 276, 4588–4596;

Kemeny-Beke A, Aradi J, Damjanovich J, Beck Z, Facsko A, Berta A, et al. (2006) Apoptotic response of uveal melanoma cells upon treatment with chelidonine, sanguinarine and chelerythrine. Cancer Lett; 237:67-75;

Kikuzaki H, Hisamoto M, Hirose K, Akiyama K, Taniguchi H. (2002) Antioxidant properties of ferulic acid and its related compounds. J Agric Food Chem. 50: 2161-2168;

Kim, M.M., Clinger, J.D., Masayesva, B.G., Ha, P.K., Zahurak, M.L., Westra, W.H. and Califano,

J.A. (2004) Mitochondrial DNA quantity increases with histopathologic grade in premalignant and malignant head and neck lesions. Clin. Cancer Res., 10, 8512-8515;

Kim, Y.S., Yang, C.T., Wang, J., Wang, L., Li, Z.B., Chen, X., Liu, S.J., (2008). Effects of 654 targeting moiety, linker, bifunctional chelator, and molecular charge on biological 655 properties of 64Cu-labeled triphenylphosphonium cations. Med. Chem. 51 (10), 656 2971–2984;

Kim, M.Y., Trudel, L.J., et al., (2009). Apoptosis induced by capsaicin and resveratrol in colon carcinoma cells requires nitric oxide production and caspase activation. Anticancer Res. 29 (10), 3733–3740;

Kinnally, K., Peixoto, P., Ryu, S., Dejean, L. (2011) Is mPTP the gatekeeper for necrosis, apoptosis, or both? BBA - Molecular Cell Research vol. 1813 (4) pp. 616-622;

Ko, Y.H., Pedersen, P.L., Geschwind, J.F., (2001). Glucose catabolism in the rabbit VX2 tumor model for liver cancer: characterization and targeting hexokinase. Cancer Lett. 173, 83–91;

Kolevzon, N., Kuflik, U., Shmuel, M., Benhamron, S., Ringel, I., Yavin, E. (2011) Multiple Triphenylphosphonium Cations as a Platform for the Delivery of a Pro-Apoptotic Peptide. Pharm Res. Jun 2. [Epub ahead of print];

Koppenol WH, Bounds PL, Dang CV. (2011) Otto Warburg's contributions to current concepts of cancer metabolism. Nat Rev Cancer. 11(5):325-37;

Krasutsky, P. (2006) Birch bark research and development. Nat. Prod. Rep. vol. 23 (6) pp. 919;

Kroemer, G., Galluzzi, L. & Brenner, C. (2007) Mitochondrial membrane permeabilization in cell death. Physiol. Rev. 87, 99–163;

Kurtoglu and Lampidis. (2009) From delocalized lipophilic cations to hypoxia: Blocking tumor cell mitochondrial function leads to therapeutic gain with glycolytic inhibitors. Mol. Nutr. Food Res. vol. 53 (1) pp. 68-75;

Kuznetsova LP, Nikol'skaia EB, Sochilina EE, Faddeeva MD. (2002) Inhibition by various alkaloids of acetylcholinesterase and butyrylcholinesterase from human blood. Zh Evol Biokhim Fiziol;38:28-31;

Lagouge, M., Argmann, C., Gerhart-Hines, Z., Meziane, H., Lerin, C., Daussin, F., et al. (2006) Resveratrol improves mitochondrial function and protects against metabolic disease by activating SIRT1 and PGC-1α. Cell 127, 1109–1122;

Lee B, Lee SJ, Park SS, Kim SK, Kim SR, Jung JH, et al. (2008) Sanguinarine-induced G1-phase arrest of the cell cycle results from increased p27KIP1 expression mediated via activation of the Ras/ERK signaling pathway in vascular smooth muscle cells. Arch Biochem Biophys 471:224-31;

Lee, H., Yin, P., Yu, T., Chang, Y., Hsu, W., Kao, S., Chi, C., Liu, T., Wei, Y. (2001) Accumulation of mitochondrial DNA deletions in human oral tissues - effects of betel quid chewing and oral cancer. Mutat Res. vol. 493 (1-2) pp. 67-74;

Lee, K. W. and Lee, H. J. (2006) The roles of polyphenols in cancer chemoprevention. *Biofactors 26*,

105-121;

Letasiova S, Jantova S, Cipak L, Muckova M (2006) Berberine antiproliferative activity in vitro and induction of apoptosis/necrosis of the U937 and B16 cells. Cancer Lett 239:254–262;

Letasiova S, Jantova S, Miko M, Ovadekova R, Horvathova M (2006) Effect of berberine on proliferation, biosynthesis of macromolecules, cell cycle and induction of intercalation with DNA, ds-DNA damage and apoptosis in Ehrlich ascites carcinoma cells. J Pharm Pharmacol 58:263–270;

Letasiova S, Jantova S, Muckova M, Theiszova M (2005) Antiproliferative activity of berberine in vitro and in vivo. Biomed Pap Med Fac Univ Palacky Olomouc Czech Repub 149:461–463;

Leu TH, Maa MC. (2002) The molecular mechanisms for the antitumorigenic effect of curcumin. Curr Med Chem Anticancer Agents. 2: 357-370;

Li, R., Ying, X., Zhang, Y., Ju, Y., Wang, X., Yao, H., Men, Y., Tian, W., et al. (2010) All-trans retinoic acid stealth liposomes prevent the relapse of breast cancer arising from the cancer stem cells. Journal of Controlled Release pp. 1-59;

Li, Y., Wang, J., Wientjes, M., Au, J. (2011) Delivery of nanomedicines to extracellular and intracellular compartments of a solid tumor. Adv Drug Deliv Rev pp. 1-11;

Lin HL, Liu TY, Wu CW, Chi CW (1999) Berberine modulates expression of *mdr1* gene product and the responses of digestive track cancer cells to paclitaxel. Br J Cancer 81:416–422;

Lin JP, Yang JS, Lee JH, Hsieh WT, Chung JG (2006) Berberine induces cell cycle arrest and apoptosis in human gastric carcinoma SNU-5 cell line. World J Gastroenterol 12:21–28;

Lin C-C, Lin S-Y, Chung J-G, Lin J-P, Chen C-W, Kao S-T (2006b) Down-regulation of cyclin B1 and up-regulation of Wee1 by berberine promotes entry of leukemia cells into the G2/M-phase of the cell cycle. Anticancer Res 26:1097–1104;

Lin ZX, Hoult JR, Raman A. (1999) Sulphorhodamine B assay for measuring proliferation of a pigmented melanocyte cell line and its application to the evaluation of crude drugs used in the treatment of vitiligo. J Ethnopharmacol. 66:141-50;

Liu, S., Ginestier, C., Ou, S., Clouthier, S., Patel, S., Monville, F., Korkaya, H., Heath, A., et al. (2011) Breast cancer stem cells are regulated by mesenchymal stem cells through cytokine networks. Cancer Research. vol. 71 (2) pp. 614-24;

López-Rios, F., Sánchez-Aragó, M., García-García, E., Ortega, A., Berrendero, J., et al. (2007) Loss of the Mitochondrial Bioenergetic Capacity Underlies the Glucose Avidity of Carcinomas. Cancer Research vol. 67 (19) pp. 9013-9017;

Lopus M, Panda D. (2006) The benzophenanthridine alkaloid sanguinarine perturbs microtubule assembly dynamics through tubulin binding. A possible mechanism for its antiproliferative activity. Febs J. 273:2139-50;

Lyng, M., Laenkholm, A., Pallisgaard, N., Ditzel, H. (2008) Identification of genes for normalization of real-time RT-PCR data in breast carcinomas. BMC Cancer vol. 8 (1) pp.

20;

Ma, X., Dahiya, S., Richardson, E., Erlander, M., Sgroi, D. (2009) Gene expression profiling of the tumor microenvironment during breast cancer progression. Breast Cancer Res. vol. 11 (1) pp. R7;

Mackraj I, Govender T, Gathiram P. (2008) Sanguinarine. Cardiovasc Ther;26:75-83;

Maher JC, Krishan A, Lampidis TJ (2004) Greater cell cycle inhibition and cytotoxicity induced by 2-deoxy-D-glucose in tumor cells treated under hypoxic vs aerobic conditions. Cancer Chemother Pharmacol; 53:116–122;

Maiti, M. and Kumar, G. (2006) Molecular aspects on the interaction of protoberberine, benzophenanthridine, and aristolochia group of alkaloids with nucleic acid structures and biological perspectives. Med Res Rev. 2007 Sep;27(5):649-95;

Makhey D, Gatto B, Yu C, Liu A, Liu LF, LaVoie E, Edmond J (1995) Protoberberine alkaloids and related compounds as dual inhibitors of mammalian topoisomerase I and II. Med Chem Res 5:1–12;

Malikova J, Zdarilova A, Hlobilkova A, Ulrichova J. (2006) The effect of chelerythrine on cell growth, apoptosis, and cell cycle in human normal and cancer cells in comparison with sanguinarine. Cell Biol Toxicol; 22:439-53;

Malikova, J., Zdarilova, A. and Hlobikova, A. (2006) Effects of sanguinarine and chelerythrine on the cell cycle and apoptosis. Biomed Pap Med Fac Univ Palacky Olomouc Czech Repub. 150(1):5–12;

Manach C, Williamson G, Morand C, Scalbert A, Rémésy C. (2005) Bioavailability and bioefficacy of polyphenols in humans: I. Review of 97 bioavailability studies. Am J Clin Nutr. 81: 230S-242S;

Manach, C., Scalbert, A., Morand, C., Remesy, C. and Jimenez, L. (2004) Polyphenols: food sources and bioavailability. *Am. J. Clin. Nutr. 79*, 727-747;

Mandal S, Guptan P, Owusu-Ansah E, Banerjee U (2006) Mitochondrial regulation of cell cycle progression during development as revealed by the tenured mutation in Drosophila. Dev Cell 9:843–854;

Mani, S., Guo, W., Liao, M., Eaton, E., Ayyanan, A., Zhou, A., Brooks, M., Reinhard, F., et al. (2008) The epithelial-mesenchymal transition generates cells with properties of stem cells. Cell. vol. 133 (4) pp. 704-15;

Mantena S, Sharma S, Katiyar S (2006) Berberine, a natural product, induces G1-phase cell cycle arrest and caspase-3-dependent apoptosis in human prostate carcinoma cells. Mol Cancer Ther 5:296–308;

Mantena SK, Sharma SD, Katiyar SK (2006b) Berberine inhibits growth, induces G1 arrest and apoptosis in human epidermoid carcinomaA431 cells by regulatin Cdki-Cdk–cyclin cascade, disruption of mitochondrial membrane potential and cleavage of caspace-3 and PARP. Carcinogenesis. 27(10):2018-27;

Marchetti, P., Zamzami, N., Joseph, B., Schraen-Maschke, S., Méreau-Richard, C., Constantini, P.,

et al. (1999) The novel retinoid 6-[3-(1-adamantyl)- 4-hydroxyphenyl]-2-naphtalene carboxylic acid can trigger apoptosis through a mitochondrial pathway independent of the nucleus. Cancer Res. 59, 6257–6266;

Marques, M. P. M., Borges, F., Sousa, J. B., Calheiros, R., Garrido, J., Gaspar, A., Antunes, F., Diniz, C. and Fresco, P. (2006) Cytotoxic and COX-2 inhibition properties of Hydroxycinnamic derivatives. *Lett. Drug Design Discov. 3*, 316-320;

Marroquin, L., Hynes, J., Dykens, J., Jamieson, J, Will, Y. (2007) Circumventing the Crabtree Effect: Replacing Media Glucose with Galactose Increases Susceptibility of HepG2 Cells to Mitochondrial Toxicants. Toxicological Sciences vol. 97 (2) pp. 539-547;

Masaki, H.; Okamoto, N.; Sakaki, S.; Sakurai, H. (1997) Protective Effects of Hydroxybenzoic Acids and their Esters on Cell Damage Induced by Hydroxyl Radicals and Hydrogen Peroxides. Biol. Pharm. Bull. 20, 304-308;

Mathupala, S., Ko, Y., Pedersen, P. (2006) Hexokinase II: Cancer's double-edged sword acting as both facilitator and gatekeeper of malignancy when bound to mitochondria. Oncogene. vol. 25 (34) pp. 4777-4786;

Matkar SS, Wrischnik LA, Hellmann-Blumberg U. (2008) Sanguinarine causes DNA damage and p53-independent cell death in human colon cancer cell lines. Chem Biol Interact; 172:63-71;

Mayevsky, A. (2009) Mitochondrial function and energy metabolism in cancer cells: past overview and future perspectives. Mitochondrion 9, 165-179;

Meulmeester E, Jochemsen AG. (2008) p53: a guide to apoptosis. Curr Cancer Drug Targets. 8:87-97;

Mezhybovska, M., Yudina, Y., Abhyankar, A., Sjolander, A. (2008) Beta-Catenin is involved in alterations in mitochondrial activity in non-transformed intestinal epithelial and colon cancer cells. British Journal of Cancer. vol. 101 (9) pp. 1596-1605;

Michelakis, E., Sutendra, G., Dromparis, P., Webster, L., Haromy, A., et al. (2010) Metabolic Modulation of Glioblastoma with Dichloroacetate. Science Translational Medicine. vol. 2 (31) pp. 31ra34-31ra34;

Mikes V, Dadak V (1983) Berberine derivatives as cationic fluorescent probes for the investigation of the energized state of mitochondria. Biochim Biophys Acta 723:231–239;

Min YD, Yang MC, Lee KH, Kim KR, Choi SU, Lee KR (2006) Protoberberine alkaloids and their reversal activity of P-gp expressed multidrug resistance (MDR) from the rhizome of *Coptis japonica* Makino. Arch Pharm Res 29:757–761;

Mitchell P, Moyle J (1967). Chemiosmotic hypothesis of oxidative phosphorylation. Nature 213: 137–139;

Mitscher LA, Drake S, Gollapudi SR, Okwute SK. (1987) A modern look at folkloric use of anti-infective agents. J Nat Prod; 50:1025-40.

Miyamoto, S., Murphy, A., Brown, J. (2008) Akt mediates mitochondrial protection in cardiomyocytes through phosphorylation of mitochondrial hexokinase-II. Cell Death

Differ. vol. 15 (3) pp. 521-529;

Mizumachi, T., Suzuki, S., Naito, A., Carcel-Tullois, J., Evans, T., Spring, P., et al. (2008) Increased mitochondrial DNA induces acquired docetaxel resistance in head and neck cancer cells. Oncogene. vol. 27 (6) pp. 831-8;

Modica-Napolitano, JS, and Aprille, JR. (2001) Delocalized lipophilic cations selectively target the mitochondria of carcinoma cells. Adv Drug Deliv Rev; 49: 63-70;

Modica-Napolitano, J., Kulawiec, M., Singh, K. (2007) Mitochondria and human cancer. Curr Mol Med. vol. 7 (1) pp. 121-31;

Moll UM, Zaika A. (2001) Nuclear and mitochondrial apoptotic pathways of p53. FEBS Lett; 493:65-9;

Morrison, B.J., Andera, L., Reynolds, B.A., Ralph, S.J., Neuzil, J. (2009) Future use of mitocans against tumour-initiating cells? Mol. Nutr. Food Res. 53, 147–153;

Mukhopadhyay, A., Ni, L., Yang, C. S. & Weiner, H. (2005) Bacterial signal peptide recognizes HeLa cell mitochondrial import receptors and functions as a mitochondrial leader sequence. Cell. Mol. Life Sci. 62, 1890–1899;

Mullauer, F., Kessler, J., Medema, J. (2009) Betulinic acid induces cytochrome c release and apoptosis in a Bax/Bak-independent, permeability transition pore dependent fashion. Apoptosis. vol. 14 (2) pp. 191-202;

Murphy, MP. (1997) Selective targeting of bioactive compounds to mitochondria. Trends Biotechnol. vol. 15 (8) pp. 326-30;

Naito, A., Cook, C., Mizumachi, T., Wang, M., Xie, C., Evans, T., Kelly, T., Higuchi, M. (2008) Progressive tumor features accompany epithelial-mesenchymal transition induced in mitochondrial DNA-depleted cells. Cancer Science. vol. 99 (8) pp. 1584-1588;

Naderi, A., Liu, J., Francis, G. (2011) A feedback loop between BEX2 and ErbB2 mediated by c-Jun signaling in breast cancer. Int J Cancer pp.

Neve, R., Chin, K., Fridlyand, J., Yeh, J., Baehner, F., Fevr, T., Clark, L., Bayani, N., et al. (2006) A collection of breast cancer cell lines for the study of functionally distinct cancer subtypes. Cancer Cell. vol. 10 (6) pp. 515-27;

Nguyen and Hussain (2007). The role of the mitochondria in mediating cytotoxicity of anti-cancer therapies. J Bioenerg Biomembr. vol. 39 (1) pp. 13-21;

Nithipongvanitch R, Ittarat W, Velez JM, Zhao R, St Clair DK, Oberley TD (2007). Evidence for p53 as guardian of the cardiomyocyte mitochondrial genome following acute adriamycin treatment. J Histochem Cytochem; 55:629-39.

Nomura, E., Hosoda, A., Morishita, H., Murakami, A., Koshimizu, K., Ohigashi, H. and Taniguchi, H. (2002) Synthesis of novel polyphenols consisted of ferulic and gallic acids, and their inhibitory effects on phorbol ester-induced Epstein-Barr virus activation and superoxide generation. *Bioorg. Med. Chem. 10*, 1069-1075;

Notario, B., Zamora, M., Vinas, O. & Mampel, T. (2003) All-trans-retinoic acid binds to and

inhibits adenine nucleotide translocase and induces mitochondrial permeability transition. Mol. Pharmacol. 63, 224–231;

Nyalendo, C., Sartelet, H., Barette, S., Ohta, S., Gingras, D., Béliveau, R. (2009) Identification of membrane-type 1 matrix metalloproteinase tyrosine phosphorylation in association with neuroblastoma progression. BMC Cancer. vol. 9 (1) pp. 422;

Oakman, C., Viale, G., Di Leo, A. (2010) Management of triple negative breast cancer. The Breast. vol. 19 (5) pp. 312-321;

Oliveira, P. J., Santos, D. J. and Moreno, A. J. (2000) Carvedilol inhibits the exogenous NADH dehydrogenase in rat heart mitochondria. *Arch. Biochem. Biophys. 374*, 279-285;

Oliveira, P. J., Coxito, P. M., Rolo, A. P., Santos, D. L., Palmeira, C. M. and Moreno, A. J. (2001) Inhibitory effect of carvedilol in the high-conductance state of the mitochondrial permeability transition pore. *Eur. J. Pharmacol. 412*, 231-237;

Orr, G., Verdier-Pinard, P., McDaid, H., Horwitz, S. (2003) Mechanisms of Taxol resistance related to microtubules. Oncogene. vol. 22 (47) pp. 7280-7295;

Orrenius S. (2007) Reactive oxygen species in mitochondria-mediated cell death. Drug Metab Rev; 39: 443-455;

Ortega, A., Sánchez-Áragó, M., Giner-Sanchez, D., Sanchez-Cenizo, L., Willers, I, et al. (2009) Glucose avidity of carcinomas. Cancer Letters. vol. 276 (2) pp. 125-35;

Ott, M., Robertson, J.D., Gogvadze, V., Zhivotovsky, B., Orrenius, S., (2002). Cytochrome c release from mitochondria proceeds by a two-step process. Proc. Natl. Acad. Sci. USA 99, 1259–1263;

Ottino, P., Duncan, J.R., (1997). Effect of alpha-tocopherol succinate on free radical and lipid peroxidation levels in BL6 melanoma cells. Free Radic. Biol. Med. 22, 1145–1151;

Palacios, C.; Cespon, C.; Martin de la Vega, C, et la. (2001) Lauryl gallate inhibits the activity of protein tyrosine kinase c-Src purified from human platelets. J. Enzyme. Inhib. 16, 527;

Pan JF, Yu C, Zhu DY, Zhang H, Zeng JF, Jiang SH, Ren JY (2002) Identification of three sulfate-conjugated metabolites of berberine chloride in healthy volunteer's urine after oral administration. Acta Pharmacol Sin 23:77–82;

Pavlova, N., Savinova, O., Nikolaeva, S., Boreko, E., Flekhter, O. (2003) Antiviral activity of betulin, betulinic and betulonic acids against some enveloped and non-enveloped viruses. Fitoterapia. vol. 74 (5) pp. 489-92;

Pantaleo, M., Astolfi, A., Nannini, M., Paterini, P., Piazzi, G., Ercolani, G., Brandi, G., et al. (2008) Gene expression profiling of liver metastases from colorectal cancer as potential basis for treatment choice. Br J Cancer vol. 99 (10) pp. 1729-1734;

Pedersen, P., Mathupala, S., Rempel, A., Geschwind, J., Ko, Y. (2002) Mitochondrial bound type II hexokinase: a key player in the growth and survival of many cancers and an ideal prospect for therapeutic intervention. Biochim Biophys Acta. vol. 1555 (1-3) pp. 14-20;

Pedersen. P. (2008) Voltage dependent anion channels (VDACs): a brief introduction with a focus

on the outer mitochondrial compartment's roles together with hexokinase-2 in the "Warburg effect" in cancer. JOURNAL OF BIOENERGETICS AND BIOMEMBRANES Volume 40, Number 3, 123-126;

Peetla, C., Bhave, R., Vijayaraghavalu, S., Stine, A., Kooijman, E. and Labhasetwar, V. (2010) Drug resistance in breast cancer cells: biophysical characterization of and doxorubicin interactions with membrane lipids. *Mol. Pharm. 7*, 2334-2348;

Pellegrini and Mak. (2010) Tumor immune therapy: Lessons from infection and implications for cancer - Can IL-7 help overcome immune inhibitory networks?. Eur. J. Immunol. vol. 40 (7) pp. 1852-1861

Pereira, G. C., Branco, A. F., Matos, et al. (2007) Mitochondrially targeted effects of berberine [Natural Yellow 18, 5,6-dihydro-9,10-dimethoxybenzo(g)-1,3-benzodioxolo(5,6-a) quinolizinium] on K1735-M2 mouse melanoma cells: comparison with direct effects on isolated mitochondrial fractions. J. Pharmacol. Exp. Ther. 323, 636-649;

Pereira CV, Machado NG, Oliveira PJ. (2008) Mechanisms of berberine (natural yellow 18)-induced mitochondrial dysfunction: interaction with the adenine nucleotide translocator. Toxicol Sci. 105(2): 408-17;

Pereira, C. V., Moreira, A. C., Pereira, S. P., Machado, N. G., Carvalho, F. S., Sardao, V. A. and Oliveira, P. J. (2009) Investigating drug-induced mitochondrial toxicity: a biosensor to increase drug safety? *Curr. Drug Saf. 4*, 34-54;

Petros, J., Baumann, A., Ruiz-Pesini, E., Amin, M., Sun, C., Hall, J., Lim, S., et al. (2005) mtDNA mutations increase tumorigenicity in prostate cancer. Proc. Natl Acad. Sci. USA 102, 719–724;

Pi G, Ren P, Yu J, Shi R, Yuan Z, Wang C. (2008) Separation of sanguinarine and chelerythrine in Macleaya cordata (Willd) R. Br. based on methyl acrylate-codivinylbenzene macroporous adsorbents. J Chromatogr A;1192:17-24.

Plescia, J., Saiz, W., Xia, F., Pennati, M., Zaffaroni, N., Daidone, M., Meli, M., Dohi, T., et al. (2005) Rational design of shepherdin, a novel anticancer agent. Cancer Cell. vol. 7 (5) pp. 457-68;

Prasad, K.N., Edwards-Prasad, J., (1982). Effects of tocopherol (vitamin E) acid succinate on morphological alterations and growth inhibition in melanoma cells in culture. Cancer Res. 42, 550–555;

Rajan, P., Vedernikova, I., Cos, P., Berghe, D. V., Augustyns, K. and Haemers, A. (2001) Synthesis and evaluation of caffeic acid amides as antioxidants. *Bioorg. Med. Chem. Lett. 11*, 215-217;

Ralph, S., Rodriguez-Enriquez, S., Neuzil, J., Moreno-Sanchez, R. (2010) Bioenergetic pathways in tumor mitochondria as targets for cancer therapy and the importance of the ROS-induced apoptotic trigger. Molecular Aspects of Medicine. vol. 31 (1) pp. 29-59;

Ralph, S. J. and Neuzil, J. (2009) Mitochondria as targets for cancer therapy. *Mol. Nutr. Food. Res. 53*, 9-28;

Rasola and Bernardi. (2011) Mitochondrial permeability transition in Ca2+-dependent apoptosis and necrosis. Cell Calcium pp. 1-12;

Repesh LA, Drake SR, Warner MC, Downing SW, Jyring R, Seftor EA, et al. (1993) Adriamycin-induced inhibition of melanoma cell invasion is correlated with decreases in tumor cell motility and increases in focal contact formation. Clin Exp Metastasis;11:91-102;

Repesh LA. (1989) A new in vitro assay for quantitating tumor cell invasion. Invasion Metastasis. 9:192-208;

Reyes R, Ramirez G, Delgado NM (2004) Fluorescent berberine binding as a marker of internal glycosaminoglycans sulfate in bovine oocytes and sperm cells. Arch Androl 50:327–332;

Rob A. Cairns, Isaac S. Harris & Tak W. Mak. (2011) Regulation of cancer cell metabolism. Nature Reviews Cancer 11, 85-95;

Robert A. Gatenby & Robert J. Gillies. (2004) Why do cancers have high aerobic glycolysis? Nature Reviews Cancer 4, 891-899;

Robert Allan Weinberg (2007) The biology of cancer. Garland Science, Taylor & Francis Group, LLC.

Roleira, F. M., Siquet, C., Orru, E., et al (2010) Lipophilic phenolic antioxidants: correlation between antioxidant profile, partition coefficients and redox properties. *Bioorg. Med. Chem. 18*, 5816-5825;

Rolo, A. P., Oliveira, P. J., Moreno, A. J. and Palmeira, C. M. (2000) Bile acids affect liver mitochondrial bioenergetics: possible relevance for cholestasis therapy. *Toxicol. Sci. 57*, 177-185;

Ross, M. F., Filipovska, A., Smith, R. A., Gait, M. J. & Murphy, M. P. (2004) Cell-penetrating peptides do not cross mitochondrial membranes even when conjugated to a lipophilic cation: evidence against direct passage through phospholipid bilayers. Biochem. J. 383, 457–468;

Rossignol, R., Gilkerson, R., Aggeler, R., Yamagata, K., Remington, S., Capaldi, R. (2004) Energy substrate modulates mitochondrial structure and oxidative capacity in cancer cells. Cancer Research. vol. 64 (3) pp. 985-93;

Sardão VA, Oliveira PJ, Holy J, Oliveira CR, and Wallace KB (2007) Vital imaging of H9c2 myoblasts exposed to tert-butylhydroperoxide: characterization of morphological features of cell death. BMC Cell Biol 8:11;

Sardao, V. A., Pereira, S. L. and Oliveira, P. J. (2008) Drug-induced mitochondrial dysfunction in cardiac and skeletal muscle injury. Expert Opin. Drug Saf. 7, 129-146;

Sardao, V. A., Oliveira, P. J., Holy, J., Oliveira, C. R. and Wallace, K. B. (2009) Doxorubicin-induced mitochondrial dysfunction is secondary to nuclear p53 activation in H9c2 cardiomyoblasts. Cancer Chemother. Pharmacol. 64, 811-827;

Sasaki, R., Suzuki, Y., et al. (2008). DNA polymerase gamma inhibition by vitamin K3 induces mitochondria-mediated cytotoxicity in human cancer cells. Cancer Sci. 99 (5), 1040–1048;

Sastre J, Pallardo FV, and Vina J (2000) Mitochondrial oxidative stress plays a key role in aging and apoptosis. *IUBMB Life* **49:**427–435;

Schubert, A., Grimm, S. (2004). Cyclophilin D, a component of the permeability transition-pore, is an apoptosis repressor. Cancer Res. 64, 85–93;

Schulz, T., Thierbach, R., Voigt, A., Drewes, G., Mietzner, B., Steinberg, P., Pfeiffer, A., Ristow,M. (2005) Induction of Oxidative Metabolism by Mitochondrial Frataxin Inhibits Cancer Growth: Otto Warburg revisited. Journal of Biological Chemistry vol. 281 (2) pp. 977-981;

Seitz S., Korsching E., Weimer J., Jacobsen A. et al. (2006) Genetic background of different cancer cell lines influences the gene set involved in chromosome 8 mediated breast tumor suppression. Genes, Chromosomes and Cancer Volume 45, Issue 6, pages 612–627;

Seifen E, Adams RJ, Riemer RK. (1979) Sanguinarine: a positive inotropic alkaloid which inhibits cardiac Na+,K+-ATPase. Eur J Pharmacol; 60:373-7.

Selak, M., Armour, S., Mackenzie, E., Boulahbel, H., Watson, D., Mansfield, K., Pan, Y., et al. (2005) Succinate links TCA cycle dysfunction to oncogenesis by inhibiting HIF-alpha prolyl hydroxylase. Cancer Cell. vol. 7 (1) pp. 77-85;

Sellar, G., Li, L., Watt, K., Nelkin, B., Rabiasz, G., Stronach, E., Miller, E., Porteous, D., et al. (2001) BARX2 induces cadherin 6 expression and is a functional suppressor of ovarian cancer progression. Cancer Research. vol. 61 (19) pp. 6977-81

Selina Kaye Sutton (2005) How does mitochondrial heteroplasmy affect cell proliferation? Thesis in Master of Science School of Biological Sciences University of Canterbury, New Zealand;

Serafim, T. L., Oliveira, P. J., Sardao, V. A., Perkins, E., Parke, D. and Holy, J. (2008) Different concentrations of berberine result in distinct cellular localization patterns and cell cycle effects in a melanoma cell line. Cancer Chemother. Pharmacol. 61, 1007-1018;

Serafim, T. L., Marques, M. P., Borges, F. and Oliveira, P. J. (2008b) Mitochondria as a target for novel chemotherapeutic agents based on phenolic acids. J. Theor. Exp. Pharm. 1, 3-13;

Shaw, J. M. and Winge, D. R. (2009) Shaping the mitochondrion: mitochondrial biogenesis, dynamics and dysfunction. Conference on Mitochondrial Assembly and Dynamics in Health and Disease. *EMBO Rep. 10*, 1301-1305;

Sheridan C, Kishimoto H, Fuchs RK, Mehrotra S, Bhat- Nakshatri P, Turner CH, et al. (2006) CD44+/CD24- breast cancer cells exhibit enhanced invasive properties: an early step necessary for metastasis. Breast Cancer Res; 8:R59;

Shipitsin M, Campbell LL, Argani P, Weremowicz S, et al. (2007) Molecular definition of breast tumor heterogeneity. Cancer Cell. 11:259-273;

Shitan N, Tanaka M, Terai K, Ueda K, Yazaki K (2007) Human MDR1 and MRP1 recognize berberine as their transport substrate. Biosci Biotechnol Biochem 71:242–245;

Shukla S, Wu CP, Ambudkar SV. (2008) Development of inhibitors of ATP-binding cassette drug transporters: present status and challenges. Expert Opin Drug Metab Toxicol; 4:205-23;

Shulman, O., Laitman, Y., Vilan, A., Leviav, A., Friedman, E. (2006) Monoclonal origin of anatomically distinct basal cell carcinomas. J Invest Dermatol vol. 126 (3) pp. 676-9;

Simonnet, H., Alazard, N., Pfeiffer, K., Gallou, C., Beroud, C., Demont, J., Bouvier, R., et al. (2002) Low mitochondrial respiratory chain content correlates with tumor aggressiveness in renal cell carcinoma. Carcinogenesis. vol. 23 (5) pp. 759-68;

Skehan P, Storeng R, Scudiero D, Monks A, McMahan J, et al. (1990) New colorimetric cytotoxicity assay for anticancer-drug screening. J Natl Cancer Inst 82:1107–1112;

Slaninova I, Taborska E, Bochorakova H, Slanina J (2001) Interaction of benzo[c]phenanthridine and protoberberine alkaloids with animal and yeast cells. Cell Biol Toxicol 17(1):51–63;

Smolarczyk, R., Cichon, T., Graja, K., Hucz, J., Sochanik, A., Szala, S. (2006) Antitumor effect of RGD-4C-GG-D(KLAKLAK)2 peptide in mouse B16(F10) melanoma model. Acta Biochim Pol. vol. 53 (4) pp. 801-5;

Smolkova, K, Bellance N, Scandurra F, Ge´not E, Gnaiger E, et al. (2010) Mitochondrial bioenergetic adaptations of breast cancer cells to aglycemia and hypoxia. J Bioenerg Biomembr 42: 55–67;

Solaini, G., Sgarbi, G., Baracca, A. (2010) Oxidative phosphorylation in cancer cells. BBA – Bioenergetics. pp. 1-9;

Son, S., Lobkowsky, E. B. and Lewis, B. A. (2001) Caffeic acid phenethyl ester (CAPE): synthesis and X-ray crystallographic analysis. Chem. Pharm. Bull. (Tokyo) 49, 236-238;

Stockwin, L., Yu, S., Borgel, S., Hancock, C., Wolfe, T., Phillips, L., Hollingshead, M., Newton, D. (2010) Sodium dichloroacetate selectively targets cells with defects in the mitochondrial ETC. Int J Cancer. vol. 127 (11) pp. 2510-9;

Subudhi, U., Das, K., Paital, B., Bhanja, S., Chainy, G. (2008) Alleviation of enhanced oxidative stress and oxygen consumption of L-thyroxine induced hyperthyroid rat liver mitochondria by vitamin E and curcumin. Chem. Biol. Interact. 173 (2), 105–114;

Szliszka, E., Czuba, Z. P., Domino, M., Mazur, B., Zydowicz, G. and Krol, W. (2009) Ethanolic extract of propolis (EEP) enhances the apoptosis- inducing potential of TRAIL in cancer cells. *Molecules 14*, 738-754;

T. Galgon, W. Wohlrab and B. Draeger. (2005) Betulinic acid induces apoptosis in skin cancer cells and differentiation in normal human keratinocytes. Exp. Dermatol. 14, 736–743;

Taanman J-W (1999) The mitochondrial genome: structure, transcription, translation and replication. Biochim Biophys Acta 1410: 103 –123;

Tan, B., Skipworth, R., Stephens, N., Wheelhouse, N., Gilmour, H., de Beaux, A., et al. (2009) Frequency of the mitochondrial DNA 4977bp deletion in oesophageal mucosa during the progression of Barrett's oesophagus. European Journal of Cancer. vol. 45 (5) pp. 736-740;

Taylor and Turnbull. (2007) Mitochondrial DNA transcription: regulating the power supply. Cell. vol. 130 (2) pp. 211-3;

Taylor WR, Stark GR (2001) Regulation of the G2/M transition by p53. Oncogene 20:1803–1815

Temkin V, Huang Q, Liu H, Osada H, Pope RM. Inhibition of ADP/ATP exchange in receptor-interacting protein-mediated necrosis. Mol Cell Biol 26: 2215–2225, 2006;

Thaddeus S. Stappenbeck* and Hiroyuki Miyoshi. (2009) The Role of Stromal Stem Cells in Tissue Regeneration and Wound Repair. Science. Vol. 324 (5935) pp. 1666-1669;

Thomas and Cookson. (2009) The role of PTEN-induced kinase 1 in mitochondrial dysfunction and dynamics. Int J Biochem Cell Biol. vol. 41 (10) pp. 2025-35;

Thundathil J, Filion F, Smith LC. (2005) Molecular control of mitochondrial function in preimplantation mouse embryos. Mol Reprod Dev. 71:405-13;

Tlsty and Hein. (2001) Know thy neighbor: stromal cells can contribute oncogenic signals. Curr Opin Genet Dev. vol. 11 (1) pp. 54-9;

Toogood, PL. (2008) Mitochondrial drugs. Curr Opin Chem Biol. vol. 12 (4) pp. 457-63;

Trachootham, D., Zhang, H., et al., (2008). Effective elimination of fludarabine-resistant CLL cells by PEITC through a redox-mediated mechanism. Blood;

Trachootham, D., Alexandre, J., et al. (2009). Targeting cancer cells by ROS-mediated mechanisms: a radical therapeutic approach? Nat. Rev. Drug Discovery 8, 579–591;

Van Den Bogert BC, Kernebeek Gv, Leij Ld, Kroon AM (1986) Inhibition of mitochondrial protein synthesis leads to proliferation arrest in the G1-phase of the cell cycle. Cancer Lett 32:41–51;

Vander Heiden, M., Cantley, L., Thompson, C. (2009) Understanding the Warburg Effect: The Metabolic Requirements of Cell Proliferation. Science. vol. 324 (5930) pp. 1029-1033;

Vaseva, A. V. and Moll, U. M. (2009) The mitochondrial p53 pathway. Biochim. Biophys. Acta 1787, 414-420;

Vaupel, P., Kallinowski, F., Okunieff, P. (1989) Blood flow, oxygen and nutrient supply, and metabolic microenvironment of human tumors: a review. Cancer Research. vol. 49 (23) pp. 6449-65;

Vavreckova C, Gawlik I, Muller K. (1996) Benzophenanthridine alkaloids of Chelidonium majus; I. Inhibition of 5- and 12-lipoxygenase by a non-redox mechanism. Planta Med. 62:397-401;

Viktorsson, K., Lewensohn, R., Zhivotovsky, B. (2005). Apoptotic pathways and therapy resistance in human malignancies. Adv. Cancer Res. 94, 143–196;

Vinothini, G., Murugan, R., Nagini, S. (2010) Mitochondria-mediated apoptosis in patients with adenocarcinoma of the breast: Correlation with histological grade and menopausal status. The Breast. pp. 1-7;

Vogel VJ (1990) American Indian medicine, University of Oklahoma Press, Norman;

Volkmar Weissig and Gerard G. M. D'Souza (2010) Mitochondria-Targeted Drug Delivery. Targeted Delivery of Small and Macromolecular Drugs. Chapter 11. 255-273;

Wahl H, Tan L, Griffith K, Choi M, Liu JR. (2007) Curcumin enhances Apo2L/TRAIL-induced apoptosis in chemoresistant ovarian cancer cells. Gynecol Oncol. 105: 104-112;

Wallace, D., Singh, G., Lott, M., Hodge, J., Schu, T., Lezza, A., Elsas, L., Nikoskelainen, E. (1988)

Mitochondrial DNA mutation associated with Leber's hereditary optic neuropathy. Science. 242: 1427–1430;

Wang, J., Yang, C.T., Kim, Y.S., Sreerama, S.G., Cao, Q., Li, Z.B., He, Z., Chen, X., Liu, S. (2007). 727 64Cu-Labeled triphenylphosphonium and triphenylarsonium cations as highly 728 tumor-selective imaging agents. J. Med. Chem. 18 (21), 5057–5069 50;

Wang, S. J., Zhang, Z. Q., Zhao, Y. H., Ruan, J. X. and Li, J. L. (2006) Simultaneous quantification of chlorogenic acid and caffeic acid in rat plasma after an intravenous administration of mailuoning injection using liquid chromatography/mass spectrometry. *Rapid Commun. Mass Spectrom. 20*, 2303-2308;

Warburg, O., Wind, F., Negelein, E. (1927) THE METABOLISM OF TUMORS IN THE BODY. J Gen Physiol. vol. 8 (6) pp. 519-30;

Weerasinghe P, Hallock S, Tang SC, Liepins A. (2001) Role of Bcl-2 family proteins and caspase-3 in sanguinarineinduced bimodal cell death. Cell Biol Toxicol; 17: 371–81.

Weinberg, F. and Chandel, N. S. (2009) Mitochondrial metabolism and cancer. *Ann. N.Y. Acad. Sci. 1177*, 66-73;

Weinberg, F., Hamanaka, R., Wheaton, W., Weinberg, S., Joseph, J., Lopez, M., Kalyanaraman, B., et al. (2010) Mitochondrial metabolism and ROS generation are essential for Kras-mediated tumorigenicity. Proceedings of the National Academy of Sciences. vol. 107 (19) pp. 8788-8793;

Werner J.H. Koopman, Leo G.J. Nijtmans, et al. (2010) Mammalian Mitochondrial Complex I: Biogenesis, Regulation, and Reactive Oxygen Species Generation. Antioxidants & Redox Signaling. 12(12): 1431-1470;

Wheelhouse, N., Lai, P., Wigmore, S., Ross, J., Harrison, D. (2005) Mitochondrial D-loop mutations and deletion profiles of cancerous and noncancerous liver tissue in hepatitis B virus-infected liver. British Journal of Cancer. vol. 92 (7) pp. 1268-1272;

Williams, J., Lucas, P., Griffith, K., Choi, M., Fogoros, S., Hu, Y., Liu, J. (2005) Expression of Bcl-xL in ovarian carcinoma is associated with chemoresistance and recurrent disease. Gynecol Oncol. vol. 96 (2) pp. 287-95;

Windler-Hart, S., Chen, K., Chenn, A. (2005) A cell behavior screen: identification, sorting, and enrichment of cells based on motility. BMC Cell Biol. vol. 6 (1) pp. 14;

Yamada and Harashima. (2008) Mitochondrial drug delivery systems for macromolecule and their therapeutic application to mitochondrial diseases. Adv Drug Deliv Rev. vol. 60 (13-14) pp. 1439-62;

Yamamoto, T., Hsu, S., et al. (2003). Green tea polyphenol causes differential oxidative environments in tumor versus normal epithelial cells. J. Pharmacol. Exp. Ther. 307 (1), 230–236;

Yang IW, Chou CC, Yung BY (1996) Dose-dependent effects of berberine on cell cycle pause and apoptosis in Balb/c 3T3 cells. Naunyn Schmiedebergs Arch Pharmacol 354:102–108;

Yang, S.E., Hsieh, M.T., et al. (2002). Down-modulation of Bcl-XL, release of cytochrome c and

sequential activation of caspases during honokiol-induced apoptosis in human squamous lung cancer CH27 cells. Biochem. Pharmacol. 63 (9), 1641–1651;

Ye, X., Wang, G., Huang, G., Bian, X., Qian, G., Yu, S. (2011) Heterogeneity of Mitochondrial Membrane Potential: A Novel Tool to Isolate and Identify Cancer Stem Cells from a Tumor Mass? Stem Cell Rev and Rep. vol. 7 (1) pp. 153-160;

Yoshida T, Tomioka I, Nagahara T, Holyst T, Sawada M, Hayes P, et al. (2004) Baxinhibiting peptide derived from mouse and rat Ku70. Biochem Biophys Res Commun. 321:961-6;

Yu, W., Sanders, B.G., Kline, K. (2003). RRR-alpha-tocopheryl succinate-induced apoptosis of human breast cancer cells involves Bax translocation to mitochondria. Cancer Res. 63, 2483–2491;

Zamzami and Kroemer. (2001) The mitochondrion in apoptosis: how Pandora's box opens. Nat Rev Mol Cell Biol. vol. 2 (1) pp. 67-71;

Zhang, T., Chen, G., Wang, Z., Wang, Z. Y., Chen, S., Chen, Z. (2001) Arsenic trioxide, a therapeutic agent for APL. Oncogene. vol. 20 (49) pp. 7146-53;

Zhang, E., Zhang, C., Su, Y., Cheng, T., Shi, C. (2011) Newly developed strategies for multifunctional mitochondria-targeted agents in cancer therapy. Drug Discov Today. vol. 16 (3-4) pp. 140-146;

Zhou, Y., Garcia-Priteo, C., Carmey, D., Xu, R., Pelicano, H., Kang, Y., Yu, W., Lou, C., Kondo, S., Liu, J., et al. (2005) OSW-1: a Natural Compound With Potent Anticancer Activity and a Novel Mechanism of Action. JNCI Journal of the National Cancer Institute. vol. 97 (23) pp. 1781-1785;

Zini, R., Morin, C., Bertelli, A., Bertelli, A. A., Tillement, J. (1999). Effects of resveratrol on the rat brain respiratory chain. Drugs Exp. Clin. Res. 25 (2–3), 87–97;

Zinkewich-Péotti, K. and Andrews, P. (1992) Loss of cis-diamminedichloroplatinum(II) resistance in human ovarian carcinoma cells selected for rhodamine 123 resistance. Cancer Research. vol. 52 (7) pp. 1902-6;

Zuo F, Nakamura N, Akao T, Hattori M (2006) Pharmacokinetics of berberine and its main metabolites in conventional and pseudo germ-free rats determined by liquid chromatography/ion trap mass spectrometry. Drug Metab Dispos 34:2064–2072.